Extractives from the *Meliaceae* & *Ptaeroxylaceae*

By

Dashnie Naidoo
BSc (HONS)(Natal)

Submitted in partial fulfillment of the requirements
for the degree of
Master of Science
in the
School of Pure and Applied Chemistry,
University of Natal,
Durban

2001

ஓம் சக்தி கணபதி வா வா
சமயே கணபதியே வா வா
னசவவோக தேவவோகம்
சொவெரோத்தகவம்
என் மகமே உன் மகமே ஆகிய
என் கண்கள் உன் கண்கள் ஆகிய
என் பார்னவ உன் பார்னவ ஆகிய
யாவரும் என் வாசகியம் ஆகிய
அம்பினசயும் ஆங்காரம் மூன்னுடைகியா
சபாகியா
ஓம் சக்தி கணபதி வா வா

Preface

The experimental work described in this thesis was carried out in the School of Pure and Applied Chemistry, University of Natal, Durban, South Africa, under the supervision of Professor D.A. Mulholland.

This study represents original work by the author and has not been submitted in any other form to another university. Where use was made of the work of others, it has been duly acknowledged in the text.

Signed:

.....

D. Naidoo
BSc (HONS) (Natal)

I hereby certify that the above statement is correct.

Signed:

.....

Professor D.A. Mulholland
Ph.D. (Natal)
Professor of Organic Chemistry,
University of Natal, Durban

Acknowledgements

I wish to express my sincere thanks to my supervisor, Professor D.A. Mulholland, for her assistance and advice throughout my project. You are surely one of the sweetest people I've met.

Thanks to my friend Mr. Philip Coombes for filling my days with the joy of laughter and making my research a wonderful experience. I will always be greatful for your assistance and friendship.

I express my gratitude to Mr. Peter Cheplogoi for initiating my success in my natural products research. You are a dear friend.

I thank Mr. Dilip Jagjivan for not only the running of the NMR spectra, but for his kind words and support throughout my research.

I thank Mr. Brett Parel for always providing me with the materials I required and for the running of the mass spectra. I'll always remember the funny experiences that put a smile on my face everytime.
Thank you Mr. Earnest Mchunu for always keeping a neat and tidy laboratory, making it a pleasure to work in.

A special thanks to Marion Horne at UNP for her assistance with the polarimeter, and Dr. Boshoff for the running of the HRMS.

I thank Dr. Milijoana Randrianarivelojosia for supplying me with the plant material that has led to my success.

Thank you Miss Farida Khan for being a great friend. Although we are miles apart, you are always close to my heart. Miss Desree Govender, thank you for bringing back the excitement into my life and for lifting my spirits. Your sweet smile always brightens my day. Your friendship I intend to keep till my endless sleep.

I thank the Natural Products Research Group, Angela, Katherine, Chantal, Tracy, Neil, Peter, Phil, Brenda and Nivan for making my MSc research a pleasurable and memorable one. For not only being my working collegues but for being like my family.

I thank Professor K.H. Pegel for his assistance in providing me with the literature data I required. I will always admire you for the wisdom you have gained over the years.

I would also like to thank all staff of the Department of Chemistry, both academic and technical, who have in some way assisted me.

I thank the photographers and internet sites for the photographs of various plants included in this work. Acknowledgements have been included in the text at the appropriate places.

I acknowledge the support of the NRF for their financial assistance.

A special thanks to my family, my mum and dad, Bruce, Dean, Cyril, Phelan and Kassandra, for all the love and support they have given me. Thank you dad for making this all possible. I owe this all to you. Your financial support and encouragement has brought me where I am today. You worked extremely hard and overcame many obstacles to accomplish all that you have. You have been the inspiration in my life. Thank you. I am proud to be your daughter. Mum, you are my source of love. Your loving, caring, helpful nature and words of wisdom have instilled in me my good qualities. You have introduced me to the wonders of God. For this I shall always be greatful.

Finally I dedicate this thesis to my beautiful sister Jenny who was left to rest in peace on 26/12/1999. She was the person we were all blessed to know and love. Jen you will always have a special place in my heart.

Praise God almighty, my creator, saviour and protector, for helping me accomplish all that I have and be what I am today.

List of Abbreviations

^{1}H NMR spectroscopy - proton nuclear magnetic resonance spectroscopy

^{13}C NMR spectroscopy - carbon-13 nuclear magnetic resonance spectroscopy

COSY - correlated spectroscopy

NOESY - nuclear Overhauser effect spectroscopy

HMBC - heteronuclear multiple bond coherence

HSQC - heteronuclear multiple quantum coherence

DEPT - distortionless enhancement by polarisation transfer

HRMS - high resolution mass spectrometry

MS - mass spectrometry

IR - infra-red

Mp - melting point

t.l.c - thin layer chromatography

s - singlet

d - doublet

t - triplet

q - quartet

m - multiplet

dd - doublet of doublets

dt - doublet of triplets

td - triplet of doublets

h - heptet

Hz - Hertz

C - concentration

p-TSA - *para*-toluene sulphonic acid

Abstract

This work is an account of the extractives from one member of the Meliaceae and one member of the Ptaeroxylaceae. In all, thirteen compounds have been isolated, of which four have not been described previously.

Neobeguea mahafalensis belongs to the *Neobeguea* genus and has been classified into the Swietenieae subfamily of the Meliaceae. *Neobeguea mahafalensis* seeds obtained from Madagascar were investigated for the presence of limonoids. This is the first time extracts of the seeds were investigated. Previous work was done on the stem bark of this species. An andirobin-type limonoid, methyl angolensate (**5**), two mexicanolide-type limonoids, mexicanolide (**6**), khayasin (**7**), and three protolimonoids, sapelin E acetate (**8**), sapelin C (**9**) and grandifoliolenone (**10**), have been isolated in this work. One of these was novel.

Cedrelopsis grevei belongs to the *Cedrelopsis* genus and has been classified into the Ptaeroxylaceae family. Extracts from the stem bark of *Cedrelopsis grevei* obtained from Madagascar yielded seven compounds, a triterpenoid, β-amyrin (**15**), a coumarin, scoparone (**16**), a limonoid, cedmiline (**14**), a triterpenoid derivative, cedashnine (**17**), a quassinoid, cedphiline (**19**), a lignan, cedpetine (**18**) as well as sitosteryl β-D-glucopyranoside (**20**). Three of these were novel.

Foreword

Part I contains all the written text and part II contains all the spectra. Where a spectrum is referred to in the text, a spectrum reference page number for part II will be provided in bold print within square brackets. Example, " the ^{1}H NMR spectrum of cedashnine (**17**) **[31]**." The ^{1}H NMR spectrum for cedashnine (**17**) is therefore available on page 31 of part II.

TABLE OF CONTENTS

PAGE NO.

Part I

Chapter 1

Introduction to Limonoids

PAGE NO.

PAGE NO.

List of Figures

List of Tables

PAGE NO.

List of Schemes

1.1 Introduction of limonoids

Limonoids are tetranortriterpenoids with a tetracyclic triterpenoid structure with a β-substituted furanyl ring at C-17α. The loss of four carbon atoms from the side chain attached to C-17 in triterpenoids results in the formation of the furan ring, which is typical of limonoids. Limonoids acquired their name from limonin (**1**), which was the first compound of this class to be isolated in 1841 from the genus *Citrus* (Rutaceae),[1] and whose structure was determined in 1960.[2] The biosynthesis of limonoids is discussed in section 1.3.

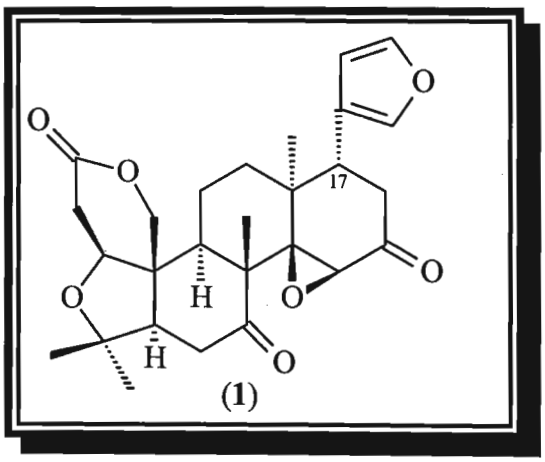

(**1**)

Fig. 1.1. Limonin (1) – First limonoid to be isolated[1]

Limonoids have been isolated from the Meliaceae, Ptaeroxylaceae, Cneoraceae, Rutaceae and Simaroubaceae families. The classification of these compounds into different classes is discussed in section 1.2.

Limonoids have been found to have a wide range of biological activities, including insect antifeedant and growth regulating properties[3], bacteriocidal, anti-viral[4] and anti-fungal activities,[3,4,5,6] anti-protozoal[7] and anti-sickling[8] properties. The biological activities of these compounds are discussed in greater detail in section 1.4.

1.2 Classification of limonoids

Taylor[9] classified the compounds from the Meliaceae into the protolimonoids and limonoids. This classification was modified by Mulholland[10] to include subsequently isolated compounds, and is given in Table 1.1. The sixteen classes of limonoids are classified according to which of the four rings of the triterpenoid nucleus has been oxidatively opened. This classification does not include the highly oxidised and rearranged limonoids from the Simaroubaceae (genus *Harrisonia*) and Ptaeroxylaceae (genus *Cedrelopsis*). Limonoids from groups I, II, IVa and IVc (Table 1.1) are discussed further since limonoids from these groups have been isolated and identified during the course of this work. The formation of the complex *Cedrelopsis* limonoids is discussed in chapter 5.

Table 1.1. Classification of protolimonoids and limonoids[10]

Class	Group	Example	Ring A	Ring B	Ring C	Ring D	Sidechain
I	Protolimonoids	2	Usually Intact	Intact	Intact	Intact	Intact
II	Havanensin	3	Intact	Intact	Intact	Intact	Furan
III	Gedunin	4	Intact	Intact	Intact	Lactone	Furan
IVa	Andirobin	5	Intact	Open	Intact	Lactone	Furan
IVb	Trijugin	6	Intact	Open	Contracted	Lactone	Furan
IVc	Mexicanolide	7	Intact	Open and recyclised	Intact	Lactone	Furan
IVd	Phragmalin	8	Intact	Open and recyclised with C-4, C-29, C-1-bridge	Intact	Lactone	Furan
IVe	Entilin	9	Modified	Cleavage of C-9, C-10-bond	Intact	Lactone	Furan
V	Methyl ivorensate	10	Open or Lactone	Open	Intact	Lactone	Furan
VI	Obacunol	11	Open or Lactone	Intact	Intact	Lactone	Furan
VII	Nimbin	12	Intact	Intact	Open	Intact	Furan
VIII	Toonafolin	13	Intact	Open or Lactone	Intact	Intact	Furan
IX	Evodulone	14	Open or Lactone	Intact	Intact	Intact	Furan
X	Prieurianin	15	Open or Lactone	Open	Intact	Intact	Furan
XIa	Carapa spirolactone	16	Contracted	Intact	Intact	Intact	Furan
XIb	Carapolide	17	Contracted	Cleavage of C-9, C-10-bond	Intact	Lactone	Furan

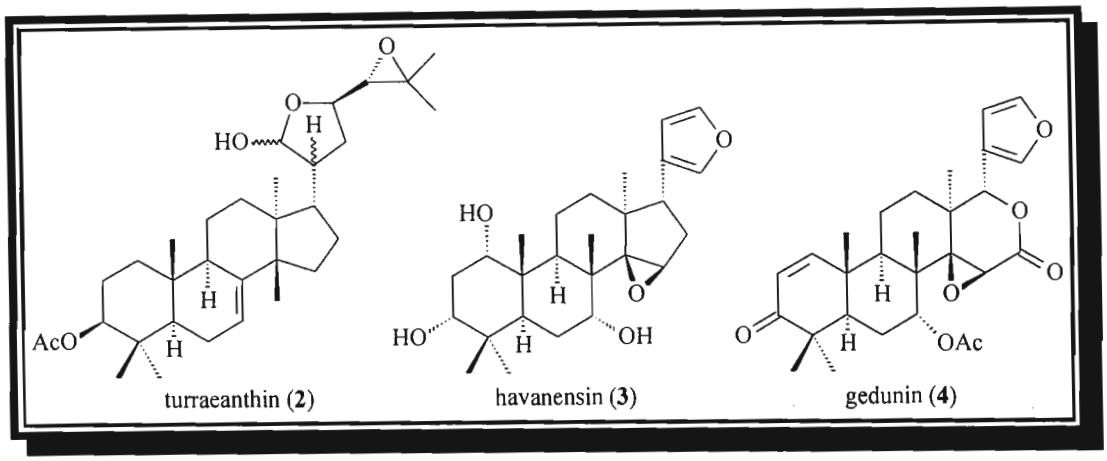

Fig. 1.2a. Examples of a protolimonoid (2), havanensin type (3) and gedunin type (4) limonoids

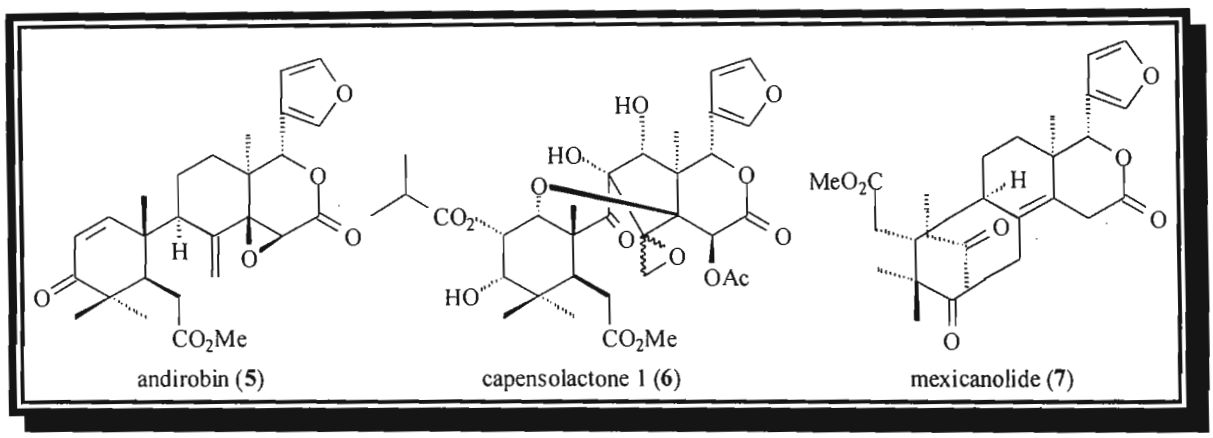

Fig. 1.2b. Examples of andirobin type (5), trijugin type (6) and mexicanolide type (7) limonoids

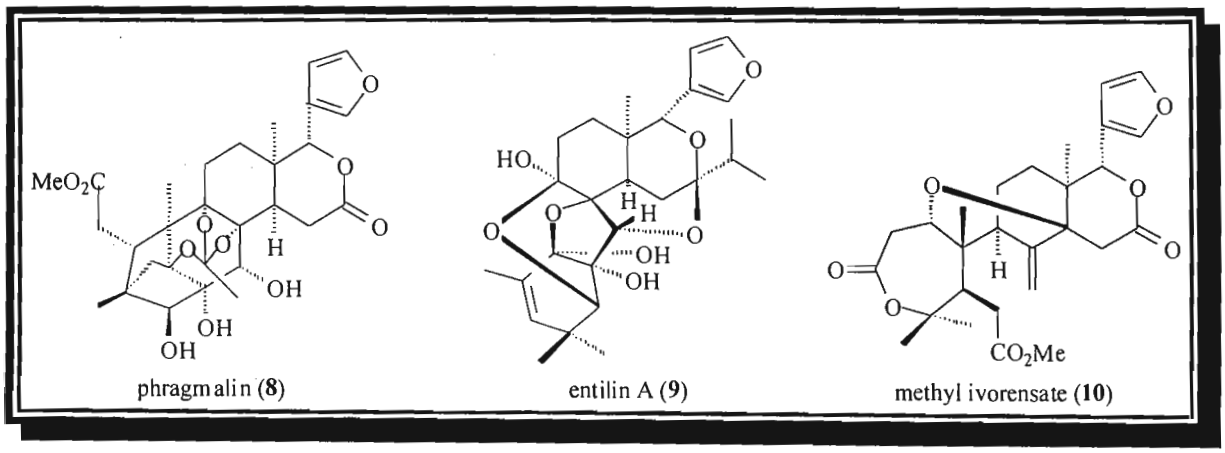

Fig. 1.2c. Examples of phragmalin type (8), entilin type (9) and methyl ivorensate type (10) limonoids

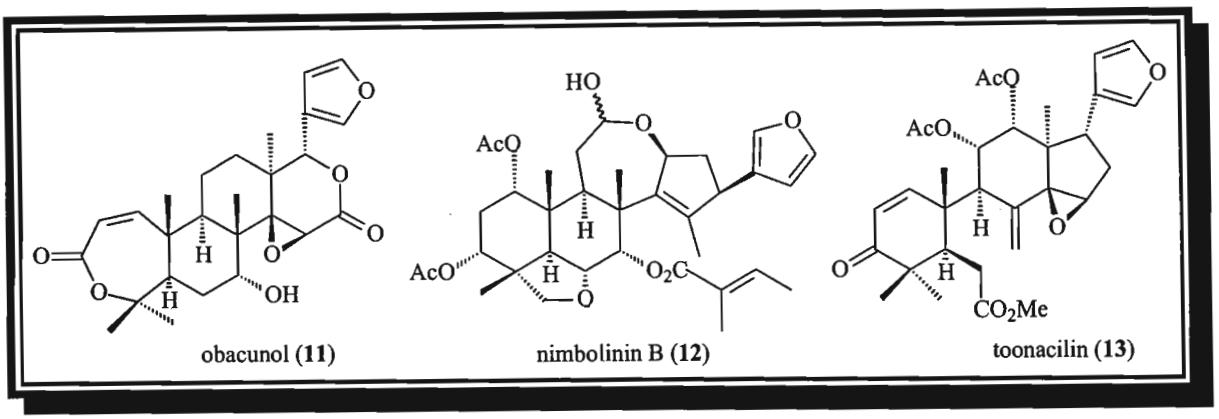

Fig. 1.2d. Examples of obacunol type (11), nimbin type (12) and toonafolin type (13) limonoids

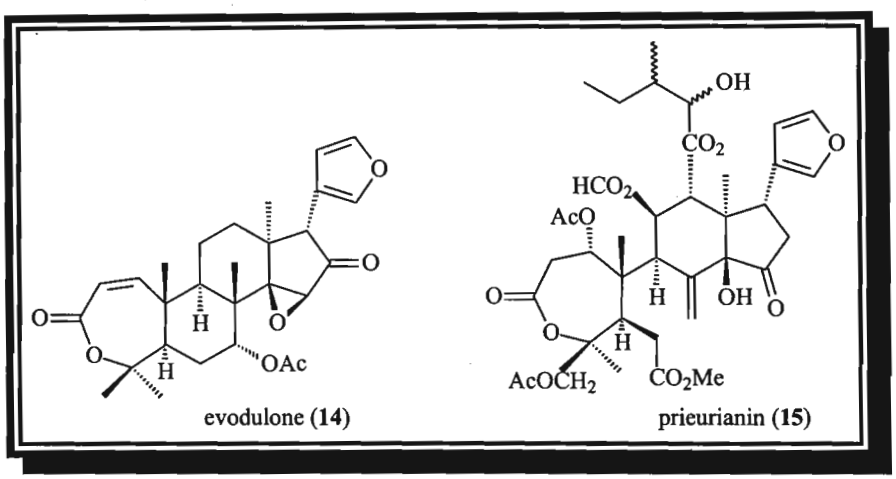

Fig. 1.2e. Examples of evodulone type (14) and prieurianin type (15) limonoids

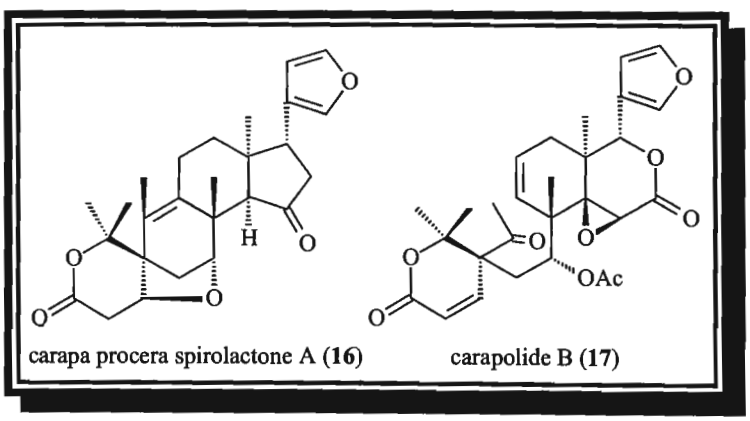

Fig. 1.2f. Examples of carapa spirolactone type (16) and carapolide type (17) limonoids

1.2.1 Group I : Protolimonoids

Protolimonoids are triterpenoid precursors of the limonoids in which the side chain is oxidised and often results in the formation of an ether ring. There are two classes of protolimonoids (Table 1.1). Class Ia compounds, for example sapelin B (**18**) and bourjotinolone A (**19**), have a β-methyl group at C-14 and a Δ^7-double bond. Class Ib compounds such as grandifoliolenone (**20**) have undergone the apo-euphol rearrangement to form a Δ^{14}-double bond with the β-methyl group at C-8, and an oxy function at C-7α.

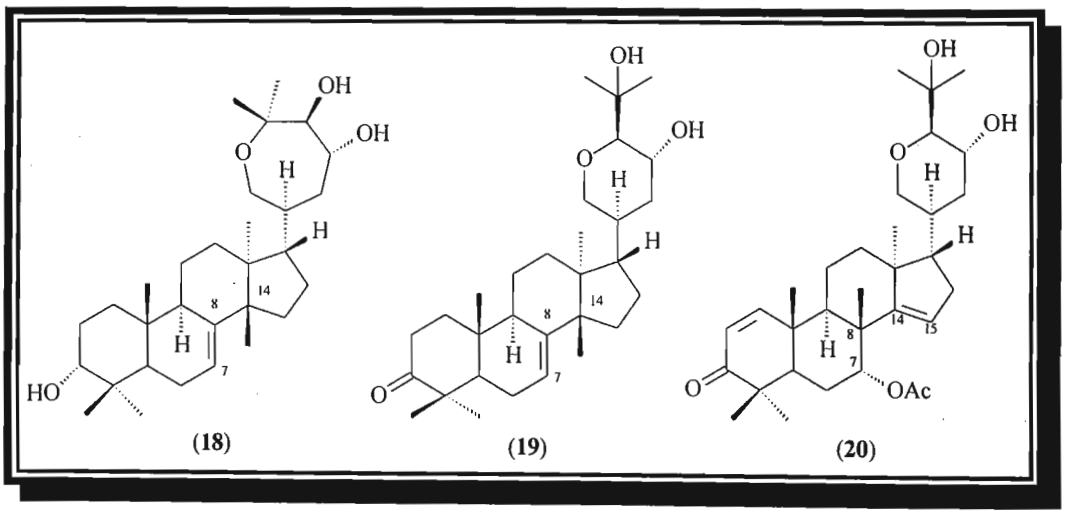

Fig. 1.3. Class Ia (18, 19) and Ib (20) protolimonoids

1.2.2 Group II : Havanensin limonoids

The four rings of the tetracyclic triterpenoid nucleus and the furan ring at C-17α remain intact. These limonoids range from simple ones such as deoxyhavanensin (**21**), azadirone (**22**) and azadiradione (**23**) to the more complex structures with further substituents on the rings, such as heudelottin C (**24**).

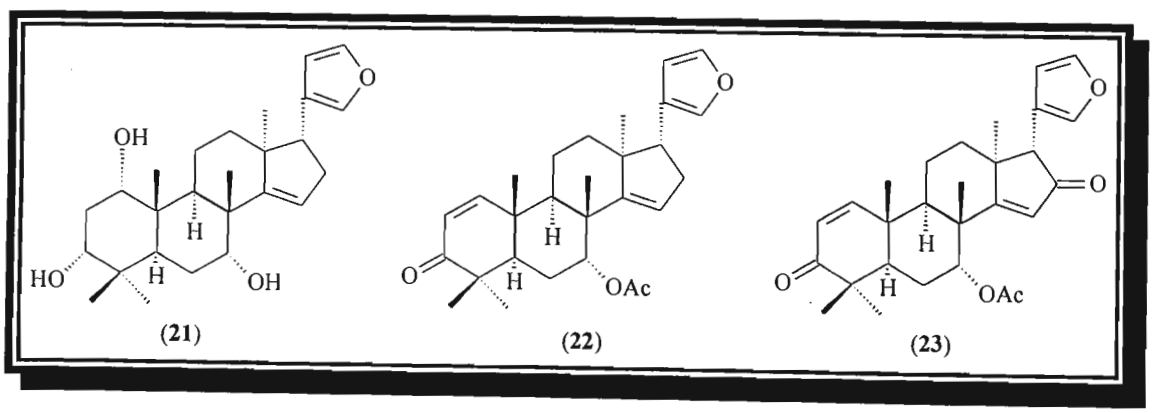

Fig. 1.4a. Simple havanensin type limonoids (21, 22, 23)

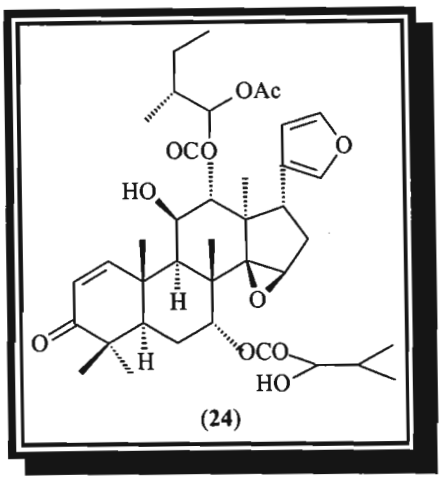

Fig. 1.4b. Complex havanensin type limonoid (24)

1.2.3 Group IVa : Andirobin limonoids

In andirobin type limonoids rings A and C remain intact while ring B is opened and ring D is lactonised. This is shown in compounds such as andirobin (**5**) and methyl angolensate (**25**).

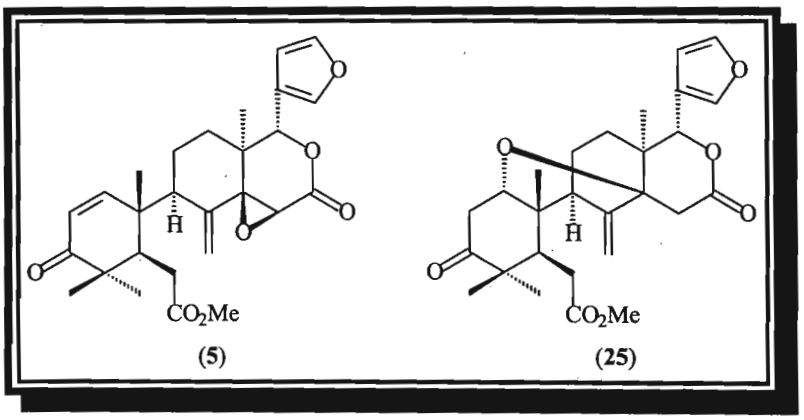

Fig. 1.5. Andirobin type limonoids (5, 25)

1.2.4 Group IVc : Mexicanolide limonoids

In this group of limonoids, rings A and C remain intact, ring B is opened and recyclised and ring D is lactonised. Examples of these types of compounds include mexicanolide itself (**7**) and swietenine (**26**).

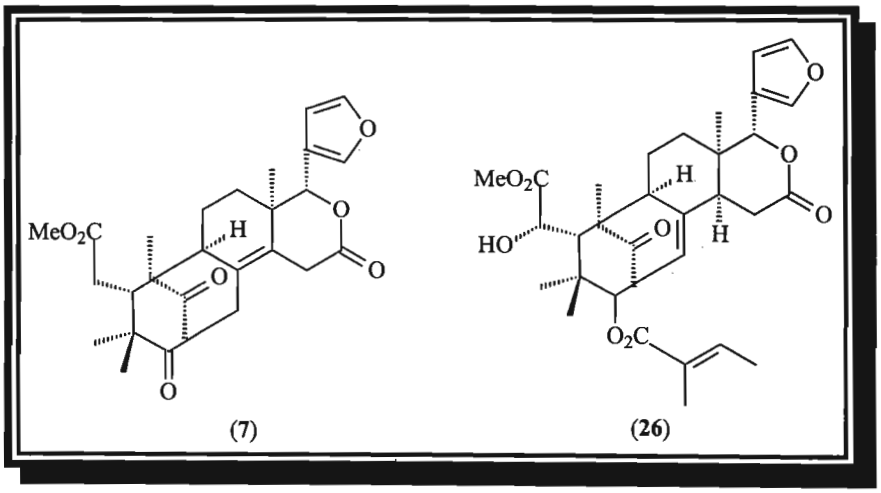

Fig. 1.6. Mexicanolide type limonoids (7, 26)

1.2.5 Biosynthetic routes of limonoid groups II, III, IVa and IVc

The inter-relationship between the limonoids from *Neobeguea mahafalensis* isolated in this work is given in scheme 1.1.

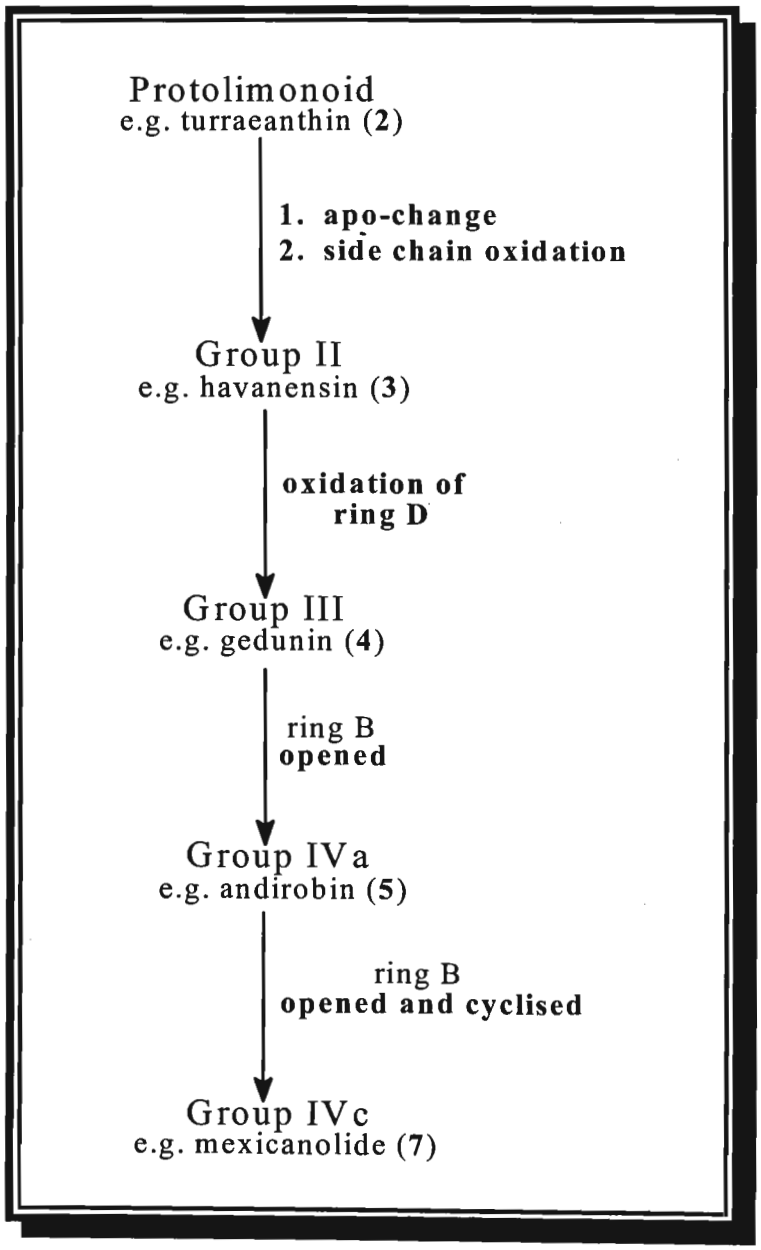

Scheme 1.1. Proposed routes in the biosynthesis of limonoids of class II, III, IVa and IVc

1.2.6 The relationship between limonoid groups II, III, IVa and IVc

Scheme 1.2 shows the relationship between the havanensin, gedunin, andirobin and mexicanolide limonoids from *Neobeguea mahafalensis* isolated in this work. The mexicanolide limonoid is the most complex type of limonoid of these classes as there have been changes to rings A, B and D of the havanensin type structure.

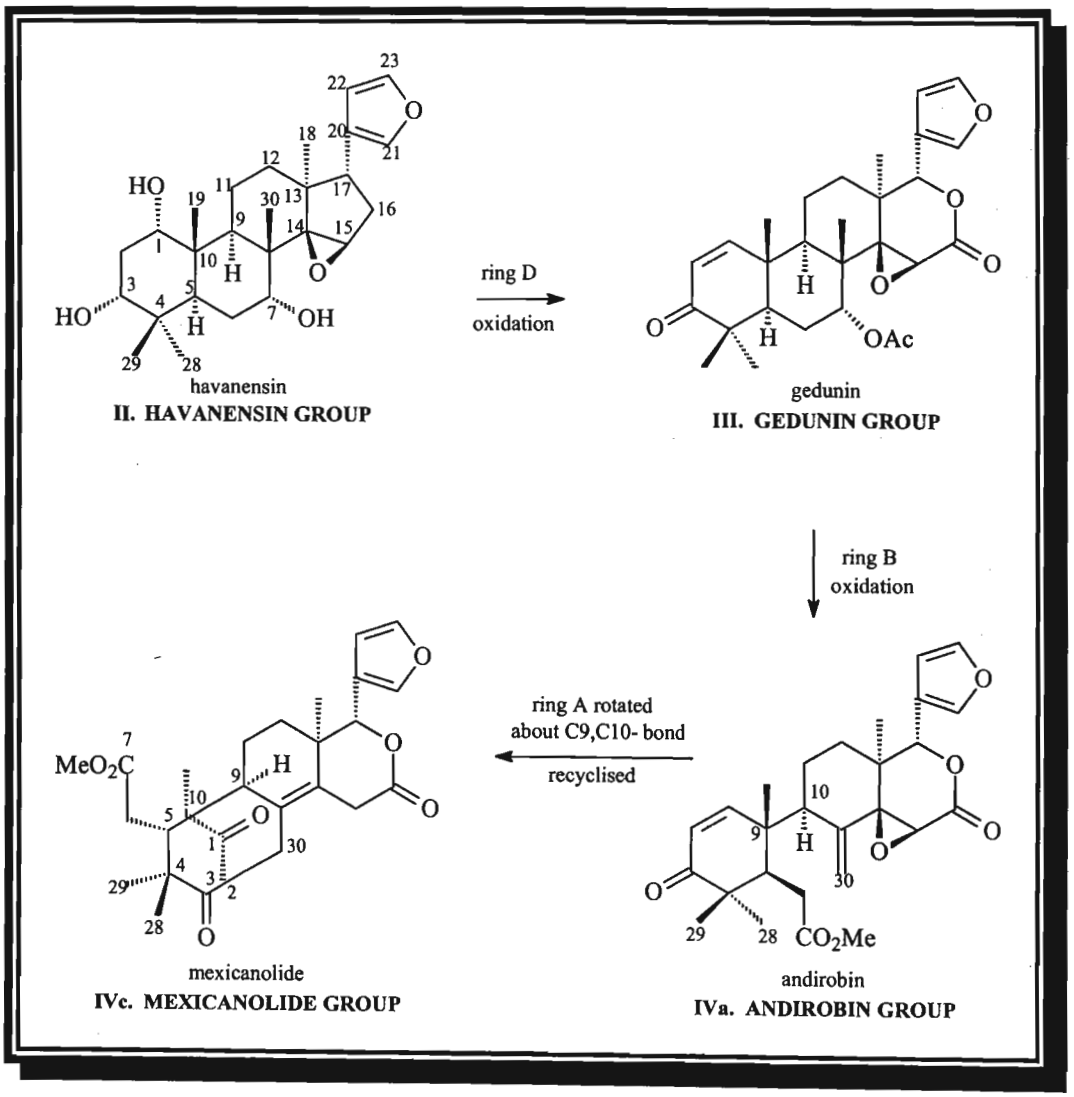

Scheme 1.2. The relationship between the limonoid groups II, III, IVa and IVc.[10]

1.3 Biosynthesis of limonoids

1.3.1 Formation of the apo-euphol structure

Barton *et al.*[2] proposed that limonoids are derived from compounds with the apo-euphol structure (**30**), and these compounds are derived from euphol (**27**) or tirucallol (**28**) or butyrospermol (**29**) (Scheme 1.3).

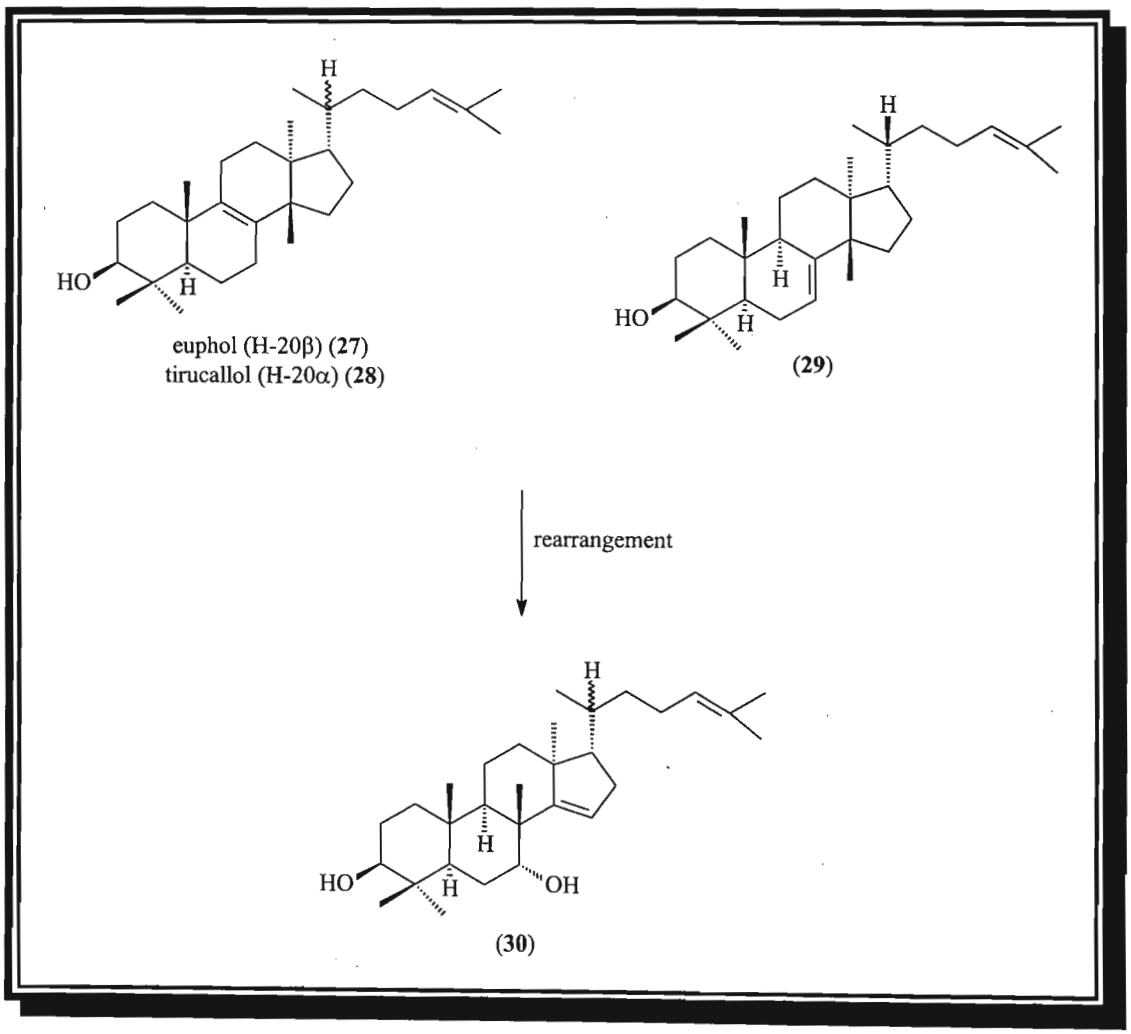

Scheme 1.3. Formation of the apo-euphol structure (30) from euphol (27), tirucallol (28) or butyrospermol (29).[2]

An alternative formation of the apo-euphol structure (**30**) is directly from squalene (**31**) *via* the dammarane ion (**32**) (scheme 1.4).[2]

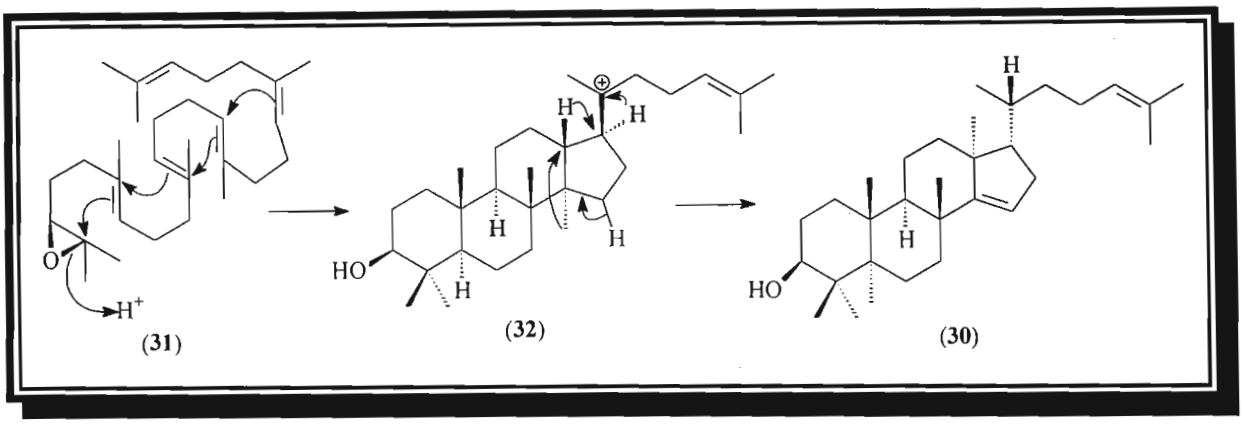

Scheme 1.4. Formation of the apo-euphol structure (30) *via* the dammarane ion (32).[2]

Two changes are necessary for the formation of limonoids, the apo-euphol rearrangement and the formation of the furan ring.

1.3.2 The apo-euphol rearrangement

This change has been accomplished by conversion of the 3β-acetate (**33**) to the apo-compound (**36**) in the laboratory.[11] Monoperphthalic acid oxidation of the Δ^7-double bond (**33**) furnishes the 7α, 8α-epoxide (**34**).[11] Treatment with boron trifluoride etherate leaves a cationic center at C-8, which results in the migration of the methyl group from C-14 to C-8 and the elimination of the proton at C-15 to give the apo-compound (**36**) (Scheme 1.5).

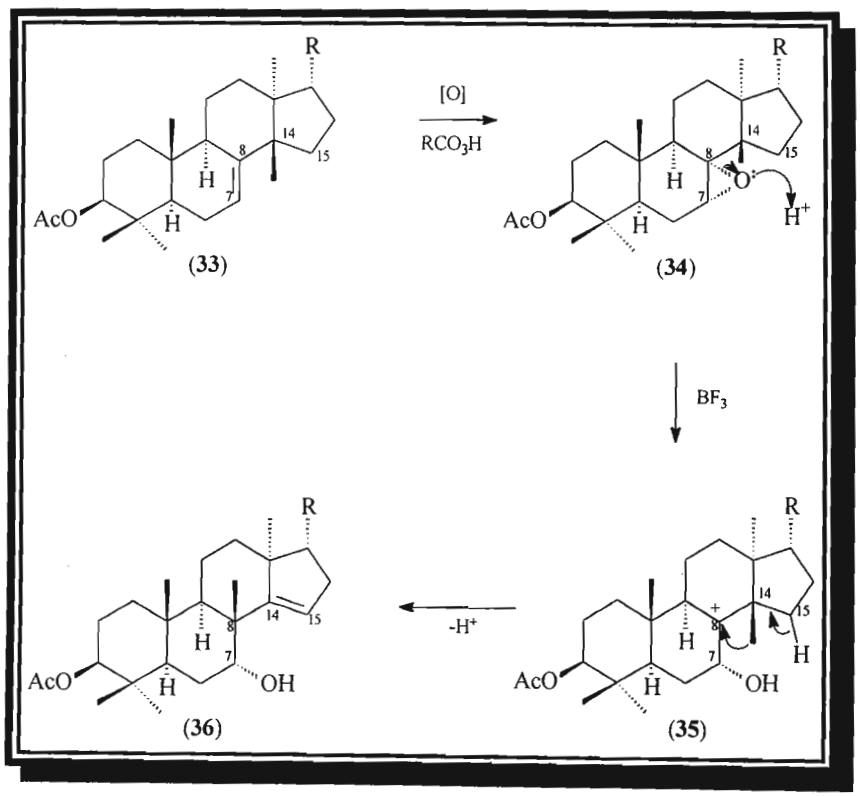

Scheme 1.5. The apo-euphol rearrangement.[11]

Glabretal (**37**) is an intermediate between the two protolimonoid groups. It has a β-methyl group at C-8, an acetate group at C-7α, and a 13, 14, 18-cyclopropane ring. The proposed formation of glabretal (**37**) is given in scheme 1.6.

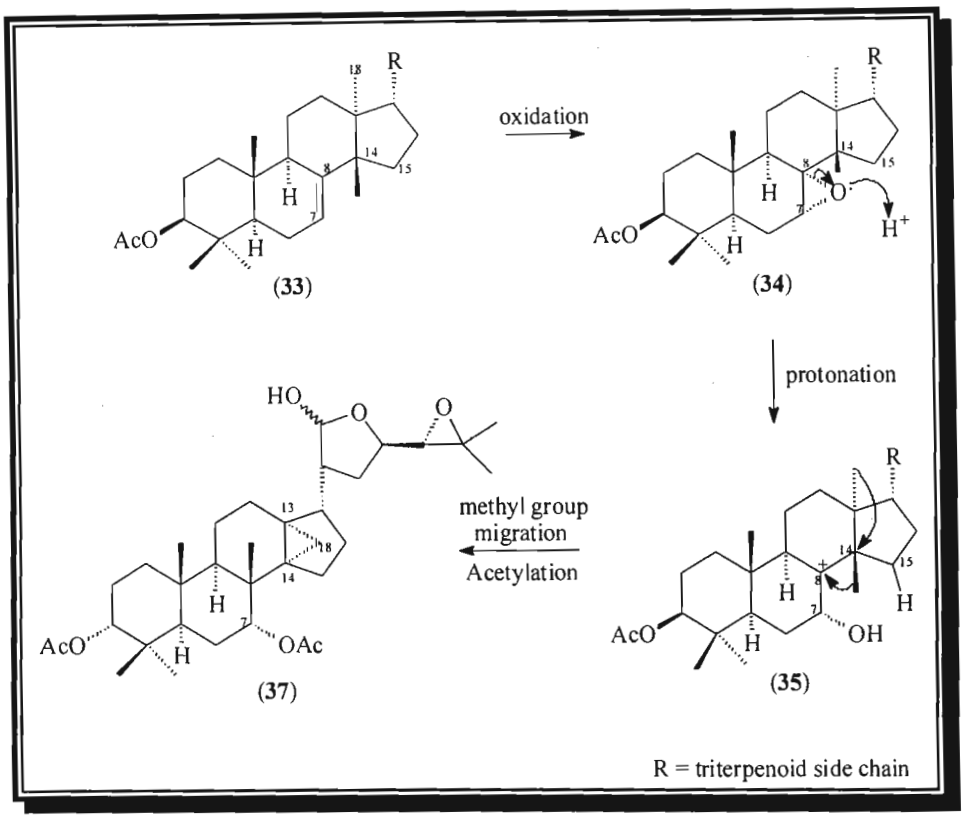

Scheme 1.6. Proposed formation of the glabretal intermediate (37)

1.3.3 Formation of the furan ring

The furan ring is formed by the oxidation and subsequent cleavage of the tirucallol side chain. Oxidation results in the formation of an aldehyde group at C-21, a hydroxy group at C-23 and a 24, 25-epoxide ring.[12] This side chain is then cyclised to form the turraeanthin (**2**) side chain (Scheme 1.7).

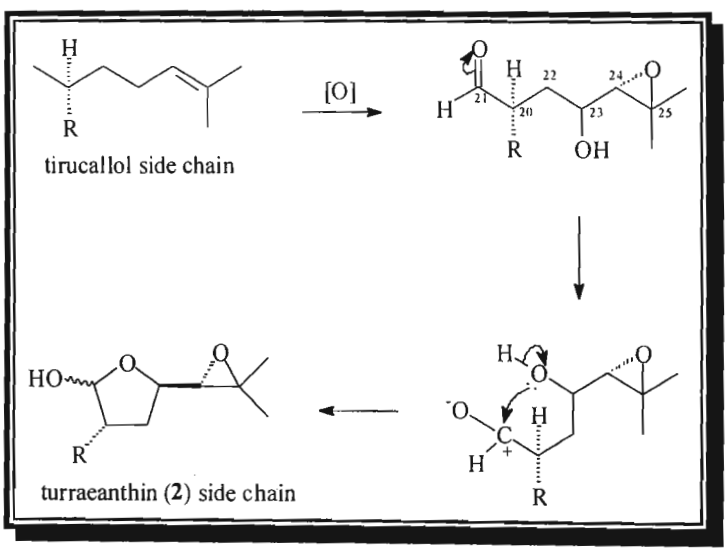

Scheme 1.7. Formation of the turraeanthin side chain[12]

Further oxidation of this side chain gives a C-24 keto group. A Baeyer-Villiger type oxidation of the C-23, C-24-bond, followed by oxidative cleavage of the C-23, C-24-bond produces the dihydrofuran ring as a result of the loss of four carbon atoms. Dehydration of this ring furnishes the β-substituted furanyl ring (Scheme 1.8).

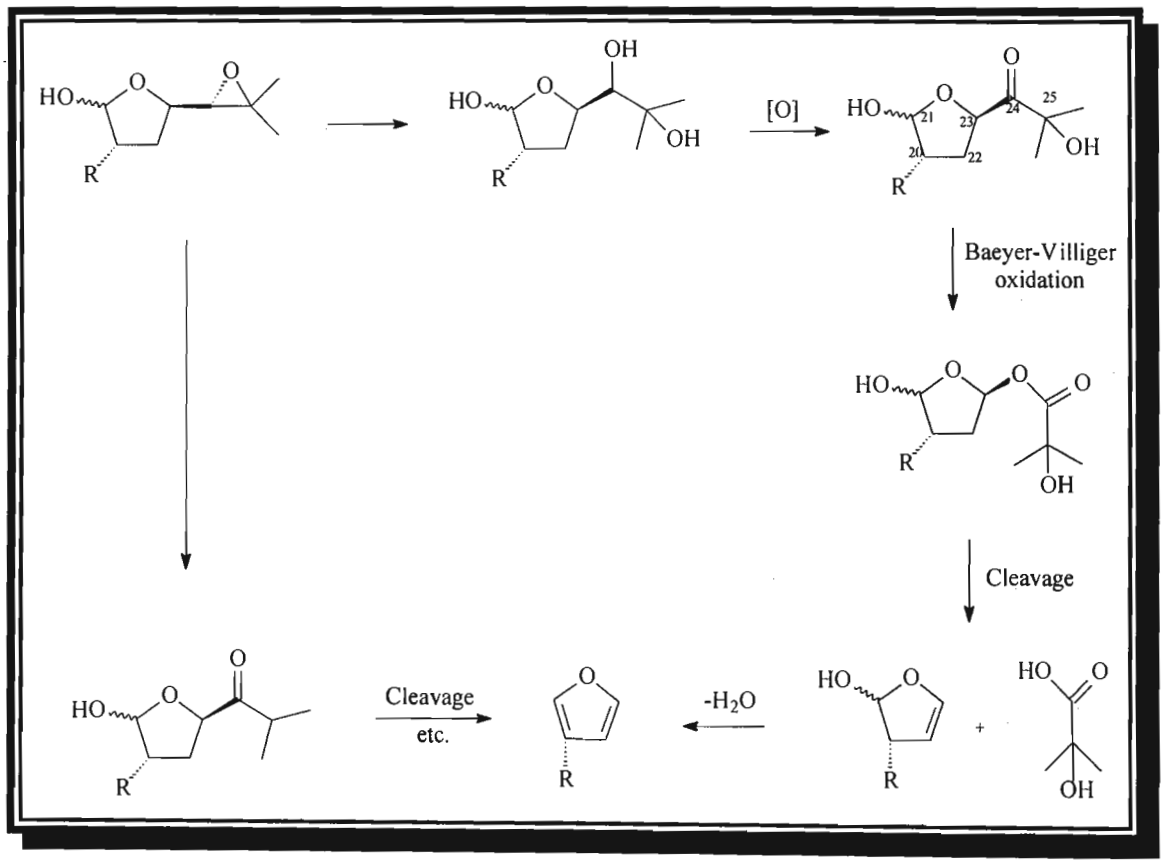

Scheme 1.8. Formation of the furan ring from the turraeanthin side chain[12]

Halsall[13] converted the turraeanthin (**2**) side chain into a furan ring in the laboratory (Scheme 1.9).

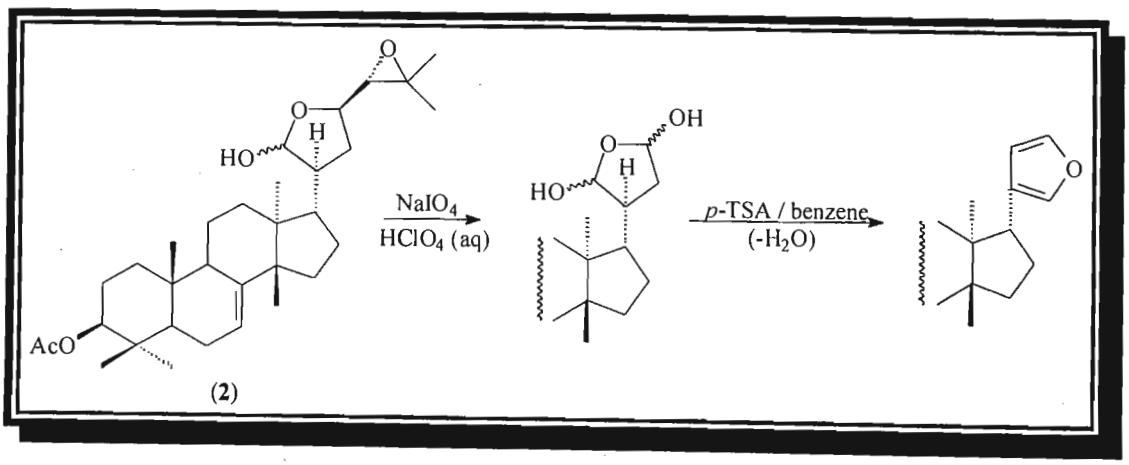

Scheme 1.9. Halsall's conversion of the turraeanthin (2) side chain into a furan ring[13]

The apo-euphol rearrangement (scheme 1.5) and the furan ring formation (schemes 1.7 and 1.8) result in the formation of group II limonoids, the simplest of the limonoid class of compounds. Azadirone (**22**) is an example of a simple group II limonoid.

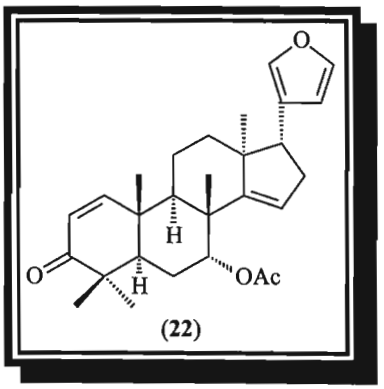

(22)

Fig. 1.7. Azadirone (22)

The Δ^{14}-double bond may be oxidised to an epoxide as in havanensin (**3**), (Scheme 1.10).

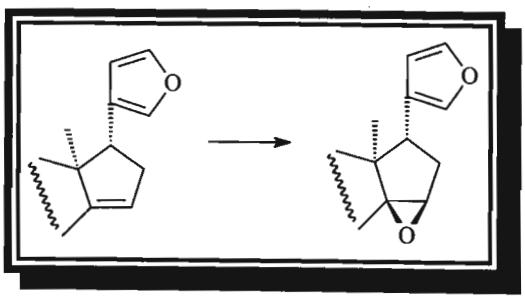

Scheme 1.10. Conversion of a cyclopentenyl ring D into a ring D epoxide[14]

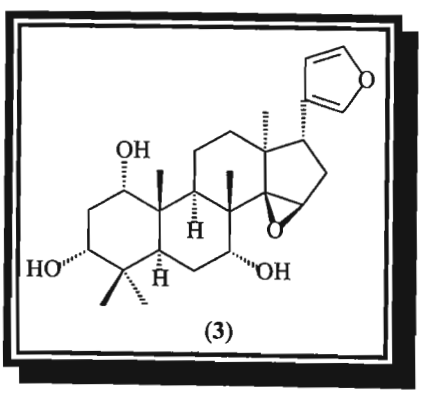

(3)

Fig. 1.8. Havanensin (3)

1.3.4 Biosynthesis of group IVa limonoids

In this group, rings B and D are oxidised to form lactones. Allylic oxidation of compounds such as 7-ketokhivorin (**38**) leads to the cyclopentenone ring formation which is followed by the 14, 15-epoxide formation. Baeyer-Villiger oxidation results in the formation of a ring D lactone. Baeyer-Villiger oxidation of ring B and subsequent ring opening and methylation leads to the $\Delta^{8(30)}$–double bond and the carbomethoxy group at C-7 (scheme 1.11). Connolly *et al.*[15] accomplished the interconversion of 7-deacetoxy-7-oxokhivorin (**39**) to andirobin (**5**) in the laboratory.

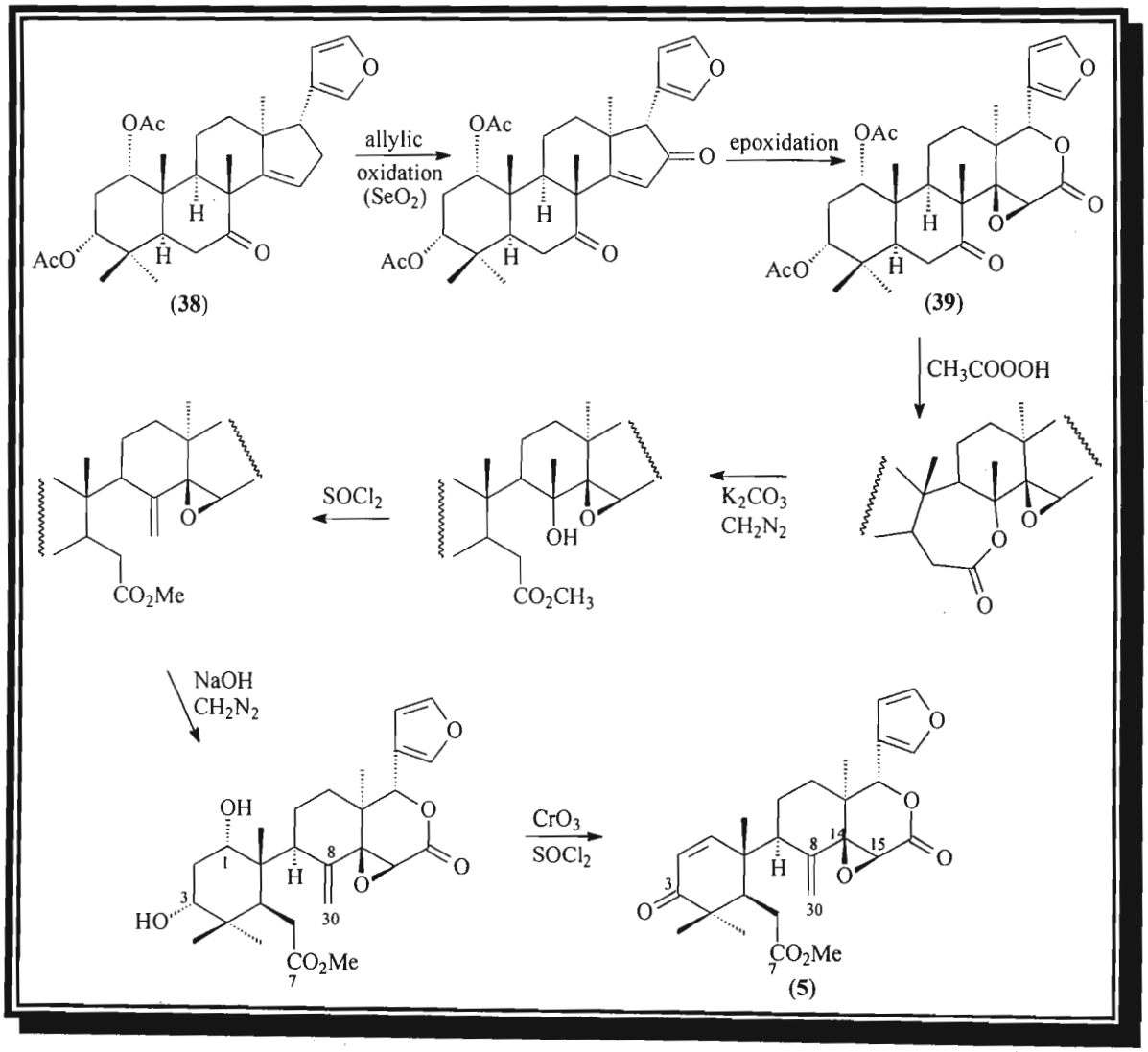

Scheme 1.11. Laboratory synthesis of andirobin (5)[15]

In the methyl angolensate type compounds, opening of the ring B is followed by the attack of the α-hydroxy group at C-1 on the diene at C-14 to form a 1, 14-ether bridge (scheme 1.12).

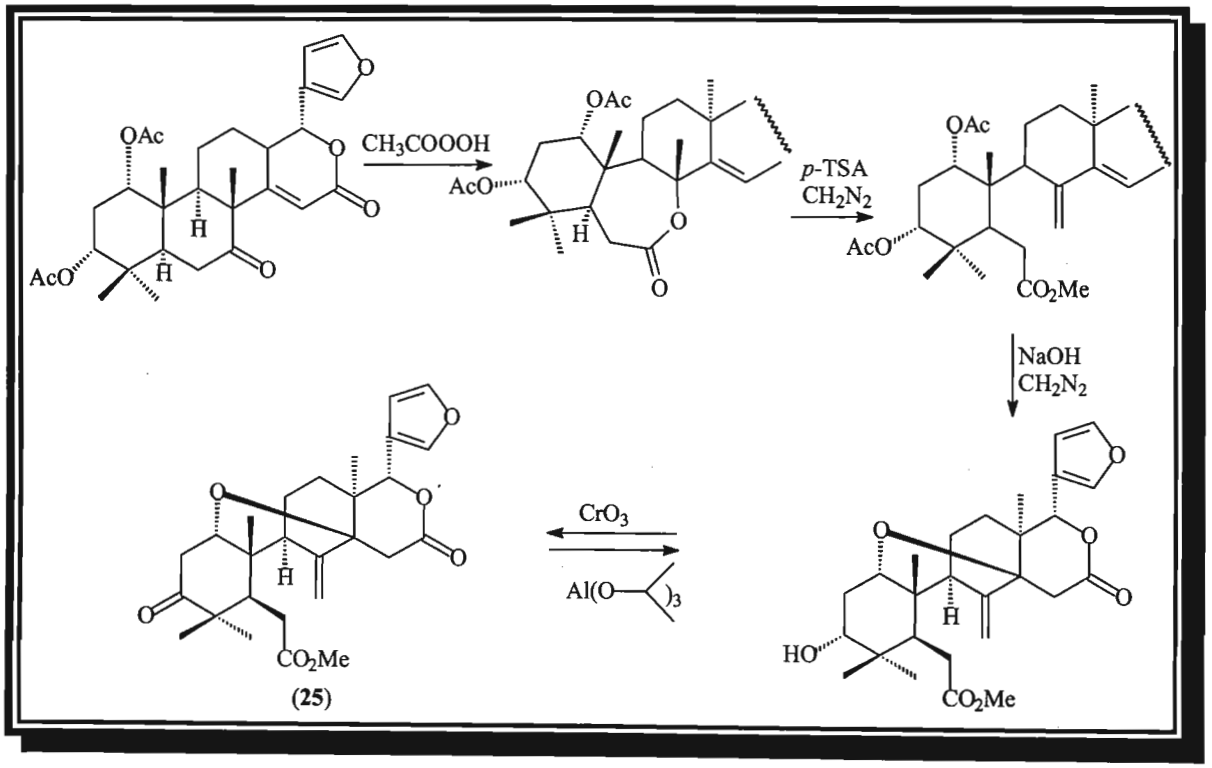

Scheme 1.12. Laboratory synthesis of methyl angolensate (25)[15]

1.3.5 Biosynthesis of group IVc limonoids

These compounds are formed by spontaneous Michael cyclisation from 1,3-diketodiene lactones of the andirobin type limonoids, and have been synthesised in the laboratory by Connolly *et al.*[16,17]

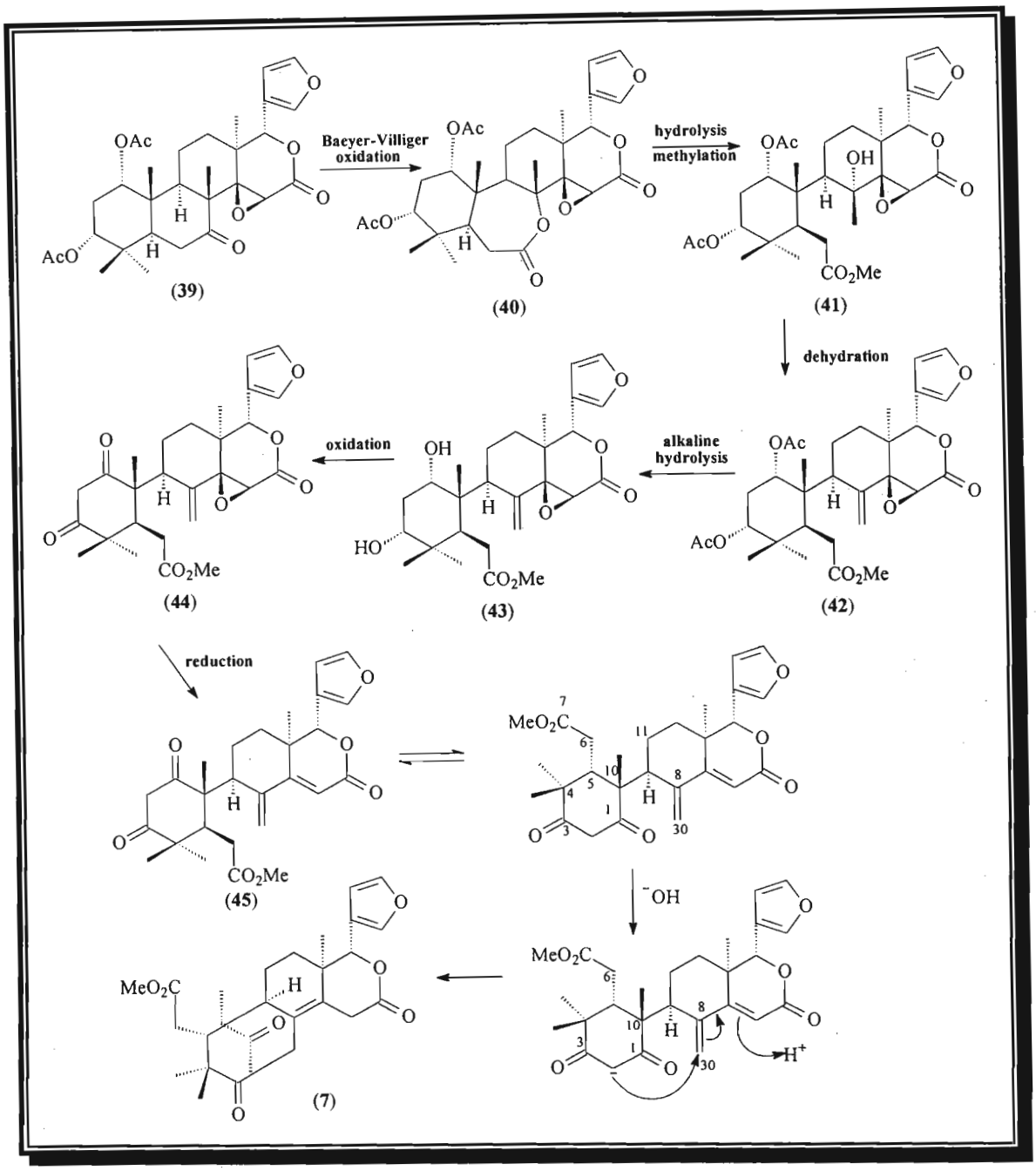

Scheme 1.13. Laboratory synthesis of group IVc limonoids[17]

Baeyer-Villiger oxidation of 7-deacetoxy-7-oxokhivorin (**39**) afforded the ε-lactone (**40**). Hydrolysis of the lactone (**40**) with potassium carbonate in aqueous methanol, and methylation with ethereal diazomethane converted the lactone into the ester (**41**). Dehydration of the ester (**41**) with thionyl chloride in pyridine resulted in the exomethylene compound (**42**). Alkaline hydrolysis of (**42**) resulted in the diol (**43**). Oxidation of the diol (**43**) afforded the β-diketone (**44**), which was reduced with chromium (II) chloride to remove the epoxide and afford the diene lactone (**45**). Cyclisation of (**45**) afforded mexicanolide (7).

1.4 Biological activity of limonoids

Great emphasis has been placed on limonoid research since limonoids have been found to have a range of biological activities. These include insect antifeedant[3,4,5,6] and growth regulating properties,[3] antimalarial, antifungal, bacteriocidal and antiviral activities,[4] anti-protozoal[7] and anti-sickling properties.[8] Research also shows anticarcinogenic activity in humans and animals.

South African traditional medicine uses species of the Meliaceae (for example *Trichilia dregeana*, *Turraea floribunda*, and *Ekebergia capensis*)[18] to treat backache, fever, stomach complaints, kidney complaints, rheumatism, and heart disease.

Several limonoids have been found to be active in the inhibition of a murine P-388 lymphocytic leukemia cell line.[19] The *Citrus* (Rutaceae) limonoids, such as limonin (**1**), nomilin (**46**), and obacunol (**11**) have been found to affect the enzyme glutathione S-transferase (GST), which is responsible for detoxifying carcinogens such as benzo[a]pyrene (BP) induced cancers. The conjugate that limonin forms is less reactive, less harmful and water-soluble which facilitates rapid excretion.[20] It seems that the furan moiety attached to the ring D in limonoids is the center for induction of GST.

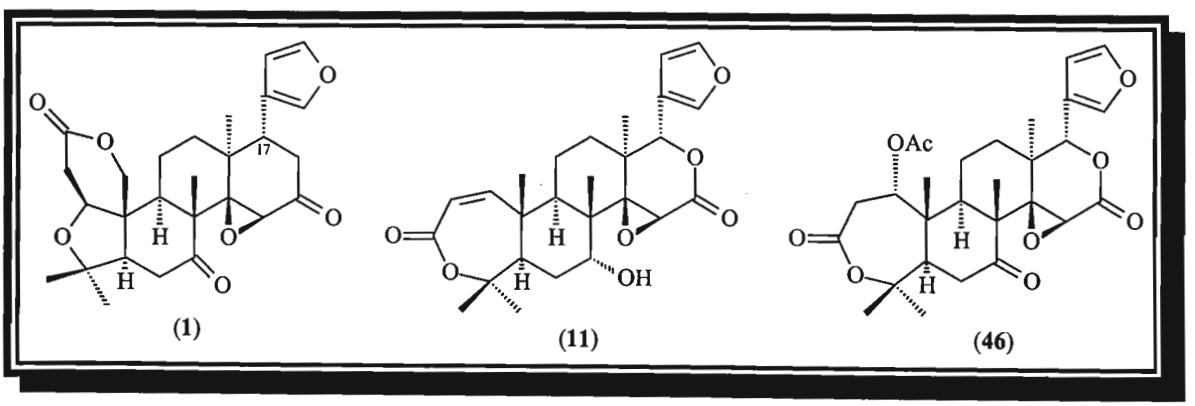

Fig. 1.9a. The *Citrus* limonoids (1, 11, 46)

The havanensin and the prieurianin type limonoids exhibit anti-cancer activity. Sendanin (**47**) is a havanensin type limonoid that is a most active agent. It is believed the 14,15-epoxy D ring and a 19, 29-lactol bridge are responsible for this anti-cancer activity.[9]

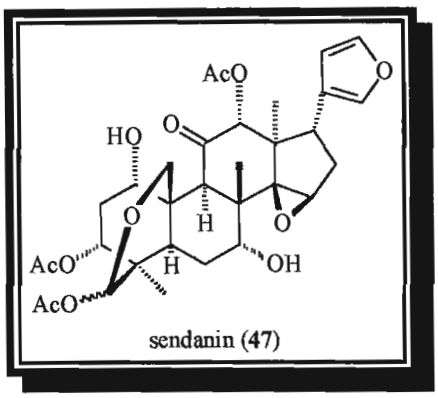

Fig. 1.9b. Sendanin (47)

Limonoids from *Swietenia* have been found to have platelet aggregation inhibiting properties.[21] The nimbin limonoids (ring-C oxidised) from *Melia volkensii* seeds from East Africa have insect anti-feedant properties. The triterpenoids showed cytotoxic selectivity against the human breast tumour line,[22] and the human solid tumour lines especially the colon tumour cell line.[23]

The limonoid volkensinin (**48**) is weakly active against six human tumour cell lines.[24] The synthetic derivative 23, 24-diketomelianin B is cytotoxic to human prostate and pancreatic cancer cell lines.[25]

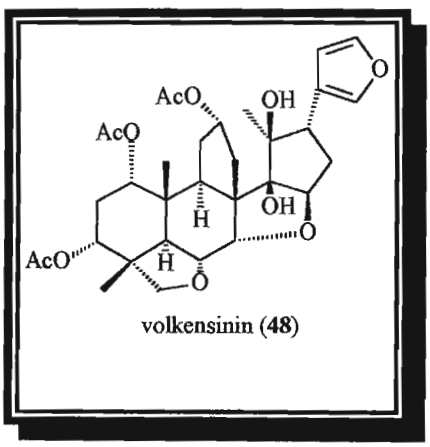

Fig. 1.9c. Volkensinin (48)

Melia volkensii
(http://www.jicakenya.org/SOFEM/treelist/Mvolkn.htm)

Limonoids are also used in the treatment of blood disorders, hepatitis, sleeplessness, boils, burns, cholera, gingivitis, malaria, measles, nausea, snakebite and syphilis.[26,27]

The plant *Azadirachta indica* shows such medicinal properties, and the active ingredient is the limonoid azadirachtin (**49**) which affects over 200 species of insects and mites.[28] Gedunin (**4**) has been found to exhibit anti-malarial activity, and methyl angolensate (**25**) exhibits anti-ulcer activity.[29,30]

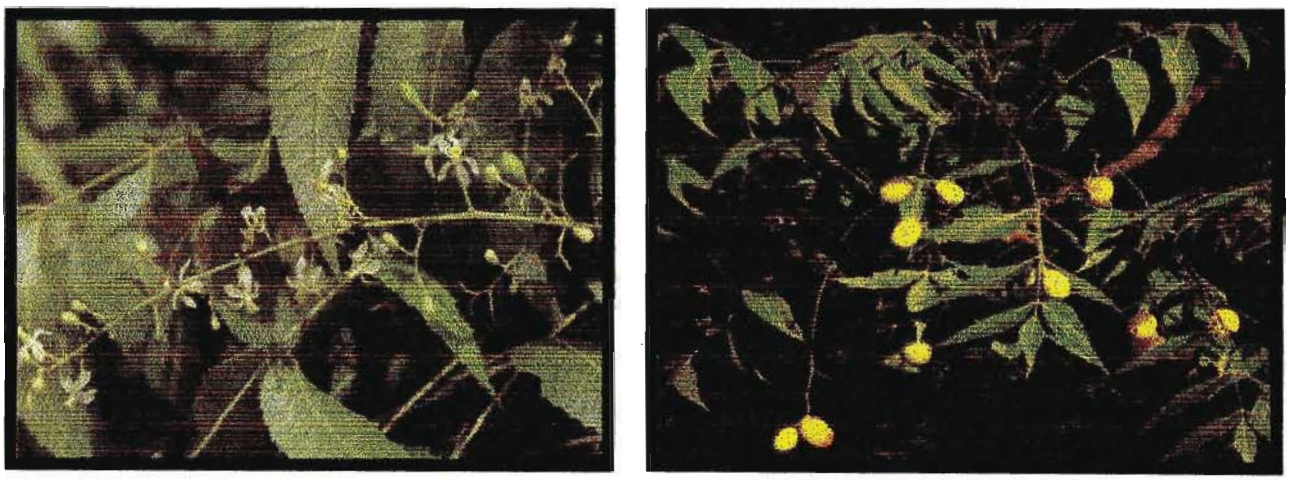

Azadirachta indica
(Photographs by GTZ and H. Schmutterer courtesy Ecoport)

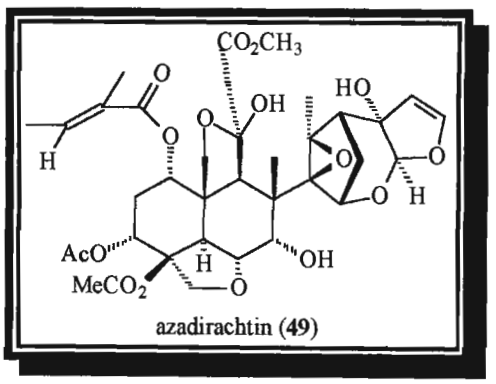

Fig. 1.9d. Azadirachtin (49)

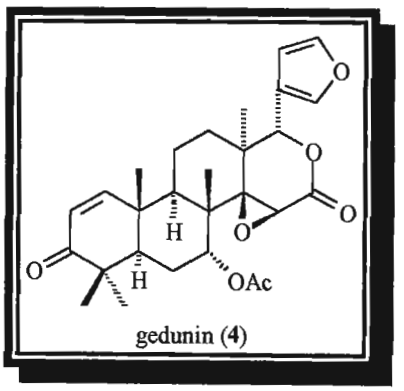

Fig. 1.9e. Gedunin (4)

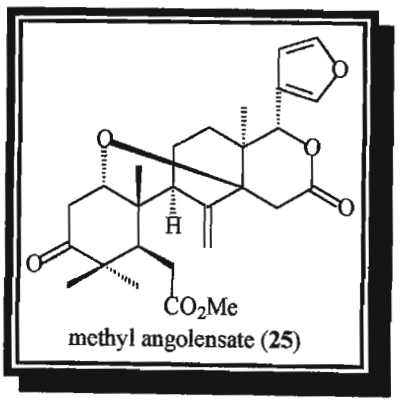

Fig. 1.9f. Methyl angolensate (25)

This research has been undertaken in the hope of isolating compounds that could be of both agricultural and medicinal significance.

1.5 References

1. Bernays, *Liebigs Ann.*, 1841, **40**, 317.
2. Arigoni, D., Barton, D.H.R., Corey, E.J. and Jeger, O., *Experientia*, 1960, **16**, 41.
3. Champagne, D.E., Koul, O., Isman, M.B., Scudder, G.G.E. and Towers, G.H.N., *Phytochemistry*, 1992, **31**, 377.
4. Huang, R.C., Okamura, H., Iwagawa, T., Tadera, K. and Nakatani, M., *Phytochemistry*, 1995, **38**, 593.
5. Kraus, W., Grimminger, W. and Sawitzki, G., *Angew. Chem. Int. Ed. Engl.*, 1978, **17**, 452.
6. Butterworth, J.H. and Morgan, E.D., *Chem. Commun.*, 1968, 23.
7. Khalid, S.A., Friedrichsen, G.M., Kharazami, A., Theander, T.G., Olsen, C.E. and Christensen, S.B., *Phytochemistry*, 1998, **49**, 1769.
8. Fall, A.B., Vanhaelen-Fastre, R. and Vanhaelen, M., *Planta Medica*, 1999, **65**, 209.
9. Taylor, D.A.H., *Progress in the Chemistry of Organic Natural Products*, 1984, **45**, 1.
10. Mulholland, D.A., Parel, B. and Coombes, P.H., *Current Org. Chem.*, 2000, **4**, 1011.
11. Buchanan, J.G.St.C. and Halsall, T.G., *Chem. Commun.*, 1969, 242.
12. Bevan, C.W.L., Ekong, D.E.U., Halsall, T.G. and Toft, P., *J. Chem. Soc.* (C), 1967, 820.
13. Buchanan, J.G.St.C. and Halsall, T.G., *J. Chem. Soc.* (C), 1970, 2280.
14. Mahomed, H.A., Ph.D Thesis, University of Natal, Durban, 1997, 14.
15. Connolly, J.D., Thornton, I.M.S. and Taylor, D.A.H., *J. Chem. Soc. Chem. Commun.*, 1970, 1205.
16. Connolly, J.D., Thornton, I.M.S. and Taylor, D.A.H., *J. Chem. Soc. Chem. Commun.*, 1971, 17.
17. Connolly, J.D., Thornton, I.M.S. and Taylor, D.A.H., *J. Chem. Soc. Perkin Trans. 1*, 1973, 2407.
18. Mulholland, D.A., *Chemistry, Biological and Pharmacological properties of African medicinal plants*, Proceedings of the first International IOCD-Symposium Victoria falls, Zimbabwe, edited by Hostettmann, K., Chinyanganya, F., Maillard, M. and Wolfender, J.-L., 1996, 199.
19. Pettit, G.R., Barton, D.H.R., Herald, C.L., Polonsky, J., Schmidt, J.M. and Connolly, J.D., *J. Nat. Prod.*, 1983, **46**, 379.
20. Lam, L.K.T., Li, Y. and Hasegawa, S., *J. Agric. Food Chem.*, 1989, **37**, 878.
21. Ekimoto, H., Irie, Y., Araki, Y., Han, G-Q., Kadota, S. and Kikuchi, T., *Planta Medica*, 1991, **57**, 56.
22. Zeng, L., Gu, Z., Fang, X., Fanwick, P.E., Chang, C., Smith, D.L. and McLaughlin, J.L., *Tetrahedron*, 1995, **51**, 2477.
23. Zeng, L., Gu, Z., Fanwick, P.E., Chang, C., Smith, D.L. and Mclaughlin, J.L., *Heterocycles*, 1995, **41**, 741.
24. Rogers, L.L., Zeng, L. and McLaughlin, J.L., *Tetrahedron Letters*, 1998, **39**, 4623.

25. Rogers, L., Zeng, L., Kozlowski, J.F., Shimada, H., Alali, F.Q., Johnson, H.A. and McLaughlin, J.L., *J. Nat. Prod.*, 1998, **61**, 64.
26. Mitra, C., *J. Indian Oilseeds*, 1957, **1**, 256.
27. Jacobson, M., *Focus on Phytochemical Pesticides*, 1988, **1**, 133.
28. Warthen, J.D.Jr., *Proc. Entomol. Soc. Wash.*, 1989, **91**, 367.
29. Khalid, S.A., Duddeck, H. and Gonzalez–Sierra, M., *J. Nat. Prod.*, 1989, **52**, 922.
30. Njar, V.C.O., Adesanwo, J.K. and Raji, Y., *Planta Medica*, 1995, **61**, 91.

Chapter 2

Introduction to Quassinoids

PAGE NO.

PAGE NO.

List of Figures

PAGE NO.

List of Schemes

2.1 Introduction of quassinoids

Quassinoids are bitter-tasting terpenoid compounds, and are found mainly in the Simaroubaceae family.

Quassinoids have a similar biosynthetic pathway to limonoids and are classified according to their basic C_{20}, C_{25}, C_{18} and C_{19} skeletons.[1] The classification of quassinoids is discussed in section 2.2.

The Simaroubaceae is a family free of limonoids, with one exception, the genus *Harrisonia*, which produces limonoids, not quassinoids.[2]

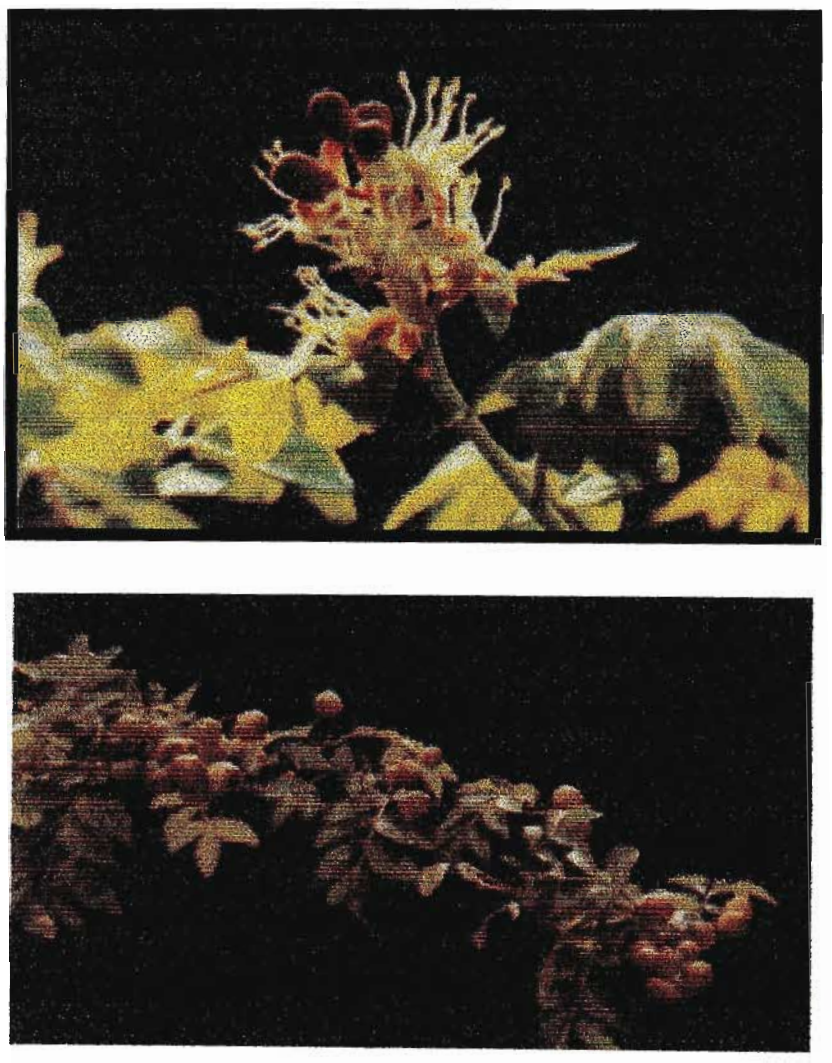

Harrisonia perforata
(http://www.ku.ac.th/AgrInfo/plant/plant2/p103.html)

The wood of *Quassia amara* L. and *Picraena excelsa* Lindt. were reported to have been used by the Aztecs as a diuretic, a laxative, and a digestive tonic. The West Indian natives carved cups out of this wood and added hot water to them and allowed this to stand for the bitter resin to be extracted into the water. This mixture was then taken to boost the appetite or help in digestion.[3]

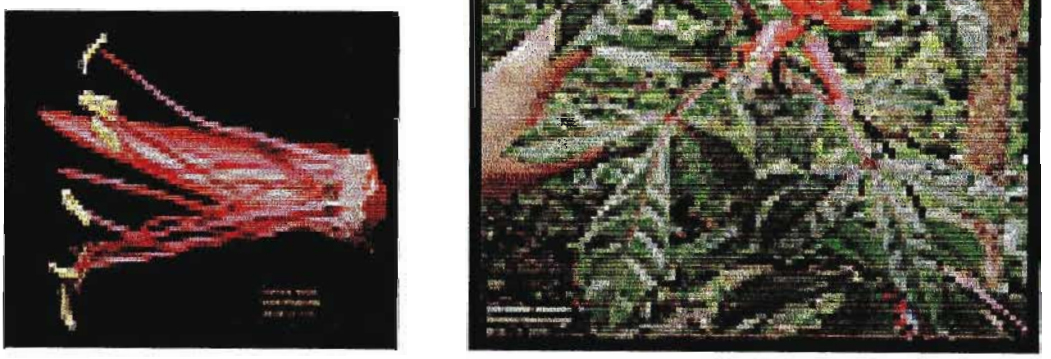

Quassia amara
(Photograph by Gerald D. Carr)

Picraena excelsa
(http://www.xs4all.nl/~margjos/nlkassi.htm)

There is a wide variety of biological activities of quassinoids which include herbal and homeopathic remedies for soothing the stomach, treatment of thrush and mouth fungal disorders, sinus, eczema,[4] anorexia nervosa, fever, blennorrhagia, malaria and liver disorders,[5] flavourants in foods, liquors and tonic wines.[3] They are also effective pesticides.[3,6]

These biological activities are further discussed in section 2.4.

2.2 Classification of quassinoids

The five basic skeletons (**A**→**E**) of the quassinoids[1] are shown in fig. 2.1. There are two different systems of numbering in use for quassinoids that have lost the C-17→C-23 part of the molecule (types **A**, **B** and **C**). The first, which will be used in this work, keeps the biogenetic numbering as shown in figure 2.1 (**A**→**C**). The second option which is used by Chemical Abstracts uses a different numbering system where the oxygen is numbered and the methyl group numbering changes as shown in figure 2.1.[7]

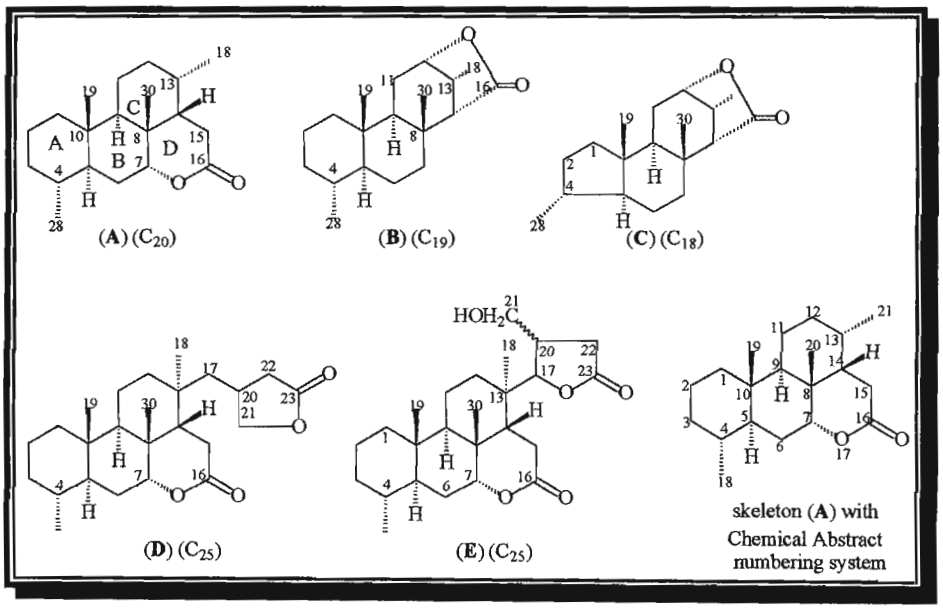

Fig. 2.1. Skeletal types (A), (B), (C), (D) and (E) of quassinoids[1, 7]

2.2.1 C_{20} quassinoids

The first compounds with the C_{20} quassinoid structure to be isolated were quassin (**1**) and neoquassin (**2**) in 1950 from the wood of *Quassia amara*.[8] Their structures, (**1**) and (**2**), were elucidated in 1962 by Valenta and co-workers.[9,10]

Quassia amara
(Photograph by Gerald D. Carr)

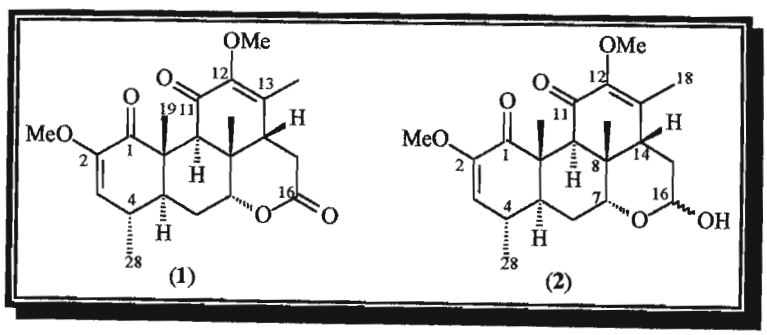

Fig. 2.2. Quassin (1) and neoquassin (2)

Quassin (**1**) has a δ-lactone, and neoquassin (**2**) has a corresponding hemiacetal.

In 1964 the C_{20} quassinoid structures of glaucarubin (**3**) and glaucarubol (**4**),[11,12] from the seeds of *Simarouba glauca* C.DC., were established.

Simarouba glauca
(Photograph by Dr. Edward F. Gilman)

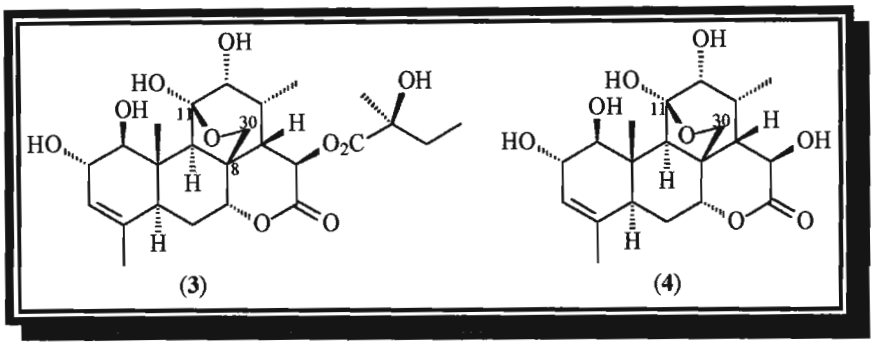

Fig. 2.3. Glaucarubin (3) and glaucarubol (4)

These quassinoids, (**3**) and (**4**), are different from quassinoids (**1**) and (**2**) in that the C-30 methyl group has been oxidised to a hydroxymethyl group, which has then formed a hemiketal linkage to a carbonyl group at C-11.

Polonsky[1] subclassified the C_{20} quassinoids on the basis of variations in the structure of ring A (fig. 2.4).

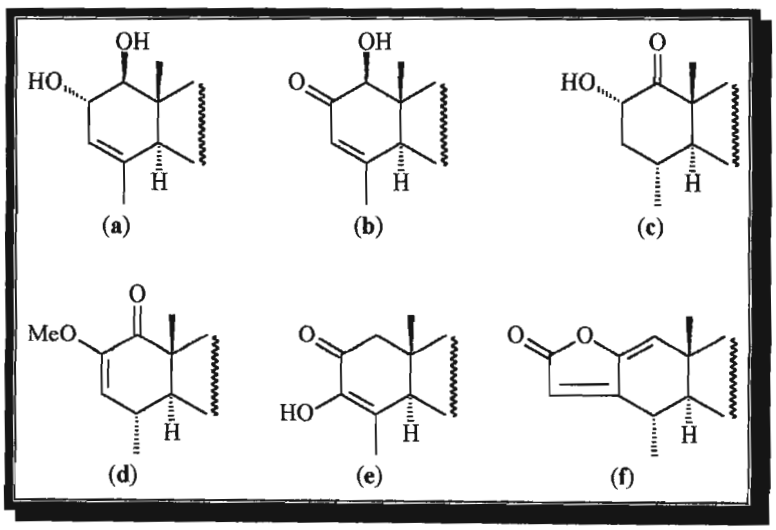

Fig. 2.4. Variations in ring A of the C_{20} quassinoid structure[1]

Polonsky[1] also noted that ring C may possess a methyl or hydroxymethyl group at position 30, and ring D may have a hydroxy group at C-15 which is generally esterified with small fatty acids.

Bruceanic acid A (**5**), isolated in 1975 from *Brucea antidysenterica* Mill,[13] was the first ring A-*seco* C_{20} quassinoid found.

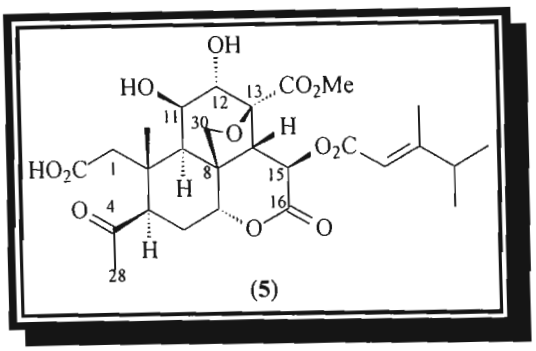

Fig. 2.5. Bruceanic acid A (5)

Shinjudilactone (**6**) isolated from *Ailanthus altissima* is a C_{20} quassinoid with rearrangement of ring C and a 12, 30-lactone linkage.[14,15]

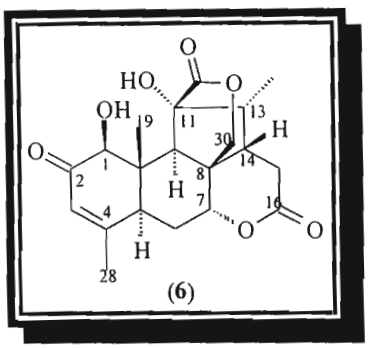

Fig. 2.6. Shinjudilactone (6)

Indaquassin B (**7**) from *Q. indica*[16] and cedronolactone D (**8**) from *Simaba cedron*[17] are C_{20} quassinoids, in which a lactone ring has formed including C-14 and C-12 rather than C-14 and C-7.

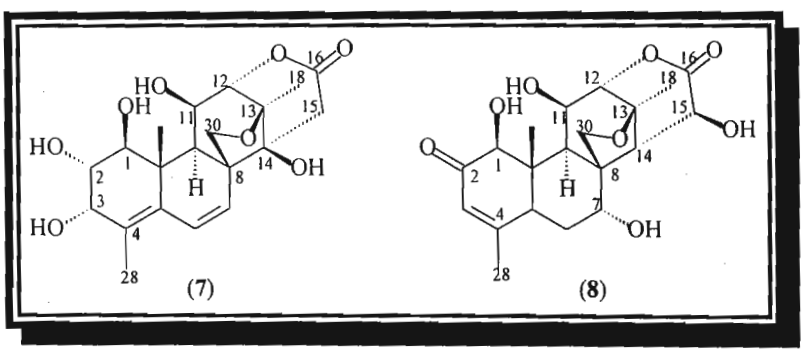

Fig. 2.7. Indaquassin B (7) and cedronolactone D (8)

Vilmorinine B (**9**) from *Ailanthus vilmoriana* Dode is a C_{20} quassinoid which has an unusual H-14α and has lost C-20.[18]

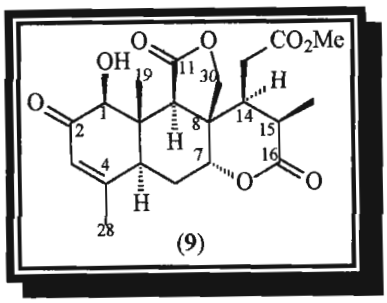

Fig. 2.8. Vilmorinine B (9)

2.2.2 C_{25} quassinoids

Simarolide (**10**) was isolated from the bark of *Simarouba amara* Aubl.[19] and is a C_{25} quassinoid similar to quassin (**1**), but has an additional five carbon atom sidechain containing a ketone at C-17 and a γ-lactone ring.

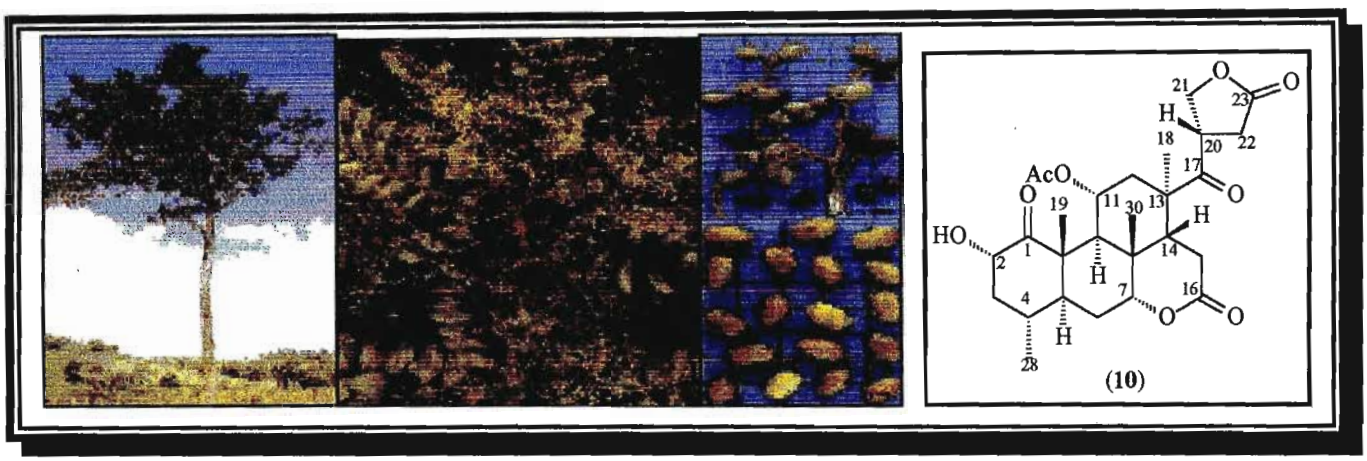

Simarouba amara
(Photograph by Harri Lorenzi www.plantarum.com.br)

Fig. 2.9. Simarolide (10)

C_{25} quassinoids type (**E**) (page 33) differ from C_{25} quassinoids type (**D**) by the mode of formation of the γ-lactone.[1] In type (**D**) the γ-lactone is formed between C-21 and C-23 and C-17 is not involved. In type (**E**) C_{25} quassinoids, C-17 is involved in the γ-lactone and C-21 is external to the ring.

In 1970 the second C_{25} quassinoid was isolated. This was picrasin A (**11**) isolated from the wood of *Picrasma quassiodes* Bennet.[20] The same compound was isolated from *P. ailanthoides* Planchon[21] and was then named nigakilactone G.

Picrasma ailanthoides
(NC State University Images by Erv Evans)

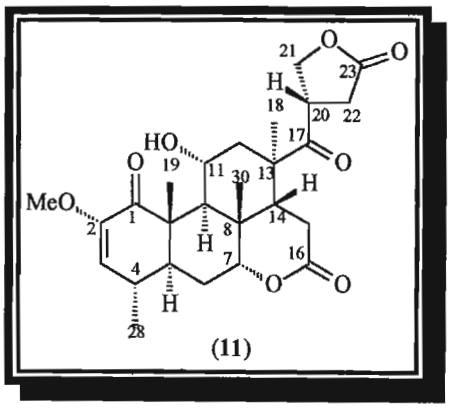

Fig. 2.10. Picrasin A (11)

Bruceantinoside A (**12**) was the first quassinoid glycoside to be fully described.[22,23]

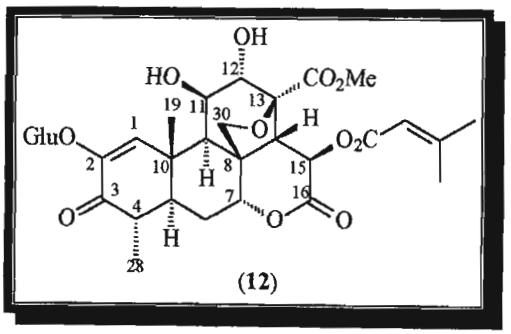

Fig. 2.11. Bruceantinoside A (12)

Odyendane (**13**) and odyendene (**14**), isolated from the stem bark of *Odyendea gabonensis* Engler,[24] were the first type (**E**) C_{25} quassinoids with the *S* configuration at C-17 to be reported.

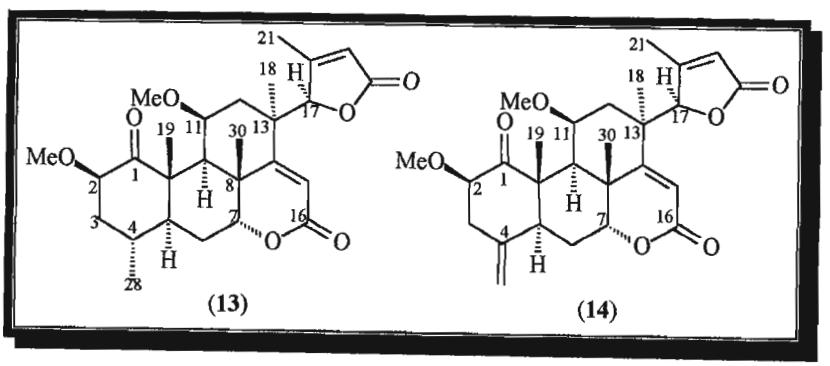

Fig. 2.12. Odyendane (13) and odyendene (14)

2.2.3 C_{19} quassinoids

The first quassinoids with a C_{19} skeleton to be isolated, were samaderine C (**15**) and samaderine B (**16**) from *Samadera indica* Gaert.[25]

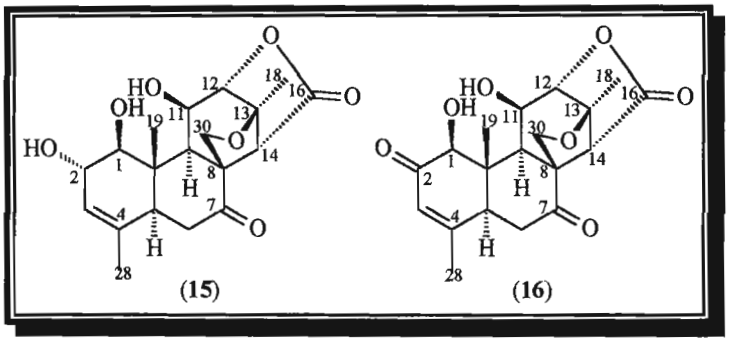

Fig. 2.13. Samaderine C (15) and samaderine B (16)

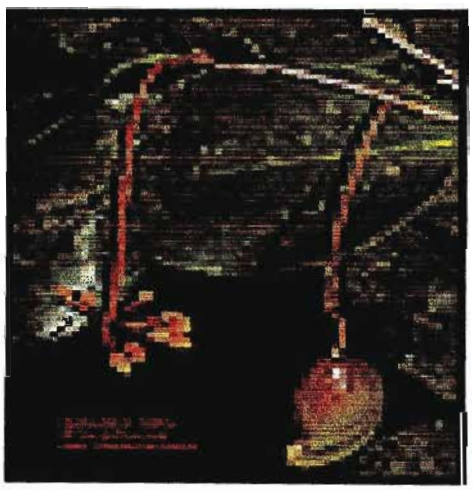

Samadera indica
(Photograph by Lani Stemmermann)

The C_{19} quassinoids such as (**15**) and (**16**) have an ether linkage between the hydroxymethyl group at C-8 and C-13 rather than C-11, and the 7, 14-δ-lactone has been replaced by a γ-lactone including C-14 and C-12.

Shinjulactone B (**17**) isolated from *Ailanthus altissima* Swingle,[26] represents a further type of C_{19} quassinoids.

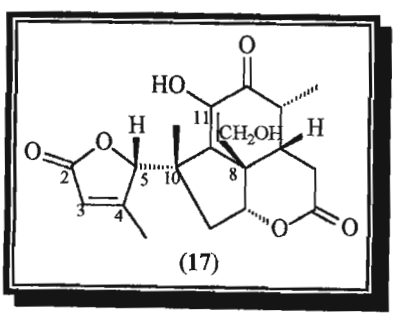

Fig. 2.14. Shinjulactone B (17)

2.2.4 C_{18} quassinoids

The C_{18} quassinoids type (**C**) differ from C_{19} quassinoids type (**B**) by the loss of one carbon atom from ring A[1] (fig. 2.1). Samaderine A (**18**) isolated from *Samadera indica*[27,28] and laurycolactone A (**19**) and B (**20**) isolated from *Eurycoma longifolia* Jack[29] (Vietnamese Simaroubaceae) are examples of the C_{18} quassinoids.

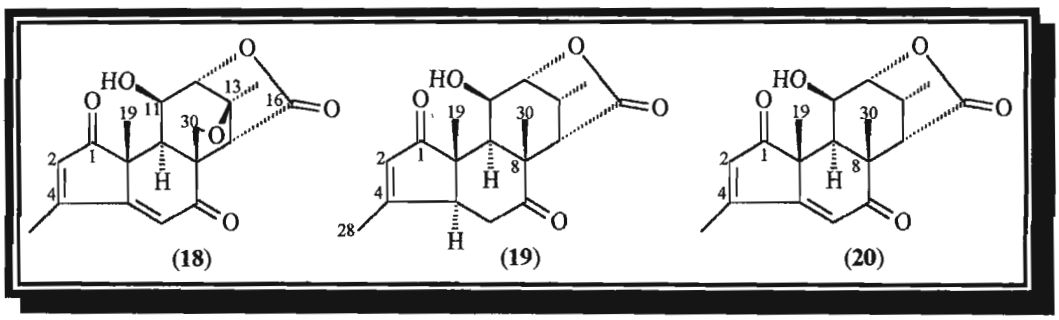

Fig. 2.15. Samaderine A (18), laurycolactone A (19) and B (20)

Eurycoma longifolia
(http://www.pasakbumi.com/trees.htm)

2.3 Biosynthesis of quassinoids

By 1964 it became apparent,[12,30,31] that quassinoids followed the same biosynthetic pathway as limonoids but were formed at a later stage. The biosynthesis of limonoids is described in chapter 1. The formation of quassinoids from apo-euphol (**21**) or from apo-tirucallol (**21**) is as follows[31] : one methyl group at C-4 and four carbon atoms at the end of the side chain are removed and C-20 to C-23 are converted to a γ-lactone ring. Ring D is oxidatively expanded and opened, and the C-16 carboxylic acid group forms a lactone ring with the 7α-hydroxy group. Oxidation of the C-17 hydroxy group then results in the basic C_{25} skeletons of simarolide (**10**) and picrasin A (**11**) (scheme 2.1).

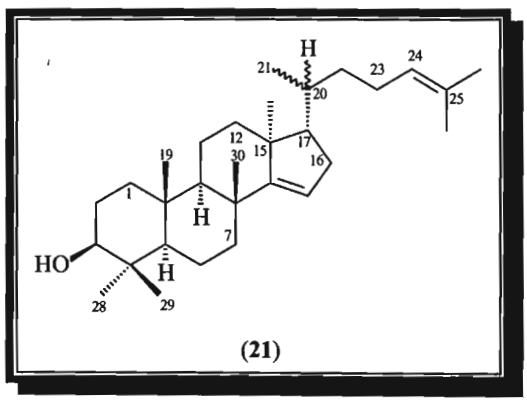

Fig. 2.16. Apo-euphol / apo tirucallol (21)

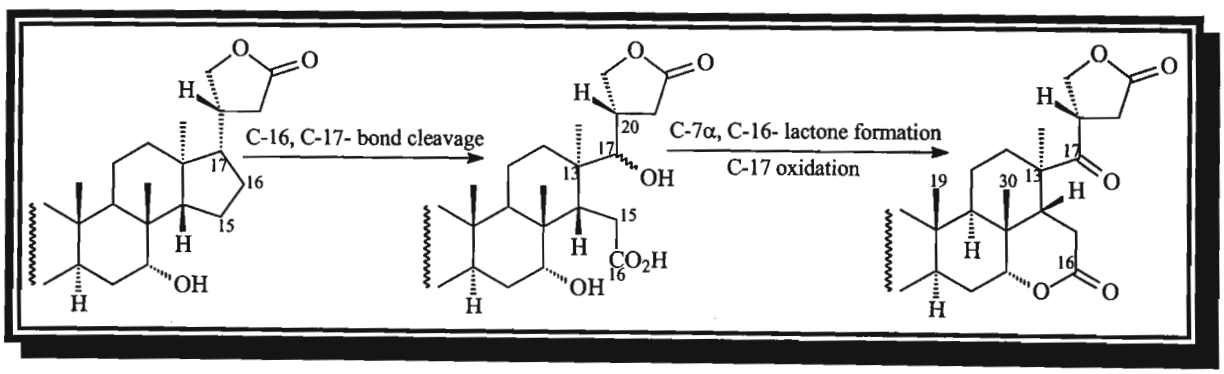

Scheme 2.1. Formation of simarolide (10)[12,30,31]

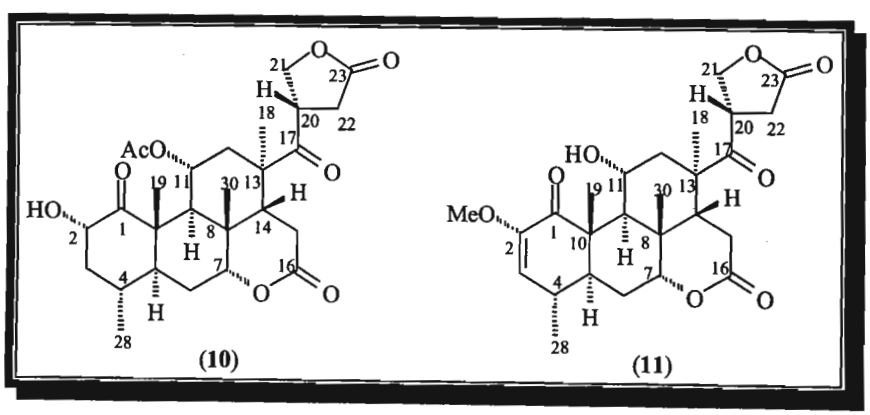

Fig. 2.17. Simarolide (10) and picrasin A (11)

The C_{25} quassinoids are considered to be intermediates in the biosynthesis of the other groups, C_{20} and C_{19}, in which the C-13, C-17-bond is cleaved if the 12, 17-dione is present or by a retro-aldol reaction of the 12-on-17-ol (scheme 2.2).[32] The loss of C-1 is also required to form C_{19} quassinoids (scheme 2.3).

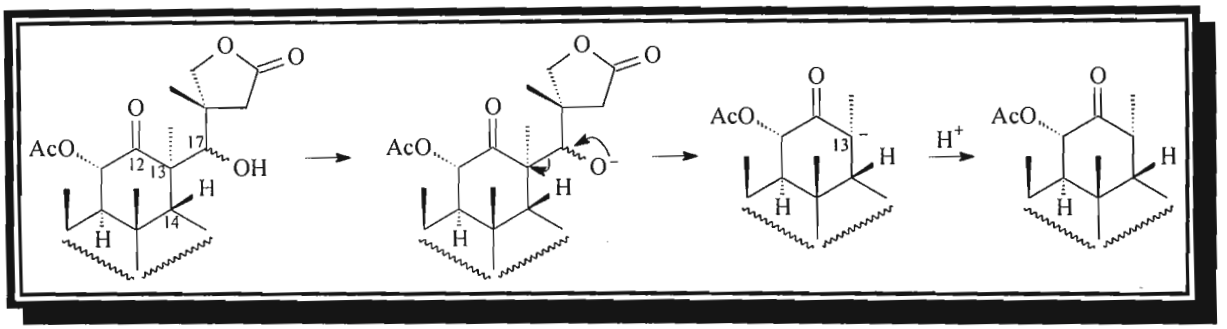

Scheme 2.2. Biosynthesis of C_{20} quassinoids by a retro-aldol reaction of the 12-on-17-ol[32]

The unusual *R* configuration at C-5 in compounds such as shinjulactone B (**17**) arises from C-1, C-2-bond cleavage of the 1, 2-diketo precursor, followed by nucleophilic attack at C-5, decarboxylation and ring B contraction (scheme 2.3).[26]

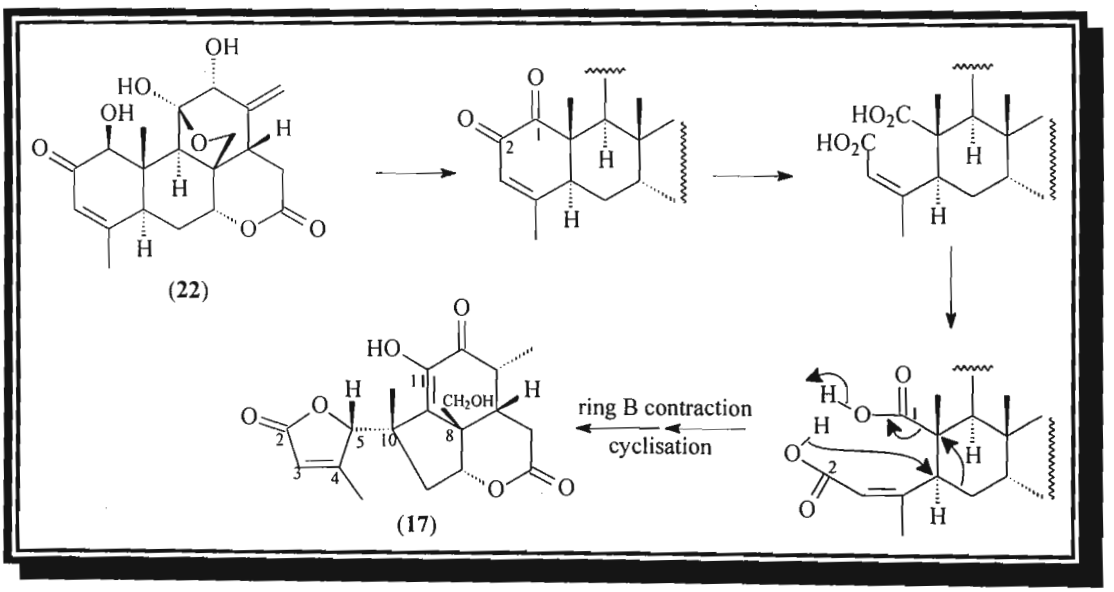

Scheme 2.3. Formation of the *R* configuration of a C_{19} quassinoid shinjulactone B (17)[26]

Ailanthone (**22**) may be converted into the C_{20} quassinoid shinjudilactone (**6**) by treatment with $NaHCO_3$ (scheme 2.4).[15]

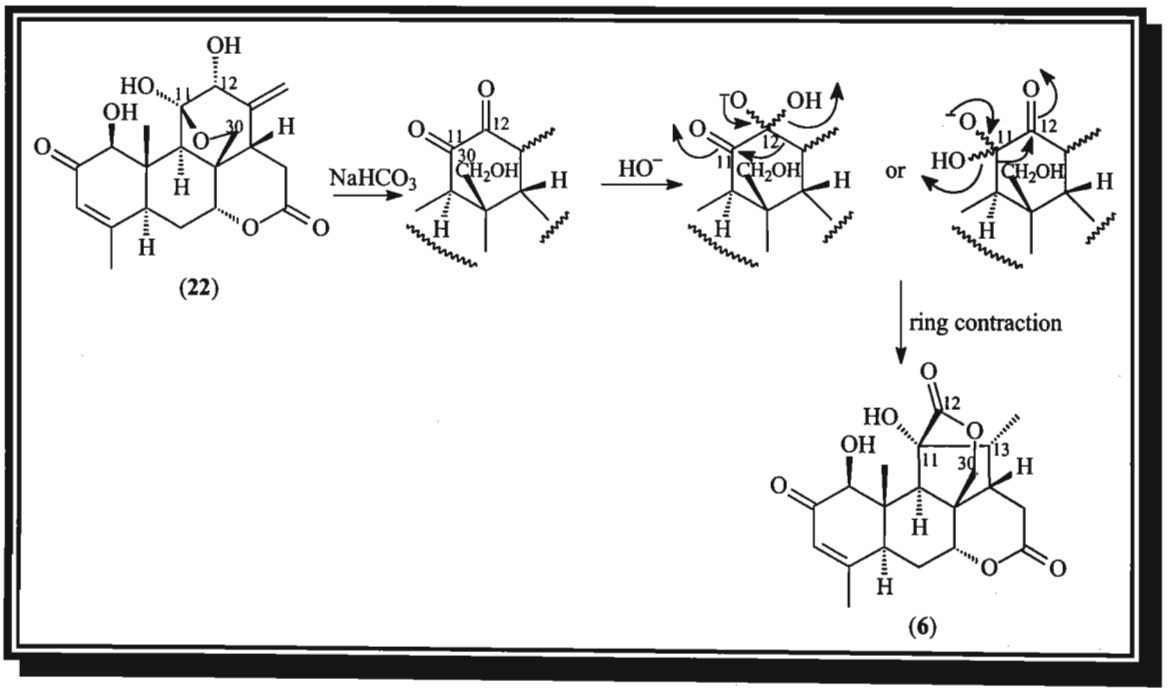

Scheme 2.4. Proposed biosynthesis of shinjudilactone (6) from ailanthone (22)[15]

2.4 Biological activity of quassinoids

Quassinoids have a wide range of biological activities such as antileukemic, antiviral, antimalarial, anti-inflammatory, antifeedant and amoebicidal activities.

Certain quassinoids display *in vivo* antileukemic activity. Bruceantin (**23**) is one such compound which is active against the P-388 lymphocytic leukemia cell line.[1] It shows activity over a wide dose range and is active against solid tumours.[1,13,33,34,35]

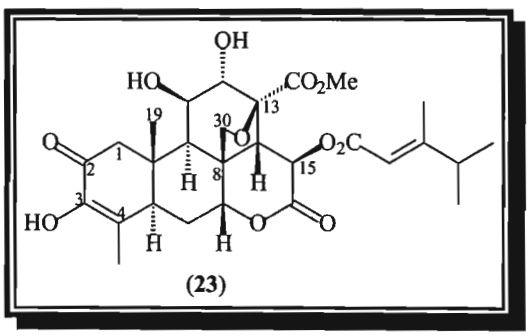

Fig. 2.18. Bruceantin (23)

The esters of brusatol (**24**), bisbrusatol (**25**) and bruceantin (**23**) have the ability to suppress DNA and protein synthesis in P-388 lymphocytic leukemia cells. These active compounds were also shown to inhibit DNA polymerase activity and purine synthesis.[36]

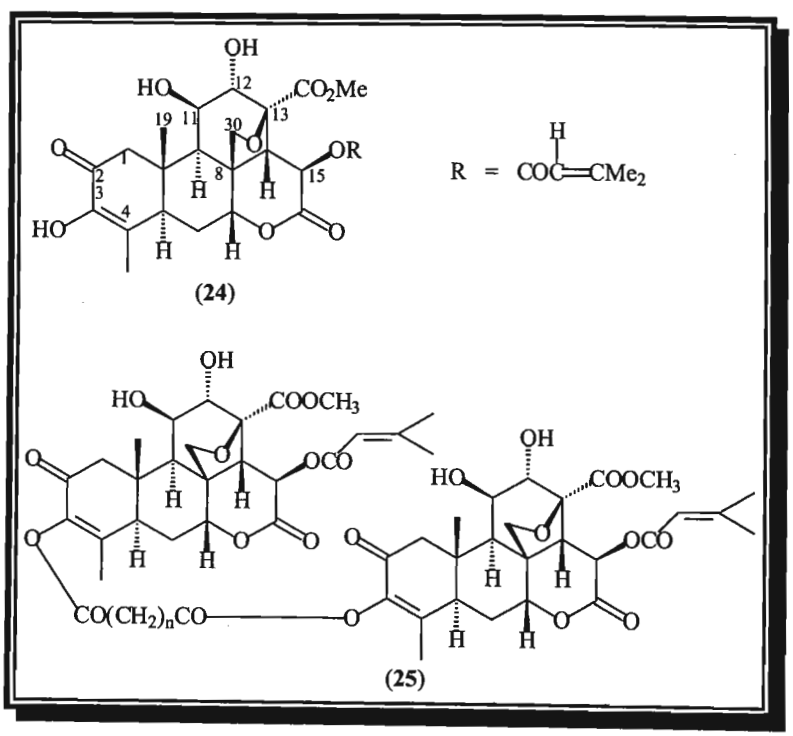

Fig. 2.19. Brusatol (24) and bisbrusatol (25)

Only quassinoids which possess the α, β-unsaturated ketol group in ring A display antineoplastic activity in the NIH murine lymphocytic leukemia P-388 system.

Undulatone (**26**)[37] is another cytotoxic quassinoid isolated from *Hannoa undulata*.

15-Deacetylsergeolide (**27**) isolated from the leaf extract of *Picrolemma pseudocoffea*[38] displays potent antileukemic activity.

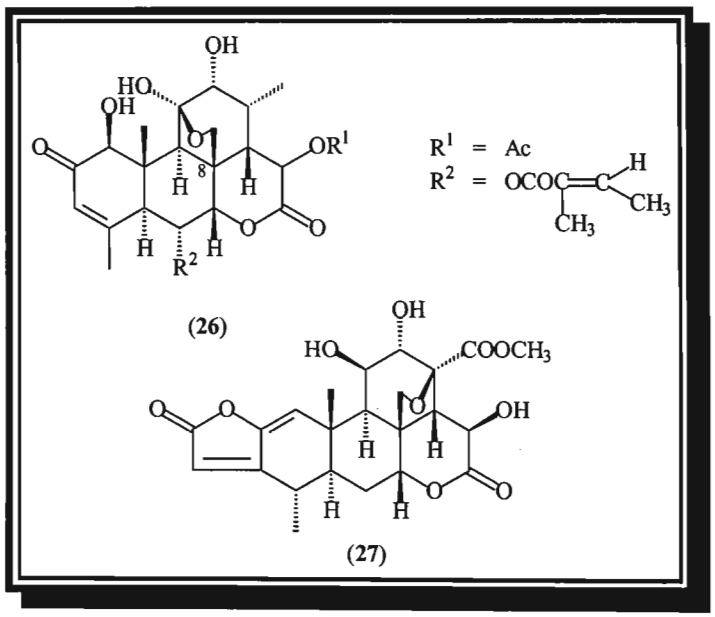

Fig. 2.20. Undulatone (26) and 15-deacetylsergeolide (27)

The quassinoid glucosides, bruceoside A (**28**) and bruceoside B (**29**) from *Brucea javanica* seeds,[21] and bruceantinoside A (**12**) and bruceantinoside B (**30**) from *Brucea antidysenterica* wood display significant antileukemic activity.[39]

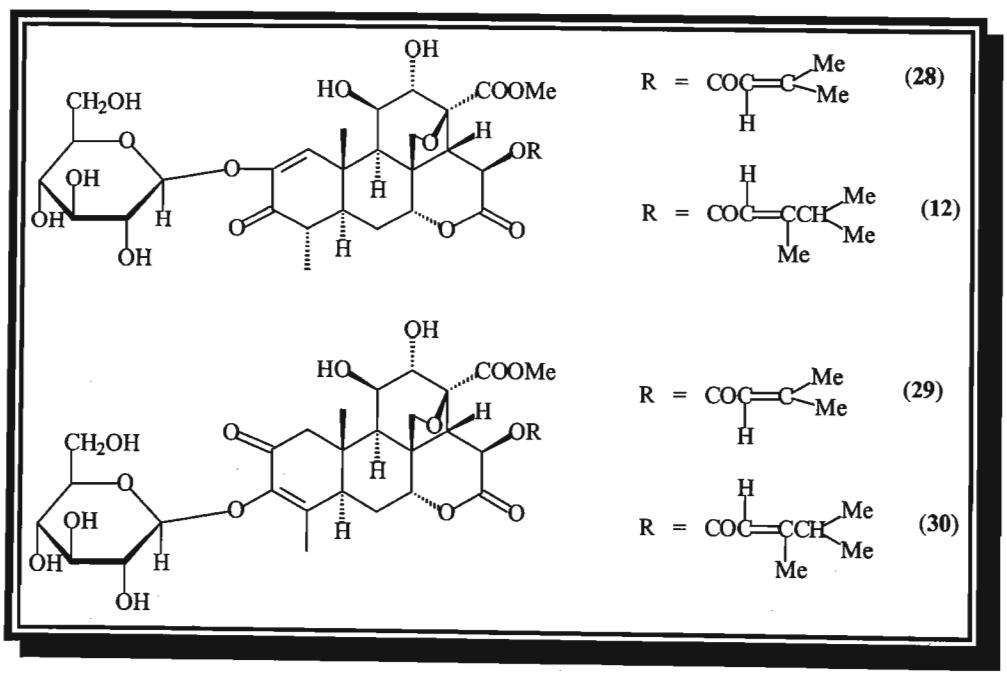

Fig. 2.21. Bruceoside A (28), bruceoside B (29), bruceantinoside A (12) and bruceantinoside B (30)

Certain quassinoids such as isobruceine A (**31**) and chaparrinone (**32**) display *in vitro* antiviral activity for example against the oncogenic Rous sarcoma virus.[1]

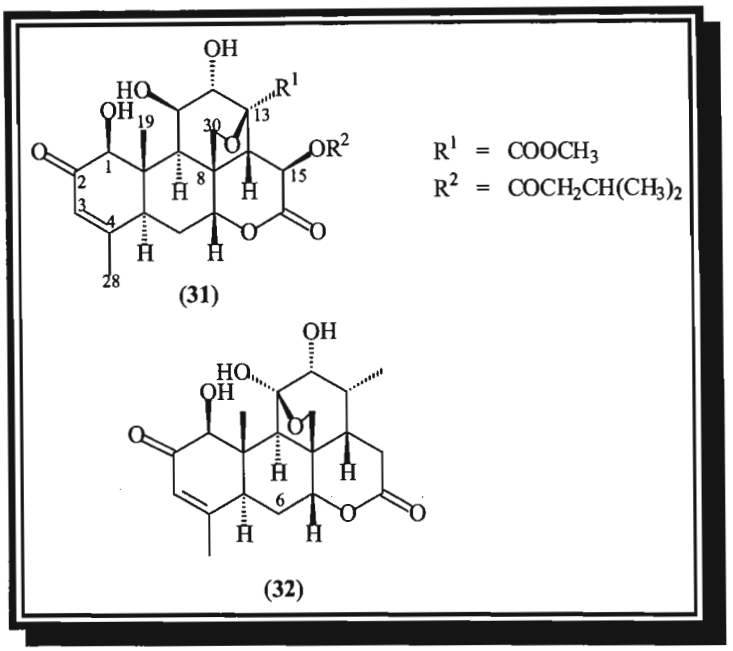

Fig. 2.22. Isobruceine A (31) and chaparrinone (32)

Certain quassinoids display *in vitro* antimalarial activity.[40] Simalikalactone D (**33**) is the most active compound. Glaucarubinone (**34**) and soularubinone (**35**) are also effective.

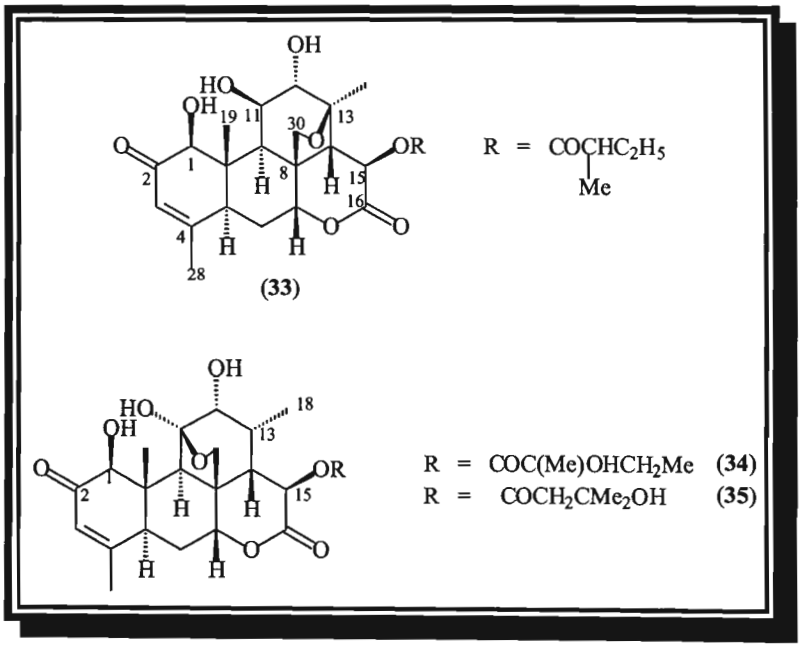

Fig. 2.23. Simalikalactone D (33), glaucarubinone (34) and soularubinone (35)

Simalikalactone D (**34**) is a potent antifeedant.[1] Glaucarubinone (**35**) and brucein B (**36**) show insecticidal properties.[1]

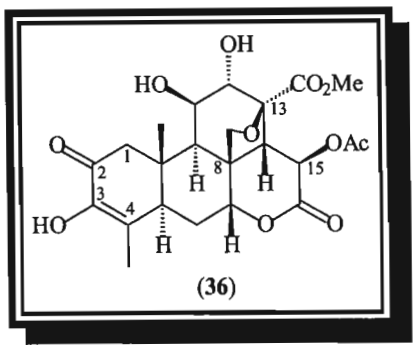

Fig. 2.24. Brucein B (36)

Extracts of many *Simarouba* species such as *Castela nicholsoni* or *Chaparro amargoso* (castamargina) have been used in Mexico and China to treat fevers, dysentery and amoebiasis. Ailanthone (**22**)[1] and glaucarubin (**3**)[1] were shown to be effective amoebicides.

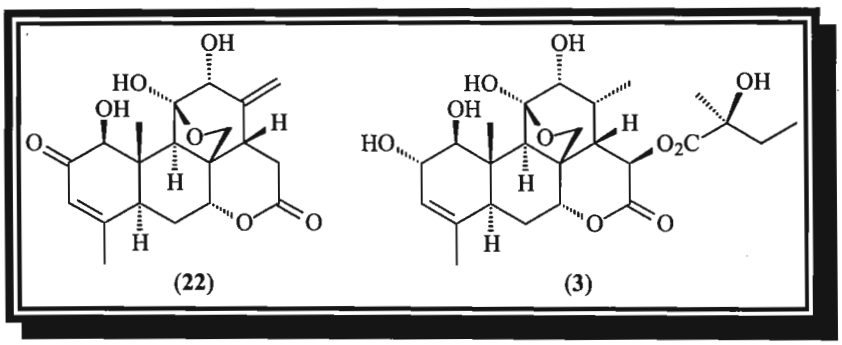

Fig. 2.25. Ailanthone (22) and glaucarubin (3)

Brusatol (**24**) and related compounds were found to be potent inhibitors of induced inflammation and arthritis in rodents.[41] The action of these anti-inflammatory quassinoids is to stabilise lysosomal membranes, thereby reducing the release of hydrolytic enzymes that cause damage to the surrounding tissues.[41]

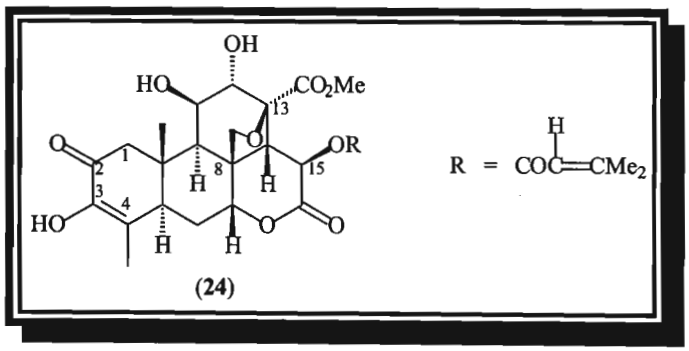

Fig. 2.26. Brusatol (24)

Since quassinoids are of important biological significance, research in this field continues, in the hope of finding biologically active quassinoids.

2.5 References

1. Polonsky J., *Progress in the Chemistry of Organic Natural Products*, 1985, **47**, 221.
2. Gibbons, S., Craven, L., Dunlop, C., Gray, A.I., Hartley, T.G. and Waterman, P.G., *Phytochemistry*, 1997, **44**, 1109.
3. http://electrocomm.tripod.com/quassia.html
4. http://www.ocnsignal.com/yangtextq.shtml
5. http://www.tropilab.com/quassia-ama.html
6. http://www.tinasherbs.com/hlistiq.htm
7. Dictionary of Natural Products, 1st edition, Chapman and Hall Ltd., London, 1994, **7**, xciii.
8. London, E., Robertson, A. and Worthington, H., *J. Chem. Soc.*, 1950, 3431.
9. Valenta, Z., Papadopoulos, S. and Podesva, C., *Tetrahedron*, 1961, **15**, 100.
10. Valenta, Z., Gray, A.H., Orr, D.E., Papadopoulos, S. and Podesva, C., *Tetrahedron*, 1962, **18**, 1433.
11. Ham, E.A., Schafer, H.M., Denkewalter, R.C. and Brink, N.G., *J. Am. Chem. Soc.*, 1954, **76**, 6066.
12. Polonsky, J., Fouquey, C.L. and Gaudemer, A., *Bull. Soc. Chim. France*, 1964, 1827.
13. Kupchan, S.M., Britton, R.W., Lacadie, J.A., Ziegler, M.F. and Sigel, C.W., *J. Org. Chem.*, 1975, **40**, 648.
14. Ishibashi, M., Tsuyuki, T., Murae, T., Hirota, H., Takahashi, T., Itai, A. and Iitaka, Y., *Bull. Chem. Soc. Jpn.*, 1983, **56**, 3683.
15. Ishibashi, M., Murae, T., Hirota, H., Naora, H., Tsuyuki, T., Takahashi, T., Itai, A. and Iitaka, Y., *Chem. Letters*, 1981, 1597.
16. Koike, K. and Ohmoto, T., *Phytochemistry*, 1993, **34**, 505.
17. Ozeki, A., Hitotsuyanagi, Y., Hashimoto, E., Itokawa, H., Takeya, K. and Alves, S. de M., *J. Nat. Prod.*, 1998, **61**, 776.
18. Takeya, K., Kobata, H., Ozeki, A., Morita, H. and Itokawa, H., *Phytochemistry*, 1998, **48**, 565.
19. Brown, W.A.C. and Sim, G.A., *Proc. Chem. Soc.*, 1964, 293.
20. Hikino, H., Ohta, T. and Takemoto, T., *Chem. Pharm. Bull.*, 1970, **18**, 1082.
21. Murae, T., Ikeda, T., Tsuyuki, T., Nishihama, T. and Takahashi, T., *Bull. Chem. Soc. Jpn.*, 1970, **43**, 969.
22. Lee, K.H., Imakura, Y., Sumida, Y., Wu, R.Y., Hall, J.H. and Huang, H. Ch., *J. Org. Chem.*, 1979, **44**, 2180.
23. Lee, K.H., Imakura, Y. and Huang, H.C., *J. Chem. Soc. Chem. Commun.*, 1977, 69.
24. Forgacs, P., Provost, J., Touche, A., Guenard, D., Thal, C. and Guilhem, J., *Tetrahedron Letters*, 1985, **26**, 3457.

25. Zylber, J. and Polonsky, J., *Bull. Soc. Chim. France*, 1964, 2016.
26. Furono, T., Ishibashi, M., Naora, H., Murae, T., Hirota, H., Tsuyuki, T., Takahashi, T., Itai, A. and Iitaka, Y., *Bull. Chem. Soc. Jpn.*, 1984, **57**, 2484.
27. Polonsky, J., Zylber, J. and Wijesekera, R.O.B., *Bull. Soc. Chim. France*, 1962, 1715.
28. Onan, K.D. and McPhail, A.T., *J. Chem, Research (S)*, 1978, 14.
29. Nguyên-Ngoc-Suong, Bhatnagar, S., Polonsky, J., Vuilhorgne, M., Prange, T. and Pascarol, C., *Tetrahedron Letters*, 1982, **23**, 5159.
30. Connolly, J.D., Overton, K.H. and Polonsky, J., *Progress in Phytochemistry*, 1970, **2**, 385.
31. Polonsky, J., *Progress in the Chemistry of Organic Natural Products*, 1973, **30**, 101.
32. Hikino, H., Ohta, T. and Takemoto, T., *Phytochemistry*, 1975, **14**, 2473.
33. Bedikian, A.Y., Valdivieso, M., Bodey, G.P., Murphy, W.K. and Freireich, E.J., *Cancer Treat. Rep.*, 1979, **63**, 1843.
34. Fong, K.L.L., Ho, D.H.W., Benjamin, R.S., Brown, N.S., Bedikian, A.Y., Yap, B.S., Wiseman, C.L., Kramer, W. and Bodey, G.P., *Pharmacol.*, 1982, **9**, 169.
35. Liesmann, J., Belt, R.J., Haas, C.D. and Hoogstraten, B., *Cancer Treat. Rep.*, 1981, **65**, 883.
36. Hall, I.H., Liou, Y.F., Okano, M. and Lee, K.H., *J. Pharm. Sci.*, 1982, **71**, 345.
37. Wani, M.C., Taylor, H.L., Thompson, J.B., Wall, M.E., McPhail, A.T. and Onan, K.D., *Tetrahedron,* 1979, **35**, 17.
38. Polonsky, J., Bhatnagar, S. and Moretti, C., *J. Nat. Prod.*, 1984, **47**, 994.
39. Okano, M., Lee, K.H., Hall, I.H. and Boettner, F.E., *J. Nat. Prod.*, 1981, **44**, 470.
40. Trager, W. and Polonsky, J., *J. Trop. Med. Hyg.*, 1981, **30**, 531.
41. Hall, I.H., Lee, K.H., Imakura, Y., Okano, M. and Johnson, A., *J. Pharm. Sci.,* 1983, **72**, 1282.

Chapter 3

Introduction to Lignans

PAGE NO.

PAGE NO.

List of Figures

List of Schemes

3.1 Introduction and classification of lignans

According to Haworth,[1] lignans are naturally occurring dimers of phenylpropanoid (C6-C3) units linked by the β-carbons of their side chains. Lignans have enormous structural diversity and are assembled from simple phenolic precursors, for example, (*E*)-coniferyl alcohol, (*E*)-*p*-coumaryl alcohol and (*E*)-sinapyl alcohol. The precursors differ only in aromatic substitution.

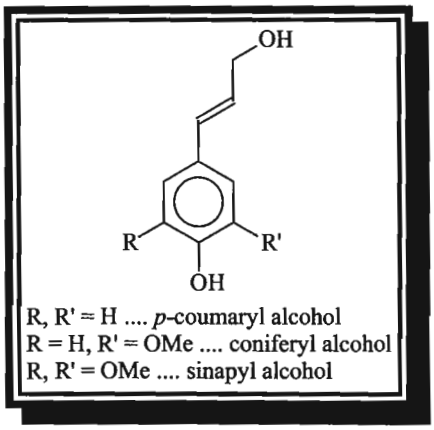

Fig. 3.1. Simple phenolic precursors

These alcohols are derived from compounds such as caffeic (**1**), ferulic (**2**) and sinapic (**3**) acids.

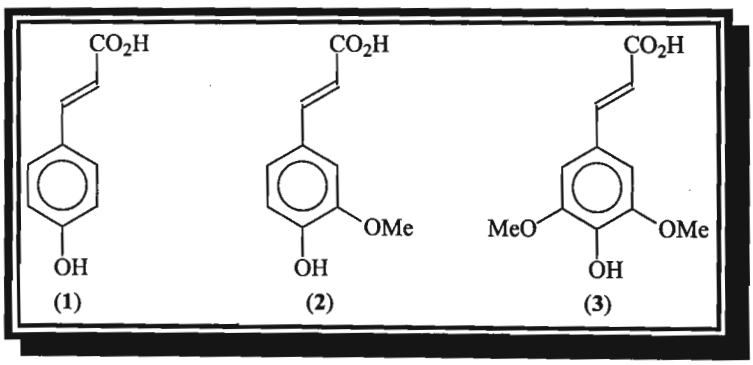

Fig. 3.2. Caffeic (1), ferulic (2) and sinapic (3) acids

Lignans (fig. 3.3) are derived by the C-8, C-8' coupling of two alcohols. Neolignans (fig. 3.4) are naturally occurring dimers that exhibit linkages other than the C-8-C-8' type.[1]

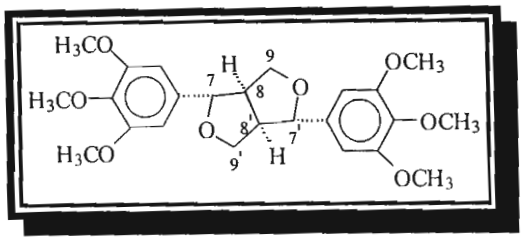

Fig. 3.3. Lignan showing the C-8-C-8' bond link

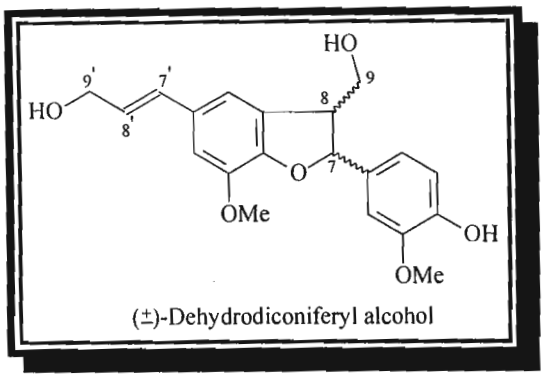

Fig. 3.4. Example of a neolignan

Lignans arise from the oxidative coupling of *p*-hydroxyphenylpropene units.[1] The biosynthesis of lignans is discussed in detail in section 3.2.

Lignans have a broad range of biological activities including anti-tumour, antimitotic and antiviral activity, and specifically inhibit certain enzymes.[1,2,3,4] Certain lignans are also known to have insect antifeedant, antibacterial and antifungal activity.[1,4] The biological activities of lignans are discussed in detail in section 3.3.

3.2 Biosynthesis of lignans

3.2.1 Reduction of cinnamic acids to form monolignols

The alcohols are derived by reduction of the corresponding cinnamic acids *via* coenzyme A esters and aldehydes. Formation of the coenzyme A ester facilitates the first reduction step by introducing a better leaving group (CoAS-) for the NADPH-dependent reaction.[3] The second reaction step, the conversion of aldehyde to alcohol, uses a further NADPH molecule and is reversible[3] (fig. 3.5).

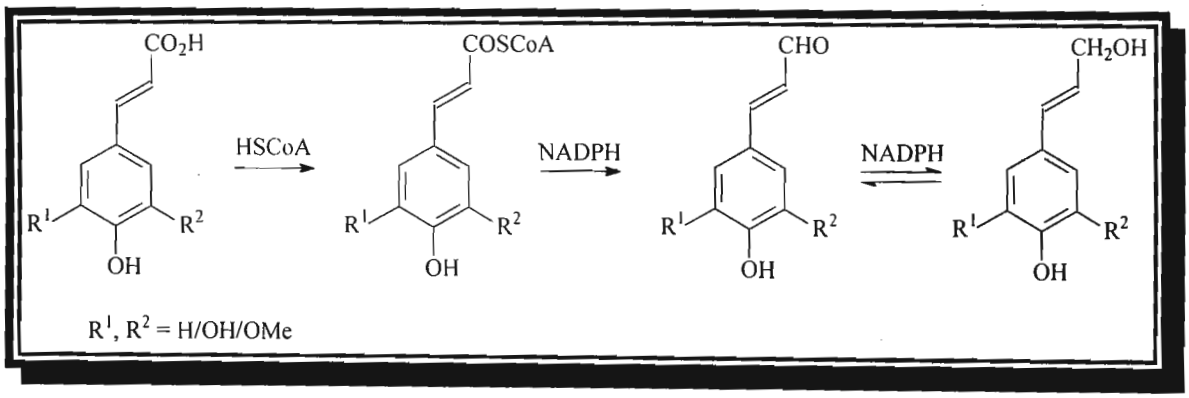

Fig. 3.5. Reduction of cinnamic acid to form the alcohol[3]

3.2.2 Oxidation of a monolignol to form a free radical

The peroxidase enzyme achieves one electron oxidation of the phenol group, which allows delocalisation of the unpaired electron, giving resonance forms as shown in scheme 3.1.

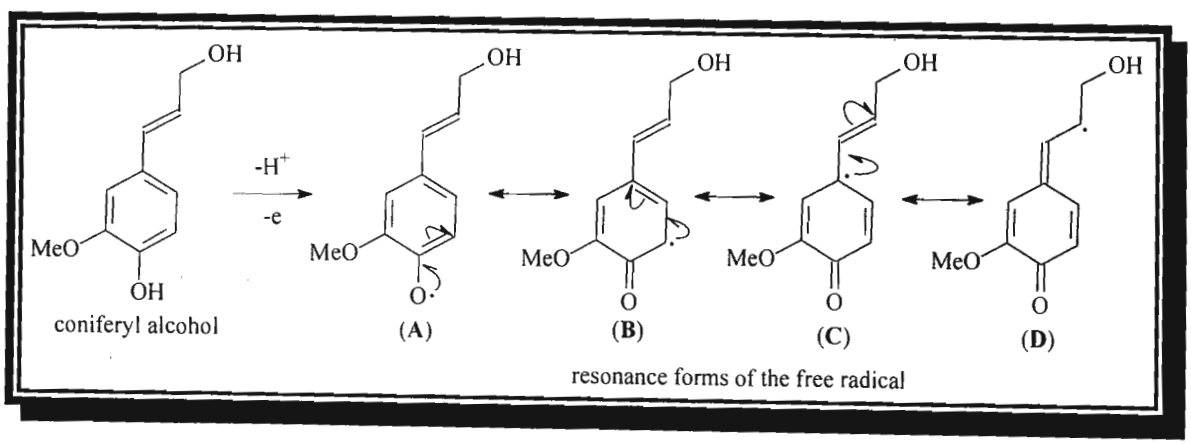

Scheme 3.1. Resonance forms of the free radical[3]

The conjugation of cinnamic acid derivatives allows the unpaired electron to be delocalised into the side chain.

3.2.3 Radical pairing to form lignans

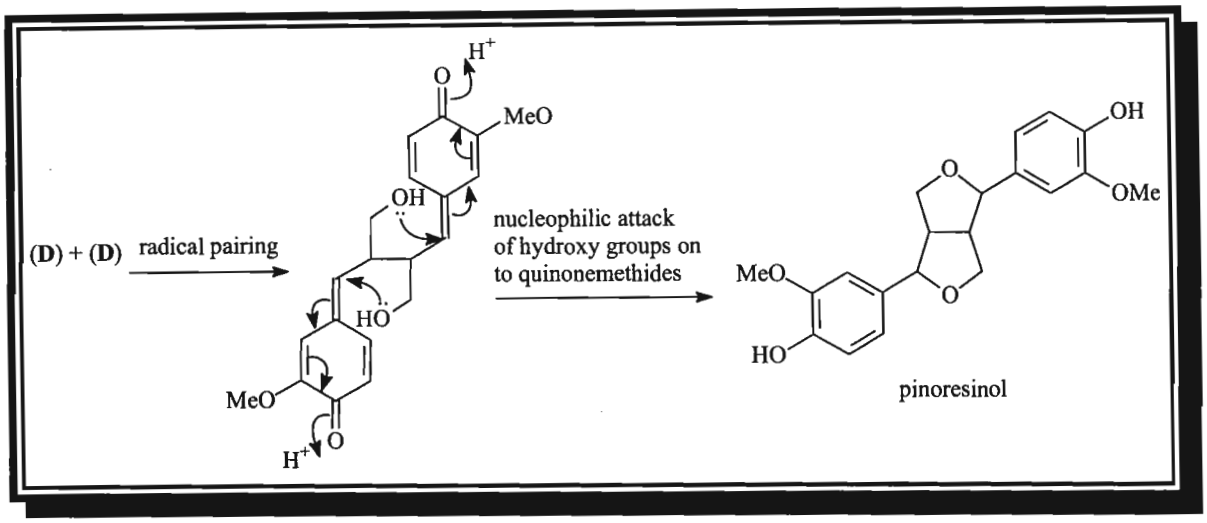

Scheme 3.2. Radical pairing to form a dimer (lignan)[3]

Radical pairing of the resonance structures provides a range of dimers (lignans). Bimolecular phenoxy radical coupling *in vivo* can lead to well defined biopolymers and oligomers such as the melanins, lignins and lignans. 'Random' bimolecular radical coupling (**A**) and stereoselective coupling (**B**) are shown below.

(A) 'Random' bimolecular radical coupling :

One electron oxidation of the monolignol, E-coniferyl alcohol, results in 'random' bimolecular radical coupling to afford initially dimeric products, such as (±)-dehydrodiconiferyl alcohols, (±)-pinoresinols, and (±)-guaiacylglycerol 8-O-4'-coniferyl alcohol ethers (scheme 3.3).[5]

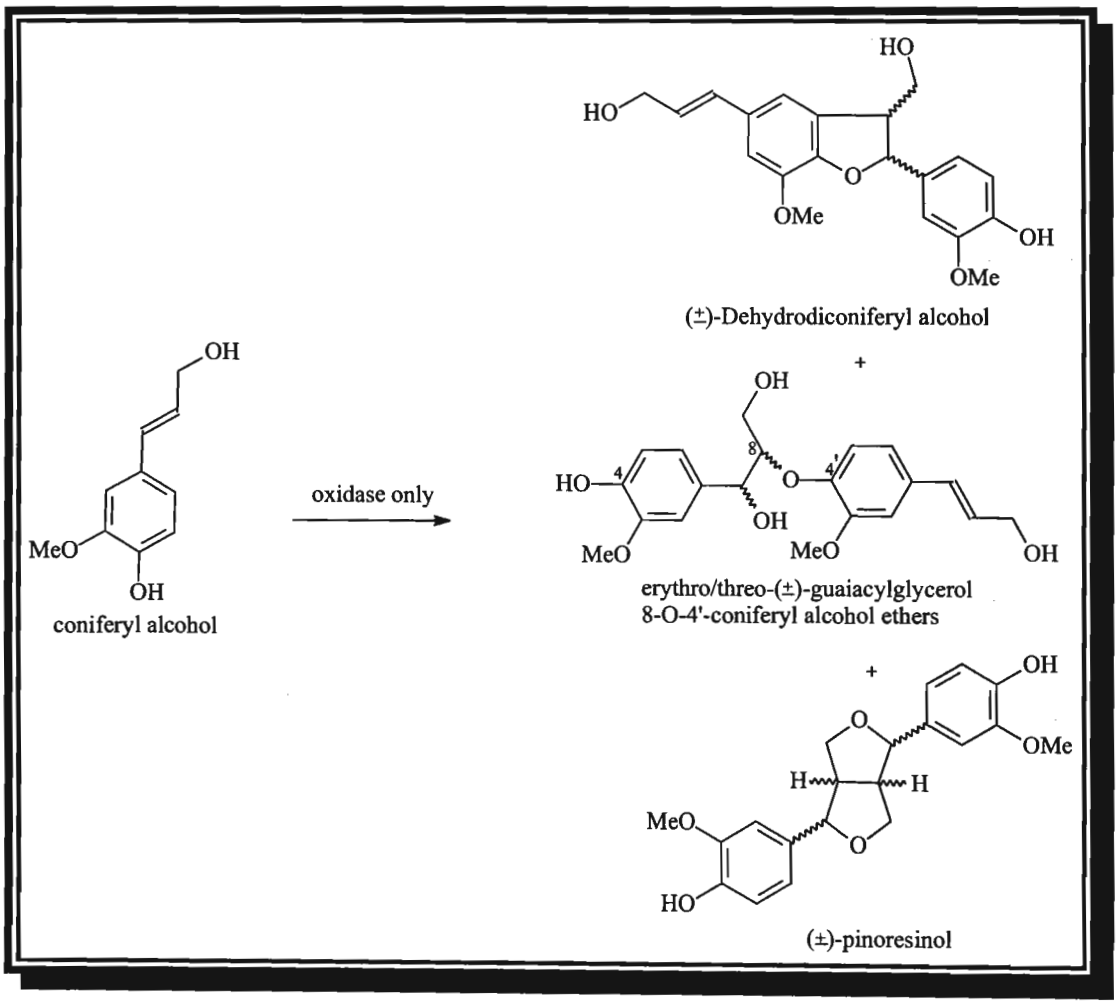

Scheme 3.3. 'Random' bimolecular radical coupling to form lignans[5]

(B) Stereoselective bimolecular coupling :

A protein coupling agent is thought to be involved in the formation of the stereospecific 8, 8'-linked lignans. The protein serves only to bind and orientate the coniferyl alcohol-derived free radicals, which then undergo stereoselective coupling. It is presumed that both radical intermediate species are bound and orientated at the '(+)-pinoresinol synthase' active site (scheme 3.4).[5]

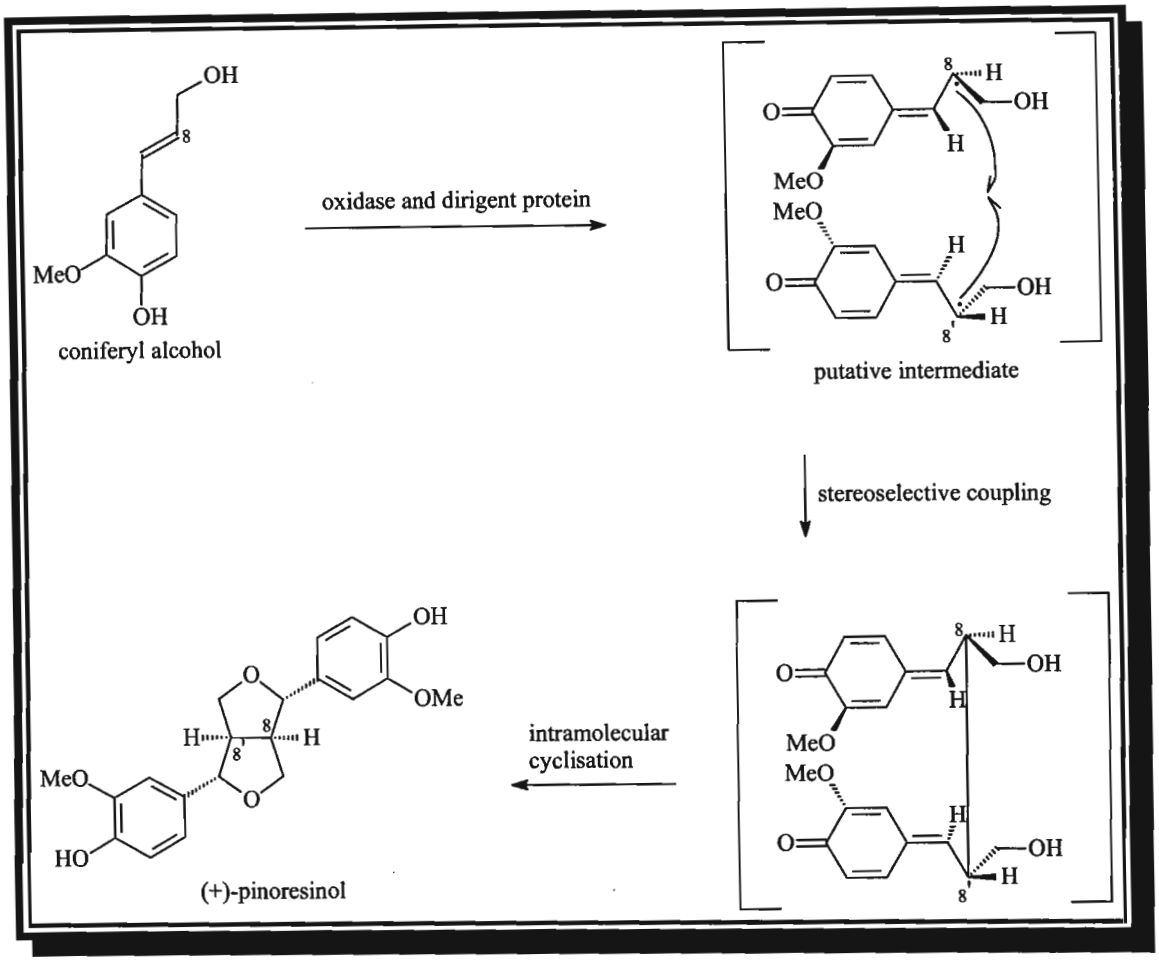

Scheme 3.4. Stereoselective coupling to form (+)-pinoresinol[5]

It has been proposed that the free radical intermediates, which are generated by the oxidase, are captured by a dirigent protein. They are bound and orientated in such a manner that coupling only results in a specific stereoisomer.[6]

According to Rouhi,[7,8] the protein dictates the monomers that will be incorporated and the type of linkage that will be formed through the specificity and orientation of their binding sites. They assemble a progenitor macromolecule from the monomers through a series of oxidations and couplings. Once the progenitor is formed, it is replaced by a direct template mechanism.[7]

3.3 Biological activity of lignans

Lignans are found in seed coats, stems, leaves, flowers and various other plant parts. Lignans display a large variety of biological activities, which include antitumour, antiviral, antifeedant, antifungal, and antioxidant activities.

Podophyllum peltatum L. is in demand in the drug trade since it has antitumour activity.[1] *Nor*-dihydroguaiaretic acid (**4**), from *Podophyllum peltatum* L., has been described as a potent anti-cancer antimetabolite *in vitro*.[1] The aryltetralin lactone podophyllotoxin (**5**) which is derived from coniferyl alcohol *via* the dibenzylbutyrolactone matairesinol (**6**), has cytotoxic properties.[3] The antimitotic effect of podophyllotoxin and other lignans occur by binding to the protein tubulin in the mitotic spindle, preventing polymerisation into microtubules.[3]

Podophyllum peltatum

(http://www.ces.ncsu.edu/depts/hort/consumer/poison/images/PodopPe4.htm)
(http://www.ces.ncsu.edu/depts/hort/consumer/poison/images/PodopPe7.htm)

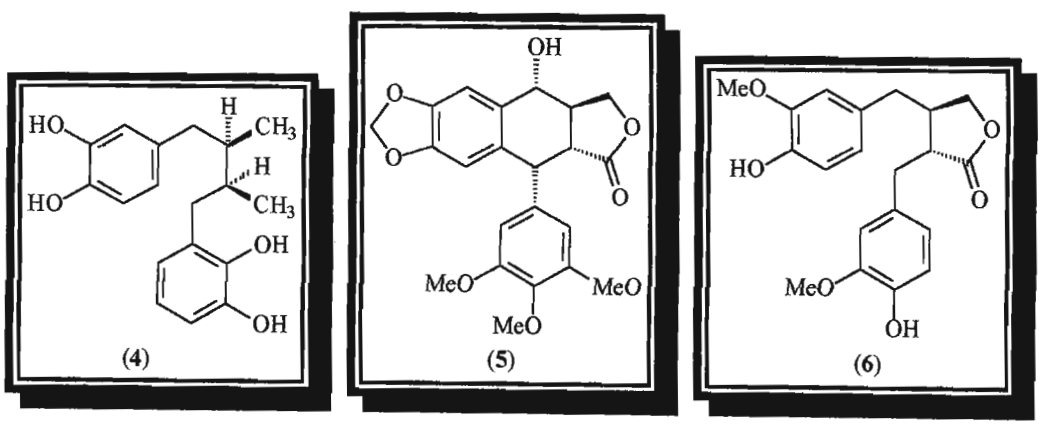

Fig. 3.6. *Nor*-dihydroguaiaretic acid (4), podophyllotoxin (5) and matairesinol (6)

The semi-synthetic derivatives of podophyllotoxin, etoposide (**7**) and teniposide (**8**) are excellent antitumour agents.[3] Etoposide (**7**) is a very effective anticancer agent which is used in the treatment of small cell lung cancer, testicular cancer and lymphomas, in combination with other anticancer drugs.[3] Teniposide (**8**) is used in the treatment of paediatric neuroblastoma. These drugs inhibit the enzyme topoisomerase II, thus preventing DNA synthesis and replication.[3]

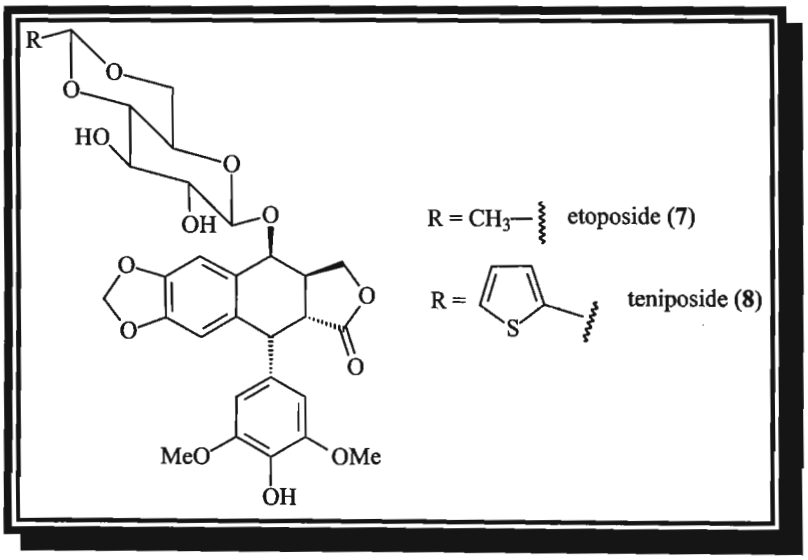

Fig. 3.7. Etoposide (7) and teniposide (8)

An extract of *Podophyllum peltatum* was observed to reduce the cytopathic effect of herpes simplex type II, influenza A and vaccinia viruses.[2] Podophyllotoxin (**5**), β-peltatin (**9**), deoxypodophyllotoxin (**10**), picropodophyllotoxin (**11**) and α-peltatin (**12**) were found to be active against measles and herpes simplex type I.[9] It was observed, that replacing the lactone ring of podophyllotoxin with a furan ring (anhydropodophyllol) results in a ten-fold reduction in the activity.

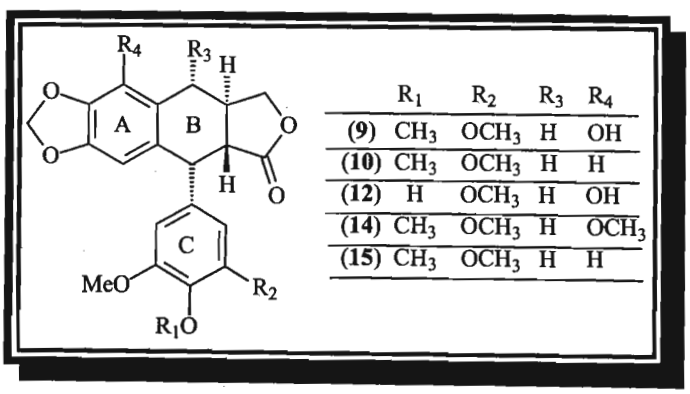

	R_1	R_2	R_3	R_4
(9)	CH_3	OCH_3	H	OH
(10)	CH_3	OCH_3	H	H
(12)	H	OCH_3	H	OH
(14)	CH_3	OCH_3	H	OCH_3
(15)	CH_3	OCH_3	H	H

Fig. 3.8. β-Peltatin (9), deoxypodophyllotoxin (10), α-peltatin (12), β-peltatin-A-methyl ether (14) and deoxypicropodophyllin (15).

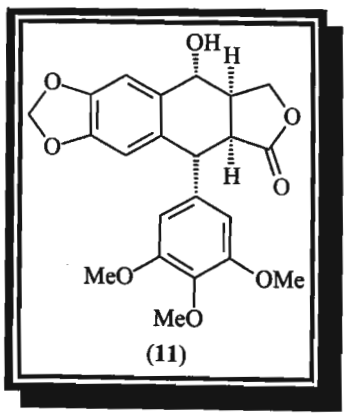

Fig. 3.9. Picropodophyllotoxin (11)

Schizandrin (**13**) has been used in the Orient as a stimulant.[1]

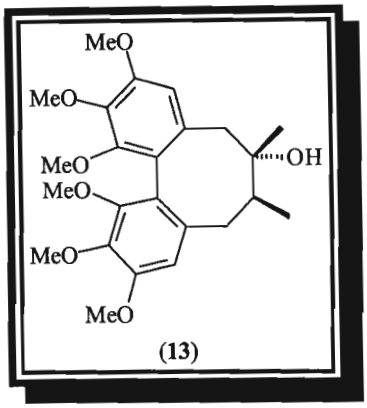

Fig. 3.10. Schizandrin (13)

Podophyllotoxin analogues such as β-peltatin-A-methyl ether (**14**), deoxypodophyllotoxin (**10**) and deoxypicropodophyllin (**15**) are effective in inhibiting insect larval growth.[2] The bisepoxylignans, kobusin (**16**) and (+)-sesamin (**17**), inhibit the growth of silkworm larvae. *p*-Benzolactone (**18**) is an insect feeding inhibitor.

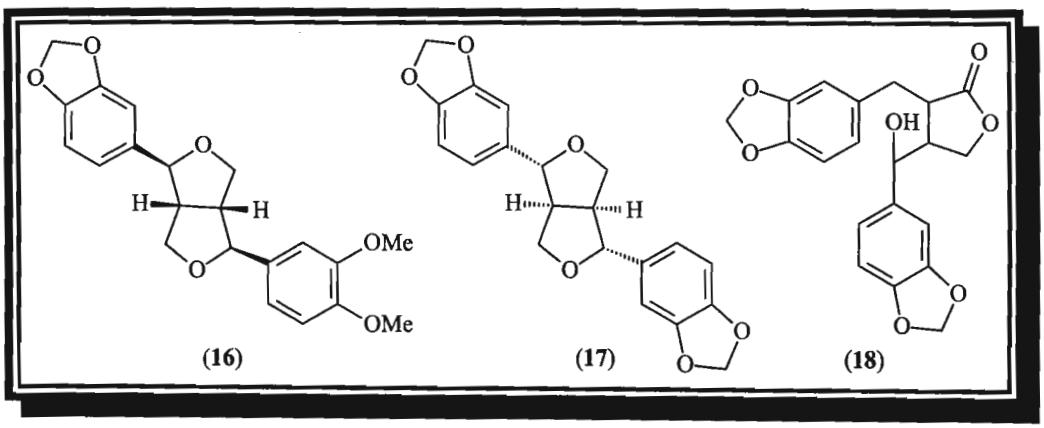

Fig. 3.11. Kobusin (16), (+)-sesamin (17) and *p*-benzolactone (18)

(+)-Sesamin (**17**) and (-)-asarinin (**19**) are the toxic ingredients in a wide variety of insecticides. Lignans such as savinin (**20**) and hinokinin (**21**), matairesinol (**6**) and its dimethyl ether (**22**) are known insecticide synergists.[2]

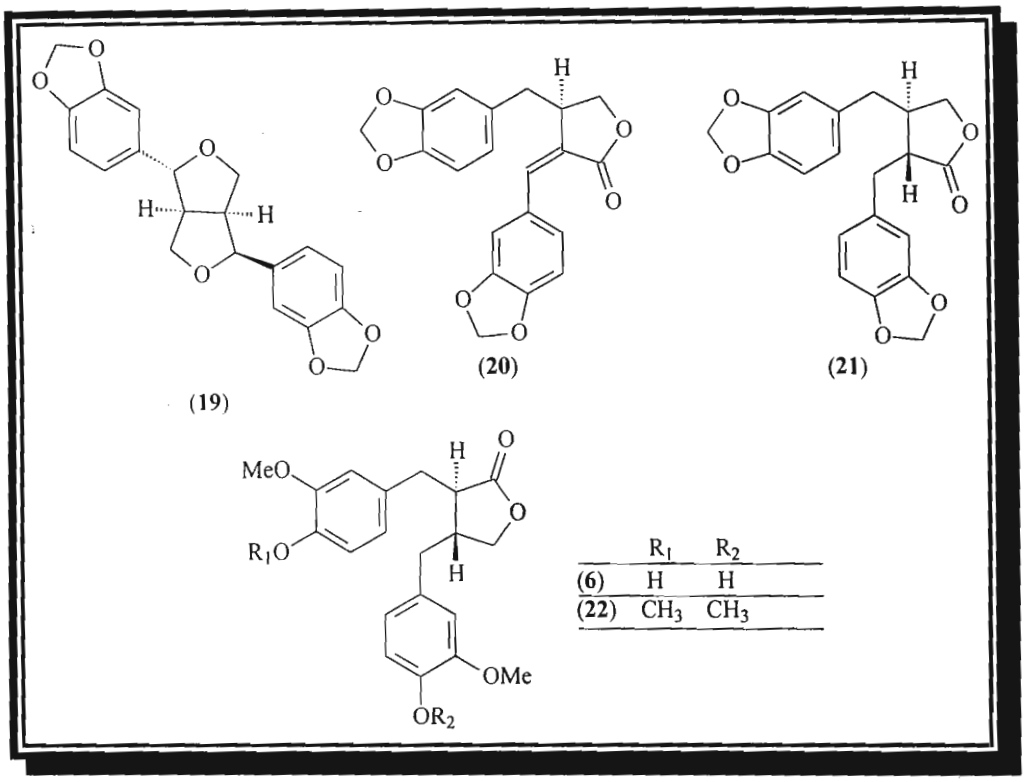

Fig. 3.12. (-)-Asarinin (19), savinin (20), hinokinin (21), matairesinol (6) and the dimethyl ether of matairesinol (22)

The neolignan, piperenone (**23**) exhibits insect antifeeding properties.[1] Hydroxymatairesinol (**24**) and matairesinol (**6**) are antifungal agents.[2]

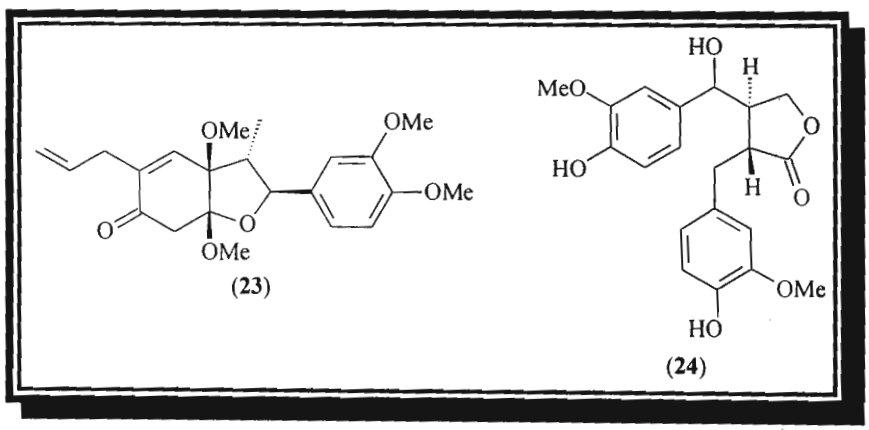

Fig. 3.13. Piperenone (23) and hydroxymatairesinol (24)

Otobain (**25**) and the co-occurring neolignans are the fungistatic ingredients of otoba butter, used in Colombia in veterinary practice.[1]

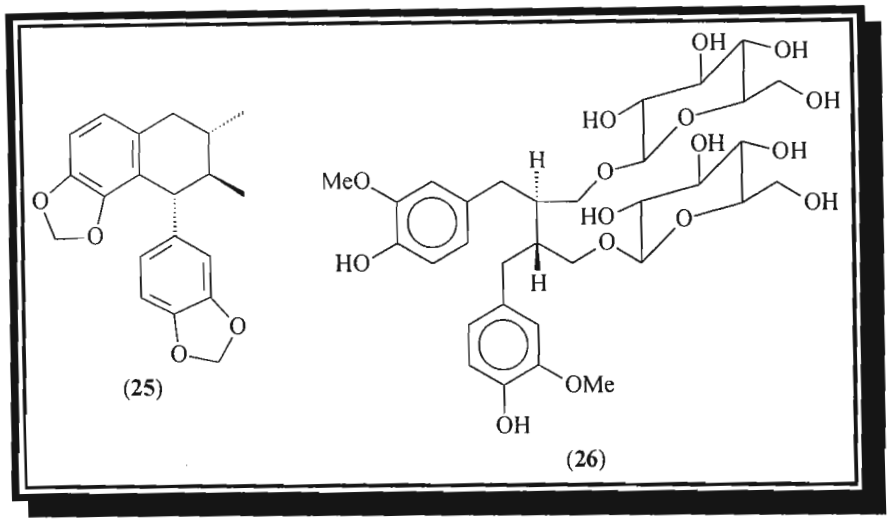

Fig. 3.14. Otobain (25) and *seco*-isolariciresinol diglucoside (26)

The flaxseed lignan, *seco*-isolariciresinol diglucoside (SDG) (**26**), is effective in the treatment of breast and colon cancer, hypercholesterolemic artherosclerosis, and lupus nephritis. SDG also exhibits anti-oxidant properties.[4]

The *Schizandra* lignans have physiological actions on man, such as activity on the central nervous system, protective activity against toxins and general stress-reducing activity.[2] Schizandrin B (**27**) is effective in protecting the liver by offering resistance to the toxic effects of digitoxin and indomethacin.[2]

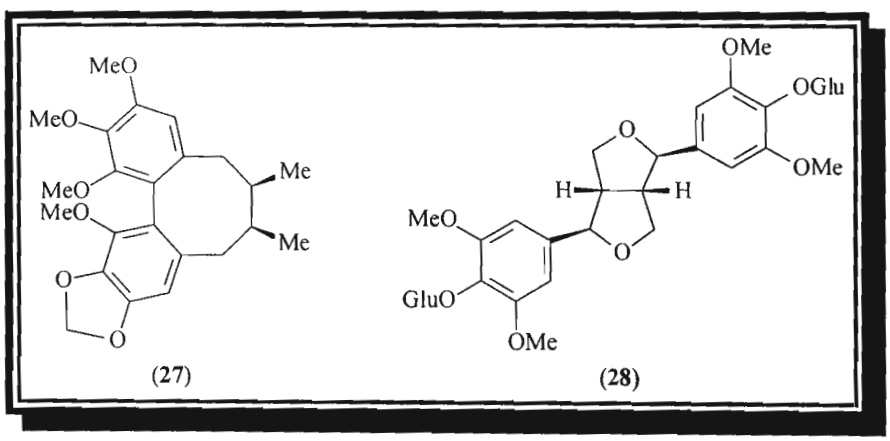

Fig. 3.15. Schizandrin B (27) and (-)-syringaresinol diglucoside (28)

The bisepoxylignan (-)-syringaresinol diglucoside (**28**) reduces the physiological response to stress in animals by reducing the weight of the adrenal gland, thymus and spleen.[2]

Enterolactone (**29**) and enterodiol (**30**) have been found in the urine of humans.[2,4] There is a possibility that the lignans possess hormonal activity in man, however, there is evidence that these lignans are possibly metabolic products of the microflora of the gut.[2] They have unusual 3'-oxidation patterns on the aromatic rings.

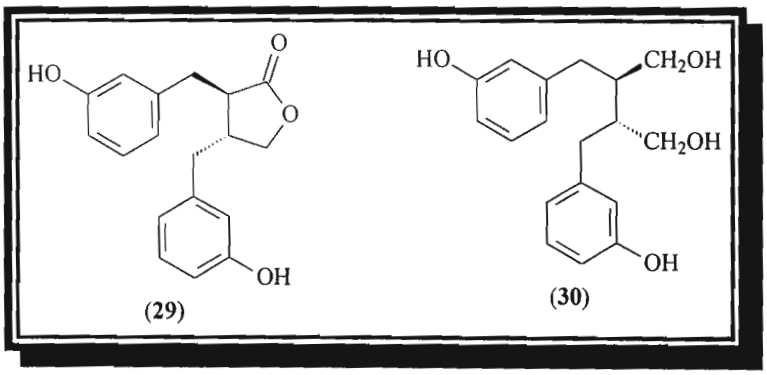

Fig. 3.16. Enterolactone (29) and enterodiol (30)

Lignan research continues today in the hope of discovering more lignans of pharmacological significance.

3.4 References

1. Gottlieb, O.R., *Progress in the Chemistry of Organic Natural Products*, 1978, **35**, 1.
2. MacRae, W.D. and Towers, G.H.N., *Phytochemistry*, 1984, **23**, 1207.
3. Dewick, P.M., *Medicinal Natural Product*, A Biosynthetic Approach, John Wiley and Sons, Chichester, New York, 1998, 120.
4. http://www.wholehealthmd.com
5. Davin, L.B., Wang, H.B., Crowell, A.L., Bedgar, D.L., Martin, D.M., Sarkanen, S. and Lewis, N.G., *Science*, 1997, **275**, 362.
6. Davin L.B. and Lewis, N.G., *Plant Physiology*, 2000, **123**, 453.
7. Rouhi, M.A., *Chemical and Engineering News*, 2000, **78**, 29.
8. Rouhi, M.A., *Chemical and Engineering News*, 2001, **79**, 52.
9. Bedows, E. and Hatfield, G.M., *J. Nat. Prod.*, 1982, **45**, 725.

Chapter 4

Foreword to Experimental

Nuclear magnetic resonance spectroscopy (NMR Spectroscopy)

Nuclear magnetic resonance spectroscopy was performed on a 400MHz Varian UNITY-INOVA NMR spectrometer. All spectra were recorded at room temperature in deuterated chloroform ($CDCl_3$) with the exception of compound (**17**) which was run in deuterated methanol. The chemical shifts were all recorded in ppm relative to TMS.

Infrared Spectroscopy (IR Spectroscopy)

The infra-red spectra were recorded using a Nicolet Impact 400D Fourier-Transform Infra-red (FT-IR) spectrometer. The crystalline compounds were analysed using KBr discs and the non-crystalline samples were dissolved in dichloromethane and analysed on a NaCl window. The spectra were calibrated against an air background.

Ultraviolet Absorption Spectrometry/ Spectroscopy (UV Spectroscopy)

The ultra-violet absorption spectra were obtained on a Varian DMS 300 UV-visible spectrometer. The solvent in which the spectra were recorded was dichloromethane.

Melting Points (mp)

Melting points were determined on a Kofler micro-hot stage melting point apparatus and are uncorrected.

Optical Rotations

Optical rotations were measured at room temperature in either methanol or chloroform using a Perkin Elmer 241 Polarimeter or an Optical Activity AA-5 Polarimeter together with a series A2 stainless steel (4 x 200 mm) unjacketed flow tube.

Mass Spectrometry

High resolution mass spectra were obtained for compounds (**7**), (**8**), (**9**), (**10**), (**17**), (**18**) and (**19**) and were recorded on a Kratos 9/50 HRMS instrument. The mass spectrometry was performed by Dr. P. Boshoff at the Cape Technikon. All other mass spectra were recorded on an Agilent MS 5975 instrument connected to GC 6890 and the mass spectrometry was performed by Mr. B. Parel at UND.

General Chromatography

The isolation process employed column and thin layer chromatographic techniques. In column chromatography, different sized columns were used ranging from 2-8 cm in diameter depending on the amount of sample available and the purification stage. Separation of crude extracts was generally carried out on a column using Merck Art. 9385 silica gel. All separations were carried out under gravity. Both the column and thin layer chromatographic techniques made use of varying ratios of dichloromethane and hexane or dichloromethane and ethyl acetate or ethyl acetate and hexane. Thin layer chromatography was carried out on 0.2 mm silica-gel, aluminium-backed plates (Merck Art. 5554). The plates were developed using anisaldehyde : conc. H_2SO_4 : methanol [1:2:97] spray reagent. The plates were first analysed under UV light (366 nm) and then by heating.

General acetylation procedure

Pyridine (1 ml) and acetic anhydride (1 ml) were added to the sample (15 mg) in a round bottom flask. The sample was left to stand at room temperature for 48 hours. Methanol (5 ml) was then added to the sample to react with the excess acetic anhydride and toluene (4 x 10 ml) was added successively to remove the pyridine. After each addition, the solvent was evaporated off on the rotavapor. Thereafter, methanol (5 x 10 ml) was added to remove the remaining toluene. The sample was then spotted on a t.l.c plate to see whether the reaction had gone to completion or needed to be separated from the starting material.

General Plant Extraction Procedure

The species in this study were collected by Dr. Milijaona Randrianarivelojosia from Madagascar. The stem bark of the *Cedrelopsis grevei* plant was investigated. The stem bark was milled and air dried, and then successively extracted with hexane, ethyl acetate and methanol using a soxhlet apparatus. The seeds of *Neobeguea mahafalensis* were investigated. The seeds were separated from the shell and both parts were ground, then successively extracted with hexane, ethyl acetate and methanol using a soxhlet apparatus. Extraction with each solvent was carried out for approximately 48 hours. The solvents from the extracts obtained were evaporated using a BUCHI rotavapor. The extraction procedure for each plant is explained in more detail in chapters five and six.

Chapter 5

Extractives from *Cedrelopsis grevei* stem bark

Photograph by Dr. Milijaona Randrianarivelojosia

PAGE NO.

PAGE NO.

List of Figures

List of Schemes

List of Tables

5.1 Introduction

Madagascar is home to a large number of medicinal plants. The Madagascan periwinkle (*Catharanthus roseus*) is one such medicinal plant, whose extractives are used to treat childhood leukaemia and Hodgkin's disease. Katrafay (*Cedrelopsis grevei*) is another Madagascan medicinal plant, whose bark relieves muscular fatigue, when soaked in bath water.[1]

Compounds previously isolated from this species include 3-acetyl-2,6-dihydroxy-4-methoxybenzaldehyde (**1**),[2] cedrelopsin (**2**),[3] greveichromenol (**3**),[4] greveiglycol (**4**),[4] peucenin (**5**),[4,5] alloptaeroxylin (**6**),[4,6] ptaeroxylinol (**7**),[7,8] heteropeucenin (**8**),[4] cedrecoumarin A (**9**),[8] and cedrecoumarin B (**10**),[8] ptaeroglycol (**11**),[7,4] ptaeroxylin (**12**),[3,5,7] cedmilinol (**13**),[1] cedmiline (**14**)[1] and β-amyrin (**15**).[1]

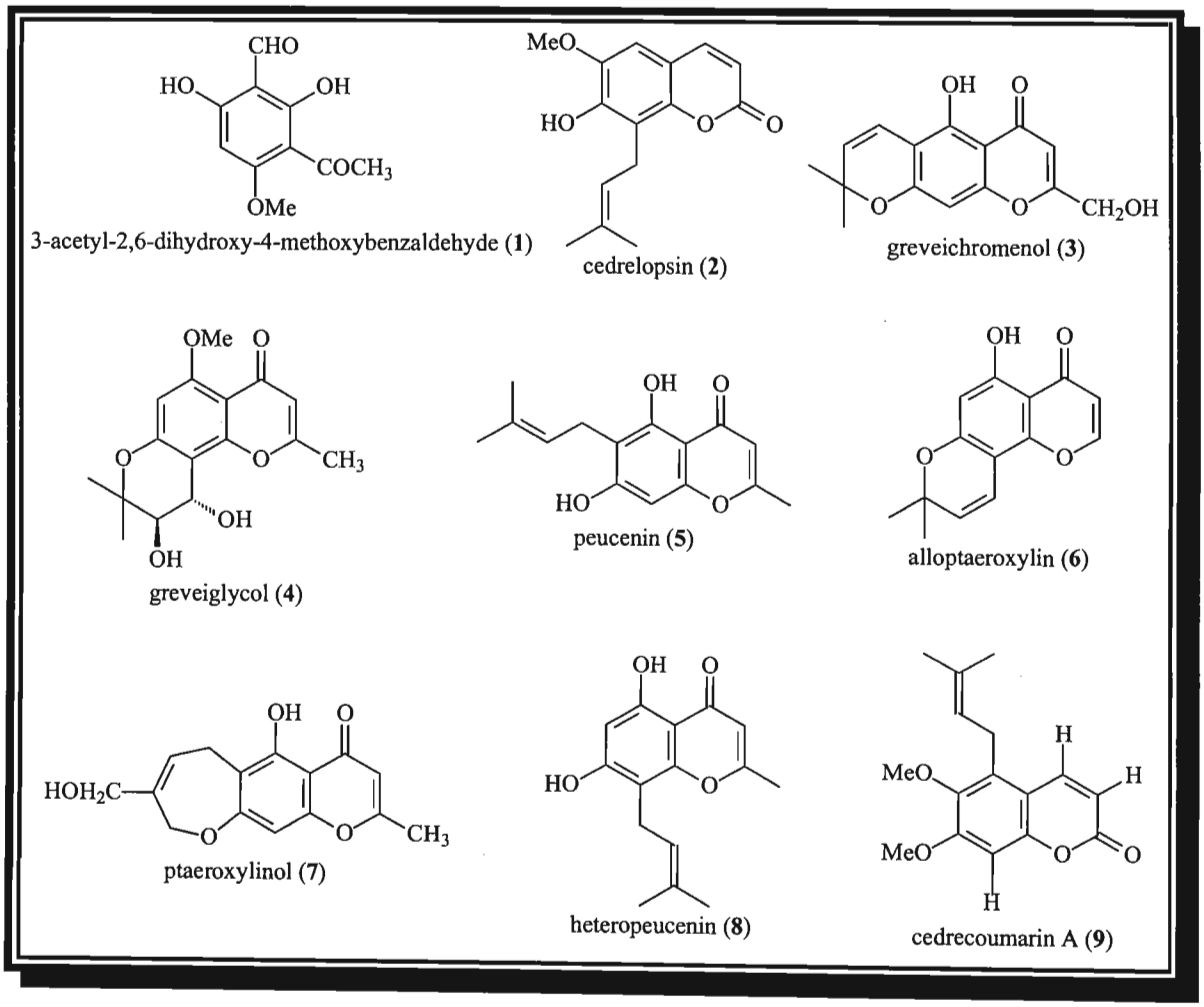

Fig. 5.1a. Compounds previously isolated from *Cedrelopsis grevei* (1, 2, 3, 4, 5, 6, 7, 8, 9)[2,3,4,5,6,7,8]

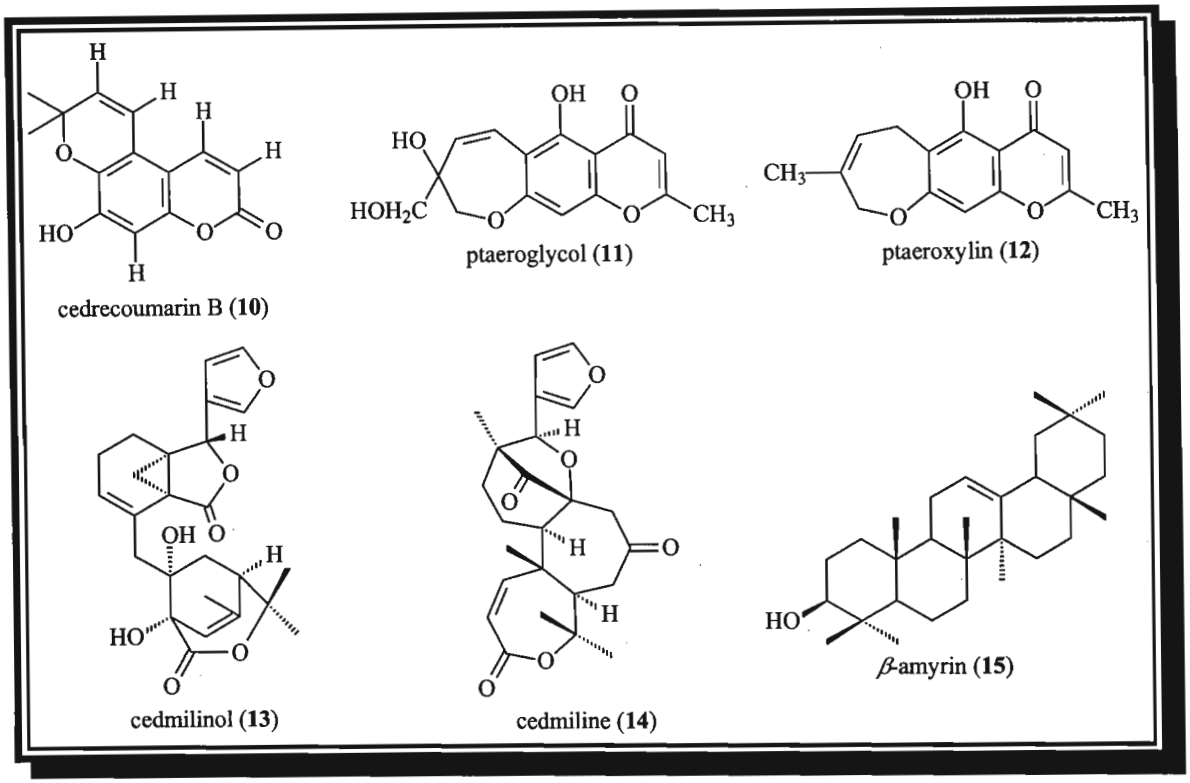

Fig. 5.1b. Compounds previously isolated from *Cedrelopsis grevei* (10, 11, 12, 13, 14, 15)[1,3,4,5,6,7,8]

Ptaeroglycol (**5**) and ptaeroxylin (**6**) have also been isolated from *Ptaeroxylon obliquum* (Ptaeroxylaceae).[7] A comparison of these pyrones from *Ptaeroxylon obliquum* and *Cedrelopsis grevei* has shown these species to be closely related.

Pennington and Styles[9] grouped the genus *Cedrelopsis* with the South African monospecific genus *Ptaeroxylon* into the Ptaeroxylaceae family since these two genera are similar in morphology and structure of the secondary xylem. The pollen of *Cedrelopsis* and *Ptaeroxylon* is also similar, unlike the Meliaceous pollen grains but similar to that of some Rutaceae.[9] However, there was insufficient evidence to place these genera in the Sapindaceae or Rutaceae. Therefore they were placed in a separate family, the Ptaeroxylaceae, and this was supported by their chemical similarities.

A recent investigation[8] showed the same types of compounds (chromones and coumarins) from a specimen of *Cedrelopsis grevei* collected in the south of Madagascar. Unexpected limonoids (cedmiline (**14**) and cedmilinol (**13**))[1] were isolated from a specimen collected in the north. Therefore a further specimen from the north was re-investigated to isolate more of these compounds, which were required for screening purposes because of their unusual structures. Additional compounds were also isolated from this specimen.

The proposed biosynthesis of cedmilinol (**13**) (scheme 5.1) and cedmiline (**14**) (scheme 5.2) are shown below starting from a limonoid such as obacunone.[1,10]

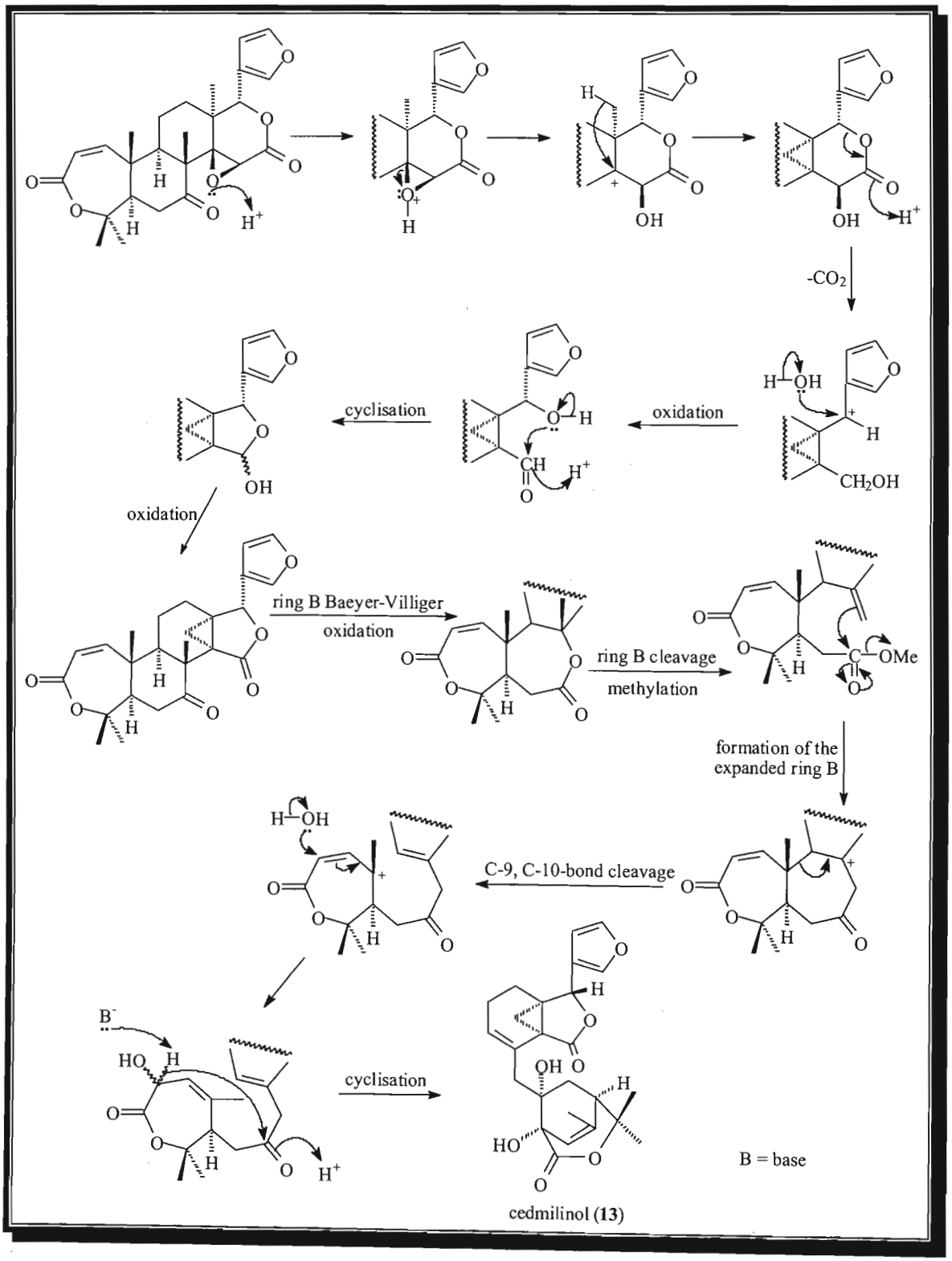

Scheme 5.1. Proposed biosynthesis of cedmilinol (13)[1,10]

Scheme 5.1 shows the formation of the cyclopropane ring at C-13 and C-14, followed by the contraction of ring D with the elimination of carbon dioxide. Ring B expansion occurs and is followed by C-9, C-10-bond cleavage and C-2, C-7-bond formation to furnish cedmilinol (**13**).[1]

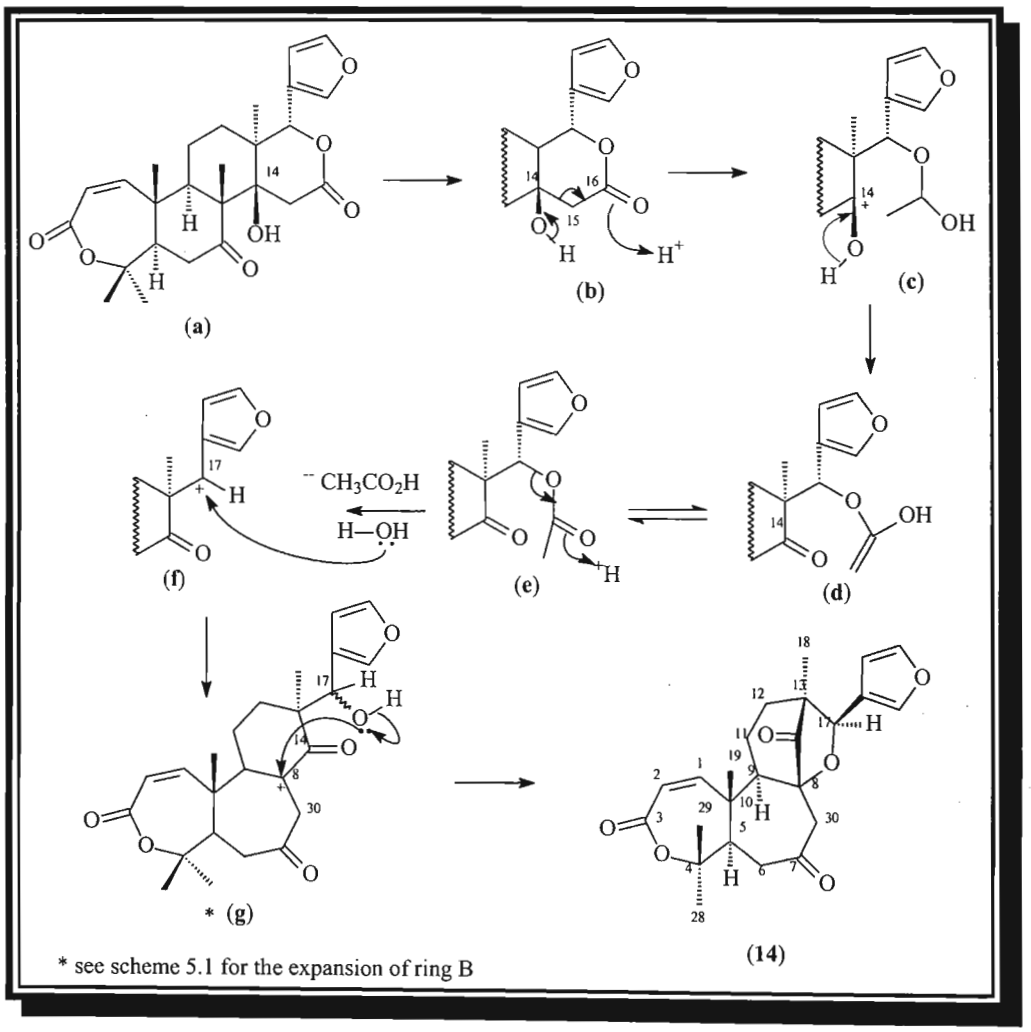

Scheme 5.2. Proposed biosynthesis of cedmiline (14)[1]

The biosynthetic pathway for cedmiline (**14**) (Scheme 5.2) has been explained by the ring D opening and the loss of acetic acid, followed by the expansion of ring B as shown previously in scheme 5.1. This is followed by an ether bond formation between C-17 and C-8 to furnish cedmiline (**14**).[1]

5.2 Discussion

Further investigation of the stem bark of a second specimen of *Cedrelopsis grevei* collected in the north of Madagascar again yielded the limonoid, cedmiline (**14**), the pentacyclic triterpenoid β-amyrin (**15**), the coumarin, scoparone (**16**), a novel triterpenoid derivative, which we name cedashnine (**17**), a novel lignan, which we name cedpetine (**18**), a novel quassinoid, which we name cedphiline (**19**) and the common phytosteryl glycoside, sitosteryl β-D-glucopyranoside (**20**).

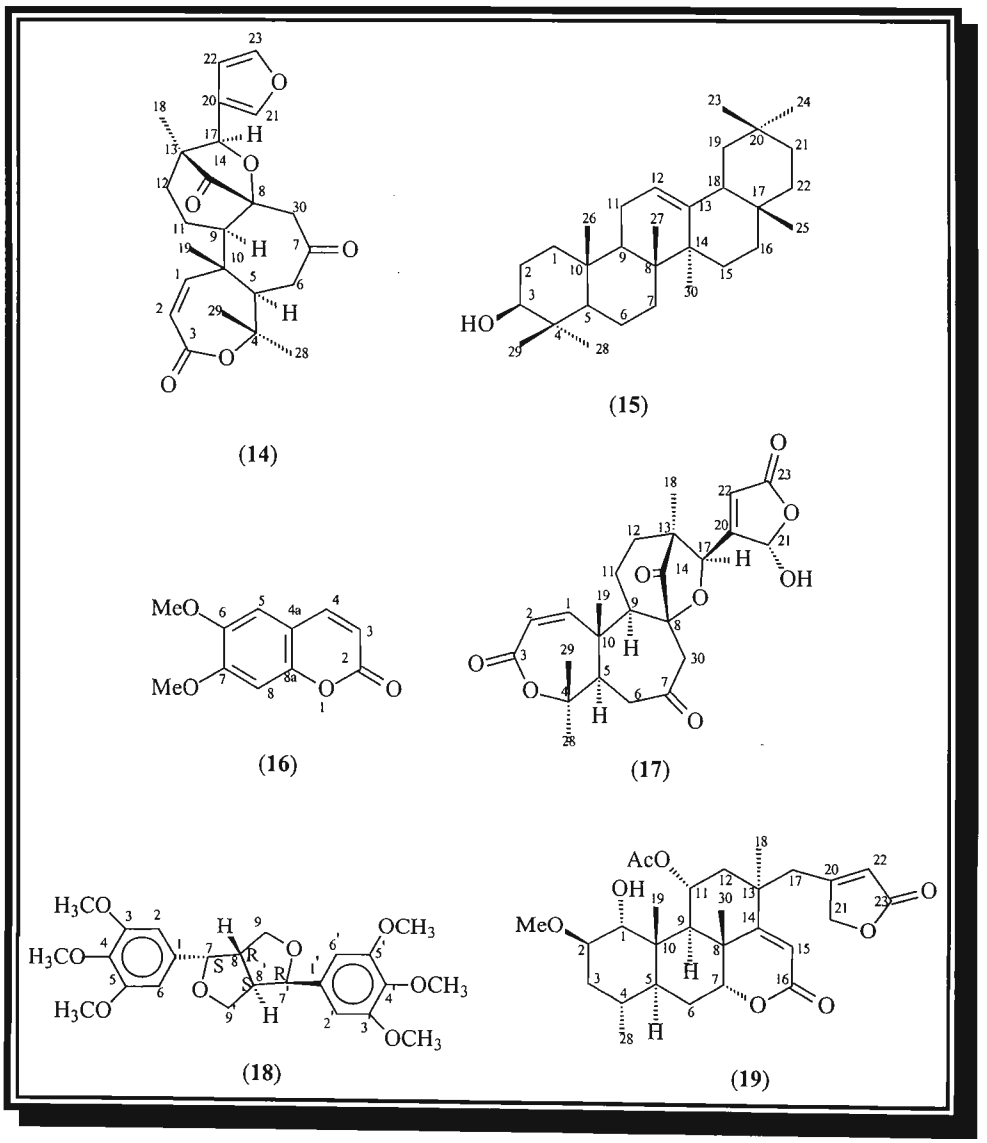

Fig. 5.2a. Compounds isolated from *Cedrelopsis grevei*

Sitosteryl β-D-glucopyranoside (**20**) was acetylated to afford the tetra-acetate (**21**).

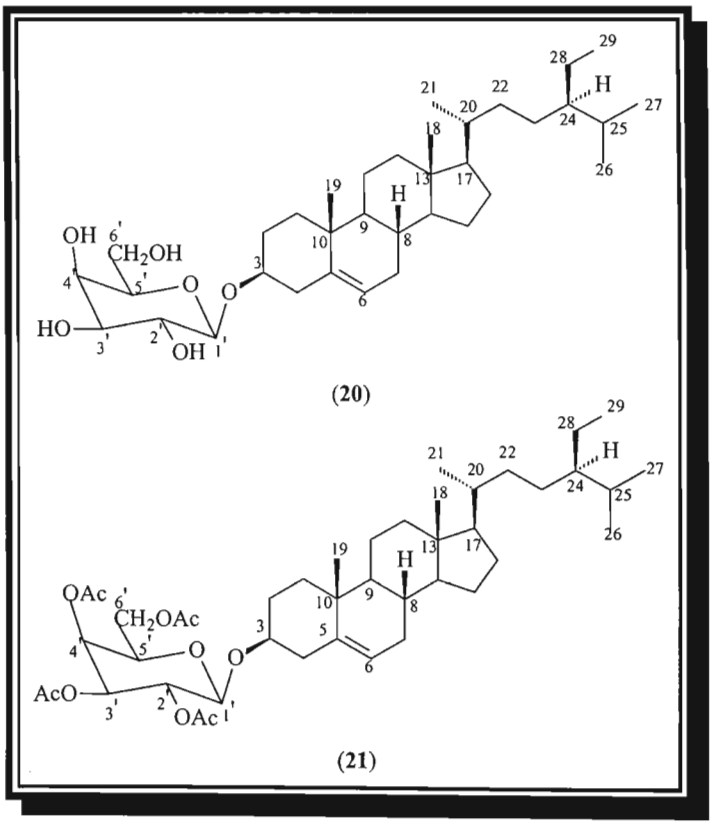

Fig. 5.2b. Compounds from *Cedrelopsis grevei*

Sitosteryl β-D-glucopyranoside (**20**) is an antineoplastic agent and is used in the drug industry to treat benign prostate hypertrophy.[11]

5.3 Structural elucidation of compounds isolated from *Cedrelopsis grevei*

Structural elucidation of cedmiline (14)

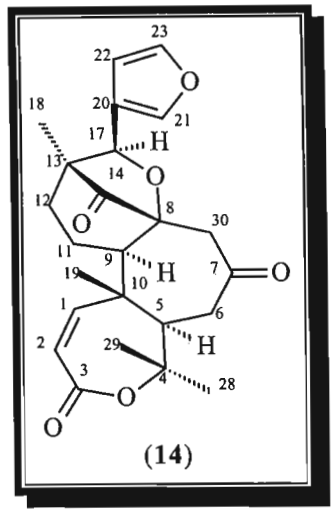

Fig. 5.3. Cedmiline (14)

Cedmiline (**14**) was isolated as a white crystalline material, mp 295-296°C. The mass spectrum **[4]** for this compound showed a molecular ion [M^+] at *m/z* 412 corresponding to the molecular formula $C_{24}H_{28}O_6$. The IR spectrum **[5]** showed C=O absorptions at 1702 cm^{-1} and 1766 cm^{-1}.

The ^1H NMR spectrum **[6]** showed the typical furan ring protons at δ_H 7.35 (H-23), 7.37 (H-21) and 6.04 (H-22) all appearing as one proton resonances. The signals at δ_C 144.12, 140.38, and 108.32 in the ^{13}C NMR spectrum **[7]** were assigned to C-23, C-21 and C-22 respectively, using the HSQC spectrum **[9-10]**.

The resonance assigned to H-17 appeared as a one proton singlet at δ_H 5.08 and showed HMBC **[11]** correlations to C-12 (δ_C 40.48), C-13 (δ_C 51.34), C-8 (δ_C 81.48), C-20 (δ_C 124.83), C-22 (δ_C 108.32), C-21 (δ_C 140.38) and C-14 (δ_C 213.58).

The H-17 resonance showed a NOESY **[13]** correlation with 3H-18 indicating the α-orientation of H-17, leaving the furan ring at C-17 with a β-orientation. The two H-12 resonances appeared as multiplets at δ_H 1.64 and 2.04 and were assigned using the HSQC spectrum **[9-10]**. The H-12 resonance at δ_H 2.04 showed a NOESY **[13]** correlation with H-17 indicating the α-orientation for this H-12 proton, leaving the H-12 resonance at δ_H 1.64 to be β-orientated.

The H-12α resonance showed a NOESY **[13]** correlation with the H-11 resonance at δ_H 1.86 which showed a NOESY **[13]** correlation with H-9, confirming that this H-11 proton was α-orientated, leaving the H-11 proton resonance at δ_H 2.04 with a β-orientation. The NOESY **[13]** correlation between H-12β and H-11β confirmed the stereochemistry of these protons. The resonance at δ_C 21.67 was assigned to C-11 using the HSQC **[9-10]** spectrum.

The two H-30 proton resonances appeared as a pair of doublets (J = 12.45 Hz) at δ_H 2.37 and 3.43 and showed COSY **[12]** correlations to each other. The H-30 resonance at δ_H 2.37 showed a NOESY **[13]** correlation with H-21 (δ_H 7.37) and H-22 (δ_H 6.04) of the furan ring which indicated that this H-30 proton was β-orientated, leaving the H-30 proton resonance at δ_H 3.43 with an α-orientation. A model of cedmiline (**14**) confirmed that the H-30 proton resonance at δ_H 2.37 had to be β-orientated for correlations between the furan ring protons and this H-30 resonance to be seen.

The HSQC **[9-10]** spectrum showed the two H-6 proton resonances occurring as double doublets at δ_H 2.47 (J = 13.00, 16.89 Hz) and δ_H 2.63 (J = 4.40, 16.89 Hz). Both these protons showed HMBC **[11]** correlations to C-5 (δ_C 52.25) and C-7 (δ_C 206.72). A double doublet signal at δ_H 2.97 (J = 4.40, 13.00 Hz) was assigned to H-5 using the HSQC **[9-10]** spectrum, and showed HMBC **[11]** correlations to C-29 (δ_C 20.65), C-10 (δ_C 47.36), C-9 (δ_C 63.81) and C-4 (δ_C 83.96).

The H-6 resonance at δ_H 2.47 showed NOESY **[13]** correlations with 3H-19 (δ_H 1.23) and 3H-29 (δ_H 1.51) which are β-orientated on biosynthetic grounds, therefore indicating the β-orientation for this H-6 proton at δ_H 2.47, leaving the H-6 proton at δ_H 2.63 to be assigned an α-orientation.

The C-19 methyl group protons (δ_H 1.23) showed HMBC **[11]** correlations to C-10 (δ_C 47.36), C-5 (δ_C 52.25), C-9 (δ_C 63.81) and C-1 (δ_C 152.18). The doublet at δ_H 6.17 (J = 13.00 Hz) was therefore assigned to H-1 using the HSQC **[9-10]** spectrum. The H-1 resonance showed COSY **[12]** coupling to H-2, which appeared as a doublet at δ_H 5.92 (J = 13.00 Hz). The signal at δ_C 119.44 was therefore assigned to C-2 using the HSQC spectrum **[9-10]**. The H-2 resonance showed HMBC **[11]** correlations to C-10 (δ_C 47.36) and to the C-3 carbonyl resonance (δ_C 166.06).

The methyl group proton singlet at δ_H 0.87 showed HMBC **[11]** correlations to C-12 (δ_C 40.48), C-13 (δ_C 51.34), C-17 (δ_C 78.78) and C-14 (δ_C 213.58) and was assigned to the 3H-18 protons. The C-18 resonance appeared at δ_C 14.79 using the HSQC **[9-10]** spectrum.

The C-19 methyl group protons (δ_H 1.23) showed NOESY **[13]** interactions with the three proton singlet at δ_H 1.51 (3H-29) **[13]**. The remaining methyl group proton singlet at δ_H 1.43 was assigned to the C-28 methyl group protons. The 3H-28 protons showed NOESY **[13]** interactions with H-5 (δ_H 2.97) which, in turn, showed NOESY **[13]** interactions with H-9 (δ_H 2.04). The resonance at δ_C 32.26 was assigned to C-28 by use of the HSQC **[9-10]** spectrum.

The NMR data for cedmiline (**14**) are shown in table 5.1 (page 98) and agree with those previously reported for cedmiline.[1]

Structural elucidation of β-amyrin (15)

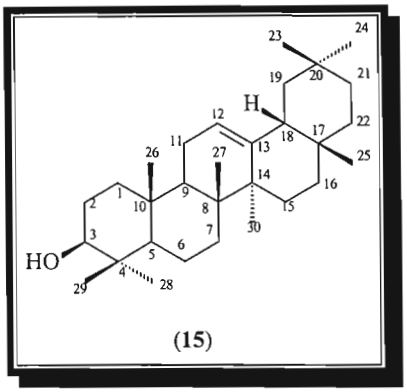

Fig. 5.4. β-Amyrin (15)

β-Amyrin (**15**) was isolated as a white crystalline material, mp 193-194 °C. The structure of this compound was determined by comparing ^{13}C NMR data from literature.[12] As a result of the mass spectrometers at UND and Cape Technikon being unavailable, a mass spectrum of β-amyrin (**15**) was not obtained. However a mass spectrum from a standard sample of β-amyrin (**15**) isolated previously in the laboratory,[13] whose ^{1}H NMR spectrum was identical with the compound isolated, showed a molecular ion [M^+] at 426 corresponding to a molecular formula of $C_{30}H_{50}O$.

The molecular formula indicated that six double bond equivalents were present in this compound. The IR spectrum **[15]** showed the presence of a hydroxy group stretching band at 3364 cm^{-1}.

The one proton oxymethine multiplet at δ_H 3.20 and the one proton olefinic triplet at δ_H 5.16 were assigned to H-3 and H-12 respectively in the ^{1}H NMR spectrum **[16]**. The H-12 resonance accounted for one of the six double bond equivalents within the triterpenoid nucleus leaving a pentacyclic triterpenoid structure. The eight tertiary methyl groups appeared at δ_H 0.77, 0.81, 0.85 (6H), 0.91, 0.94, 0.97, and 1.11 in the ^{1}H NMR spectrum **[16]**.

The resonances at δ_C 121.70 and 145.19 in the ^{13}C NMR spectrum **[17]** were assigned to the olefinic carbons. These resonances are characteristic of pentacyclic triterpenoids and were assigned to C-12 and C-13 respectively of the Δ^{12}-oleanones. The oxymethine carbon resonance at δ_C 79.04 in the ^{13}C NMR spectrum **[17]** is typical for C-3 of Δ^{12}-oleanones with a 3β-hydroxy group. Compound (**15**) was confirmed to be β-amyrin by comparison of the ^{13}C NMR data (Table 5.2, page 99) with that from the literature.[12]

Structural elucidation of scoparone (16)

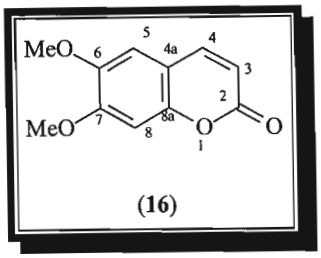

Fig. 5.5a. Scoparone (16)

This is the only simple coumarin isolated from *Cedrelopsis grevei*. It was previously isolated from a sample from the same species from the dry south of Madagascar.[8]

Scoparone (**16**) was isolated as a yellow gum. The mass spectrum **[19]** of this compound showed a molecular ion [M^+] peak at *m/z* 206, which corresponded to the molecular formula $C_{11}H_{10}O_4$. This compound contained six double bond equivalents.

The IR spectrum **[20]** showed the presence of C-H stretch bands at 2927 cm^{-1} and 2852 cm^{-1}, a carbonyl band at 1729 cm^{-1} and a C=C stretch band at 1623 cm^{-1}.

The UV absorption spectrum **[21]** showed absorptions at 344 nm (log ε 3.5), 295 nm (log ε 3.4), and 231 nm (log ε 3.8), as well as a shoulder absorption at 260 nm, which is typical for 6,7-dioxygenated coumarins.

The pair of doublets at δ_H 7.60 (J = 9.34 Hz) and 6.26 (J = 9.34 Hz) in the ^1H NMR spectrum **[22]** were assigned to H-4 and H-3 respectively. These resonances indicated the presence of a coumarin nucleus, with an unsubstituted pyrone ring. All six double bond equivalents could be assigned to this nucleus, confirming the presence of a simple coumarin.

The H-4 and H-3 resonances showed COSY **[26]** and NOESY **[27]** correlations with each other. The H-4 resonance also showed a NOESY **[27]** correlation with the singlet at δ_H 6.83, which was assigned to H-5. The H-5 resonance (δ_H 6.83) showed a NOESY **[27]** correlation with the methoxy group proton resonance at δ_H 3.90, indicating that the methoxy group was attached at C-6. The carbon resonances at δ_C 143.30, 113.52 and 107.90 were assigned to C-4, C-3 and C-5 respectively, by use of the HSQC spectrum **[24]**.

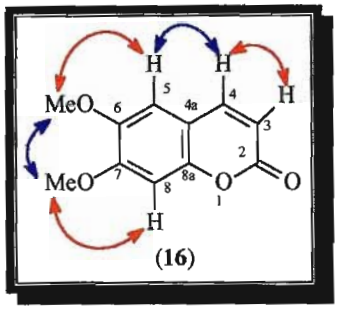

(16)

Fig. 5.5b. NOESY correlations of scoparone (16)

The C-6 methoxy group methyl proton resonance at δ_H 3.90 showed NOESY **[27]** correlations with the second methoxy group proton resonance at δ_H 3.93, which indicated that the second methoxy group was attached at C-7. The methoxy methyl group protons at C-7 (δ_H 3.93) also showed a NOESY correlation with the singlet at δ_H 6.82, which was assigned to H-8. The resonance at δ_C 99.98 was assigned to C-8 using the HSQC NMR spectrum **[24]**.

From the HSQC NMR spectrum **[24]**, resonances at δ_C 56.33 and 56.37 were assigned to the C-6 and C-7 methoxy group carbons respectively. The resonance at δ_C 111.41 showed HMBC **[25]** correlations with H-3 (δ_H 6.26), H-4 (δ_H 7.60) and H-8 (δ_H 6.82) and was assigned to C-4a. The H-3 and H-4 resonances showed HMBC **[25]** correlations with the resonance at δ_C 161.43, which was assigned to C-2. The H-8 singlet showed HMBC **[25]** correlations with C-8a (150.0), C-6 (146.31) and C-4a (δ_C 111.41). The H-5 (δ_H 6.83) resonance showed HMBC **[25]** correlations with C-7 (δ_C 152.81), C-8a (δ_C 150.00), C-6 (δ_C 146.31) and C-4 (δ_C 143.30).

The NMR data for scoparone (**16**) are shown in table 5.3, page 100.

Structural elucidation of cedashnine (17)

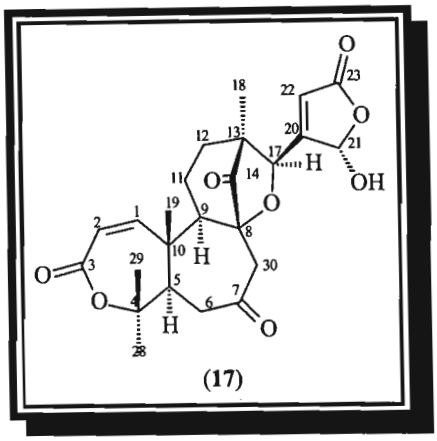

Fig. 5.6a. Cedashnine (17) - novel triterpenoid derivative

Cedashnine (**17**), a hexanortriterpenoid, was isolated as a white crystalline material, mp 220-221 °C. The mass spectrum **[29]** for this compound showed a molecular ion peak [M^+] at *m/z* 444.17759 corresponding to a molecular formula of $C_{24}H_{28}O_8$. The fragment ion peak at *m/z* 426.16951 was due to the loss of H_2O. The IR spectrum **[30]** showed bands at 1710 cm^{-1} and 1756 cm^{-1} due to carbonyl absorptions, and bands at 2861 cm^{-1} and 2921 cm^{-1} due to C-H stretching. The band at 3381 cm^{-1} was due to the hydroxy group stretching.

The NMR spectra for cedashnine (**17**) are similar to those of cedmiline (**14**). The only difference between the two compounds is the furan ring, which is in an oxidised form in cedashnine (**17**). The NMR spectra of cedashnine (**17**) were the same as those of cedmiline (**14**) in the following ways:

The resonance assigned to H-17 appeared as a one proton singlet at δ_H 5.25 and showed HMBC **[35]** correlations to C-12 (δ_C 41.43), C-13 (δ_C 51.05), C-21 (δ_C 98.00) and C-14 (δ_C 212.29). The presence of the two ketone carbonyl carbon resonances at δ_C 209.03 (C-7) and δ_C 212.29 (C-14) are the same as in cedmiline (**14**).

The two H-12 proton resonances appeared as multiplets at δ_H 1.60 and 2.06 by use of the HSQC spectrum **[33-34]** and both these resonances showed COSY **[36]** correlations with the two H-11 proton resonances at δ_H 1.88 (m) and 2.06 (m). The C-11 resonance appeared at δ_C 21.34 by use of the HSQC spectrum **[33-34]**. The two H-30 proton resonances appeared as a pair of doublets (J = 12.27 Hz) at δ_H 2.46 and 3.57 in the ^{1}H NMR spectrum **[31]**.

The H-30 resonance at δ_H 2.46 showed a NOESY **[37]** correlation with 3H-19 (δ_H 1.22), which suggested a β-orientation for this proton, leaving the H-30 resonance at δ_H 3.57 to be assigned an α-orientation. This assignment was confirmed by a NOESY **[37]** correlation between H-30α and H-5α. The two H-30 protons showed HMBC **[35]** correlations with C-7 (δ_C 209.03) and C-8 (δ_C 82.72).

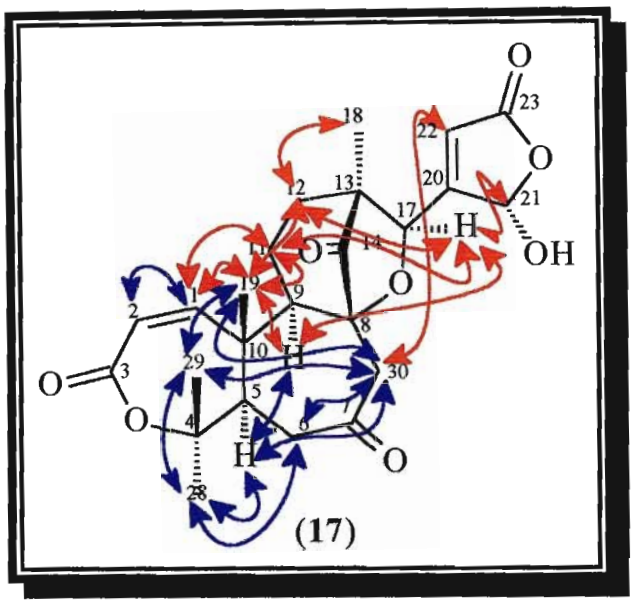

Fig. 5.6b. NOESY correlations of cedashnine (17)

The C-19 methyl group protons (δ_H 1.22) showed NOESY **[37]** interactions with the three proton singlet at δ_H 1.53 (3H-29). The singlet at δ_H 1.43 was assigned to the C-28 methyl group protons. The 3H-28 protons showed NOESY interactions with H-5 (δ_H 3.09) which, in turn, showed NOESY interactions with H-9 (δ_H 1.99) **[37]** as expected. The C-28 resonance occurred at δ_C 31.10. Both the 3H-28 and 3H-29 resonances showed HMBC **[35]** correlations with C-4 (δ_C 84.82).

The resonances assigned to the two H-6 protons appeared as double doublets at δ_H 2.46 (superimposed with one of the H-30 resonances) (J = 7.80, 16.95 Hz) and δ_H 2.78 (J = 4.02, 16.95 Hz) using the HSQC **[33-34]** spectrum. The H-6 resonance at δ_H 2.78 showed NOESY **[37]** correlations with 3H-28 and H-5 indicating it was α-orientated. Thus the other H-6 resonance (δ_H 2.46) was assigned the β-stereochemistry. The NOESY **[37]** correlations between H-6β and 3H-19 and 3H-29 confirmed the stereochemistry for this proton.

Both the H-6 resonances showed COSY **[36]** correlations with the H-5 resonance (δ_H 3.09). The resonance at δ_C 51.91 was assigned to C-5 by use of the HSQC **[33-34]** spectrum and showed HMBC **[35]** correlations with H-1 (δ_H 6.37), 3H-19 (δ_H 1.22), 3H-28 (δ_H 1.43) and 3H-29 (δ_H 1.53). The H-1 doublet at δ_H 6.37 (J = 12.87 Hz) showed coupling in the COSY **[36]** spectrum to H-2 which appeared as a doublet (J = 12.87 Hz) at δ_H 5.90. The signals at δ_C 153.99 and δ_C 118.44 were assigned to C-1 and C-2 respectively using the HSQC **[33-34]** spectrum. The C-3 lactone carbonyl carbon resonance occurred at δ_C 167.51.

The methyl group proton singlet at δ_H 0.97 showed HMBC **[35]** correlations to C-12 (δ_C 41.43), C-13 (δ_C 51.05), C-17 (δ_C 79.61) and C-14 (δ_C 212.29), and was assigned to the 3H-18 protons. The C-18 resonance appeared at δ_C 13.60 by use of the HSQC spectrum **[33-34]**.

These correlations showed that the tetracyclic structure was the same for both cedashnine (**17**) and cedmiline (**14**). However, the resonances ascribed to the furan ring protons were absent in the ^{1}H NMR spectrum of cedashnine (**17**).

Subtracting the atoms and the number of double bond equivalents required for the tetracyclic structure left $C_4H_3O_3$ and three double bond equivalents for the side chain. Double bond carbons were seen at δ_C 120.23 (C-20) and δ_C 153.99 (C-22), a lactone carbonyl carbon was present at δ_C 167.13 (C-23) and a resonance at δ_C 98.00 (C-21) indicating a carbon bonded to two oxygens were present in the ^{13}C NMR spectrum **[32]**. Two proton resonances each integrating to one proton were present as singlets at δ_H 6.10 and δ_H 6.25. The HSQC spectrum **[33-34]** showed that these proton resonances correlated with ^{13}C NMR resonances at δ_C 153.99 and δ_C 98.00 enabling their assignments as H-22 and H-21 respectively. Both C-21 and C-22 ^{13}C NMR resonances showed HMBC **[35]** correlations with H-17 supporting the proposed structure.

It is interesting that only one epimer was seen for this compound. Usually paired resonances are seen for the carbon and proton resonances because of the hemiacetal existing as a mixture of epimers at C-21. A model was constructed in order to try and explain this observation. There is a possibility of H-bonding occurring between the 8, 17-ether oxygen and the 21-hydroxy group proton if the hydroxy group is α-orientated. Evidence for this is the observed NOESY **[37]** correlation between H-21 (which would have to be β-orientated for this to occur) and the 3H-18 methyl group proton resonance. This would necessitate an *S* configuration at C-21.

The H-17 resonance showed a NOESY **[37]** correlation with 3H-18, which indicated an α-orientation of H-17. The H-12 resonance at δ_H 2.06 showed NOESY **[37]** correlations with H-17. The model of cedashnine (**17**) confirmed the α-orientation for this H-12 resonance, leaving the β-orientation for the H-12 resonance at δ_H 1.60. The H-12β and 3H-19 resonances showed NOESY **[37]** correlations with the H-11 resonance at δ_H 2.06 indicating a β-orientation for this proton, and the H-9 resonance showed a NOESY **[37]** correlation with the H-11 resonance at δ_H 1.88 confirming an α-orientation for this proton. The cedashnine (**17**) model showed that the 8, 13-bridge had to be β-orientated for it to exist.

The NMR data for cedashnine (**17**) are shown in table 5.4, page 101. Comparison of the NMR data for cedashnine (**17**) and those of cedmiline (**14**) are shown in table 5.5, page 102.

Biosynthesis of cedashnine (17)

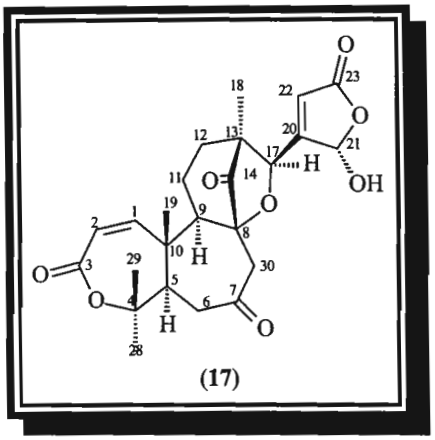

Fig. 5.6a. Cedashnine (17) - novel triterpenoid derivative

The proposed biosynthetic pathway for the tetracyclic part of cedashnine (**17**) (Scheme 5.2, page 74)[1] has been explained by ring D opening and the loss of an acetic acid residue, followed by the expansion of ring B and subsequent ether bond formation between C-17 and C-8. The modification of the triterpenoid side chain to give the butenolide structure is shown in scheme 5.3.

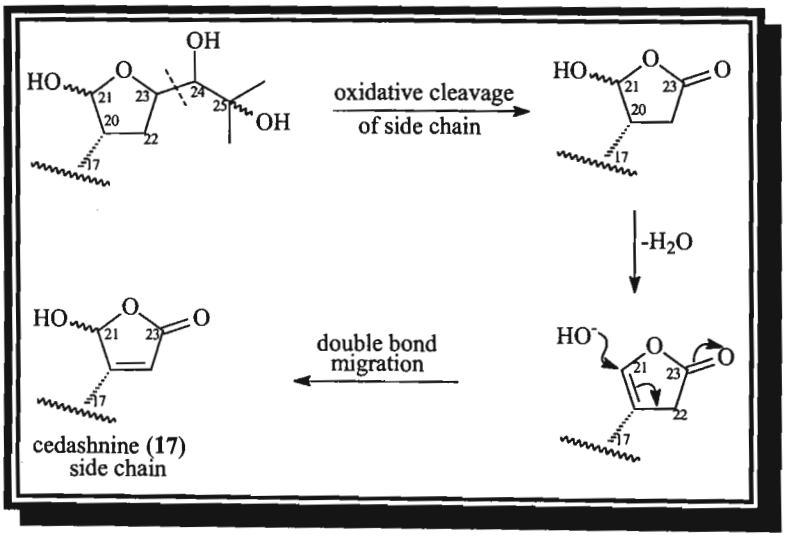

Scheme 5.3. Proposed formation of the cedashnine (17) side chain

Structural elucidation of cedpetine (18)

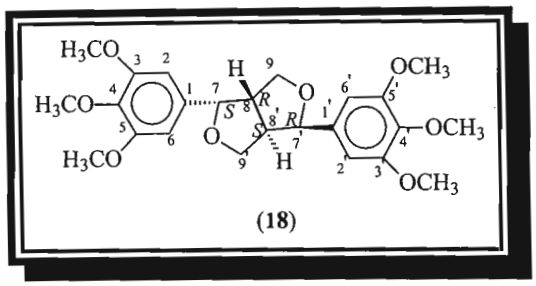

Fig. 5.7a. Cedpetine (18) - novel lignan

The lignan cedpetine (**18**) was isolated as yellow crystalline material, mp 265-266 °C. The mass spectrum **[39]** for this compound showed a molecular ion peak [M^+] at *m/z* 446.19458 corresponding to a molecular formula of $C_{24}H_{30}O_8$. The fragment ion peak at *m/z* 415.17539 showed the loss of a methoxy group. The IR spectrum **[40]** showed C-H stretching bands at 2931 cm^{-1} and 2858 cm^{-1} and C-O absorptions at 1011, 1133 and 1238 cm^{-1}. The UV absorption spectrum **[40]** showed absorptions at 272 nm (log ε 4.0) and 229 (log ε 4.6). Cedpetine (**18**) was found to be optically inactive, a zero reading was obtained when the optical rotation was measured.

Cedpetine (**18**) is a symmetrical compound and only one half of the expected number of resonances are seen in the NMR spectra. Thus only one half of the molecule will be discussed initially, then the combination of the two equivalent parts will be discussed. A singlet at δ_H 6.55 in the ^1H NMR spectrum **[41]** integrated to two protons, which indicated the presence of two equivalent non-substituted aromatic ring carbons. This singlet was assigned to H-2/6. The C-2/6 resonance appeared at δ_C 102.97 by use of the HSQC spectrum **[44]**.

The two singlets at δ_H 3.85 and 3.81 **[41]** integrated to six and three protons respectively indicating the presence of two equivalent methoxy groups and a third non-equivalent methoxy group. The resonance at δ_C 153.56 in the ADEPT NMR spectrum **[43]** was assigned to the two equivalent fully substituted aromatic ring carbons C-3 and C-5. This resonance showed HMBC **[45]** correlations to the methoxy group proton singlet at δ_H 3.85, which indicated that these two equivalent methoxy groups were attached at C-3 and C-5. The resonance at δ_C 56.46 was assigned to the C-3 and C-5 methoxy group carbons by use of the HSQC spectrum **[44]**. The methoxy groups were attached at C-3 and C-5 instead of C-2 and C-6 since the 3/5 methoxy group protons showed NOESY **[47]** correlations to the δ_H 6.55 singlet (H-2/6), which was COSY **[46]** correlated to H-7 (δ_H 4.72) (benzylic coupling).

The resonance at δ_C 137.59 was assigned to the fully substituted aromatic ring carbon C-4, and showed HMBC **[45]** correlations to the methoxy group proton singlet at δ_H 3.81. This indicated that the third methoxy group was attached at C-4. The resonance at δ_C 61.11 was assigned to the C-4 methoxy group carbon using the HSQC spectrum **[44]**.

The resonance at δ_C 136.87 in the ^{13}C NMR spectrum **[42]** was assigned to the fully substituted C-1, which showed HMBC **[45]** correlations to H-7 (δ_H 4.72) and H-8 (δ_H 3.08). The resonances at δ_C 86.18 and 54.63 were assigned to C-7 and C-8 respectively by the use of the HSQC spectrum **[44]**. The methylene carbon resonance at δ_C 72.22 was assigned to C-9, and it showed a HMBC **[45]** correlation to H-7.

The ^{13}C NMR spectrum **[42]** showed one oxygenated methine resonance at δ_C 86.18 and one oxygenated methylene resonance at δ_C 72.22. According to the mass spectrum **[39]**, each half of the lignan should contain four oxygens, three being part of the methoxy groups, leaving one oxygen atom from this half of the molecule and one from the other half to form two ether linkages. The H-7 resonance showed COSY **[46]** correlations with the H-8 and the 2H-9 resonances.

The H-8 resonance also showed COSY **[46]** correlations with the 2H-9 and the H-7 resonance. The H-7 resonance also showed COSY **[46]** correlations with H-2 and H-6 confirming that C-7 was attached at C-1 of the aromatic ring. The chemical shifts of C-7 (δ_C 86.18), C-8 (δ_C 54.63) and C-9 (δ_C 72.22) and the symmetrical nature of the molecule necessitated the ether linkages to occur between C-7 and C-9', and C-9 and C-7' and a C-C bond to occur between C-8 and C-8' as shown in figure 5.7a.

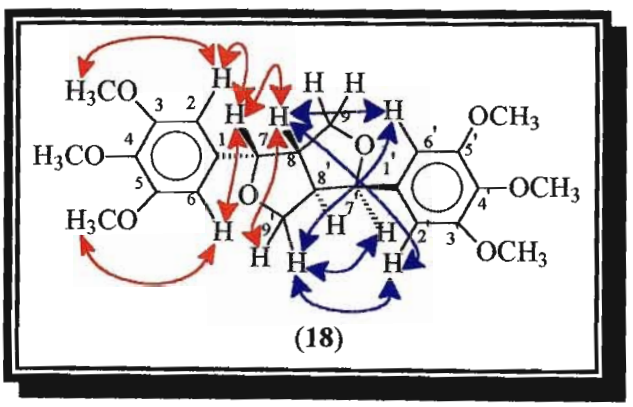

(18)

Fig. 5.7b. NOESY correlations of cedpetine (18)

An optical rotation of zero was obtained for cedpetine (**18**) which indicated that the compound was a *meso* compound. The NOESY NMR spectrum **[47]** showed correlations between the H-7 and H-8 resonances, therefore these protons are *cis* to each other.

The H-7 and H-8 resonances were arbitrarily assigned the β-stereochemistry giving the stereochemistry at C-7 and C-8 to be *S* and *R* respectively. As this is a *meso* compound, the stereochemistry at C-7' and C-8' has to be *R* and *S* respectively, giving both H-7' and H-8' the α-stereochemistry. The arbitrary assignment of the β-stereochemistry to H-7 and H-8 is justified as the molecule is symmetrical. The same final result would have been obtained if they had been assigned the α-stereochemistry, making H-7' and H-8' β-orientated.

The NMR data for cedpetine (**18**) are shown in table 5.6, page 103.

Biosynthesis of cedpetine (18)

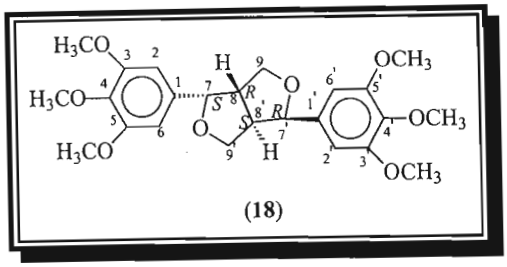

Fig. 5.7a. Cedpetine (18) - novel lignan

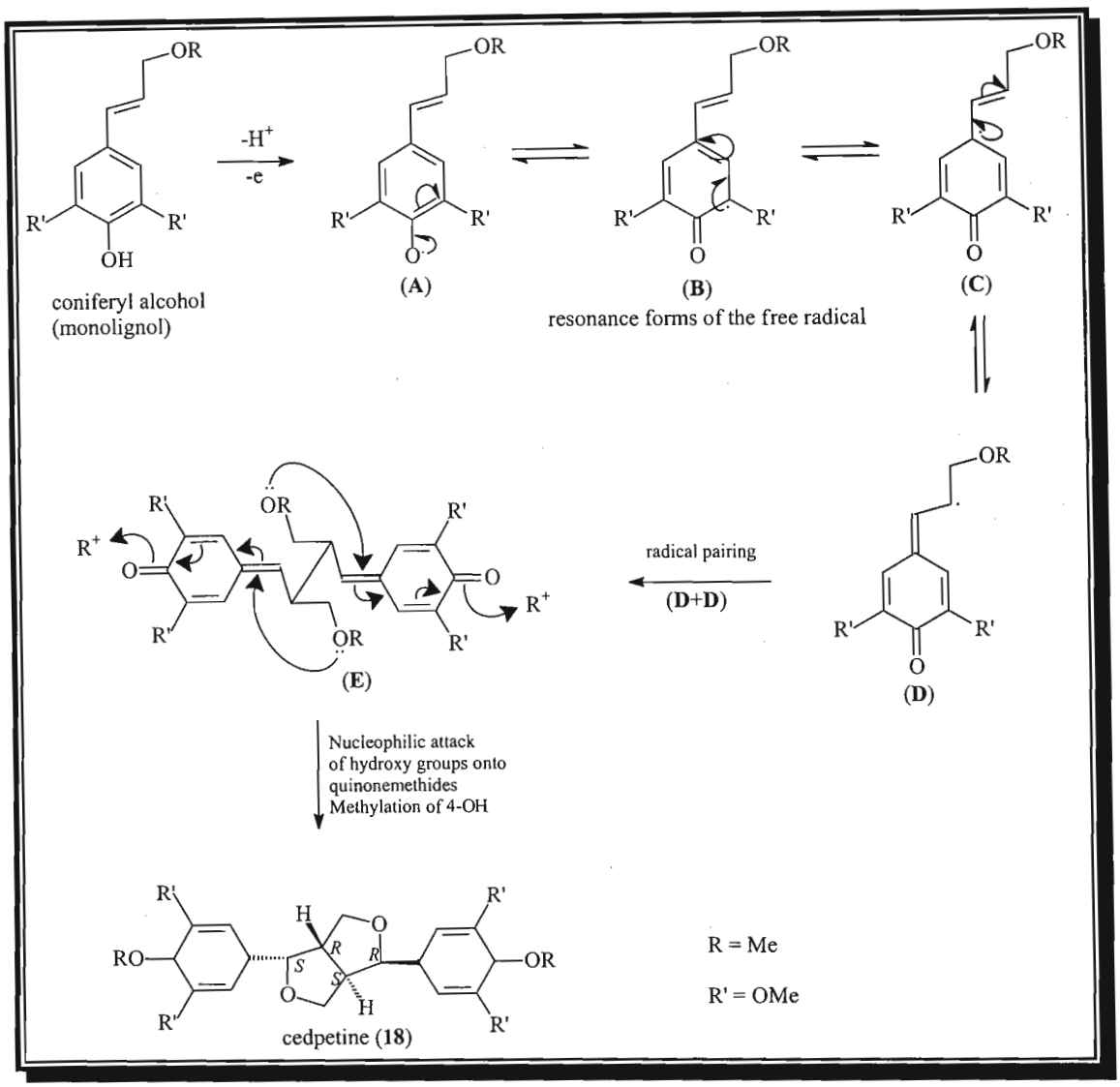

Scheme 5.4. Proposed biosynthesis of cedpetine (18)

The monolignol undergoes a one electron oxidation to result in the free radical resonance hybrids (**A**, **B**, **C** and **D**). Radical pairing of the two free radicals (**D** + **D**), results in (**E**). Nucleophilic attack of the hydroxy group oxygens onto the quinonemethides of (**E**), results in the formation of the lignan, cedpetine (**18**).

Structural elucidation of cedphiline (19)

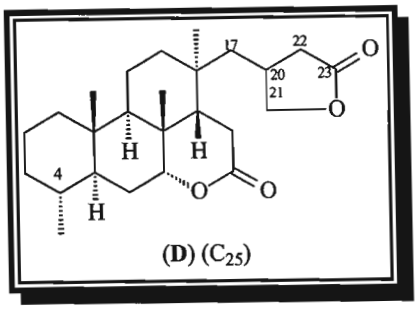

Fig. 5.8a. C_{25} quassinoid of type D

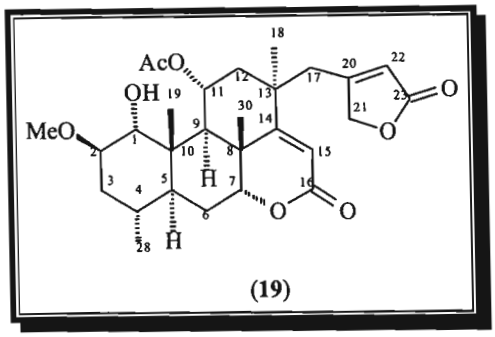

Fig. 5.8b. Cedphiline (19) - novel quassinoid

The quassinoid cedphiline (**19**) was isolated as a white crystalline material, mp 160-161 °C. The mass spectrum **[49]** for this compound showed a molecular ion peak [M^+] at *m/z* 502.25593 corresponding to the molecular formula of $C_{28}H_{38}O_8$. The fragment ion peaks at *m/z* 459.23942 and 442.23434 showed the loss of CH_3-CO and CH_3-COOH respectively as expected. The IR spectrum **[50]** showed a hydroxy stretch band at 3500 cm^{-1}, a C-H stretch bands at 2917 $cm^{-1}$and 2855 cm^{-1} and carbonyl absorptions at 1745 and 1719 cm^{-1}.

The ^{13}C NMR spectrum **[52]** showed the presence of twenty-eight carbons, including an acetate group and a methoxy group, indicating that compound (**19**) was a C_{25} quassinoid of type (**D**) (fig. 5.8a).

The three methyl group singlets in the ^1H NMR spectrum **[51]** were assigned to 3H-19 (δ_H 1.00), 3H-18 (δ_H 1.32) and 3H-30 (δ_H 1.34), based on their HMBC **[56-57]** correlations. The 3H-19 resonance showed HMBC **[56-57]** correlations to C-1 (δ_C 80.98) and C-9 (δ_C 53.78), and the 3H-30 resonance showed HMBC **[56-57]** correlations to C-7 (δ_C 78.78) and C-9 (δ_C 53.78). The 3H-18 resonance showed a HMBC **[56-57]** correlation to C-17 (δ_C 42.49). The methyl group proton doublet at δ_H 0.93 (J = 6.41 Hz) showed HMBC **[56-57]** correlations to C-3 (δ_C 37.46), C-4 (δ_C 29.12) and C-5 (δ_C 44.22) and was assigned to 3H-28. The C-28 resonance appeared at δ_C 19.99 by use of the HSQC spectrum **[54-55]**.

The H-17a and H-17b coupled protons appeared at δ_H 2.59 (J = 13.74 Hz) and 2.64 (J = 13.74 Hz) respectively in the ^1H NMR spectrum **[51]**. These protons showed HMBC **[56-57]** correlations to C-20 (δ_C 164.24), C-21 (δ_C 74.53) and C-22 (δ_C 120.13) of the butenolide ring. The doublet at δ_H 4.73 (2H, J = 1.09 Hz) and the singlet at δ_H 5.92 was assigned to 2H-21 and H-22 respectively using the HSQC spectrum **[54-55]**. The 2H-21 resonance showed HMBC **[56-57]** correlations to C-20 (δ_C 164.24) and C-22 (δ_C 120.13). The resonance at δ_C 173.14 showed HMBC **[56-57]**correlations with H-21 and H-22 and was assigned to C-23.

The carbonyl carbon resonance at δ_C 164.87 was assigned to C-16 of the ring D lactone. The C-16 resonance showed HMBC **[56-57]** correlations to the resonance at δ_H 5.83, which was assigned to H-15. The H-7 and H-9 resonances appeared at δ_H 4.14 and 1.89 respectively in the ^{1}H NMR spectrum **[51]**. The H-9 resonance (δ_H 1.89) showed HMBC **[56-57]** correlations with C-1 (δ_C 80.98), C-5 (δ_C 44.22), C-7 (δ_C 78.78), C-8 (δ_C 39.07), C-10 (δ_C 42.06), C-11 (δ_C 70.65), C-14 (δ_C 172.44), C-19 (δ_C 11.79), and C-30 (δ_C 22.97). The H-5 and H-1 resonances appeared at δ_H 1.24 and 3.08 respectively by use of the HSQC spectrum **[54-55]**.

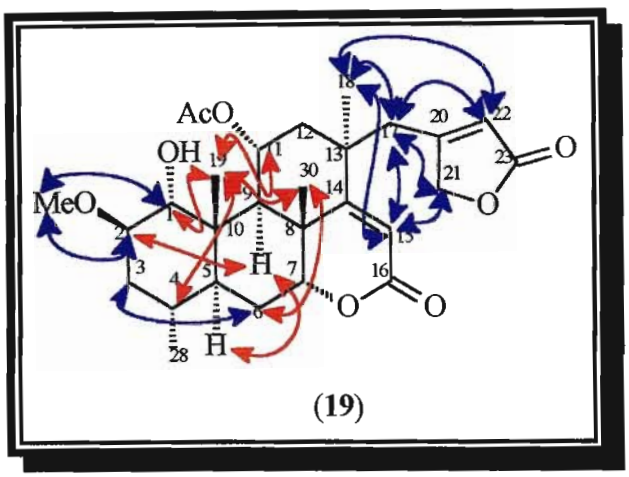

(19)

Fig. 5.8c. NOESY correlations of cedphiline (19)

The H-1 resonance (δ_H 3.08) showed COSY **[58]** correlations with the H-2 resonance at δ_H 3.08. Both of these resonances showed NOESY **[59]** correlations with the methoxy group proton singlet at δ_H 3.33. The resonances at δ_C 80.98, 80.55 and δ_C 56.60 were assigned to C-1, C-2 and the methoxy group carbon respectively by use of the HSQC spectrum **[54-55]**. The methoxy group proton resonance showed HMBC **[56-57]** correlation to C-2 (δ_C 80.55), which confirmed that the methoxy group was attached at C-2. On biosynthetic grounds, 3H-19 and 3H-30 are β-orientated and H-5, H-9, 3H-18 and 3H-28 are α-orientated. The H-1 resonance showed a NOESY **[59]** correlation with 3H-19, and the H-2 resonance showed a NOESY **[59]** correlation with H-9, which indicated the β-orientation for H-1 and the α-orientation for H-2. The methoxy group proton resonance showed a NOESY **[59]** correlation with H-1, which confirmed the β-orientation for the methoxy group.

The H-6 resonance at δ_H 1.82 showed NOESY **[59]** correlations with 3H-19 and 3H-30, which indicated a β-orientation for this H-6 proton. The C-6 resonance appeared at δ_C 25.41 and the remaining H-6α resonance appeared at δ_H 2.05 by use of the HSQC spectrum **[54-55]**. Both the H-6α and H-6β resonances were seen to be coupled in the COSY spectrum **[58]** to H-5 and H-7.

The two H-3 proton resonances appeared at δ_H 0.90 and 2.08 in the ^{1}H NMR spectrum **[51]**. The H-3 resonance at δ_H 0.90 showed NOESY **[59]** correlations with H-2 (δ_H 3.08) and H-5 (δ_H 1.24), which indicated the α-orientation for this H-3 proton, leaving the H-3 resonance at δ_H 2.08 to be assigned a β-orientation.

The acetate group proton resonance appeared at δ_H 1.94 in the ^{1}H NMR spectrum **[51]**. The resonance at δ_C 21.77 was assigned to the methyl carbon of the acetate group by use of the HSQC spectrum **[54-55]**. The carbonyl carbon resonance of the acetate group appeared at δ_C 170.84 and showed HMBC **[56-57]** correlations with H-11 at δ_H 5.64, which indicated that the acetate group was attached at C-11 (δ_C 70.65). The H-11 resonance showed a NOESY **[59]** correlation to 3H-19, which suggested a β-orientation for this H-11 proton, leaving the acetate group with an α-orientation.

The H-11 resonance also showed HMBC **[56-57]** correlations with C-9 (δ_C 53.78), C-12 (δ_C 41.48) and C-13 (δ_C 39.58). The two H-12 resonances appeared as a doublet (J = 16.30 Hz) at δ_H 2.00 and a double doublet (J = 16.30, 5.32 Hz) at δ_H 2.42 using the HSQC spectrum **[54-55]**. The H-12 resonance at δ_H 2.42 showed a NOESY **[59]** correlation with 3H-18 which indicated an α-orientation for this H-12 proton, leaving the H-12 proton resonance at δ_H 2.00 to be assigned the β-orientation. All NOESY **[59]** correlations agreed with the model of cedphiline (**19**).

The NMR data for cedphiline (**19**) are shown in table 5.7, page 104.

Structural elucidation of sitosteryl β-D-glucopyranoside (20)

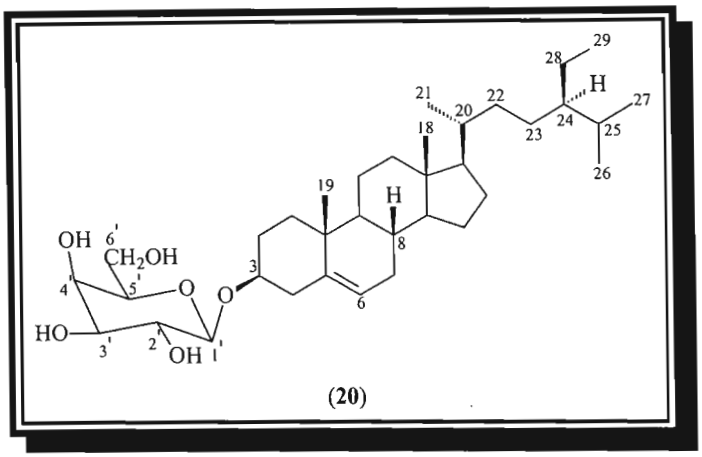

(20)

Fig. 5.9. Sitosteryl β-D-glucopyranoside (20)

Sitosteryl β-D-glucopyranoside (**20**) is a common phytosteryl glycoside. Sitosteryl β-D-glucopyranoside (**20**) was isolated as a white crystalline material, mp 269-270°C. Because sitosteryl β-D-glucopyranoside (**20**) is very polar, it was not fully soluble in solvents required for analysing the compound. Therefore the compound (**20**) was acetylated to afford the tetra-acetate (**21**), which was analysed. The tetra-acetate (**21**) structure was established from NMR spectroscopy.

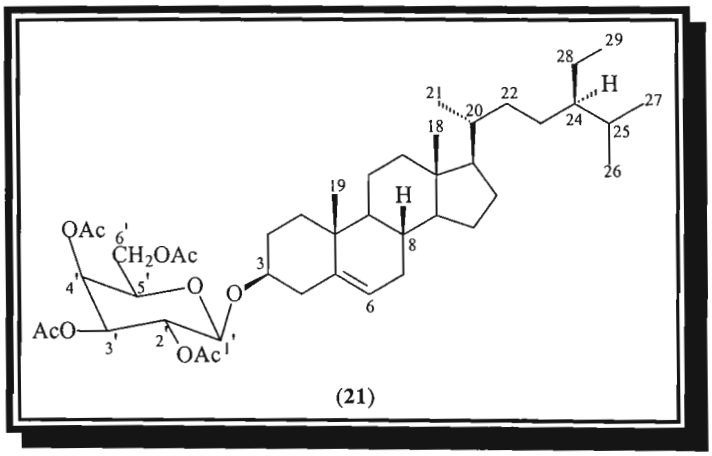

(21)

Fig. 5.10. Sitosteryl β-D-glucopyranoside tetra-acetate (21)

Sitosteryl β-D-glucopyranoside tetra-acetate (**21**) was isolated as a white crystalline material, mp 168-169°C. The IR spectrum **[61]** of sitosteryl β-D-glucopyranoside tetra-acetate (**21**) showed C-H stretch bands at 2924 cm^{-1} and 2853 cm^{-1}, a carbonyl absorption at 1750 cm^{-1} and a C-O stretching band at 1224 cm^{-1}.

The identification of sitosteryl β-D-glucopyranoside (**20**) and sitosteryl β-D-glucopyranoside tetra-acetate (**21**) were performed by comparison against literature data.[14,15]

The ^{1}H NMR spectrum **[62]** of the tetra-acetate (**21**) showed two tertiary methyl group proton resonances at δ_H 0.65 (3H-18) and δ_H 0.96 (3H-19), and four methyl resonances at δ_H 0.90 (3H-21), δ_H 0.80 (3H-26), δ_H 0.78 (3H-27) and δ_H 0.82 (3H-29). The olefinic proton resonance at δ_H 5.33 was assigned to H-6. The acetate methyl group proton resonances appeared at δ_H 2.06, 2.03, 2.00 and 1.98 in the ^{1}H NMR spectrum **[62]**.

The ^{13}C NMR spectrum **[63]** showed a resonance at δ_C 99.62 (C-1'), which indicated the presence of a single monosaccharide. The resonances at δ_C 71.67, 71.47, 68.50 and 62.08 were assigned to C-2', C-3', C-4', C-5' and C-6' of the glucopyranoside ring. The resonances at δ_C 122.17 and 140.34 were assigned to C-6 and C-5 respectively.

The NMR data for sitosteryl β-D-glucopyranoside (**20**) and sitosteryl β-D-glucopyranoside tetra-acetate (**21**) are shown in table 5.8, page 105.

5.4 Experimental

A *Cedrelopsis grevei* Baill. sample (voucher no. : 08.99 nJ. nDul) from the north west forests of Madagascar was collected and identified by Dr. M. Randrianarivelojosia of the University of Antananarivo, Madagascar.

Milled and dried stem bark (1718.2 g) of *Cedrelopsis grevei* was extracted successively using a Soxhlet apparatus with hexane, ethyl acetate and methanol. Each extraction was carried out over a period of 48 hours.

The hexane extract (143.68 g) yielded, after column chromatography over silica gel (Merck 9385) using 5 g of the extract, β-amyrin (**15**) (55 mg), scoparone (**16**) (14 mg) and a novel lignan, which we name cedpetine (**18**) (42 mg).

The ethyl acetate extract (39.03 g) yielded, after column chromatography over silica gel (Merck 9385) using 8 g of the extract, cedmiline (**14**) (50 mg), a novel quassinoid, which we name cedphiline (**19**) (45 mg) and a novel triterpenoid derivative, which we name cedashnine (**17**) (25 mg). Sitosteryl β-D-glucopyranoside (**20**) (21 mg) was also isolated from the ethyl acetate extract.

The ^{1}H NMR spectrum of the crude methanol extract indicated the presence of sugars only and was not investigated further.

5.5 Physical Data of compounds isolated from *Cedrelopsis grevei*

Physical Data for Cedmiline (14)

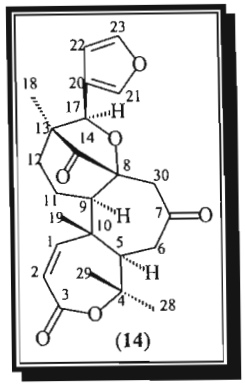

Fig. 5.3. Cedmiline (14)

Physical appearance	White crystalline material	**mp**	295-296 °C [Lit.[1] : 297-298°C]
Yield	50 mg	**Optical rotation : $[\alpha]_D^{25}$ ($CHCl_3$)**	+16.9 ° [c= 0.148] (Lit.[1] : +17.1 ° [c=0.146])
EIMS [M^+] at *m/z*	*412 ($C_{24}H_{28}O_6$ requires 412.1886)	**EIMS at *m/z***	256, 205, 149, 129, 83, 57, 43
IR : ν_{max} (NaCl) cm^{-1}	2927, 2852 (C-H stretch), 1766, 1702 (C=O)		

Table 5.1. NMR data for cedmiline (14)

C	$\delta^{13}C$ / ppm ($CDCl_3$)	δ^1H / ppm ($CDCl_3$)	HMBC (C→H)	COSY	NOESY
1	152.18 (CH)	6.17 (d, J = 13.00 Hz)	19	2	2, 11α, 19
2	119.44 (CH)	5.92 (d, J = 13.00 Hz)	1, 19	1	1
3	166.06 (C)	-	2, 28		
4	83.96 (C)	-	5, 6β, 28, 29		
5	52.25 (CH)	2.97 (dd, J = 4.40, 13.00 Hz)	1, 6α, 6β, 9, 19, 28, 29	6α, 6β	6α, 9, 28, 30α
6	46.43 (CH_2)	α) 2.63 (dd, J = 4.40, 16.89 Hz)	28, 30β	5, 6β	5, 6β, 28
		β) 2.47 (dd, J = 13.00, 16.89 Hz)		5, 6α	6α, 19, 29
7	206.72 (C)	-	6α, 6β, 30α 30β		
8	81.48 (C)	-	17, 30α 30β		
9	63.81 (CH)	2.04 (m)	5, 11β, 12α, 19, 30β		5, 11α, 18
10	47.36 (C)	-	1, 2, 5, 6α, 19		
11	21.67 (CH_2)	α) 1.86 (m)	9, 12α	9, 11β, 12α, 12β	1, 9, 12α
		β) 2.04 (m)		11α, 12α, 12β	12β, 19
12	40.48 (CH_2)	α) 2.04 (m)	11β, 17, 18	11α, 11β, 12β	11α, 17, 18
		β) 1.64 (m)		11α, 11β, 12α	11β, 18
13	51.34 (C)	-	17, 18		
14	213.58 (C)	-	17, 18, 30β		
17	78.78 (CH)	5.08 (s)	12β, 18		12α, 18, 21, 22
18	14.79 (CH_3)	0.87 (s)			9, 12α, 12β, 17, 21, 22
19	19.80 (CH_3)	1.23 (s)	1, 5		1, 6β, 11β, 29
20	124.83 (C)	-	17, 22, 23		
21	140.38 (CH)	7.37 (s)	17, 22, 23		17, 18, 30β*
22	108.32 (CH)	6.04 (s)	17, 21	23	17, 18, 23, 30β*
23	144.12 (CH)	7.35 (s)	21, 22	22	22
28	32.26 (CH_3)	1.43 (s)	29		5, 6α, 29
29	20.65 (CH_3)	1.51 (s)	5, 28		6β, 19, 28
30	45.86 (CH_2)	α) 3.43 (d, J = 12.45 Hz)	6β	30β	5, 30β
		β) 2.37 (d, J = 12.45 Hz)		30α	21*, 22*, 30α

* seen to be possible from model.

* A mass spectrum was obtained from Dr. H. Mahomed's Ph.D Thesis[12] due to the unavailability of the Cape Technikon and UND mass spectrometers.

Physical Data for β-amyrin (15)

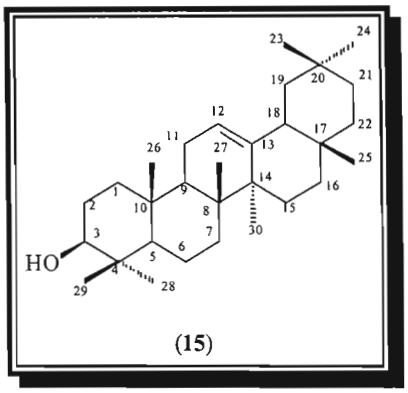

Fig. 5.4. β-Amyrin (15)

Physical appearance	White crystalline material	**mp**	193-194°C [Lit[16] : 197-197.5°C]
EIMS [M^+] at *m/z*	*426 ($C_{30}H_{50}O$ requires 426.3862)	**Optical rotation : $[\alpha]_D^{25}$ ($CHCl_3$)**	+91.0 ° [c=0.078] [Lit.[16] : +88.4°]
Yield	55 mg	**IR : ν_{max} (NaCl) cm^{-1}**	3364 (OH), 2938, 2858 (C-H stretch)

Table 5.2. ^{13}C NMR assignments of β-amyrin (15)

C	$\delta^{13}C$ / ppm ($CDCl_3$) Isolated	$\delta^{13}C$ / ppm ($CDCl_3$) Lit.[12]	C	$\delta^{13}C$ / ppm ($CDCl_3$) Isolated	$\delta^{13}C$ / ppm ($CDCl_3$) Lit.[12]	C	$\delta^{13}C$ / ppm ($CDCl_3$) Isolated	$\delta^{13}C$ / ppm ($CDCl_3$) Lit.[12]
1	38.56 (CH_2)	38.57	**11**	23.51 (CH_2)	23.52	**21**	34.71 (CH_2)	34.72
2	26.91 (CH_2)	26.92	**12**	121.70 (CH)	121.70	**22**	37.11 (CH_2)	37.12
3	79.04 (CH)	79.03	**13**	145.19 (C)	145.19	**23**	28.39 (CH_3)	28.39
4	38.75 (C)	38.77	**14**	41.69 (C)	41.70	**24**	15.48 (CH_3)	15.48
5	55.14 (CH)	55.16	**15**	26.13 (CH_2)	26.14	**25**	15.57 (CH_3)	15.57
6	18.35 (CH_2)	18.36	**16**	27.18 (CH_2)	27.22	**26**	16.78 (CH_3)	16.79
7	32.62 (CH_2)	32.64	**17**	32.48 (C)	32.48	**27**	25.98 (CH_3)	25.98
8	39.76 (C)	39.78	**18**	47.20 (CH)	47.21	**28**	28.07 (CH_3)	28.08
9	47.60 (CH)	47.62	**19**	46.80 (CH_2)	46.81	**29**	33.33 (CH_3)	33.32
10	36.92 (C)	36.94	**20**	31.08 (C)	31.08	**30**	23.68 (CH_3)	23.67

* A molecular mass was obtained from the M.Sc Thesis of Maria Kotsos[16] due to the unavailability of the Cape Technikon and UND mass spectrometers.

Physical Data for scoparone (16)

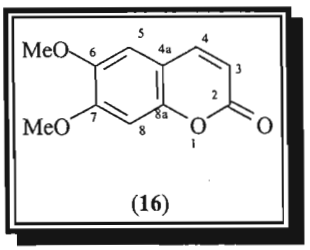

Fig. 5.5a. Scoparone (16)

Physical appearance	Yellow gum
Yield	14 mg
EIMS [M^+] at *m/z*	206 ($C_{11}H_{10}O_4$ requires 206.0579)
EIMS at *m/z*	191, 178 (M^+-CO), 163, 149, 135, 120, 79, 69, 51
IR : ν_{max} (NaCl) cm^{-1}	2927, 2852 (C-H stretch), 1729 (C=O), 1623 (C=C)
UV	344 nm (log ε 3.5), 295 nm (log ε 3.4), 231 nm (log ε 3.8)

Table 5.3. NMR data for scoparone (16)

C	$\delta^{13}C$ / ppm ($CDCl_3$)	δ^1H / ppm ($CDCl_3$)	HMBC (C→H)	COSY	NOESY
1	-	-			
2	161.43 (C)	-	3, 4		
3	113.52 (CH)	6.26 (d, J = 9.34 Hz)		4	4
4	143.30 (CH)	7.60 (d, J = 9.34 Hz)	5	3	3, 5
4a	111.41 (C)	-	3, 4, 8		
5	107.90 (CH)	6.83 (s)	4		4, 6-OMe
6	146.31 (C)	-	5, 8, 6-OMe		
7	152.81 (C)	-	5, 7-OMe		
8	99.98 (CH)	6.82 (s)			7-OMe
8a	150.0 (C)	-	4, 5, 8		
6-OMe	56.33 (CH_3)	3.90 (s)		7 OMe	5, 7-OMe
7-OMe	56.37 (CH_3)	3.93 (s)		6 OMe	6-OMe, 8

Physical Data for cedashnine (17)

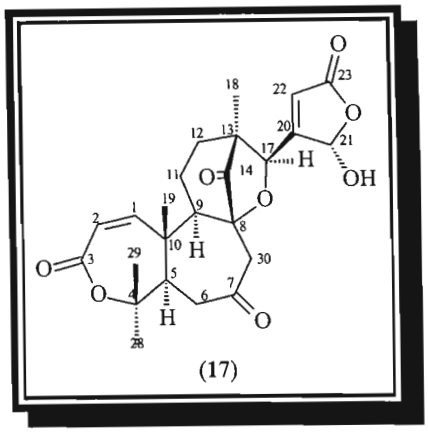

Fig. 5.6a. Cedashnine (17) – novel triterpenoid derivative

Physical appearance	White crystalline material		
mp	220-221 °C	**Yield**	25 mg
HRMS [M^+] at *m/z*	444.17759 ($C_{24}H_{28}O_8$ requires 444.17842)		
HRMS at *m/z*	426.16951 (M^+-H_2O), 316.16656, 277.07193, 258.12538, 175.10432, 121.06497, 108.05742 (100%)		
IR : ν_{max} (NaCl) cm^{-1}	3381 (OH), 2921, 2861 (C-H stretch), 1756, 1710 (C=O)		
Optical rotation : $[\alpha]_D^{25}$ (CH_3OH)	+15.38 ° [c=0.026]		

Table 5.4. NMR data for cedashnine (17)

C	$\delta^{13}C$ / ppm (CD_3OD)	δ^1H / ppm (CD_3OD)	HMBC (C→H)	COSY	NOESY
1	153.99 (CH)	6.37 (d, J = 12.87 Hz)	19	2	2, 11α, 19
2	118.44 (CH)	5.90 (d, J = 12.87 Hz)		1	1
3	167.51 (C)	-			
4	84.82 (C)	-	2, 28, 29		
5	51.91 (CH)	3.09 (dd, J = 4.02, 7.80 Hz)	1, 19, 28, 29	6α, 6β	6α, 9, 28, 30α
*6	46.15 (CH_2)	α) 2.78 (dd, J = 4.02, 16.95 Hz)	30β	5, 6β	5, 6β, 28
		β) 2.46 (dd, J = 7.80, 16.95 Hz)		5, 6α	6α, 19, 29
7	209.03 (C)	-	6β, 30α, 30β		
8	82.72 (C)	-	30α, 30β		
9	64.37 (CH)	1.99 (m)	19, 30β	11α	5, 11α, 17
10	48.50 (C)	-	2, 19		
*11	21.34 (CH_2)	α) 1.88 (m)	12α	9, 11β, 12α, 12β	1, 9, 12α
		β) 2.06 (m)		11α, 12β	12β, 19
*12	41.43 (CH_2)	α) 2.06 (m)	17, 18	11α, 12β	11α, 17, 18
		β) 1.60 (m)		11α, 11β, 12α	11β, 18
13	51.05 (C)	-	17, 18		
14	212.29 (C)	-	17, 18, 30β		
17	79.61 (CH)	5.25 (s)	18		9, 12α, 18, 22
18	13.60 (CH_3)	0.97 (s)			12α, 12β, 17, 21, 22
19	18.58 (CH_3)	1.22 (s)	1		1, 6β, 11β, 29, 30β
20	120.23 (C)	-			
21	98.00 (CH)	6.25 (s)	17		18, 22, 30β
22	153.99 (CH)	6.10 (s)	17		17, 18, 21
23	167.13 (C)	-			
28	31.10 (CH_3)	1.43 (s)	29		5, 6α, 29
29	19.77 (CH_3)	1.53 (s)	28		6β, 19, 28
*30	44.58 (CH_2)	α) 3.57 (d, J = 12.27 Hz)		30β	5, 30β
		β) 2.46 (d, J = 12.27 Hz)		30α	19, 21, 30α

* CH_2 correlations could not be seen in the HSQC spectrum since the sample was very weak. The COSY, NOESY and HMBC correlations confirmed the assignments of the resonances.

A comparison of cedmiline (14) and cedashnine (17)

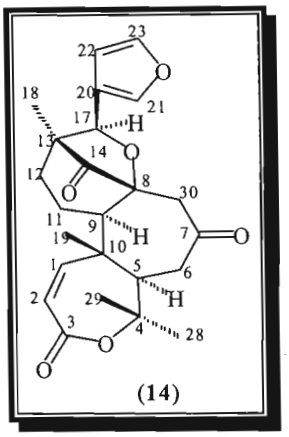

Fig. 5.3. Cedmiline (14)

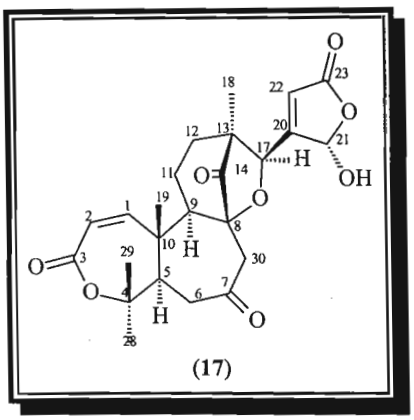

Fig. 5.6a. Cedashnine (17)

Table 5.5. Comparison of NMR data for cedmiline (14) and cedashnine (17)

C	$\delta^{13}C$ / ppm ($CDCl_3$) cedmiline (14)	$\delta^{13}C$ / ppm (CD_3OD) cedashnine (17)	$\delta^{1}H$ / ppm ($CDCl_3$) cedmiline (14)	$\delta^{1}H$ / ppm (CD_3OD) cedashnine (17)
1	152.18 (CH)	153.99 (CH)	6.17 (d, J = 13.00 Hz)	6.37 (d, J = 12.87 Hz)
2	119.44 (CH)	118.44 (CH)	5.92 (d, J = 13.00 Hz)	5.90 (d, J = 12.87 Hz)
3	166.06 (C)	167.51 (C)	-	-
4	83.96 (C)	84.82 (C)	-	-
5	52.25 (CH)	51.91 (CH)	2.97 (dd, J = 4.40, 13.00 Hz)	3.09 (dd, J = 4.02, 7.80 Hz)
6	46.43 (CH_2)	46.15 (CH_2)	α) 2.63 (dd, J = 4.40, 16.89 Hz)	α) 2.78 (dd, J = 4.02, 16.95 Hz)
			β) 2.47 (dd, J = 13.00, 16.89 Hz)	β) 2.46 (dd, J = 7.80, 16.95 Hz)
7	206.72 (C)	209.03 (C)	-	-
8	81.48 (C)	82.72 (C)	-	-
9	63.81 (CH)	64.37 (CH)	2.04 (m)	1.99 (m)
10	47.36 (C)	48.50 (C)	-	-
11	21.67 (CH_2)	21.34 (CH_2)	α) 1.86 (m)	α) 1.88 (m)
			β) 2.04 (m)	β) 2.06 (m)
12	40.48 (CH_2)	41.43 (CH_2)	α) 2.04 (m)	α) 2.06 (m)
			β) 1.64 (m)	β) 1.60 (m)
13	51.34 (C)	51.05 (C)	-	-
14	213.58 (C)	212.29 (C)	-	-
17	78.78 (CH)	79.61 (CH)	5.08 (s)	5.25 (s)
18	14.79 (CH_3)	13.60 (CH_3)	0.87 (s)	0.97 (s)
19	19.80 (CH_3)	18.58 (CH_3)	1.23 (s)	1.22 (s)
20	124.83 (C)	120.23 (C)	-	-
21	140.38 (CH)	98.00 (CH)	7.37 (s)	6.25 (s)
22	108.32 (CH)	153.99 (CH)	6.04 (s)	6.10 (s)
23	144.12 (CH)	167.13 (C)	7.35 (s)	-
28	32.26 (CH_3)	31.10 (CH_3)	1.43 (s)	1.43 (s)
29	20.65 (CH_3)	19.77 (CH_3)	1.51 (s)	1.53 (s)
30	45.86 (CH_2)	44.58 (CH_2)	α) 3.43 (d, J = 12.45 Hz)	α) 3.57 (d, J = 12.27 Hz)
			β) 2.37 (d, J = 12.45 Hz)	β) 2.46 (d, J = 12.27 Hz)

Physical Data for cedpetine (18)

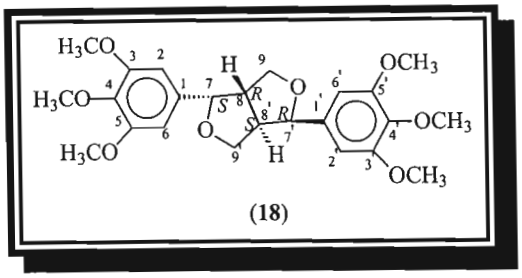

Fig. 5.7a. Cedpetine (18) - novel lignan

Physical appearance	Yellow crystalline material
Yield	42 mg
mp	265-266 °C
HRMS [M^+] at *m/z*	446. 19458 ($C_{24}H_{30}O_8$ requires 446.19407)
HRMS at *m/z*	415.17539 (3.99%) (M^+-CH_3O), 248.10536 (11.91%), 224.10455 (13.33%), 207.10265 (39.42%), 195.06635 (48.25%), 181.08615 (43.36%)
Optical rotation : $[\alpha]_D^{25}$ ($CHCl_3$)	0 ° [c=0.102]
IR : ν_{max} (NaCl) cm^{-1}	2931, 2858 (C-H stretch), 1011, 1133, 1238 (C-O)
UV	272 nm (log ε 4.0), 229 nm (log ε 4.6)

Table 5.6. NMR data for cedpetine (18)

C	$\delta^{13}C$ / ppm ($CDCl_3$)	δ^1H / ppm ($CDCl_3$)	HMBC (C→H)	COSY	NOESY
1, 1'	136.87 (2C)	-	2/6, 7, 8, 2'/6', 7', 8'		
2/6, 2'/6'	102.97 (4CH)	6.55 (s)	3/5-OMe, 6/2, 7, 3'/5'-OMe, 6'/2', 7'	7, 7'	3/5-OMe, 7, 8, 9α, 3'/5'-OMe, 7', 8', 9'α
3/5, 3'/5'	153.56 (4C)	-	2/6, 3/5-OMe, 2'/6', 3'/5'-OMe		
4, 4'	137.59 (2C)	-	2/6, 4-OMe, 2'/6', 4'-OMe		
7, 7'	86.18 (2CH)	4.72 (d, J = 3.85 Hz)	2/6, 8, 9α, 9β, 2'/6', 8', 9'α, 9'β	2/6, 8, 9α, 9β, 2'/6', 8', 9'α, 9'β	2/6, 8, 9β, 2'/6', 8', 9'β
8, 8'	54.63 (2CH)	3.08 (d, J = 1.65 Hz)	7, 9α, 9β, 8, 7', 9'α, 9'β, 8'	7, 9α, 9β, 7', 9'α, 9'β	2/6, 7, 9α, 2'/6', 7', 9'α
9, 9'	72.22 ($2CH_2$)	α) 4.28 (t, J = 6.78, 2.20 Hz)	7, 7'	7, 8, 9β, 7', 8', 9'β	2/6, 8, 9β, 2'/6', 8', 9'β
		β) 3.91 (dd, J = 9.16, 3.11 Hz)		7, 8, 9α, 7', 8', 9'α	7, 9α, 7', 9'α
4-OMe, 4'-OMe	61.11 ($2CH_3$)	3.81 (s, 3H)			
3/5-OMe, 3'/5'-OMe	56.46 ($4CH_3$)	3.85 (s, 6H)			2/6, 2'/6'

Physical Data for cedphiline (19)

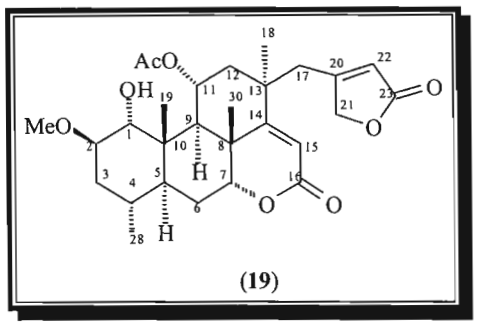

Fig. 5.8b. Cedphiline (19) - novel quassinoid

Physical appearance	White crystalline material	**IR : ν_{max} (NaCl) cm^{-1}**	3500 (OH), 2917, 2855 (C-H stretch), 1745, 1719 (C=O)
mp	160-161 °C	**Optical rotation : $[\alpha]_D^{25}$ ($CHCl_3$)**	-43.97 ° [c=0.348]
Yield	45 mg	**HRMS $[M^+]$ at *m/z***	502.25593 ($C_{28}H_{38}O_8$ requires 502.25667)
HRMS at *m/z*	85.06565 (100%), 119.08579 (19.48%), 345.20736 (18.59%), 410.2087 (27.90%), 442.23434 (M^+-CH_3COOH) (21.08%), 459.23942 (M^+-CH_3C=O) (7.61%)		

Table 5.7. NMR data for cedphiline (19)

C	$\delta^{13}C$ / ppm ($CDCl_3$)	δ^1H / ppm ($CDCl_3$)	HMBC (C→H)	COSY	NOESY
1	80.98 (CH)	3.08 (m)	9, 19	2	4, 19, OMe
2	80.55 (CH)	3.08 (m)	1, 3α, OMe	1, 3β, 3α	5, 9, OMe
3	37.46 (CH_2)	α) 0.90 (m)	28	2, 3β, 4	2, 3β, 5
		β) 2.08 (m)		2, 3α	2, 3α, OMe
4	29.12 (CH)	1.38 (m)	28	3α	1, 19
5	44.22 (CH)	1.24 (m)	9, 19, 28	6α, 6β	2, 3α, 9, 28
6	25.41 (CH_2)	α) 2.08 (m)		5, 6α, 7	6α, 7
		β) 1.82 (dd, J = 14.01, 2.75 Hz)		5, 6β, 7	6β, 7, 19, 30
7	78.78 (CH)	4.14 (m)	9, 30	6β, 6α	6α, 6β, 30
8	39.07 (C)	-	9, 15, 30		
9	53.78 (CH)	1.89 (d, J = 5.64 Hz)	1, 7, 11, 12β, 19, 30	11	2, 5
10	42.06 (C)	-	9, 19		
11	70.65 (CH)	5.64 (m)	9, 12β	9, 12β, 12α	12α, 12β, 19
12	41.48 (CH_2)	α) 2.42 (dd, J = 16.30, 5.32 Hz)	11, 17a, 17b, 18	11, 12β	11, 12β, 18
		β) 2.00 (d, J = 16.30 Hz)		11, 12α	11, 12α
13	39.58 (C)	-	11, 12β, 12α, 17a, 17b, 18		
14	172.44 (C)	-	9, 12β, 15, 17b, 18, 30		
15	116.36 (CH)	5.83 (s)			17a, 18, 21
16	164.87 (C)	-	15		
17	42.49 (CH_2)	a) 2.59 (d, J = 13.74 Hz)	12α, 18	17b	15, 18, 21, 22
		b) 2.64 (d, J = 13.74 Hz)		17a	18, 21, 22
18	31.16 (CH_3)	1.32 (s)	12β, 12α, 17a, 17b		15, 17a, 17b
19	11.79 (CH_3)	1.00 (s)	1, 9		1, 4, 6β, 11, 30
20	164.24 (C)	-	17a, 17b, 21, 22		
21	74.53 (CH_2)	4.73 (2H) (d, J = 1.09 Hz)	17a, 17b, 22		15, 17a, 17b, 30
22	120.13 (CH)	5.92 (s)	17a, 17b, 21		17a, 17b, 30
23	173.14 (C)	-	21, 22		
28	19.99 (CH_3)	0.93 (d, J = 6.41 Hz)			5
30	22.97 (CH_3)	1.34 (s)	7, 9		6β, 7, 19, 21, 22
OAc Me	21.77 (CH_3)	1.94 (s)			
OMe	56.60 (CH_3)	3.33 (s)			1, 2, 3β
OAc C=O	170.84 (C=O)	-	11, AcO Me		

Physical data for sitosteryl β-D-glucopyranoside (20) and sitosteryl β-D-glucopyranoside tetra-acetate (21)

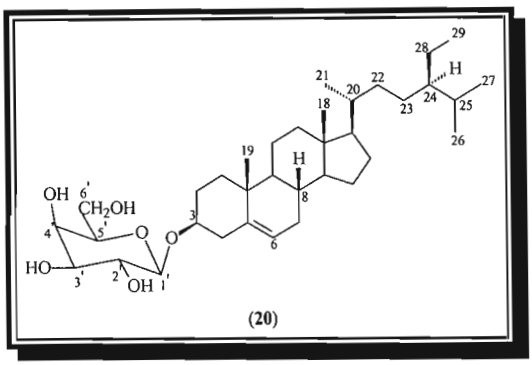

Fig. 5.9. Sitosteryl β-D-glucopyranoside (20)

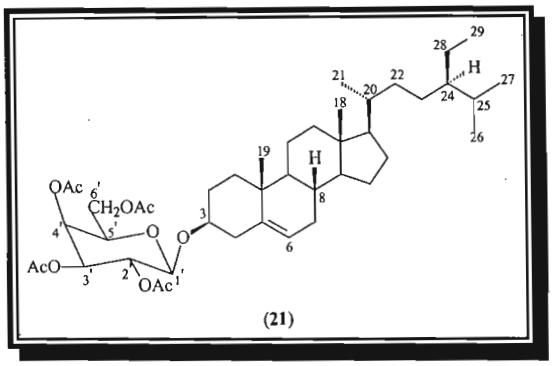

Fig. 5.10. Sitosteryl β-D-glucopyranoside tetra-acetate (21)

The acetylation procedure is given in chapter 4, page 67.

Sitosteryl β-D-glucopyranoside (20)		Sitosteryl β-D-glucopyranoside tetra-acetate (21)			
Physical appearance	White crystalline material	**Physical appearance**	White crystalline material	**Yield**	20 mg
mp	269-270 °C (Lit.[11] : 283-286 °C)	**mp**	168-169 °C (Lit.[17] : 169-170 °C)		
Yield	21 mg	**Optical rotation : $[\alpha]_D^{25}$ ($CHCl_3$)**	-13.33° [c=0.110] (Lit.[17] : -34.5° [c=0.39])		
		IR : ν_{max} (NaCl) cm^{-1}	2924, 2853 (C-H stretch), 1750 (C=O) 1224 (C-O)		

Table 5.8. NMR data for sitosteryl β-D-glucopyranoside tetra-acetate (21)

H	δ^1H / ppm ($CDCl_3$) Isolated	δ^1H / ppm ($CDCl_3$) Lit.[14]	H	δ^1H / ppm ($CDCl_3$) Isolated	δ^1H / ppm ($CDCl_3$) Lit.[14]
3α	3.46 (m)	3.49 (m)	6'b	4.25 (dd, J = 4.95, 12.18 Hz)	4.26 (dd, J = 4.8, 12.2 Hz)
6	5.33 (m)	5.36 (m)	2', 3', 4', 6' OAc Me	1.98 (s), 2.00 (s), 2.03 (s), 2.06 (s)	2.00 → 2.08
1'	4.57 (d, J = 7.88 Hz)	4.59 (d, J = 7.9 Hz)	18	0.65 (s)	0.68 (s)
2'	4.96 (dd, J = 7.87, 9.71 Hz)	4.96 (dd, J = 7.9, 9.5 Hz)	19	0.96 (s)	0.99 (s)
3'	5.22 (t, J = 9.71 Hz)	5.20 (t, J = 9.5 Hz)	21	0.90 (d, J = 6.59 Hz)	0.92 (d, J = 6.4 Hz)
4'	5.10 (t, J = 9.71 Hz)	5.08 (t, J = 9.8 Hz)	26	0.80 (d, J = 7.6 Hz)	0.84 (d, J = 7.3 Hz)
5'	3.65 (m)	3.68 (ddd, J = 2.4, 4.8, 9.8 Hz)	27	0.78 (d, J = 7.4 Hz)	0.81 (d, J = 7.0 Hz)
6'a	4.16 (dd, J = 2.20, 12.18 Hz)	4.11 (dd, J = 2.4, 12.2 Hz)	29	0.82 (t, J = 7.14 Hz)	0.85 (t, J = 7.6 Hz)

C	δ^{13}C / ppm ($CDCl_3$) Isolated	δ^{13}C / ppm ($CDCl_3$) Lit.[15]	C	δ^{13}C / ppm ($CDCl_3$) Isolated	δ^{13}C / ppm ($CDCl_3$) Lit.[15]	C	δ^{13}C / ppm ($CDCl_3$) Isolated	δ^{13}C / ppm ($CDCl_3$) Lit.[15]
1	37.17	37.2	14	56.74	56.7	27	19.81	19.8
2	29.43	29.4	15	24.28	24.2	28	23.05	23.0
3	80.07	80.0	16	28.22	28.2	29	11.97	11.9
4	38.89	38.9	17	56.03	56.0	1'	99.62	99.6
5	140.34	140.3	18	11.84	11.8	2'	71.47	71.4
6	122.17	122.1	19	19.34	19.3	3'	71.67	71.6
7	31.92	31.9	20	36.11	36.1	4'	68.50	68.5
8	31.84	31.8	21	19.00	19.0	5'	62.08	62.1
9	50.14	50.1	22	33.92	33.9	6'	62.08	62.1
10	36.70	36.7	23	26.02	26.0	2', 3', 4', 6' OAc Me	20.77, 20.72, 20.65, 20.61	20.7, 20.6
11	21.03	21.0	24	45.81	45.8	2', 3', 4', 6' OAc C=O	170.73, 170.37, 169.42	170.7, 170.3, 169.4, 169.3
12	39.71	39.7	25	29.12	29.1			
13	42.31	42.3	26	18.76	18.7			

5.6 References

1. Mulholland, D.A., Mahomed, H.A., Kotsos, M., Randrianarivelojosia, M., Lavaud, C., Massiot, G. and Nuzillard, J.-M., *Tetrahedron*, 1999, **55**, 11547.
2. Schulte, K.E., *Arch. Pharm. (Weinheim. Ger.)*, 1973, **306**, 857.
3. Eshiett, I.T. and Taylor, D.A.H., *J. Chem. Soc. (C)*, 1968, 481.
4. Dean, F.M. and Robinson, M.L., *Phytochemistry*, 1971, **10**, 3221.
5. McCabe, P.H., McCrindle, R. and Murray, R.D.H., *J. Chem. Soc. (C)*, 1967, 145.
6. Dean, F.M. and Taylor, D.A.H., *J. Chem. Soc. (C)*, 1966, 114.
7. Dean, F.M., Parton, B., Somvichien, N. and Taylor, D.A.H., *Tetrahedron Letters*, 1967, **36**, 3459.
8. Mulholland, D.A., Kotsos, M., Mahomed, H.A. and Randrianarivelojosia, M., *Nig. J. Nat. Prod. and Med.*, 1999, **3**, 15.
9. Styles, B.T. and Pennington, T.D., *Blumea*, 1975, **22**, 476.
10. Mulholland, D.A., Parel, B. and Coombes, P.H., *Current Organic Chemistry*, 2000, **4**, 1011.
11. Dictionary of Natural Products, Version 10:1, Chapman and Hall Electronic Publishing Division, London, 2001.
12. Mahomed, H.A., Ph.D Thesis, University of Natal, Durban, 1997, 95 (I), 150 (II).
13. Kotsos, M., M.Sc Thesis, University of Natal, Durban, 1997, 133.
14. Basnet, P., Kadota, S., Terashima, S., Shimizu, M. and Namba, T., *Chem. Pharm. Bull.*, 1993, **41**, 1238.
15. Matida, A.K., Rossi, M.H., Blumenthal, E.E.A., Schuquel, I.T.A., Malheiros, A. and Vidotti, G.J., *An. Assoc. Bras. Quím.*, 1996, **45**, 147.
16. Bhattacharyya, J. and Baros, C.B., *Phytochemistry*, 1986, **25**, 274.
17. Ramaiah, P.A., Lavie, D., Budhiraja, R.D., Sudhir, S. and Garg, K.N., *Phytochemistry*, 1984, **23**, 143.

Chapter 6

Extractives from *Neobeguea mahafalensis* seeds

Photograph by Dr. Milijaona Randrianarivelojosia

PAGE NO.

PAGE NO.

List of Tables

List of Schemes

List of Figures

6.1 Introduction

Neobeguea mahafalensis is a Madagascan medicinal plant, which belongs to the *Neobeguea* genus of the Meliaceae family. *Neobeguea* is commonly referred to as 'Handy' by the indigenous people.[1] A previous investigation of the jointly extracted wood and bark of this species by Taylor,[2] yielded pseudrelone A2 (**3**). Kotsos[3] recently isolated β-amyrin (**1**), stigmasterol (**2**) and neobeguin (**4**) from the bark of *Neobeguea mahafalensis*.

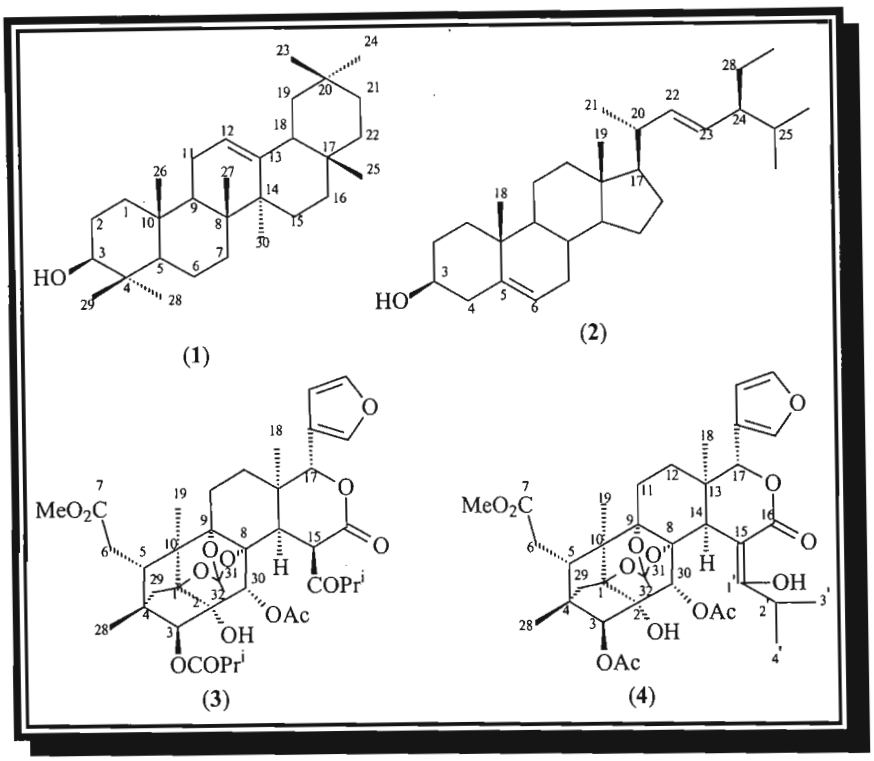

Fig. 6.1. Compounds previously isolated from *Neobeguea mahafalensis*

β-Amyrin (**1**) is a common triterpenoid that has also been isolated from *Cedrelopsis grevei* (Ptaeroxylaceae) in this work. The highly oxidised limonoids (**3**) and (**4**) were of interest, therefore the seeds of *Neobeguea mahafalensis* were investigated to see if they contained similar compounds. This is the first time that the seeds of *Neobeguea mahafalensis* have been worked on and a range of different compounds were isolated.

Neobeguea is related to other members of the Swietenioideae, especially *Khaya*.[2,4] It was previously noted that *Neobeguea* is more advanced since it yields limonoids of higher complexity than the *Khaya* genus.[2] My work shows that *Neobeguea* contains a range of compounds from protolimonoids to limonoids that range in complexity, but are not as complex as those isolated from the bark and wood. The limonoids isolated from the bark and wood are of the phragmalin class, but those that have been isolated from the seeds belong to the andirobin and mexicanolide classes.

6.2 Discussion

The seeds of *Neobeguea mahafalensis* were separated from their shells and both the seeds and the shells were investigated separately. It was interesting to see that the seeds yielded the three limonoids, methyl angolensate (**5**), mexicanolide (**6**), khayasin (**7**), and the shells yielded three protolimonoids, the novel sapelin E acetate (**8**), sapelin C (**9**) and grandifoliolenone (**10**).

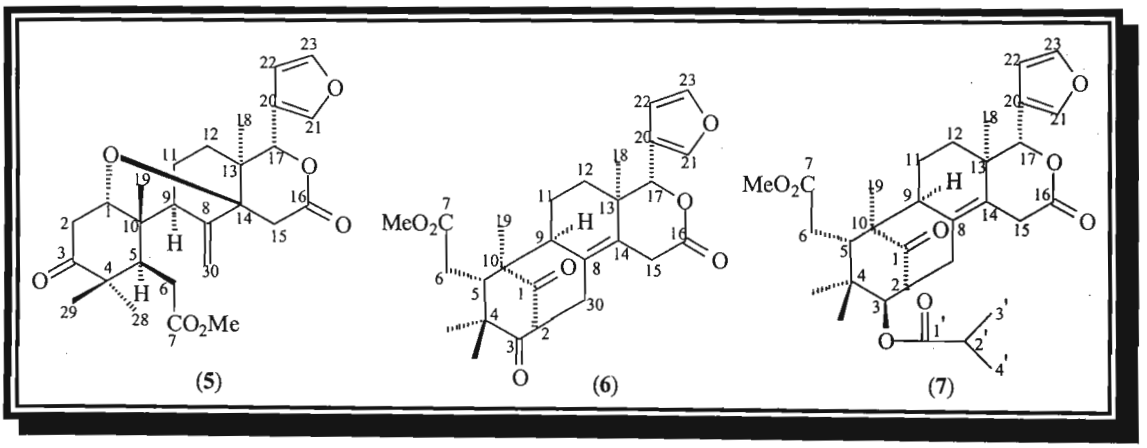

Fig. 6.2a. Limonoids isolated from *Neobeguea mahafalensis* seeds

Methyl angolensate (**5**) is an anti-ulcer agent.[5,6]

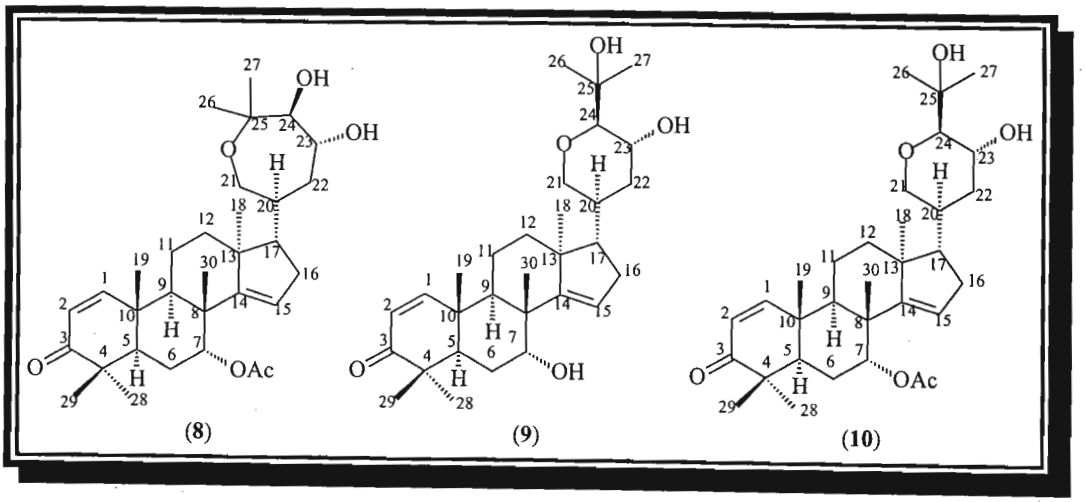

Fig. 6.2b. Protolimonoids isolated from *Neobeguea mahafalensis* seeds

Sapelin E acetate (**8**) is a novel compound. The 7-deacetyl analogue has been isolated previously.

Structural elucidation of methyl angolensate (5)

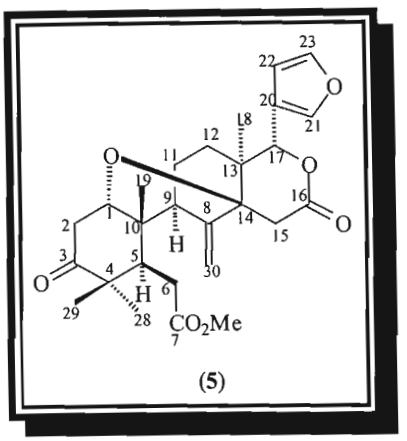

Fig. 6.3. Methyl angolensate (5)

Methyl angolensate (**5**) was isolated as a white crystalline material, mp 206-207 °C. Methyl angolensate (**5**) is a known compound and was isolated previously from *Xylocarpus moluccensis*,[7] *Carapa procera*,[8] *Entandrophragma angolense*,[9] *Khaya senegalensis*[10,11] and *Khaya grandifoliola*.[12] It is biologically active and exhibits anti-ulcer properties.[6]

The mass spectrum **[66]** for this compound showed a molecular ion [M^+] at *m/z* 470, which corresponds to the molecular formula $C_{27}H_{34}O_7$. The fragment ion peak at *m/z* 439 showed the loss of OCH_3 as expected. The IR spectrum **[67]** showed C-H stretch bands at 2931 cm^{-1} and 2859 cm^{-1}, a carbonyl band at 1740 cm^{-1} and C-O stretching bands at 1247 cm^{-1} and 1035 cm^{-1}.

The four methyl group singlets were assigned to 3H-18 (δ_H 0.84), 3H-19 (δ_H 0.92), 3H-28 (δ_H 1.02) and 3H-29 (δ_H 1.17) based on their HMBC correlations. The 3H-18 resonance showed HMBC **[74-75]** correlations with C-12 (δ_C 29.24), C-13 (δ_C 41.37), C-14 (δ_C 80.15) and C-17 (δ_C 79.56). The 3H-19 resonance showed HMBC **[74-75]** correlations with C-1 (δ_C 77.16), C-5 (δ_C 42.86), C-9 (δ_C 49.83) and C-10 (δ_C 43.97). Both the 3H-28 and 3H-29 resonances showed HMBC **[74-75]** correlations with C-3 (δ_C 212.82), C-4 (δ_C 48.00) and C-5 (δ_C 42.86). The 3H-28 resonance also showed HMBC **[74-75]** correlations with C-29 (δ_C 21.60) and the 3H-29 resonance showed HMBC **[74-75]** correlations with C-28 (δ_C 25.81). The NOESY **[77]** correlation between 3H-28 and H-5 (δ_H 2.84) confirmed that the 3H-28 resonance occurred at δ_H 1.02. The resonances at δ_C 13.71 and 21.44 were assigned to C-18 and C-19 respectively using the HSQC **[71-73]** spectrum.

The furanyl ring protons appeared at δ_H 7.41 (H-21), δ_H 6.36 (H-22) and δ_H 7.36 (H-23) in the ^1H NMR spectrum **[68]**. The C-20 (δ_C 120.75), C-21 (δ_C 140.73), C-22 (δ_C 109.87), and C-23 (δ_C 142.71) resonances were assigned using the HSQC **[71-73]** and HMBC **[74-75]** spectra. The C-20 (δ_C 120.75), C-21 (δ_C 140.73), and C-22 (δ_C 109.87) resonances showed HMBC **[74-75]** correlations to the methine carbon proton singlet at δ_H 5.64, which was assigned to H-17. The resonance at δ_C 79.56 could be assigned to C-17 using the HSQC **[71-73]** spectrum, and it showed HMBC **[74-75]** correlations to 3H-18 (δ_H 0.84). The H-17 resonance showed NOESY **[77]** correlations to H-21, H-22 and the H-12 proton at δ_H 1.86.

The two H-12 resonances showed COSY **[76]** correlations with the two H-11 proton resonances at δ_H 1.56 and 2.21. The H-11 resonance at δ_H 1.56 showed a NOESY **[77]** correlation with 3H-18 indicating this H-11 proton resonance was α-orientated. The H-11 resonance at δ_H 2.21 showed a NOESY **[77]** correlation with 3H-19, which confirmed that this resonance was β-orientated. The resonance at δ_C 23.68 was assigned to C-11 by use of the HSQC spectrum **[71-73]**. The H-11α resonance also showed a NOESY **[77]** correlation with the H-12 proton resonance at δ_H 1.09 confirming that this proton was α-orientated, leaving the H-12 resonance at δ_H 1.86 with a β-orientation. The NOESY **[77]** correlation between H-17 and H-12β confirmed the β-orientation for both these protons.

The C-16 lactone carbonyl carbon appeared at δ_C 170.10 in the ^{13}C NMR spectrum **[69]** and showed HMBC **[74-75]** correlations to the two H-15 protons at δ_H 2.56 and 2.89. Both the C-15 protons showed HMBC **[74-75]** correlations to the fully substituted carbon resonance at δ_C 80.15. This resonance (δ_C 80.15) showed HMBC **[74-75]** correlations to H-12α and 3H-18 and was assigned to C-14.

The C-14 resonance also showed HMBC **[74-75]** correlations with the methine resonance at δ_C 77.16. This methine resonance showed HMBC **[74-75]** correlations to H-5 (δ_H 2.84), H-9, (δ_H 2.15) and 3H-19 (δ_H 0.92) and was assigned to C-1. The H-1 resonance occurred as a double doublet (J = 4.03, 10.16 Hz) at δ_H 3.50, which was split by the two H-2 protons at δ_H 2.48 and δ_H 2.86 in the COSY NMR spectrum **[76]**. These correlations confirmed the presence of the 1, 14-oxygen bridge of andirobin type limonoids. The H-1 resonance showed a NOESY **[77]** correlation with 3H-19, indicating that the H-1 was β-orientated. A model of methyl angolensate (**5**) indicated that a 1α, 14β-bridge was possible.

The H-2 resonance at δ_H 2.48 showed a NOESY **[77]** correlation with 3H-28 (δ_H 1.02), indicating an α-orientated for this proton, leaving the H-2 resonance at δ_H 2.86 to be assigned the β-orientation. The NOESY **[77]** correlations between H-2β and 3H-19 and 3H-29 confirmed the β-orientation for this H-2 proton. The carbonyl carbon resonance at δ_C 212.82 was assigned to C-3 and showed HMBC **[74-75]** correlations with H-1, the two H-2 protons, 3H-28 and 3H-29.

The carbomethoxy group at C-7 (δ_C 173.84) and the exocyclic methylene group with carbon resonances at δ_C 145.71 (C-8) and δ_C 111.52 (C-30) indicated that ring B was opened. The two non-equivalent methylene group proton resonances occurred at 4.87 (H-30a) and δ_H 5.12 (H-30b). The C-8 resonance (δ_C 145.71) showed HMBC **[74-75]** correlations with H-30a, which showed NOESY **[77]** correlations with 3H-18. The H-30b resonance showed NOESY **[77]** correlations with H-11β and 3H-19.

The methoxy group protons appeared as a three proton singlet at δ_H 3.69 in the ^{1}H NMR spectrum **[68]**, and showed HSQC **[71-73]** correlations to the methoxy carbon resonance at δ_C 52.06. The methoxy group protons showed HMBC **[74-75]** correlations to C-7 (δ_C 173.84), which showed HMBC **[74-75]** correlations to the two H-6 protons at δ_H 2.23 and 2.60. The resonance at δ_C 32.63 was assigned to C-6 by use of the HSQC spectrum **[71-73]**.

The NMR data for methyl angolensate (**5**) are shown in table 6.1, page 131.

Biosynthesis of methyl angolensate (5)

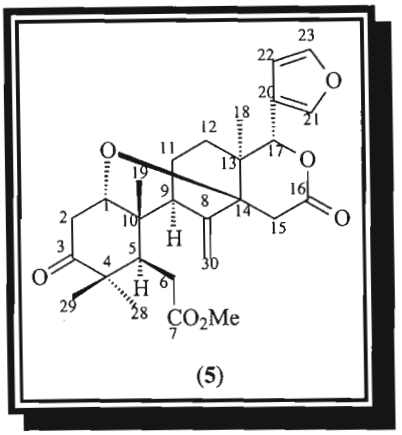

Fig. 6.3. Methyl angolensate (5)

Methyl angolensate (**5**) is formed by ring B opening of a compound such as (**A**). After ring B opening is achieved, the α-hydroxy group at C-1 adds to the α, β-unsaturated lactone system (Michael addition) at C-14, to form a 1, 14-ether bridge. Methyl angolensate (**5**) has been synthesised previously in the laboratory by Connolly *et al.* (scheme 6.1).

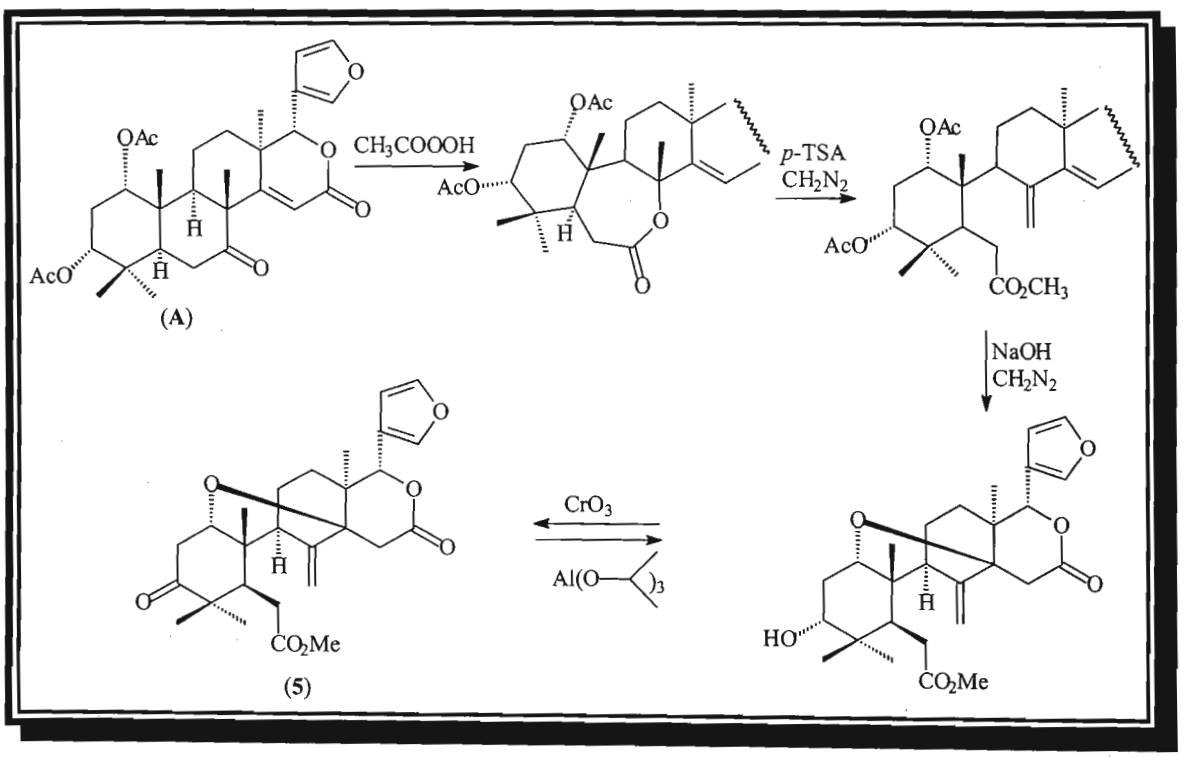

Scheme 6.1. Laboratory synthesis of methyl angolensate (5)[13]

Structural elucidation of mexicanolide (6)

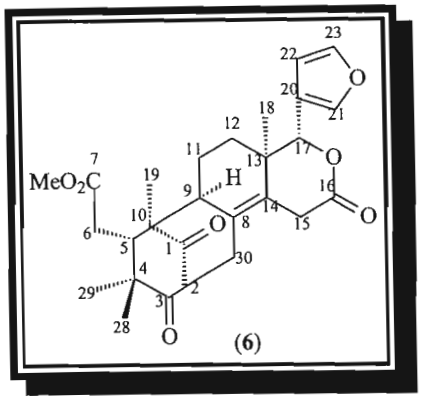

Fig. 6.4. Mexicanolide (6)

Mexicanolide (**6**) is a known limonoid, which was isolated as a white crystalline material, mp 215-216 °C. Mexicanolide (**6**) has been isolated previously from *Carapa procera*,[14] *Xylocarpus moluccensis*,[15] *Xylocarpus granatum*,[16] *Khaya senegalensis*,[17] *Khaya madagascariensis*[17] and *Khaya grandifoliola*.[12] The mass spectrum **[79]** of mexicanolide (**6**) showed the molecular ion [M^+] at *m/z* 468, which corresponds to the molecular formula $C_{27}H_{32}O_7$. The IR spectrum **[80]** showed C-H stretch bands at 2930 and 2853 cm^{-1}, a carbonyl absorption at 1732 cm^{-1}, and C-O stretching bands at 1260 and 1035 cm^{-1}.

The presence of only four methyl groups and a carbomethoxy group but no $\Delta^{8(30)}$-double bond (exocyclic methylene group) indicated the mexicanolide type of structure. Because of the cyclisation step in the biosynthesis of mexicanolide (**6**) (scheme 6.2, page 119), 3H-28 has become β-orientated and 3H-19 and 3H-29 have become α-orientated.

The four methyl group singlets were assigned to 3H-18 (δ_H 0.99), 3H-19 (δ_H 0.85), 3H-28 (δ_H 0.97) and 3H-29 (δ_H 1.23) based on their HMBC **[87-89]** correlations. The 3H-18 resonance showed HMBC **[87-89]** correlations with C-12 (δ_C 28.79), C-13 (δ_C 37.99), C-14 (δ_C 133.86) and C-17 (δ_C 80.67). The 3H-19 resonance showed HMBC **[87-89]** correlations with C-1 (δ_C 211.01), C-5 (δ_C 40.15) and C-10 (δ_C 49.40). The 3H-29 resonance showed HMBC **[87-89]** correlations with C-2 (δ_C 50.50), C-3 (δ_C 213.00), C-4 (δ_C 54.28), C-5 (δ_C 40.15) and C-6 (δ_C 32.29). The 3H-28 resonance showed HMBC **[87-89]** correlations with C-5 (δ_C 40.15), C-10 (δ_C 49.40) and C-29 (δ_C 17.97). The resonances at δ_C 17.38, 17.90, 21.93 and 17.97 were assigned to C-18, C-19, C-28 and C-29 respectively by use of the HSQC spectrum **[84-86]**.

The furanyl protons H-21, H-23 and H-22 appeared at δ_H 7.56, δ_H 7.38 and δ_H 6.47 respectively in the ^{1}H NMR spectrum **[81]**. The resonances at δ_C 141.61, 142.79 and 109.96 were assigned to C-21, C-23 and C-22 respectively by use of the HSQC spectrum **[84-86]**. The H-17 singlet appeared at δ_H 5.25 and showed HMBC **[87-89]** correlation to C-13 (δ_C 37.99), C-14 (δ_C 133.86), C-18 (δ_C 17.38), C-20 (δ_C 120.33), C-21 (δ_C 141.61) and C-22 (δ_C 109.96). The resonance at δ_C 80.67 was assigned to C-17 using the HSQC spectrum **[84-86]**.

The C-16 and C-7 resonances appeared further upfield at δ_C 169.87 and 173.59 respectively since they are esters. The resonances at δ_C 125.33 and 133.86 were assigned to the double bond carbon resonances C-8 and C-14 respectively using the HMBC spectrum **[87-89]**. The C-8 resonance showed a HMBC **[87-89]** correlation with the H-30 proton resonance at δ_H 3.19. The C-14 resonance showed HMBC **[87-89]** correlations with the H-17, H-18 and the two H-30 resonances (δ_H 2.29 and 3.19).

The methoxy group methyl proton singlet appeared at δ_H 3.71 and showed a HMBC **[87-89]** correlation with C-7. The resonance at δ_C 52.23 was assigned to the carbon of the methoxy group using the HSQC spectrum **[84-86]**.

The multiplets at δ_H 1.11 and 1.84 were assigned to the H-12 protons using the HSQC spectrum **[84-86]**. The H-12 resonance at δ_H 1.84 showed a NOESY **[91]** correlation to H-17, which indicated a β-orientation for this H-12 resonance, leaving the H-12 resonance at δ_H 1.11 to be assigned the α-orientation. The H-5 resonance (δ_H 2.74) showed NOESY **[91]** correlations with H-17 and 3H-28, which confirmed the β-configuration for H-5 as expected.

The resonance at δ_C 36.45 was assigned to C-30 by use of the HSQC spectrum **[84-86]**. The H-30 resonance at δ_H 3.19 showed NOESY **[91]** correlations with 3H-19 indicating the α-orientation for this H-30 resonance and leaving the H-30 resonance at δ_H 2.29 with a β-orientation. The H-30α resonance showed HMBC **[87-89]** correlations to C-1 (δ_C 211.01), C-2 (δ_C 50.50), C-3 (δ_C 213.00), C-8 (δ_C 125.33), and C-14 (δ_C 133.86).

The C-15 resonance appeared at δ_C 32.96 in the ^{13}C NMR spectrum **[82]** and showed HSQC **[84-86]** correlations to the two H-15 proton resonances at δ_H 3.45 and 3.48. The H-15 resonance at δ_H 3.45 showed NOESY **[91]** correlations with 3H-18 and H-30α indicating an α-orientation for this proton, leaving the H-15 resonance at δ_H 3.48 to be assigned the β-orientation. The C-11 resonance appeared at δ_C 18.57 and showed HSQC **[84-86]** correlations to the two H-11 proton resonances at δ_H 1.76 and 1.82. The H-11 resonance at δ_H 1.76 showed NOESY **[91]** correlations with 3H-29, indicating an α-orientation for this proton, leaving the H-11 resonance at δ_H 1.82 with a β-orientation.

The NMR data for mexicanolide (**6**) are shown in table 6.2, page 132.

Biosynthesis of mexicanolide (6)

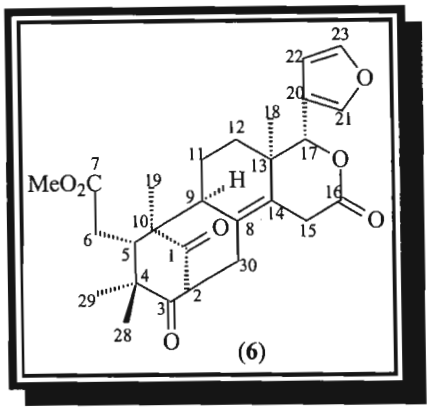

Fig. 6.4. Mexicanolide (6)

Mexicanolide (**6**) is thought to form by ring B opening and oxidation of the C-1 and C-3 hydroxy groups to ketones. This is followed by rotation about the C-9, C-10-bond and Michael addition of C-2 to the $\Delta^{8(30)}$-double bond.[18] This proposal is supported by the laboratory synthesis of mexicanolide by Connolly *et al.* given in scheme 6.2.

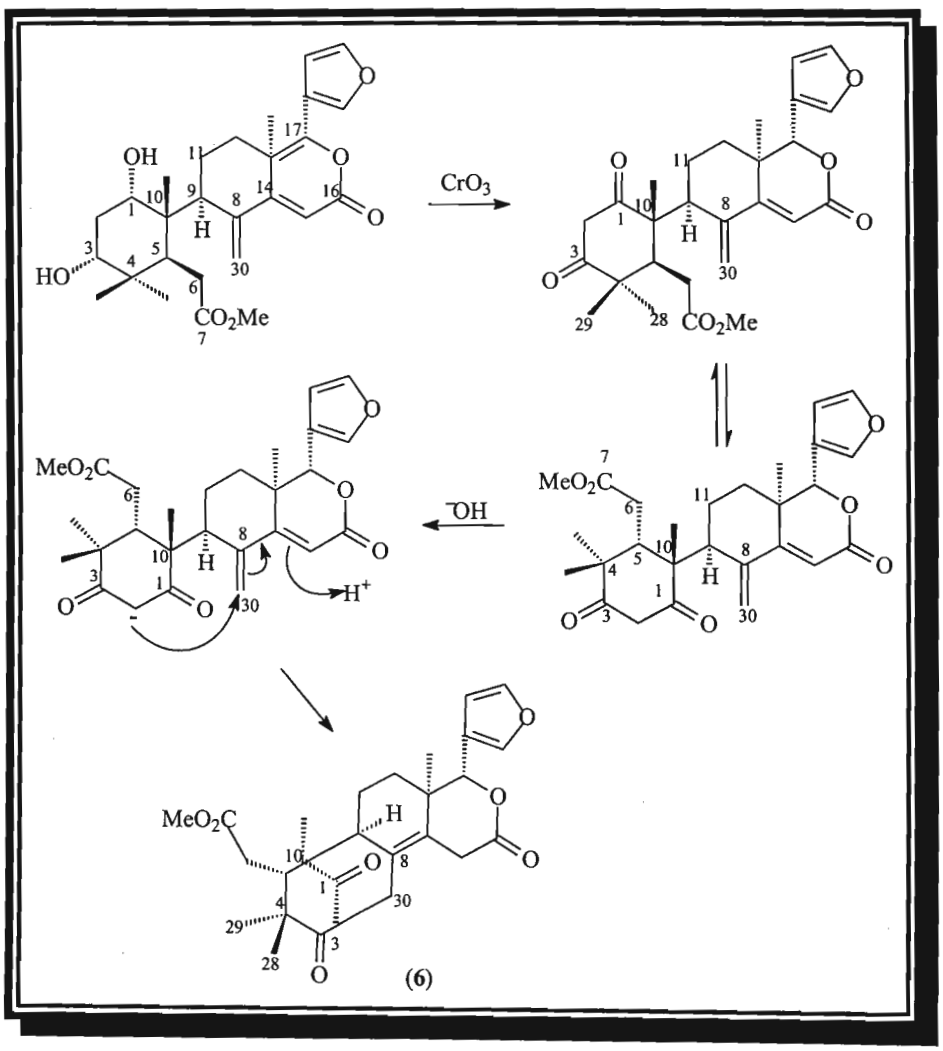

Scheme 6.2. Proposed biosynthesis of mexicanolide (6)[18]

Structural elucidation of khayasin (7)

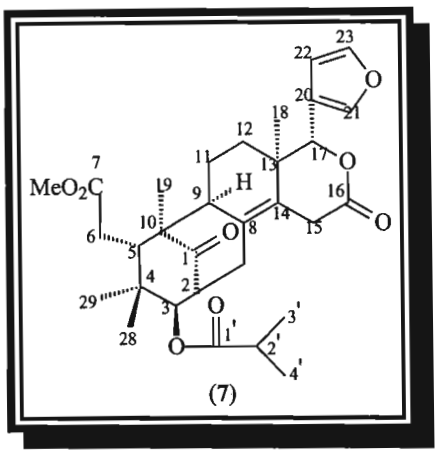

Fig. 6.5. Khayasin (7)

Khayasin (**7**) was isolated as a white crystalline material, mp 113-115 °C. The mass spectrum **[93]** showed the molecular ion [M^+] at *m/z* 540.27251, which corresponds to the molecular formula $C_{31}H_{40}O_8$. The fragment ion peak at *m/z* 509.25296 showed the loss of OCH_3 as expected. The mass spectrum **[93]** also showed a fragment ion [M^+-C_4H_7OH] at *m/z* 468.21381, indicating the above structure to be correct. The IR spectrum **[94]** showed C-H stretch bands at 2982 cm^{-1} and 2889 cm^{-1}, a carbonyl band at 1736 cm^{-1} and C-O bands at 1251 cm^{-1} and 1042 cm^{-1}.

Khayasin (**7**) is a known compound that has been previously isolated from *Khaya senegalensis*,[10,14,19] *Khaya grandifoliola*[17] and *Khaya madagascariensis*.[17]

Khayasin (**7**) is very similar to mexicanolide (**6**). The only difference between compound (**7**) and compound (**6**) is the 2-methyl propionate group at C-3 of khayasin (**7**). The C-3 resonance appeared as an oxygenated methine resonance at δ_C 78.02 in the ^{13}C NMR spectrum **[96]**. The C-3 resonance of mexicanolide (**6**) appeared at δ_C 213.00. A doublet at δ_H 4.93 (J = 9.89 Hz) was assigned to H-3 using the HSQC **[98-99]** and HMBC **[100-101]** spectra. The C-3 resonance (δ_C 78.02) showed HMBC **[100-101]** correlations to H-5 (δ_H 3.21), 3H-28 (δ_H 0.69), 3H-29 (δ_H 0.78), and the two H-30 protons at δ_H 2.08 and 2.77.

The H-3 resonance showed NOESY **[103]** correlations with 3H-28, 3H-29 and H-2 (δ_H 3.13). The 3H-28 resonance showed NOESY **[103]** correlations with the two methyl group proton resonances H-3' (δ_H 1.20) and H-4' (δ_H 1.20) of the 2-methyl propionate group.

The H-3'/ 4' resonances showed COSY **[102]** correlations with H-2' at δ_H 2.61. The H-3, H-2', and H-3'/ 4' resonances showed HMBC **[100-101]** correlations with the ester carbonyl carbon at δ_C 176.61, which was assigned to C-1'. The resonance at δ_C 34.42 was assigned to C-2' by use of the HSQC **[98-99]** spectrum. The resonance at δ_H 1.20 is not a clear doublet and the ^{13}C NMR resonances for C-3' and C-4' occurred at δ_C 19.92, and 18.52 respectively indicating restricted rotation.

A model of khayasin (**7**) showed the α-orientation of H-2. The H-2 resonance showed a NOESY **[103]** correlation with H-3 which indicated an α-orientation at H-3 and a β-orientation for the ester group at C-3. These correlations were confirmed using the khayasin (**7**) model.

The resonances at δ_C 23.14, δ_C 20.57 and δ_C 33.18 were assigned to C-28, C-29 and C-30 respectively by use of the HSQC **[98-99]** spectrum, and the fully substituted C-4 resonance appeared further upfield at δ_C 38.47 in compound (**7**) than in compound (**6**) (δ_C 54.28).

The rest of the ^1H NMR and ^{13}C NMR spectra of khayasin (**7**) are very similar to those of mexicanolide (**6**).

The NMR data for khayasin (**7**) are shown in table 6.3, page 133.

Structural elucidation of sapelin E acetate (8)

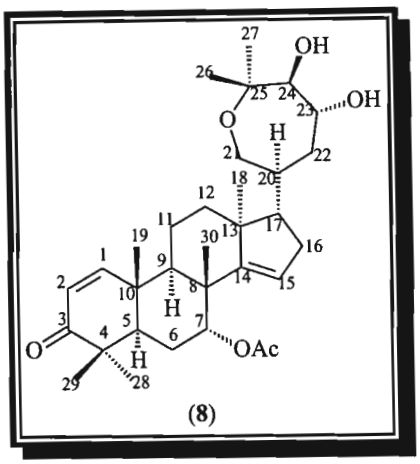

Fig. 6.6. Sapelin E acetate (8)

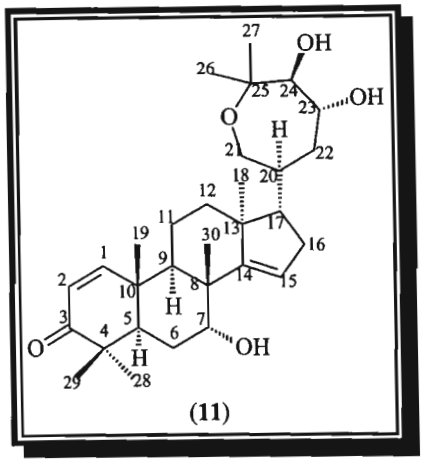

Fig. 6.7. Sapelin E (11)

Sapelin E acetate (**8**) was isolated as a white crystalline material, mp 206-207 °C. Although the molecular ion [M^+] at *m/z* 528 was not clear in the mass spectrum **[105]**, the fragment ions [M^+-H_2O] and [M^+-CH_3COOH] were seen at *m/z* 510.33442 and 468.32224 respectively, indicating the above structure with the molecular formula $C_{32}H_{48}O_6$ to be correct. The fragment ion [M^+-$2H_2O$] at *m/z* 492.32009 showed the loss of two water molecules. The IR spectrum **[106]** showed a band at 3437 cm^{-1} due to hydroxy stretching, C-H stretch bands at 2931 cm^{-1} and 2859 cm^{-1}, carbonyl bands at 1735 cm^{-1} and 1673 cm^{-1} and C-O bands at 1249 cm^{-1} and 1031 cm^{-1}.

Sapelin E acetate (**8**) is a novel compound and is the 7-acetyl derivative of the known compound sapelin E (**11**), which has been isolated previously from *Entandrophragma cylindricum*.[20]

The five tertiary methyl group singlets were assigned to 3H-18 (δ_H 0.96), 3H-19 (δ_H 1.14), 3H-28 (δ_H 1.05), 3H-29 (δ_H 1.05) and 3H-30 (δ_H 1.17) based on their HMBC **[112-114]** correlations. The 3H-18 resonance showed HMBC **[112-114]** correlations with C-12 (δ_C 34.05), C-13 (δ_C 46.32), C-14 (δ_C 159.17) and C-17 (δ_C 54.21). The 3H-19 resonance showed HMBC **[112-114]** correlations with C-1 (δ_C 158.40), C-5 (δ_C 46.17), C-9 (δ_C 38.47) and C-10 (δ_C 39.83). The 3H-28 and 3H-29 resonances appeared together at δ_H 1.05 and showed HMBC **[112-114]** correlations with C-3 (δ_C 204.74), C-4 (δ_C 44.15) and C-5 (δ_C 46.17). The C-28 resonance appeared at δ_C 21.27 and showed HMBC **[112-114]** correlations with 3H-29. The C-29 resonance appeared at δ_C 19.95 and showed HMBC **[112-114]** correlations with 3H-28. The 3H-30 resonance showed HMBC **[112-114]** correlations with C-7 (δ_C 74.68), C-8 (δ_C 42.72), C-9 (δ_C 38.47) and C-14 (δ_C 159.17). The resonances at δ_C 27.35 and δ_C 27.03 were assigned to C-18 and C-19 respectively using the HSQC spectrum **[110-111]**.

The two methyl group singlets δ_H 1.14 and δ_H 1.29 were assigned to 3H-26 and 3H-27 respectively based on their HMBC **[112-114]** and NOESY **[116]** correlations. Both the 3H-26 and the 3H-27 resonances showed HMBC **[112-114]** correlations with C-24 (δ_C 80.75) and C-25 (δ_C 76.18). The resonances at δ_C 22.42 and δ_C 26.29 were assigned to C-26 and C-27 respectively using the HSQC spectrum **[110-111]**, and both these resonances showed HMBC **[112-114]** correlations with H-24 (δ_H 3.41). The C-26 resonance showed HMBC **[112-114]** correlations with 3H-27, and C-27 showed HMBC **[112-114]** correlations with 3H-26. The 3H-26 resonance showed a NOESY **[116]** correlation with H-23 (δ_H 3.79), and the 3H-27 resonance showed a NOESY **[116]** correlation with H-24 (δ_H 3.41). Based on previous studies, the H-23 resonance is β-orientated and the H-24 resonance is α-orientated. This indicated that the 3H-26 resonance was β-orientated and the 3H-27 resonance was α-orientated.

The H-23 and H-24 resonances showed coupling to each other in the COSY NMR spectrum **[115]**. The H-23 resonance was also seen to couple with both the H-22 resonances at δ_H 1.62 and δ_H 1.96 in the COSY NMR spectrum **[115]**. The H-23 resonance also showed a NOESY **[116]** correlation with H-17 (δ_H 1.89). The H-24 resonance showed HMBC **[112-114]** correlation with C-22 (δ_C 37.91), C-23 (δ_C 68.09), C-25 (δ_C 76.18), C-26 (δ_C 22.42) and C-27 (δ_C 26.29), and H-24 also showed NOESY **[116]** correlations with H-20 (δ_H 1.89), the H-21 resonance at δ_H 3.59 and the H-22 resonance at δ_H 1.62, indicating the α-orientation for all these resonances, and leaving the H-21 resonance at δ_H 3.49 and the H-22 resonance at δ_H 1.96 to be assigned the β-orientation.

The two H-21 resonances showed COSY **[115]** coupling with each other. The H-21α resonance showed NOESY **[116]** correlations with H-20 (δ_H 1.89), H-24 and 3H-27 confirming the α-orientation for all these resonances. The H-21β resonance showed a NOESY **[116]** correlation with H-17. The H-21α resonance showed a HMBC **[112-114]** correlation with C-25. The resonance at δ_C 36.36 was assigned to C-20 using the HSQC spectrum **[110-111]**.

The two H-22 resonances showed coupling to each other in the COSY NMR spectrum **[115]**. The H-22α resonance showed a COSY **[115]** correlation with H-20. The H-22β resonance showed a NOESY **[116]** correlation with 3H-18, which is possible because of the free rotation about the C-17, C-20-bond.

The two H-16 resonances at δ_H 1.99 and 2.22 showed COSY **[115]** coupling to each other and NOESY **[116]** correlations with H-15 (δ_H 5.28). The C-15 double bond carbon resonance was seen to occur at δ_C 119.05 by use of the HSQC spectrum **[110-111]**.

The typical H-1, H-2 pair of alkene doublets appeared at δ_H 7.14 (d, J = 10.26) and δ_H 5.83 (d, J = 10.26) respectively in the ^{1}H NMR spectrum **[107]**, and showed coupling with each other in the COSY **[115]** spectrum. The resonances at δ_C 158.40 and δ_C 125.43 were assigned to C-1 and C-2 respectively using the HSQC spectrum **[110-111]**. The H-1 resonance showed HMBC **[112-114]** correlations with C-5 (δ_C 46.17), C-9 (δ_C 38.47), C-10 (δ_C 39.83) and the C-3 carbonyl resonance at δ_C 204.74.

The singlet at δ_H 1.92 in the ^{1}H NMR spectrum **[107]** was assigned to the methyl group protons of the acetate group. The acetate methyl group proton resonance showed a HMBC **[112-114]** correlation with the carbonyl group resonance of the acetate at δ_C 170.14, and NOESY **[116]** correlations with the 2H-6 (δ_H 1.76) and H-7 (δ_H 5.20) resonances. The resonance at δ_C 21.16 was assigned to the methyl group carbon of the acetate by use of the HSQC spectrum **[110-111]**. The H-7 resonance showed a NOESY **[116]** correlation with 3H-30, confirming a β-orientation for the H-7 proton, leaving the acetate group at C-7 with the α-orientation. The 2H-6 proton resonance showed COSY **[115]** correlations with H-5 (δ_H 2.15) and H-7 (δ_H 5.20). The H-5 resonance showed a NOESY **[116]** correlation with 3H-28 and the 2H-6 resonance showed NOESY **[116]** correlations with 3H-28 and 3H-29.

The two H-12 proton resonances appeared at δ_H 1.66 and δ_H 1.85, and showed COSY **[115]** coupling to each other. The two H-11 resonances appeared at δ_H 1.57 and δ_H 1.68 and were seen to be coupled to each other in the COSY **[115]** spectrum. The H-12 resonance at δ_H 1.66 and the H-11 resonance at δ_H 1.68 showed NOESY **[116]** correlations with 3H-19 and 3H-30 indicating the β-orientation for these protons, leaving the H-11 resonance at δ_H 1.57 and the H-12 resonance at δ_H 1.85 with the α-orientation.

A model of sapelin E acetate (**8**) confirmed that the NOESY correlations given above were possible. Acetylation of sapelin E acetate (**8**) was attempted but it was not possible to purify the product since a very small amount of sample was used and phthalate contamination occurred.

The NMR data for sapelin E acetate (**8**) are shown in table 6.4, page 134.

Structural elucidation of sapelin C (9)

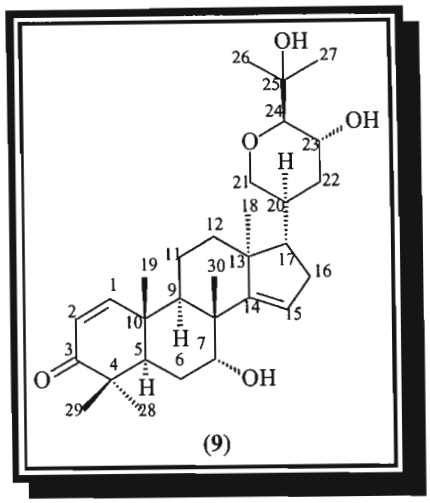

(9)

Fig. 6.8a. Sapelin C (9)

Sapelin C (**9**) was isolated as a white crystalline material, mp 238-239 °C. The molecular ion [M^+] at *m/z* 486 was not clear in the mass spectrum **[118]** which is typical for tertiary alcohols. However, a fragment ion peak due to the loss of water was seen at *m/z* 468.32474, which corresponded to the formula $C_{30}H_{44}O_4$ (requires 468.32396). From this the molecular formula of $C_{30}H_{46}O_5$ could be deduced. The IR spectrum **[119]** showed a band at 3387 cm^{-1} due to hydroxy stretching, C-H stretch bands at 2926 cm^{-1} and 2859 cm^{-1}, a carbonyl band at 1730 cm^{-1} and C-O bands at 1253 cm^{-1} and 1072 cm^{-1}.

Sapelin C (**9**) is a known compound that has also been previously isolated from *Entandrophragma cylindricum*.[20]

As a result of the small amount of sapelin C (**9**) isolated, it was not possible to obtain a good set of NMR spectra. In addition, a HMBC spectrum could not be obtained because of problems experienced with the NMR spectrometer. The structure of sapelin C (**9**) was confirmed by comparison with literature data of similar known compounds.[21,22]

The seven methyl carbon resonances appeared at δ_C 28.66, 27.63, 27.12, 24.01, 21.45, 19.57 and 18.93. These carbon resonances corresponded to the proton resonances at δ_H 1.30, 1.13, 1.14, 1.26, 1.07, 0.96 and 1.13 by use of the HSQC **[122-123]** spectrum. Two methyl carbon resonances (δ_C 18.93 and 27.63) correlated to the proton resonance at δ_H 1.13.

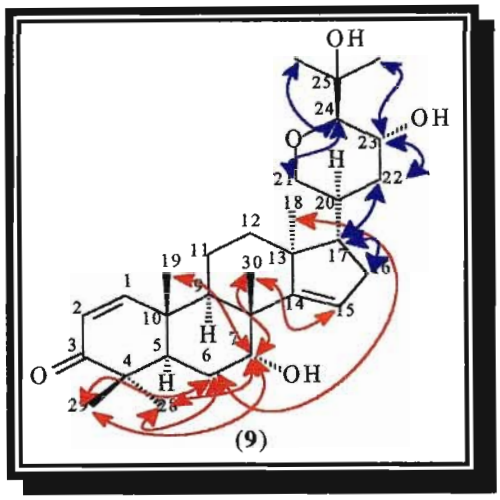

Fig. 6.8b. NOESY correlations for sapelin C (9)

The two H-22 proton resonances appeared at δ_H 1.51 and 2.03 and showed COSY **[124]** coupling to each other and with the H-23 proton resonance. Based on previous studies,[23] H-23 is β-orientated and H-24 α-orientated. The H-23 resonance (δ_H 3.86) showed a NOESY **[125]** correlation with the H-22 resonance at δ_H 2.03, indicating the β-orientation for this H-22 proton, and leaving the H-22 proton resonance at δ_H 1.51 with the α-orientation. The H-22β resonance showed a NOESY **[125]** correlation with H-17 (δ_H 2.33). The H-23 resonance was seen to be coupled to H-24 (δ_H 2.89) in the COSY **[124]** spectrum. The two H-21 resonances appeared at δ_H 3.43 and 3.96 and were seen to be coupled to each other in the COSY **[124]** spectrum. The H-24 resonance also showed a NOESY **[125]** correlation with the H-21 resonance at δ_H 3.43 which was assigned the α-orientation, leaving the H-21 resonance at δ_H 3.96 with the β-orientation.

The two methine carbon resonances at δ_C 64.36 and 86.55 were assigned to C-23 and C-24 respectively by use of the HSQC **[122-123]** spectrum. The methylene carbon resonance at δ_C 36.25 and the oxygenated methylene carbon resonance at δ_C 70.02 were assigned to C-22 and C-21 respectively using the HSQC **[122-123]** spectrum. The fully substituted carbon resonance at δ_C 74.27 was assigned to C-25.

The H-17 resonance showed COSY **[124]** and NOESY **[125]** correlations with the 2H-16 resonance at δ_H 2.06. The C-14 and C-15 double bond resonances appeared at δ_C 161.53 and 120.25 respectively in the ^{13}C NMR spectrum **[121]**. The typical H-1 and H-2 doublets appeared at δ_H 7.11 (J = 10.26 Hz) and 5.81 (J = 10.26 Hz) respectively and showed COSY **[124]** coupling to each other. The resonances at δ_C 158.34 and 125.47 were assigned to C-1 and C-2 respectively by use of the HSQC **[122-123]** spectrum. The carbonyl resonance at δ_C 205.22 was assigned to C-3.

The oxygenated methine resonance at δ_C 71.79 was assigned to C-7. Since a hydroxy group was attached at C-7 instead of an acetate group, the H-7 resonance was found further upfield at δ_H 3.97. The H-7 resonance showed a COSY **[124]** correlation with the 2H-6 resonance (δ_H 1.85).

The two H-12 resonances appeared at δ_H 1.56 and 1.96. The stereochemistry for these protons could not be established and the H-11 resonances could not be assigned. Acetylation of sapelin C (**9**) was attempted but unsuccessful because of a weak sample and phthalate contamination.

The NMR data for sapelin C (**9**) are shown in table 6.5, page 135.

Structural elucidation of grandifoliolenone (10)

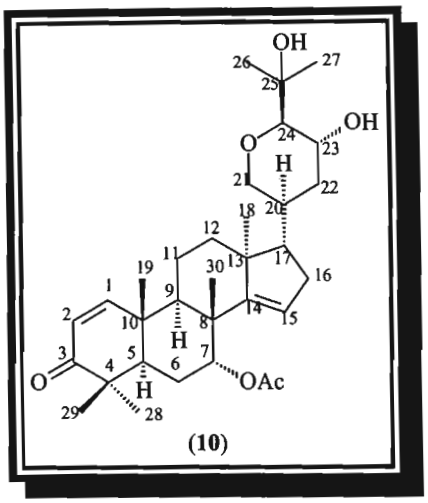

(10)

Fig. 6.9. Grandifoliolenone (10)

Grandifoliolenone (**10**) was isolated as a white crystalline material, mp 203-204 °C. The molecular ion peak was not clear in the mass spectrum **[127]**, however, a fragment ion peak due to the loss of water was seen at *m/z* 510.33137 which corresponded to the formula $C_{32}H_{46}O_5$ (requires 510.33453). From this the molecular formula of $C_{32}H_{48}O_6$ was deduced. The IR spectrum **[128]** showed a band at 3413 cm^{-1} due to hydroxy stretching, C-H stretch bands at 2926 cm^{-1} and 2854 cm^{-1} and carbonyl bands at 1740 cm^{-1} and 1673 cm^{-1}.

Grandifoliolenone (**10**) is a known compound that has also been previously isolated from *Khaya grandifoliola*.[24,25] This compound (**10**) is very similar to sapelin C (**9**). The only difference between the two compounds is the 7-acetyl group present in grandifoliolenone (**10**).

The methyl group proton resonance of the acetate group appeared at δ_H 1.93 in the ^1H NMR spectrum **[129]**. The H-7 resonance appeared further downfield at δ_H 5.21 and the H-15 resonance appeared at δ_H 5.31 in the ^1H NMR spectrum **[129]**.

The H-7 resonance showed a COSY **[134]** correlation with H-6β (δ_H 1.75) and the H-15 resonance showed a COSY **[134]** correlation with H-16α (δ_H 2.21). The H-7 resonance showed a NOESY **[135]** correlation with the 3H-30 methyl resonance which is β-orientated on biosynthetic grounds. This confirmed the β-orientation for H-7, leaving an α-orientation for the acetate group at C-7.

The oxygenated fully substituted carbon resonance at δ_C 74.23 and the oxygenated methine carbon resonances at δ_C 64.36 and 86.58 and the methylene carbon resonance at δ_C 70.05 were assigned to C-25, C-23, C-24, and C-21 respectively by comparison with ^{13}C NMR data of sapelin C (**9**). The resonances at δ_H 3.85, 2.88, 3.43, and 3.95 were assigned to H-23, H-24, and two H-21 protons respectively by use of the HSQC spectrum **[132-133]**.

Some ^{13}C / ^{1}H NMR correlations could not be seen in the weak HSQC **[132-133]** spectrum. Therefore some resonances could not be assigned.

Acetylation of grandifoliolenone (**10**) was also attempted but unsuccessful since a small amount of starting material was used and phthalate contamination occurred. However, thin layer chromatographic analysis of the acetylation products of sapelin C (**9**) and grandifoliolenone (**10**) showed that the same acetylation product had been produced for both compounds as expected.

The NMR data for grandifoliolenone (**10**) are shown in table 6.6, page 136.

4.4 Experimental

A specimen of *Neobeguea mahafalensis* Leroy seeds (voucher no. : 02.00 / nJ. nDul) from the forests of Madagascar was obtained and identified by Dr. M. Randrianarivelojosia of the University of Antananarivo, Madagascar. The voucher specimen is retained at the University of Antananarivo.

The seeds and shell were separated and both were separately ground and extracted successively in a Soxhlet apparatus with hexane, ethyl acetate and methanol. Each extraction was carried out over a period of 48 hours.

The hexane extract (12 g) of the seed shells yielded, after column chromatography over silica gel (Merck 9385), the three protolimonoids, the novel sapelin E acetate (**8**) (11 mg), sapelin C (**9**) (7 mg) and grandifoliolenone (**10**) (9 mg).

The ethyl acetate extract (7 g) of the seeds yielded the three limonoids, methyl angolensate (**5**) (18 mg), mexicanolide (**6**) (19 mg) and khayasin (**7**) (23 mg).

The ^{1}H NMR spectra of the crude hexane and methanol extracts of the seeds and the crude ethyl acetate and methanol extracts of the seed shells did not show the presence of any compounds of interest. Therefore these crude extracts were not investigated further.

Physical Data for methyl angolensate (5)

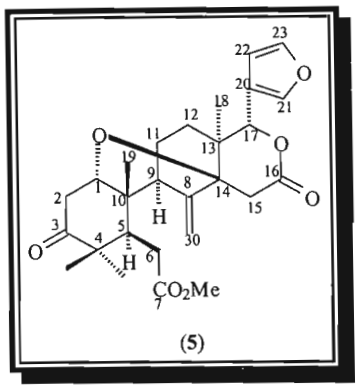

Fig. 6.3. Methyl angolensate (5)

Physical appearance	White crystalline material	**mp**	206-207 °C (Lit.[6] 212-214 °C)
Yield	18 mg	**Optical rotation : $[\alpha]_D^{25}$ ($CHCl_3$)**	-19.58 ° [c=0.19] (Lit.[6] $[\alpha]_D^{30}$: -43 ° [c=2])
EIMS [M^+] at *m/z*	470 ($C_{27}H_{34}O_7$ requires 470.2305)	**IR : ν_{max} (NaCl) cm^{-1}**	2931, 2859 (C-H stretch), 1740 (C=O), 1247, 1035 (C-O)
EIMS at *m/z*	439 [M^+-OCH_3], 359, 332, 243, 210, 177, 149, 105 (100%), 79, 41		

Table 6.1. NMR data for methyl angolensate (5)

C	$\delta^{13}C$ / ppm ($CDCl_3$)	δ^1H / ppm ($CDCl_3$)	HMBC (C→H)	COSY	NOESY
1	77.16 (CH)	3.50 (dd, *J* = 4.03, 10.16 Hz)	2α, 2β, 5, 9, 19	2α, 2β	2α, 2β, 19
2	39.38 (CH_2)	α) 2.48 (dd, *J* = 4.03, 10.16 Hz)	1	1, 2β	1, 2β, 28
		β) 2.86 (m)		1, 2α	1, 2α, 19, 12β, 29
3	212.82 (C)	-	1, 2α, 2β, 28, 29		
4	48.00 (C)	-	6a, 6b, 28, 29, 2β		
5	42.86 (CH)	2.84 (m)	1, 6a, 6b, 19, 28, 29	6a, 6b	6b, 9, 28
6	32.63 (CH_2)	a) 2.23 (d, *J* = 16.48 Hz)	5	5, 6a	6b
		b) 2.60 (d, *J* = 16.48 Hz)		5, 6b	5, 6a, 28, 29
7	173.84 (C)	-	6a, 6b, OMe		
8	145.71 (C)	-	11β, 30a		
9	49.83 (CH)	2.15 (d, *J* = 4.39 Hz)	12α, 19	11α	5, 11α
10	43.97 (C)	-	2α, 2β, 5, 6a, 9, 11α, 19		
11	23.68 (CH_2)	α) 1.56 (m)	12α	9, 11β, 12β, 12α	9, 11β, 12α, 18
		β) 2.21 (d, *J* = 4.39 Hz)		11α, 12β	11α, 19, 30b
12	29.24 (CH_2)	α) 1.09 (dd, *J* = 4.58 Hz)	9, 18	12β, 11α	11α, 12β, 22
		β) 1.86 (dd, *J* = 4.76 Hz)		11α, 11β, 12α	2β, 12α, 17
13	41.37 (C)	-	12β, 15β, 18		
14	80.15 (C)	-	1, 2β, 9, 12α, 15β, 15α, 18		
15	33.72 (CH_2)	α) 2.89 (d, *J* = 7.79 Hz)		15β	15β, 18
		β) 2.56 (d, *J* = 7.79 Hz)		15α	15α, 19
16	170.10 (C)	-	15α, 15β		
17	79.56 (CH)	5.64 (s)	18		12β, 18, 21, 22
18	13.71 (CH_3)	0.84 (s)	12β		11α, 15α, 17, 21, 22, 30a
19	21.44 (CH_3)	0.92 (s)	1, 2β, 5, 9		1, 2β, 11β, 15β, 30b
20	120.75 (C)	-	17, 21, 22, 23		
21	140.73 (CH)	7.41 (s)	17, 22, 23	22	17, 18
22	109.87 (CH)	6.36 (d, *J* = 0.91 Hz)	17, 21	21, 23	12α, 17, 18, 23
23	142.71 (CH)	7.36 (d, *J* = 1.65 Hz)	21, 22	22	22
28	25.81 (CH_3)	1.02 (s)	2β, 29		2α, 5, 6b, OMe
29	21.60 (CH_3)	1.17 (s)	2β, 5, 28		2β, 6b
30	111.52 (CH_2)	a) 4.87 (s)	11β	30b	15α, 18, 30b
		b) 5.12 (s)		30a	11β, 15α, 19, 30a
OMe	52.06 (CH_3)	3.69 (s)			28

Physical Data for mexicanolide (6)

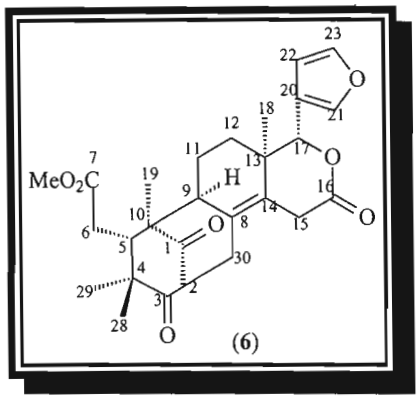

Fig. 6.4. Mexicanolide (6)

Physical appearance	White crystalline material	**mp**	215-216 °C (Lit.[6] 222-227 °C)
Yield	19 mg	**Optical rotation : $[\alpha]_D^{25}$ ($CHCl_3$)**	-78.76 ° [c=0.23] (Lit.[6] –100 °)
EIMS [M^+] at *m/z*	468 ($C_{27}H_{32}O_7$ requires 468.2148)	**EIMS at *m/z***	438, 408, 249, 218, 189, 135, 95, 43
IR : ν_{max} (NaCl) cm^{-1}	2930, 2853 (C-H stretch), 1732 (C=O), 1260, 1035 (C-O)		

Table 6.2. NMR data for mexicanolide (6)

C	$\delta^{13}C$ / ppm ($CDCl_3$)	$\delta^{1}H$ / ppm ($CDCl_3$)	HMBC (C→H)	COSY	NOESY
1	211.01 (C)	-	19, 28, 30α		
2	50.50 (CH)	2.09 (m)	5, 29, 30α		11β, 29, 30β
3	213.00 (C)	-	29, 30α		
4	54.28 (C)	-	5, 6, 29		
5	40.15 (CH)	2.74 (dd, *J* = 4.76, 12.82 Hz)	6, 19, 28, 29	6	11β, 17, 28
6	32.29 (CH_2)	2.45 (2H, *J* = 4.76, 12.82 Hz)	5, 29	5	19, 28, 29
7	173.59 (C)	-	5, 6, OMe		
8	125.33 (C)	-	30α		
9	77.20 (CH)	1.87 (m)			18
10	49.40 (C)	-	5, 6, 19, 28		
11	18.57 (CH_2)	α)1.76 (m)		11β, 12α	29
		β)1.82 (m)		11α, 12α	2, 5
12	28.79 (CH_2)	α)1.11 (m)	18	12β, 11α, 11β	
		β)1.84 (m)		12α	17
13	37.99 (C)	-	17, 18		
14	133.86 (C)	-	17, 18, 30α, 30β		
15	32.96 (CH_2)	α)3.45 (d, *J* = 19.1 Hz)			18, 30α
		β)3.48 (d, *J* = 19.1 Hz)			
16	169.87 (C)	-			
17	80.67 (CH)	5.25 (s)	18		5, 12β, 21, 22
18	17.38 (CH_3)	0.99 (s)	17		9, 15α
19	17.90 (CH_3)	0.85 (s)	5		6, 30α
20	120.33 (C)	-	17, 23		
21	141.61 (CH)	7.56 (s)	17, 22	22	17, 28
22	109.96 (CH)	6.47 (s)	17, 21	21, 23	17, 23, 28
23	142.79 (CH)	7.38 (s)		22	22
28	21.93 (CH_3)	0.97 (s)	19		5, 6, 21, 22
29	17.97 (CH_3)	1.23 (s)	5, 28		2, 6, 11α
30	36.45 (CH_2)	α)3.19 (m)		30β	15α, 19, 30β
		β)2.29 (dd, *J* = 11.36 Hz)		30α	2, 30α
OMe	52.23 (CH_3)	3.71 (s)			

Physical Data for khayasin (7)

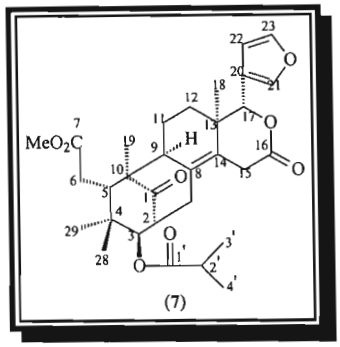

Fig. 6.5. Khayasin (7)

Physical appearance	White crystalline material	**mp**	113-115 °C (Lit.[6] 114-116 °C)
Yield	23 mg	**Optical rotation : $[\alpha]_D^{25}$ ($CHCl_3$)**	-106.05 ° [c=0.344] (Lit.[6] -165 °)
HRMS [M^+] at *m/z*	540.27251 ($C_{31}H_{40}O_8$ requires 540.27232)	**IR : ν_{max} (NaCl) cm^{-1}**	2982, 2889 (C-H stretch), 1736 (C=O), 1251, 1042 (C-O)
HRMS at *m/z*	509.25296 (M^+-OCH_3), 468.21381 (M^+-C_4H_7OH), 444.24963 (44.53%), 416.25741 (100%), 328.20344 (21.39%), 210.12553 (26.31%), 173.09632 (18.47%), 149.02459 (32.34%), 83.95364 (23.31%), 71.04965 (51.82%)		

Table 6.3. NMR data for khayasin (7)

C	$\delta^{13}C$ / ppm ($CDCl_3$)	δ^1H / ppm ($CDCl_3$)	HMBC (C→H)	COSY	NOESY
1	218.16 (C)	-	19, 30β, 2		
2	48.06 (CH)	3.13 (m)	3, 30β	3, 30α, 30β	3, 30α, 30β
3	78.02 (CH)	4.93 (d, J = 9.89 Hz)	5, 28, 29, 30α, 30β	2	2, 28, 29
4	38.47 (C)	-			
5	40.77 (CH)	3.21 (dd, J = 4.03, 8.79 Hz)	3, 6, 19, 28, 29	6	6, 11β, 17, 28
6	33.48 (CH_2)	2.35 (2H, J = 8.79 Hz)	5	5	5, 19, 28, 29
7	174.17 (C)	-	5, 6, OMe		
8	127.78 (C)	-	2, 15β, 30α, 30β		
9	52.22 (CH)	2.02 (m)	5, 19, 30β	2H-11, 12α, 15α, 15β	11α, 15α, 19
10	38.47 (C)	-	5, 6, 28, 29		
11	18.75 (CH_2)	1.75 (2H, m)		9, 12α, 12β	5, 9, 12α, 12β
12	29.11 (CH_2)	α) 1.08 (m)	18	2H-11, 12β	11α, 12β, 21, 22
		β) 1.74 (m)		2H-11, 12α	12α, 17, 21, 22
13	38.12 (C)	-	11, 12β, 15β, 17, 18		
14	131.70 (C)	-	15β, 17, 18, 30α, 30β		
15	33.19 (CH_2)	α) 3.44 (dt, J = 2.56, 20.88 Hz)		15β, 30α	9, 15β, 18
		β) 3.73 (m)		15α	15α, 17, 21, 22, 2', 3', 4'
16	169.75 (C)	-	15β		
17	80.72 (CH)	5.64 (s)	12β, 18		5, 12β, 15β, 21, 22, 3', 4'
18	17.73 (CH_3)	1.03 (s)	12α, 12β, 17		15α, 21, 22
19	16.65 (CH_3)	1.12 (s)			6, 9, 29
20	120.61 (C)	-	17, 21, 22, 23		
21	141.70 (CH)	7.52 (s)	17, 22, 23	22	12α, 12β, 15β, 17, 18
22	109.91 (CH)	6.45 (s)	17, 21	21, 23	12α, 12β, 15β, 17, 18, 23
23	142.80 (CH)	7.38 (s)	21, 22	22	22
28	23.14 (CH_3)	0.69 (s)			3, 5, 6, 29, 3', 4', OMe
29	20.57 (CH_3)	0.78 (s)			3, 6, 19, 28
30	33.18 (CH_2)	α) 2.08 (m)		2, 15α, 30β	2, 30β
		β) 2.77 (dd, J = 1.74, 15.11 Hz)	3	2, 30α	2, 30α, 15β
1'	176.61 (C)	-	3, 2',3' ,4'	-	
2'	34.42 (CH)	2.61 (h, J = 6.96 Hz)	3', 4'	3', 4'	15β, 3', 4'
3'	19.92 (CH_3)	*1.20 (m)	2'	2'	15β, 17, 28, OMe, 2'
4'	18.52 (CH_3)	*1.20 (m)	2'	2'	15β, 17, 28, OMe, 2'
OMe	52.05 (CH_3)	3.67 (s)			28, 3', 4'

* resonances superimposed.

Physical data for sapelin E acetate (8)

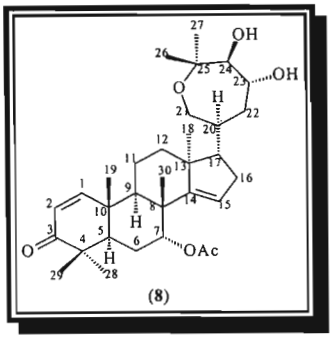

Fig. 6.6. Sapelin E acetate (8)

Physical appearance	White crystalline material	**mp**	206-207 °C
Yield	11 mg	**Optical rotation : $[\alpha]_D^{25}$ ($CHCl_3$)**	+6.0 ° [c=0.120]
HRMS [M^+-H_2O] at *m/z*	510.33442 ($C_{32}H_{46}O_5$ requires 510.33453)	**IR : ν_{max} (NaCl) cm^{-1}**	3437 (OH), 2931, 2859 (C-H stretch), 1735, 1673 (C=O), 1249, 1031 (C-O)
HRMS at *m/z*	492.32009 [M^+-$2H_2O$], 468.32224 [M^+-CH_3COOH], 395.25858 (24.55%), 368.2343 (24.18%), 309.21958 (37.66%), 308.214 (31.20%), 150.10454 (100%), 137.09696 (74.16%), 107.08566 (34.15%), 57.07034 (70.75%)		

Table 6.4. NMR data for sapelin E acetate (8)

C	$\delta^{13}C$ / ppm ($CDCl_3$)	$\delta^{1}H$ / ppm ($CDCl_3$)	HMBC (C→H)	COSY	NOESY
1	158.40 (CH)	7.14 (d, *J* = 10.26 Hz)	19	2	2, 19
2	125.43 (CH)	5.83 (d, *J* = 10.26 Hz)		1	1
3	204.74 (C)	-	1, 28, 29		
4	44.15 (C)	-	2, 28, 29		
5	46.17 (CH)	2.15 (d, *J* = 3.66 Hz)	1, 19, 28, 29	6	6, 28
6	23.81 (CH_2)	(2H) 1.76 (m)		5, 7	5, 7, OAc, 28, 29
7	74.68 (CH)	5.20 (bs)	30	6	6, 30, OAc
OAc C=O	170.14 (C)	-	OAc Me		
8	42.72 (C)	-	30		
9	38.47 (CH)	2.18 (m)	1, 19, 30		18
10	39.83 (C)	-	1, 2, 19		
11	16.75 (CH_2)	*α)1.57 (m)		11β, 12α, 12β	11β, 12α
		*β)1.68 (m)		11α, 12α, 12β	11α, 12β, 19, 30
12	34.05 (CH_2)	α)1.85 (m)	18	12β, 11α, 11β	11α, 12β
		β)1.66 (m)		12α, 11α, 11β	11β, 12α, 19, 30
13	46.32 (C)	-	18		
14	159.17 (C)	-	18, 30		
15	119.05 (CH)	5.28 (bs)		16β	16α, 16β, 30
16	35.02 (CH_2)	α)1.99 (m)		16β	15, 16β, 22α
		β)2.22 (m)		15, 16α	15, 16α, 22β
17	54.21 (CH)	1.89 (m)	18		21β, 23, 30
18	27.35 (CH_3)	0.96 (s)			9, 20, 21β, 22β
19	27.03 (CH_3)	1.14 (s)	2		1, 11β, 12β
20	36.36 (CH)	1.89 (m)		21β, 22α, 22β	18, 21α, 24
21	64.27 (CH_2)	α)3.59 (d, *J* = 10.07 Hz)		21β	20, 21β, 24, 27
		β)3.49 (d, *J* = 10.07 Hz)		20, 21α	17, 18, 21α
22	37.91 (CH_2)	α)1.62 (m)	24	20, 22β, 23	16α, 22β, 23, 24
		β)1.96 (m)		20, 22α, 23	16β, 18, 22α, 23
23	68.09 (CH)	3.79 (td, *J* = 2.57, 6.50 Hz)	24	22α, 22β, 24	17, 22α, 22β, 24, 26
24	80.75 (CH)	3.41 (d, *J* = 8.98 Hz)	26, 27	23	20, 21α, 22α, 23, 27
25	76.18 (C)	-	21α, 24, 26, 27		
26	22.42 (CH_3)	1.14 (s)	27, 24		23
27	26.29 (CH_3)	1.29 (s)	26, 24		21α, 24
28	21.27 (CH_3)	1.05 (s)	29		5, 6
29	19.95 (CH_3)	1.05 (s)	28		6
OAc Me	21.16 (CH_3)	1.92 (s)			6, 7
30	19.03 (CH_3)	1.17 (s)			7, 15, 17

* These proton resonances were not clearly visible in the HSQC spectrum [**110-111**].

Physical data for sapelin C (9)

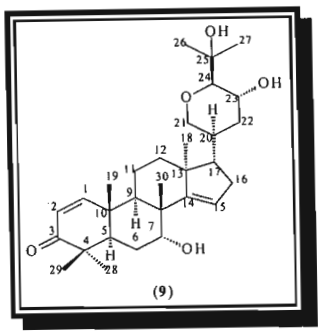

(9)

Fig. 6.8. Sapelin C (9)

Physical appearance	White crystalline material	**mp**	238-239 °C (Lit.[6] : 243-246 °C)
Yield	7 mg	**Optical rotation : $[\alpha]_D^{25}$ ($CHCl_3$)**	0.0 ° [c=0.01] (Lit.[6] : -14 ° [c=0.8]) sample too small to measure
HRMS [M^+-H_2O] at *m/z*	468.32474 ($C_{30}H_{44}O_4$ requires 468.32396)	**IR : ν_{max} (NaCl) cm^{-1}**	3387 (OH), 2926, 2859 (C-H stretch), 1730 (C=O), 1253, 1072 (C-O)
HRMS at *m/z*	428.294 (60.80%), 326.22492 (100%), 219.1381 (87.84%), 159.11721 (44.97%), 137.09674 (70.89%), 107.08549 (54.51%), 57.0704 (72.34%)		

Table 6.5. NMR data for sapelin C (9)

C	δ^{13}C/ppm ($CDCl_3$)	δ^1H/ppm ($CDCl_3$)	COSY	NOESY
1	158.34 (CH)	7.11 (d, *J* = 10.26 Hz)	2	2, 7, 28, 29
2	125.47 (CH)	5.81 (d, *J* = 10.26 Hz)	1	1
3	205.22 (C)	-		
4	44.23 (C)	-		
5	46.56 (CH)	2.38 (dd, *J* = 3.39, 12.00 Hz)	6	28, 29
6	24.29 (CH_2)	1.85 (2H) (dd, *J* = 3.39, 6.87 Hz)	5, 7	18
7	71.79 (CH)	3.97 (bs)	6	15, 19, 28, 29
8	44.82 (C)	-		
*9	36.80 (CH)	1.89 (m)	5	
10	40.06 (C)	-		
*11	16.49 (CH_2)	ξ a) 1.93 (m)	11b	
		ξ b) 2.20 (dd, *J* = 6.04, 12.09 Hz)	11a	
12	34.85 (CH_2)	ξ a) 1.56 (m)	12b	
		ξ b) 1.96 (m)	12a	
13	46.56 (C)	-		
14	161.53 (C)	-		
15	120.25 (CH)	5.51 (bs)	17	7, 28, 29
16	35.75 (CH_2)	(2H) 2.06 (m)	17	17
17	52.33 (CH)	2.33 (m)	15, 16	16, 22β
18	21.45 (CH_3)	1.07 (s)		6
19	19.57 (CH_3)	0.96 (s)		7
*20	44.54 (CH)	1.99 (m)		
21	70.02 (CH_2)	α) 3.43 (d, *J* = 10.26 Hz)	21β	21β, 24
		β) 3.96 (d, *J* = 10.26 Hz)	21α	21α
22	36.25 (CH_2)	α) 1.51 (m)	22β, 23	
		β) 2.03 (m)	22α, 23	17, 23
23	64.36 (CH)	3.86 (m)	22α, 22β, 24	22β, 26, 27
24	86.55 (CH)	2.89 (d, *J* = 8.97 Hz)	23	21α, 27
25	74.27 (C)	-		
▲26	24.01 (CH_3)	1.26 (s)		23
▲27	28.66 (CH_3)	1.30 (s)		23, 24
*28	18.93 (CH_3)	1.13 (s)		1, 7, 15
*29	27.63 (CH_3)	1.13 (s)		1, 7, 15
30	27.12 (CH_3)	1.14 (s)		

* resonance could not be assigned but proposed by comparison with literature values (tetracyclic part[21], side ring[22]).
ξ stereochemistry could not be determined.
*,▲ interchangeable resonances.

Physical data for grandifoliolenone (10)

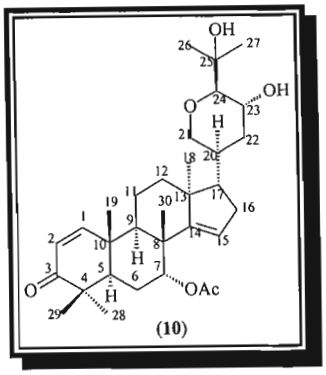

Fig. 6.9. Grandifoliolenone (10)

Appearance	White crystalline material	**mp**	203-204 °C
Yield	9 mg	**Optical rotation : $[\alpha]_D^{25}$ ($CHCl_3$)**	0.0 ° [c=0.021] sample too small to measure
HRMS [M^+-H_2O] at *m/z*	510.33137 ($C_{32}H_{46}O_5$ requires 510.33453)	**IR : ν_{max} (NaCl) cm^{-1}**	3413 (OH), 2926, 2854 (C-H stretch), 1740, 1673 (C=O)
HRMS at *m/z*	506.30131, 491.27659, 453.26764, 439.25055, 384.23209, 368.2289, 308.21428, 293.18741		

Table 6.6. NMR data for grandifoliolenone (10)

C	δ^{13}C/ppm ($CDCl_3$)	δ^1H/ppm ($CDCl_3$)	COSY	NOESY
1	158.36 (CH)	7.14 (d, J = 10.17 Hz)	2	2, 22α
2	125.47 (CH)	5.84 (d, J = 10.17 Hz)	1	1
3	204.71 (C)	-		
4	42.77 (C)	-		
5	46.39 (CH)	2.15 (m)		28, 29
*6	23.85 (CH_2)	α)1.29 (m)		
		β)1.75 (m)	7, OAc	7, 28, 29
7	74.84 (CH)	5.21 (bs)	6β	6β, 12β, 30
OAc Me	21.18 (CH_3)	1.93 (s)	6β	
8	44.16 (C)	-		
*9	38.68 (CH)	2.16 (m)		
10	39.75 (C)	-		
*11	16.84 (CH_2)	α)1.68 (s)		
		β)1.54 (s)		16β, 23, 24
*12	34.95 (CH_2)	α)1.66 (m)		
		β)1.78 (m)		7
13	46.18 (C)	-		
14	159.00 (C)	-		
15	119.55 (CH)	5.31 (d, J = 2.38 Hz)	16α	30
*16	34.95 (CH_2)	α) 2.21 (s)	15, 16β	
		β) 1.99 (s)	16α	11β, 23
*17	52.39 (CH)	1.88 (s)		19, 22β
18	19.06 (CH_3)	1.14 (s)		22β
19	20.35 (CH_3)	0.95 (s)		17
*20	(CH)			
21	70.05 (CH_2)	α)3.43 (dd, J = 2.29, 11.63 Hz)	21β	21β, 24
		β)3.95 (d, J = 11.63 Hz)	21α	21α
*22	36.26 (CH_2)	α)1.89 (d, J = 2.29 Hz)	22β	1
		β)1.63 (d, J = 4.49 Hz)	22α	17, 30
23	64.36 (CH)	3.85 (td, J = 4.49, 9.98 Hz)	24	11β, 16β, 26
24	86.58 (CH)	2.88 (d, J = 9.98 Hz)	23	11β, 21α, 27
25	74.23 (C)	-		
26	24.07 (CH_3)	1.26 (s)		23
27	28.61 (CH_3)	1.30 (s)		24
*28	21.24 (CH_3)	1.05 (s)		5, 6β
*29	27.04 (CH_3)	1.05 (s)		5, 6β
30	27.31 (CH_3)	1.19 (s)		7, 15, 22β

* resonances are interchangeable.

* the resonances could not be assigned because of weak spectra but are assigned by comparison with literature values.[21,22]

6.6 References

1. Dr. M. Randrianarivelojosia, Personal Communication.
2. Taylor, D.A.H., *Flora Neotropica*. Monograph No. 28 Meliaceae Chemotaxonomy, 1981, 450.
3. Mulholland, D.A., Kotsos, M.P., Randrianarivelojosia, M., *Phytochemistry*, 1999, **52**, 1141.
4. Mulholland, D.A., and Taylor, D.A.H., *Phytochemistry*, 1988, **27**, 1741.
5. Taylor, D.A.H., *Butterworth*, 1984, 353.
6. Njar, V.C.O., Adesanwo, J.K. and Raji, Y., *Planta Medica*, 1995, **61**, 91.
7. Connolly, J.D., MacLellan, M., Okorie, D.A. and Taylor, D.A.H., *J. Chem. Soc. Perkin Trans. 1*, 1976, 1993.
8. Sondengam, B.L., Kamga, C.S., Kimbu, S.F. and Connolly, J.D., *Phytochemistry*, 1981, **20**, 173.
9. Akisanya, A., Bevan, C.W.L., Hirst, J., Halsall, T.G. and Taylor, D.A.H., *J. Chem. Soc.*, 1960, 3827.
10. Adesogan, E.K. and Taylor, D.A.H., *J. Chem. Soc. (C)*, 1968, 1974.
11. Adesida, G.A., Adesogan, E.K. and Taylor, D.A.H., *Chem. Commun.*, 1967, 790.
12. Bevan, C.W.L., Ekong, D.E.U. and Taylor, D.A.H., *Nature*, 1965, 1323.
13. Connolly, J.D., Thornton, I.M.S. and Taylor, D.A.H., *J. Chem. Soc. Chem. Commun.*, 1970, 1205.
14. Bevan, C.W.L., Powell, J.W. and Taylor, D.A.H., *J. Chem. Soc.*, 1963, 980.
15. Taylor, D.A.H., *Phytochemistry*, 1983, **22**, 1297.
16. Ng, A.S. and Fallis, A.G., *Can. J. Chem.*, 1979, **57**, 3088.
17. Adesida, G.A., Adesogan, E.K., Okorie, D.A. and Taylor, D.A.H., *Phytochemistry*, 1971, **10**, 1845.
18. Connolly, J.D., Thornton, I.M.S. and Taylor, D.A.H., *J. Chem. Soc. Perkin Trans. 1*, 1973, 2407.
19. Adesogan, E.K., Bevan, C.W.L., Powell, J.W. and Taylor, D.A.H., *Chem. Commun.*, 1966, 27.
20. Chan, W.R., Taylor, D.R., Yee, T., *J. Chem. Soc. (C)*, 1971, 2662.
21. Mulholland, D.A., Monkhe, T.V., Taylor, D.A.H. and Rajab, M.S., *Phytochemistry*, 1999, **52**, 123.

22. Itokawa, H., Kishi, E., Morita, H. and Takeya, K., *Chem. Pharm. Bull.*, 1992, **40**, 1053.
23. Mulholland, D.A., Parel, B. and Coombes, P.H., *Current Organic Chemistry*, 2000, **4**, 1011.
24. Connolly, J.D. and McCrindle, R., *Chem. Commun.*, 1967, 1193.
25. Connolly, J.D. and McCrindle, R., *J. Chem. Soc. (C)*, 1971, 1715.

Conclusion

The findings contained in this work have proved to be interesting as novel compounds have been isolated.

The investigation of the *Cedrelopsis grevei* species provided a variety of compounds. It was interesting to isolate two limonoid-related compounds. Cedmiline (**14**) had been previously isolated by Dr. Hamdani Mahomed as novel. Cedashnine (**17**) is similar to cedmiline (**14**) and the difference between these structures is the butenolide ring instead of the limonoid furan ring, which makes the structure of cedashnine (**17**) novel.

Of particular interest was the isolation of the quassinoid, cedphiline (**19**). This quassinoid is not only novel with regard to its structure, but also with regard to its occurrence. This is the first case of a quassinoid being isolated from the Ptaeroxylaceae family. Quassinoids have only been found in the Simaroubaceae family so this confirms the link between the Ptaeroxylaceae and Simaroubaceae families suggested by Mulholland[♦] based on similarities with limonoid structures.

The lignan, cedpetine (**18**), is novel with regard to its structure and occurrence. This is the first case where the *meso* isomer of a symmetrical lignan with six methoxy groups have been isolated. It is also the first reported lignan from the Ptaeroxylaceae family.

The other three compounds, β-amyrin (**15**), scoparone (**16**) and sitosteryl β-D-glucopyranoside (**20**), isolated from *Cedrelopsis grevei* are common compounds that have been isolated many times previously. Sitosteryl β-D-glucopyranoside (**20**) is an antineoplastic agent.

A variety of compounds have been isolated from the *Neobeguea mahafalensis* species. Three known limonoids, methyl angolensate (**5**), mexicanolide (**6**) and khayasin (**7**) have been isolated. Methyl angolensate (**5**) is an anti-ulcer agent.

Three protolimonoids, sapelin E acetate (**8**), sapelin C (**9**) and grandifoliolenone (**10**) have also been isolated from this source. Sapelin E acetate (**8**) has not been reported previously although sapelin E (**11**) is known.

The three novel compounds (**17**), (**18**) and (**19**) from *Cedrelopsis grevei* and the novel compound (**8**) from *Neobeguea mahafalensis* have been sent to the National Cancer Institute in the United States of America for anti-cancer and anti-HIV screening.

♦ Mulholland, D.A., *J. Nat. Prod.*, 2002, in press.

Finally, Madagascar proves to be a land of miracles, providing a vast range of unique plant species that have evolved differently from the rest of the world. Scientists will continue to investigate this land in the search for compounds that will contribute to new and better drugs to treat human diseases.

Appendix

Structures of compounds isolated in this work

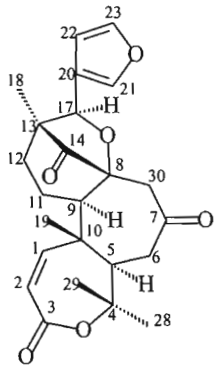

Cedmiline (14)

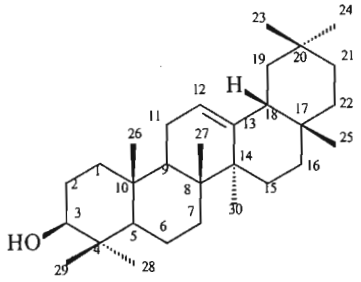

β–Amyrin (15)

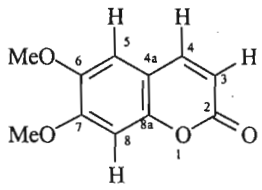

Scoparone (16)

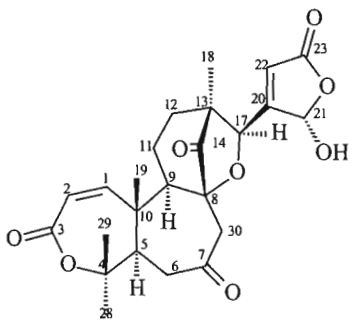

Cedashnine (17)

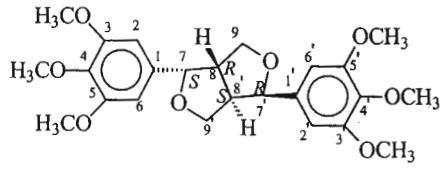

Cedpetine (18)

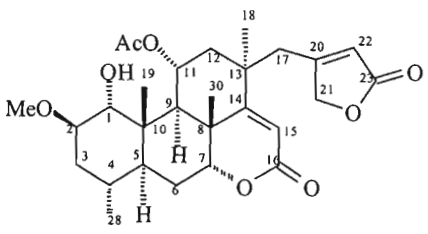

Cedphiline (19)

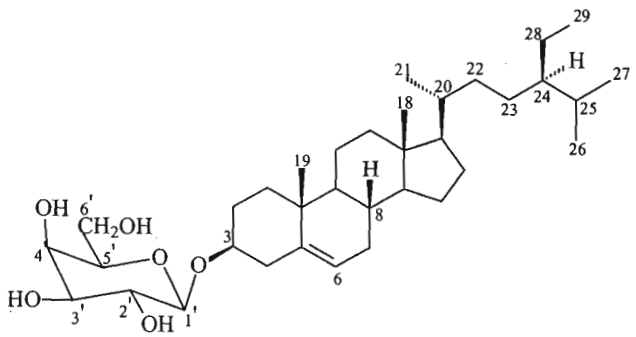

Sitosteryl β-D-glucopyranoside (20)

Compounds isolated from *Cedrelopsis grevei*

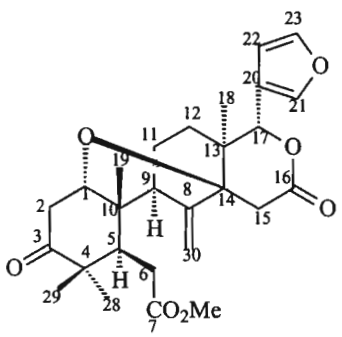

Methyl angolensate (5)

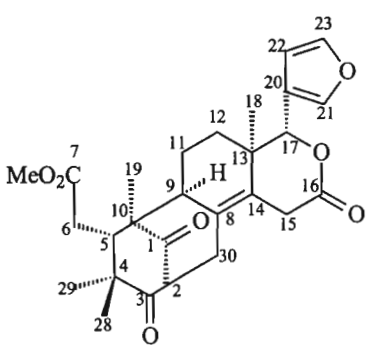

Mexicanolide (6)

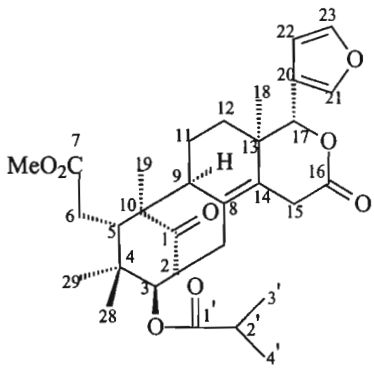

Khayasin (7)

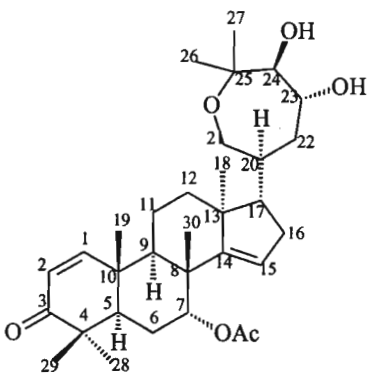

Sapelin E acetate (8)

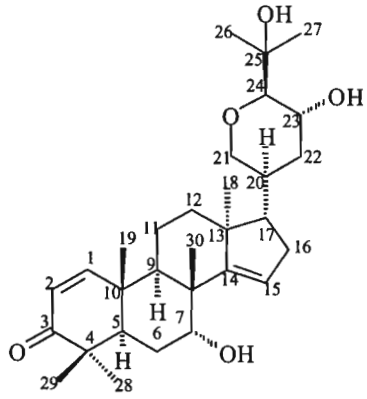

Sapelin C (9)

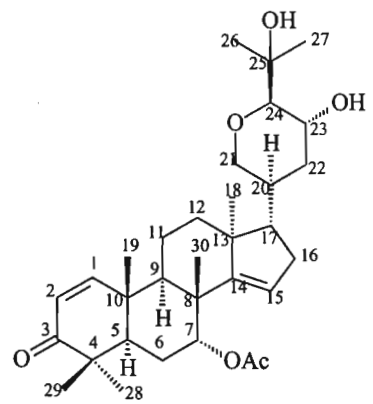

Grandifoliolenone (10)

Compounds isolated from *Neobeguea mahafalensis*

Part II

Spectra

CONTENTS **PAGE NO.**

Extractives from *Cedrelopsis grevei* stem bark

Photograph by Dr. Milijaona Randrianarivelojosia

Cedmiline (14)

Mass spectrum	**[4]**
IR spectrum	**[5]**
^{1}H NMR	**[6]**
^{13}C NMR	**[7]**
ADEPT	**[8]**
HSQC	**[9]**
Expanded HSQC	**[10]**
HMBC	**[11]**
COSY	**[12]**
NOESY	**[13]**

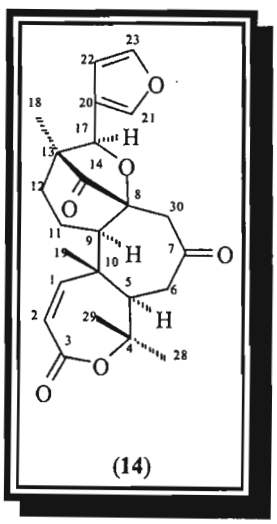

Cedmiline (14)

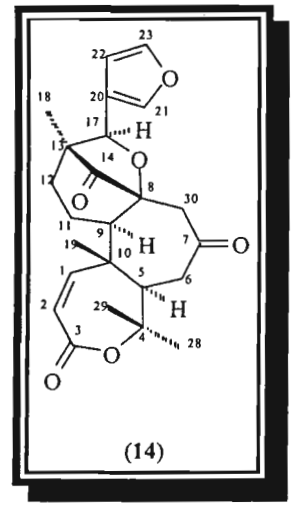

(14)

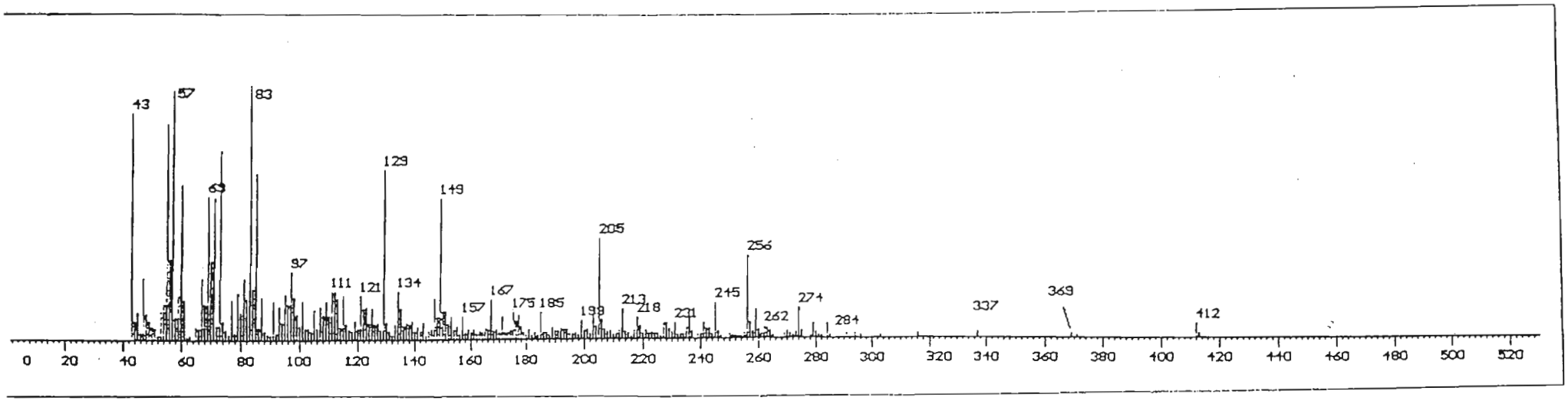

Mass spectrum of cedmiline (14)

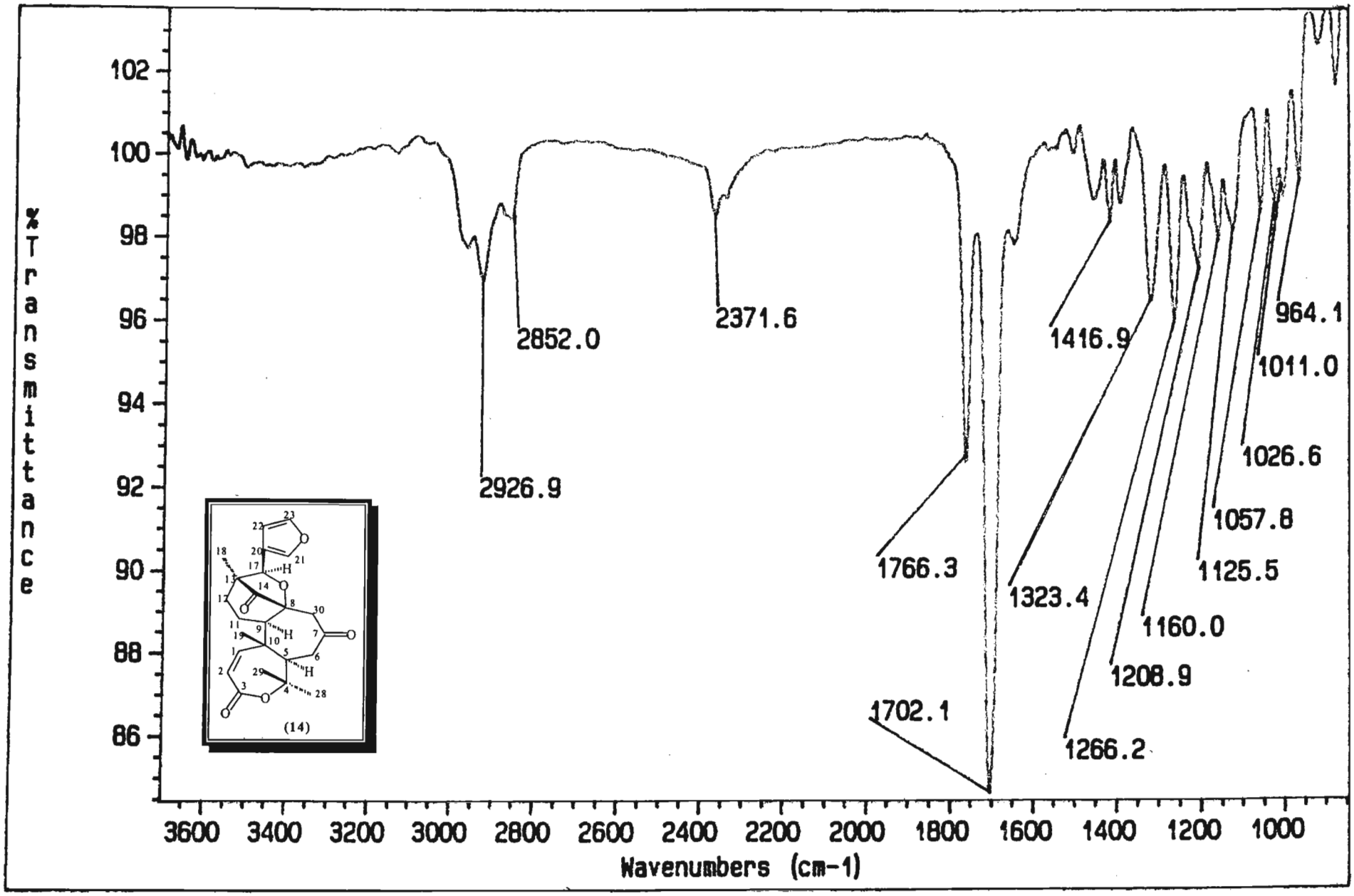

IR spectrum of cedmiline (14)

hdn92.dn-92 in cdcl3
probe=3mmID

(14)

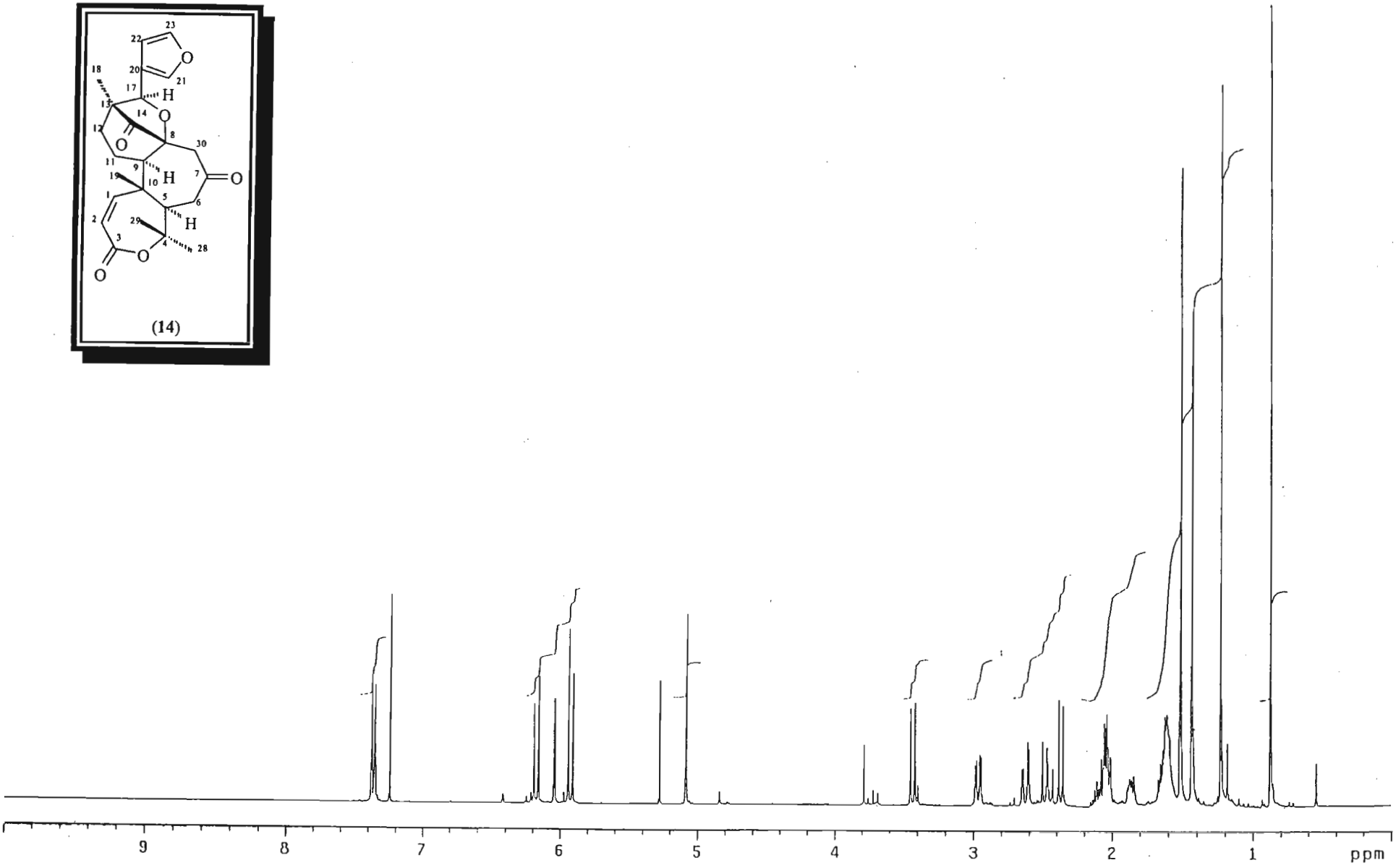

^{1}H NMR spectrum of cedmiline (14)

cdn92.dn-92 in cdcl3
probe=3mmID

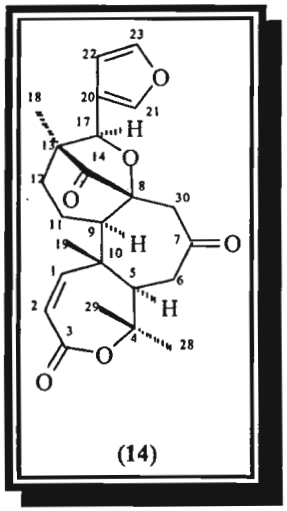

(14)

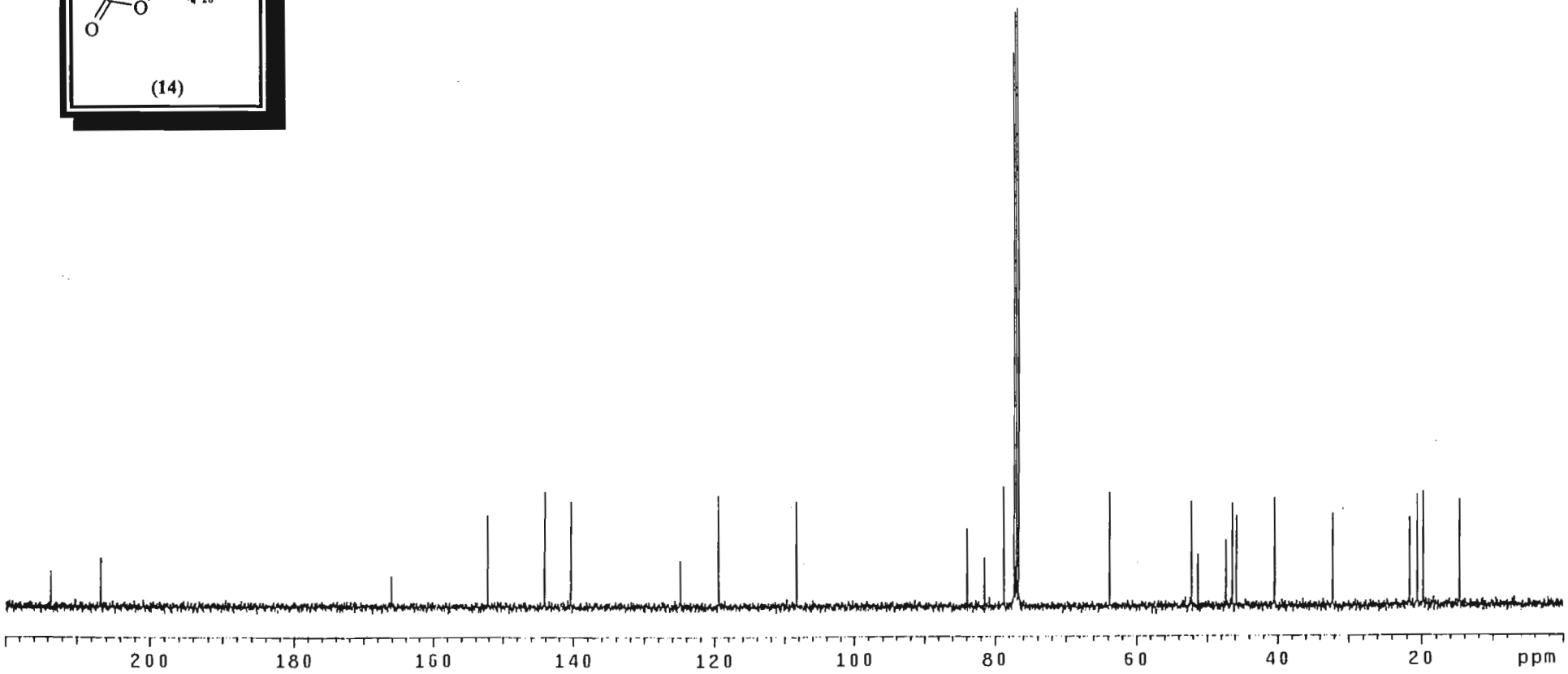

^{13}C NMR spectrum of cedmiline (14)

ddn92.dn=92 in cdcl3
probe=3mmI0

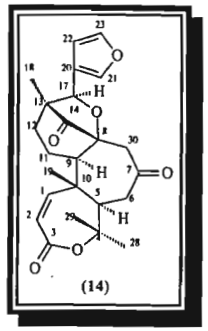

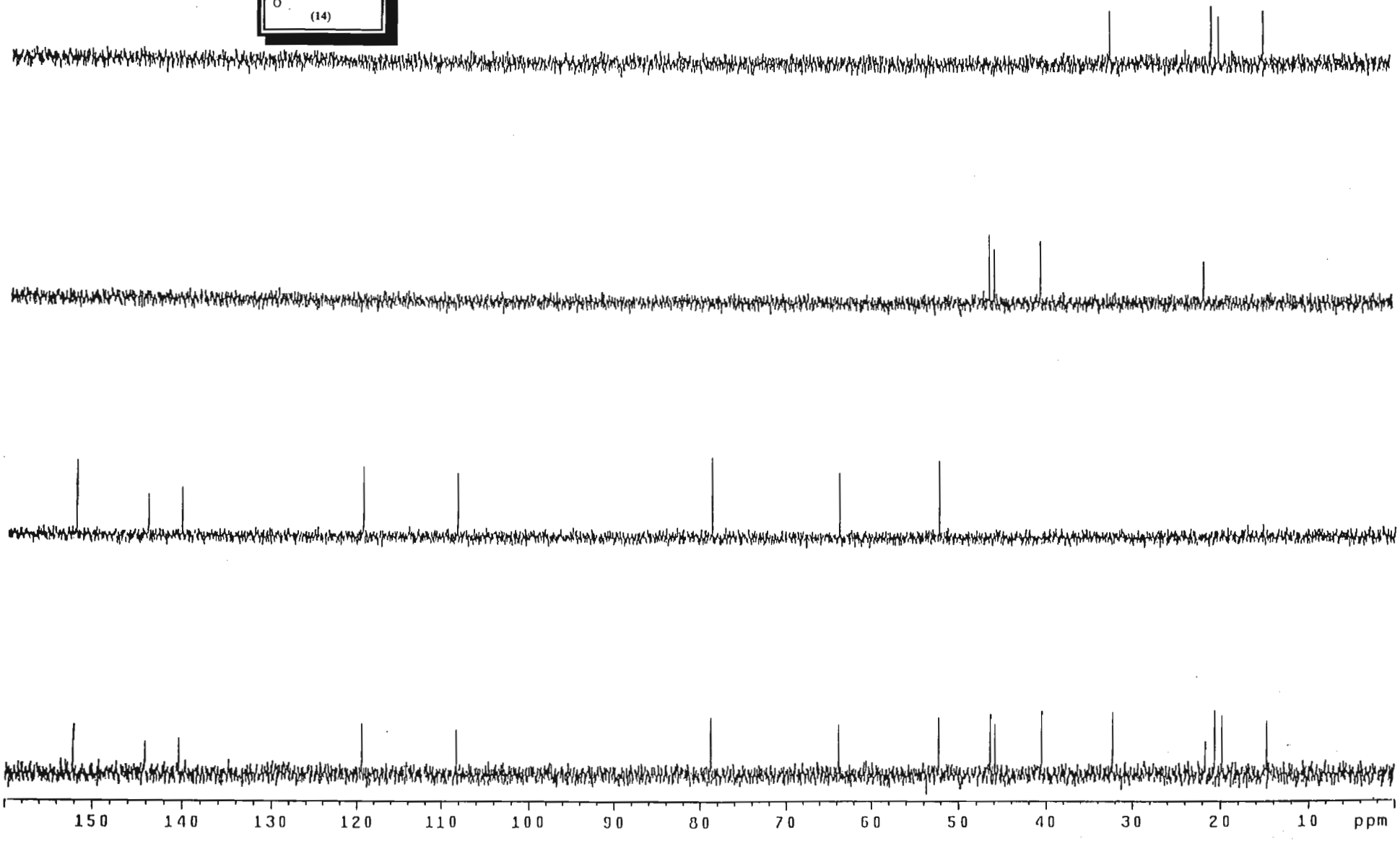

ADEPT NMR spectrum of cedmiline (14)

HQdn92.dn-92 in cdcl3
Gradient HSQC expt.

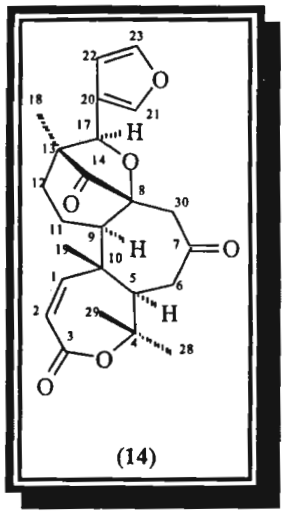

(14)

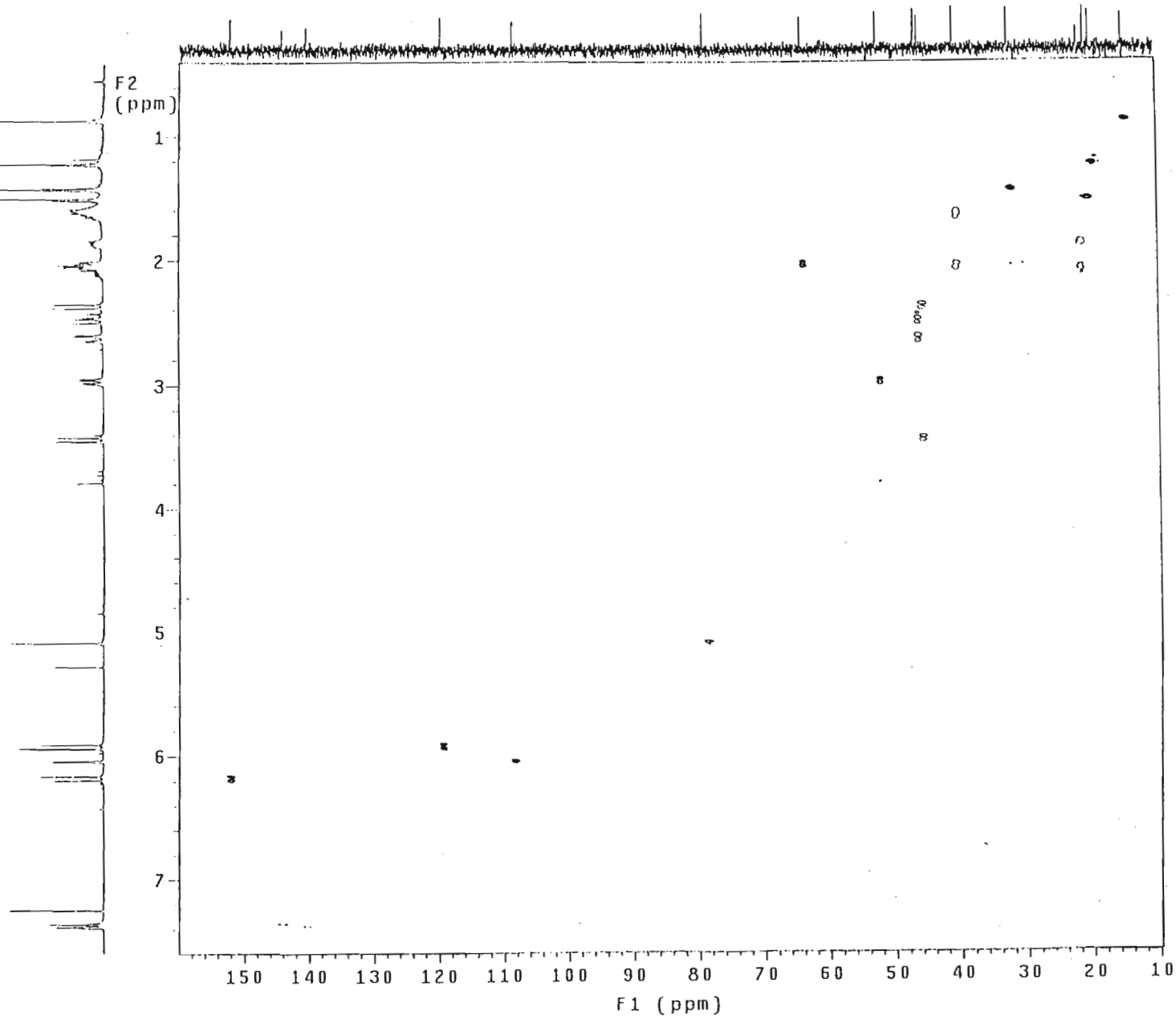

HSQC NMR spectrum of cedmiline (14)

HQdn92.dn-92 in cdcl3
Gradient HSQC expt.

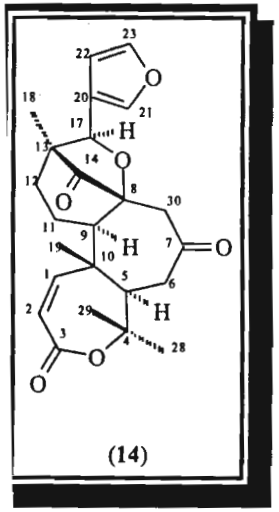

(14)

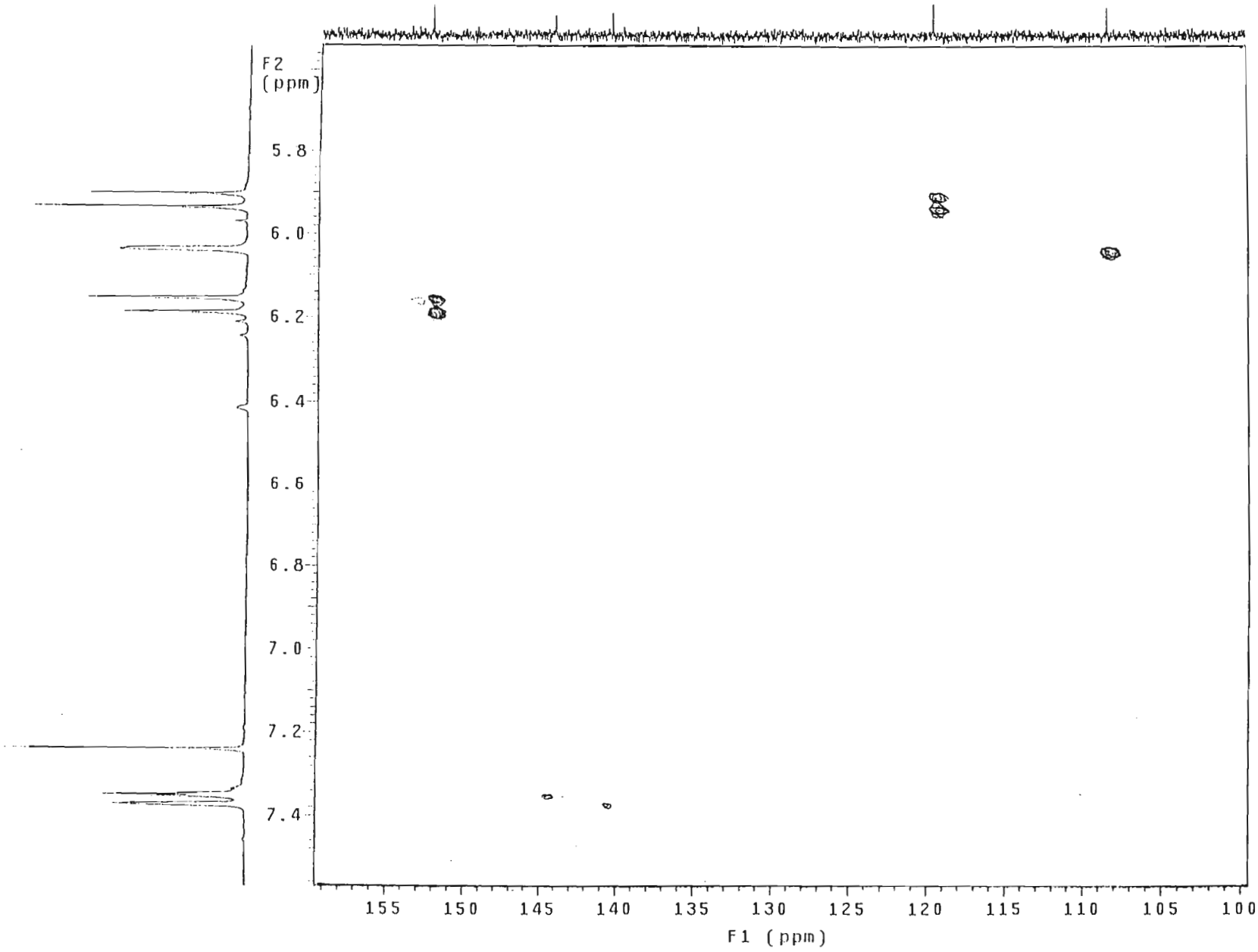

HSQC NMR spectrum of cedmiline (14)

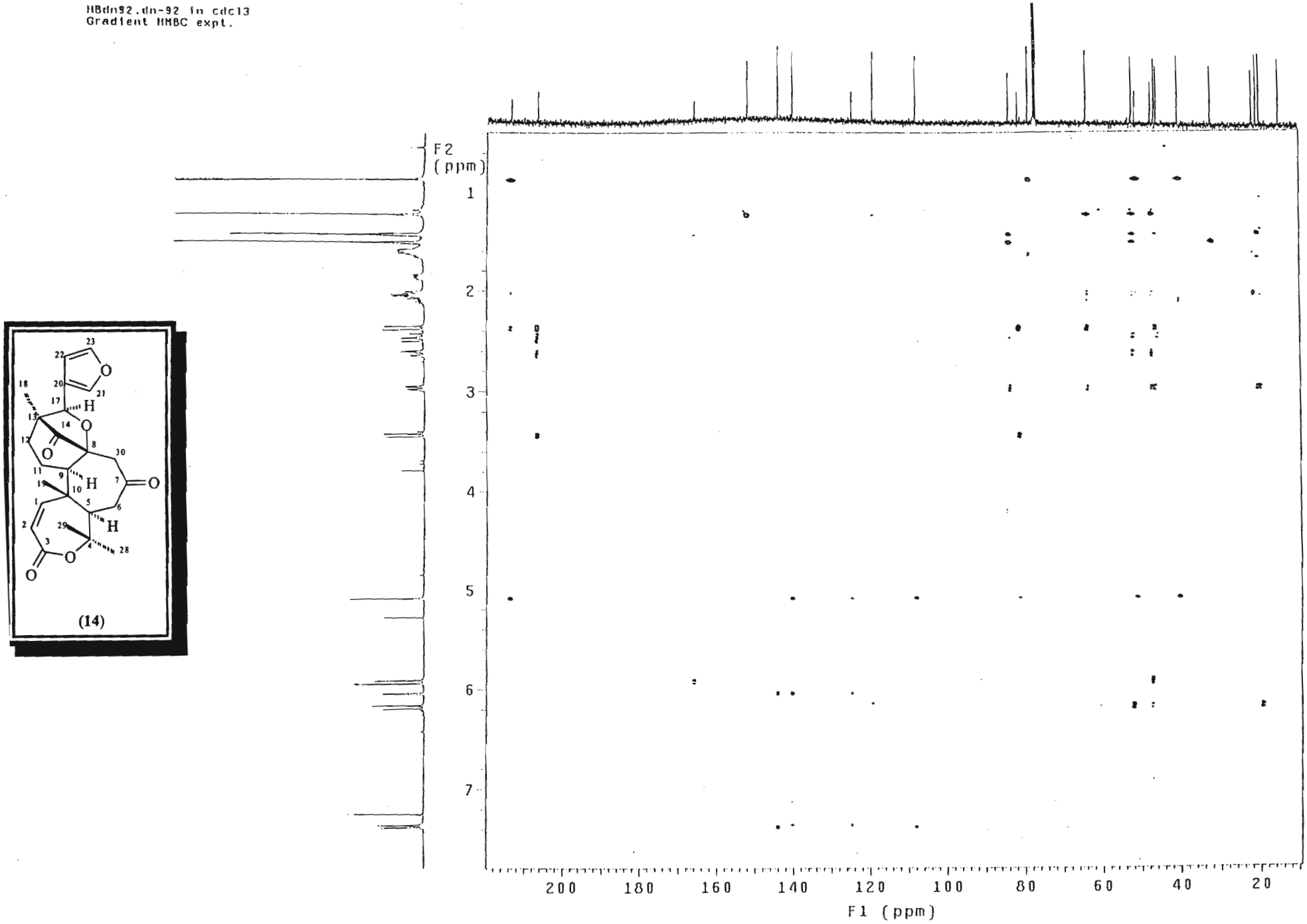

(14)

HMBC NMR spectrum of cedmiline (14)

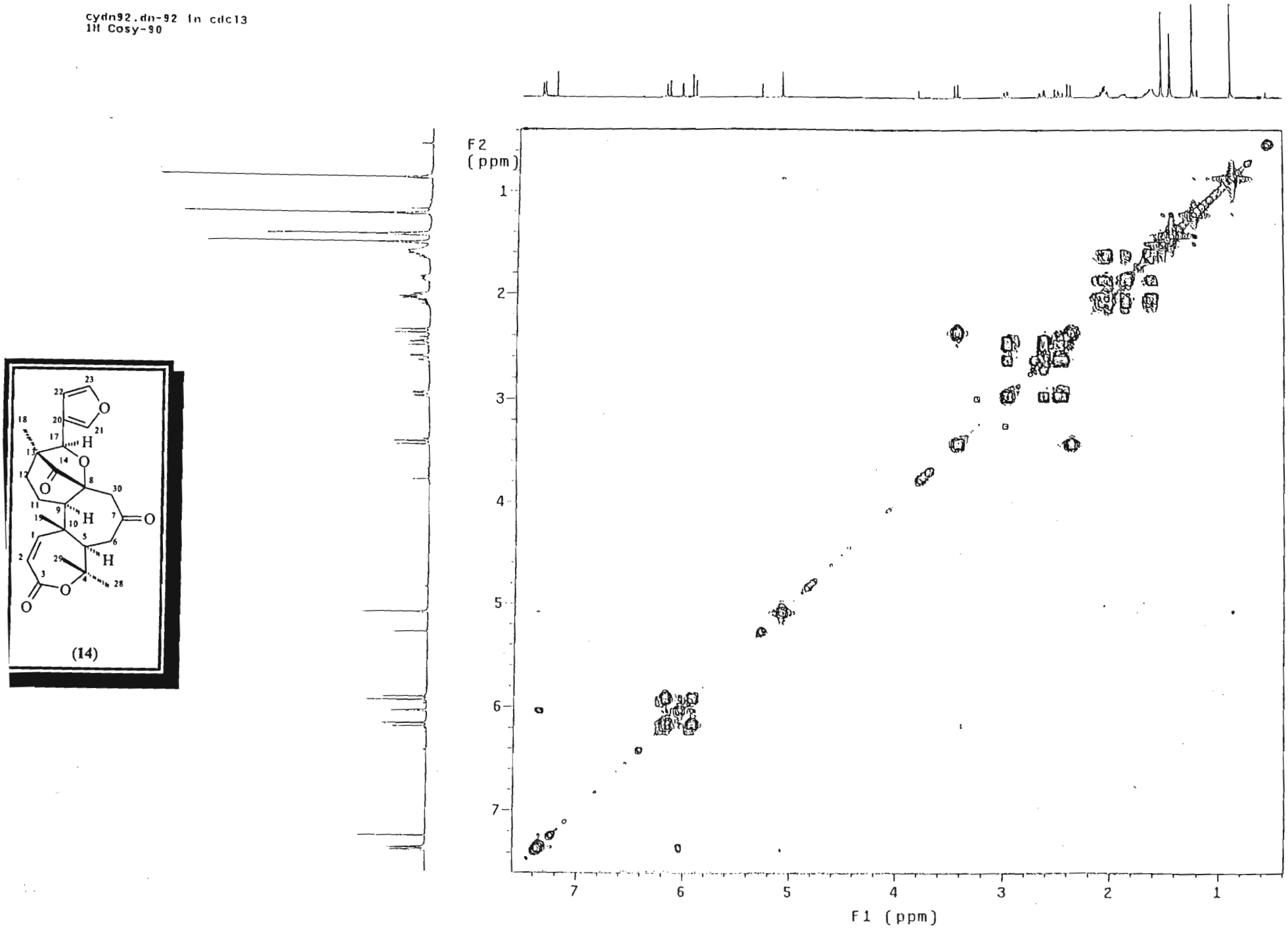

(14)

COSY NMR spectrum of cedmiline (14)

NOdn92.dn-92 in cdcl3
NOESY expt.

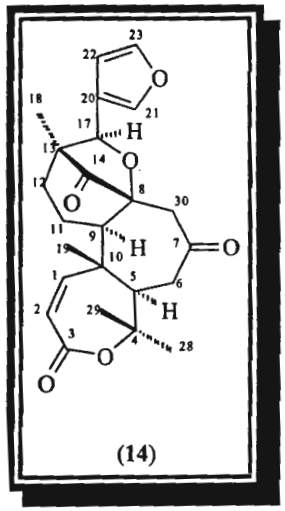

(14)

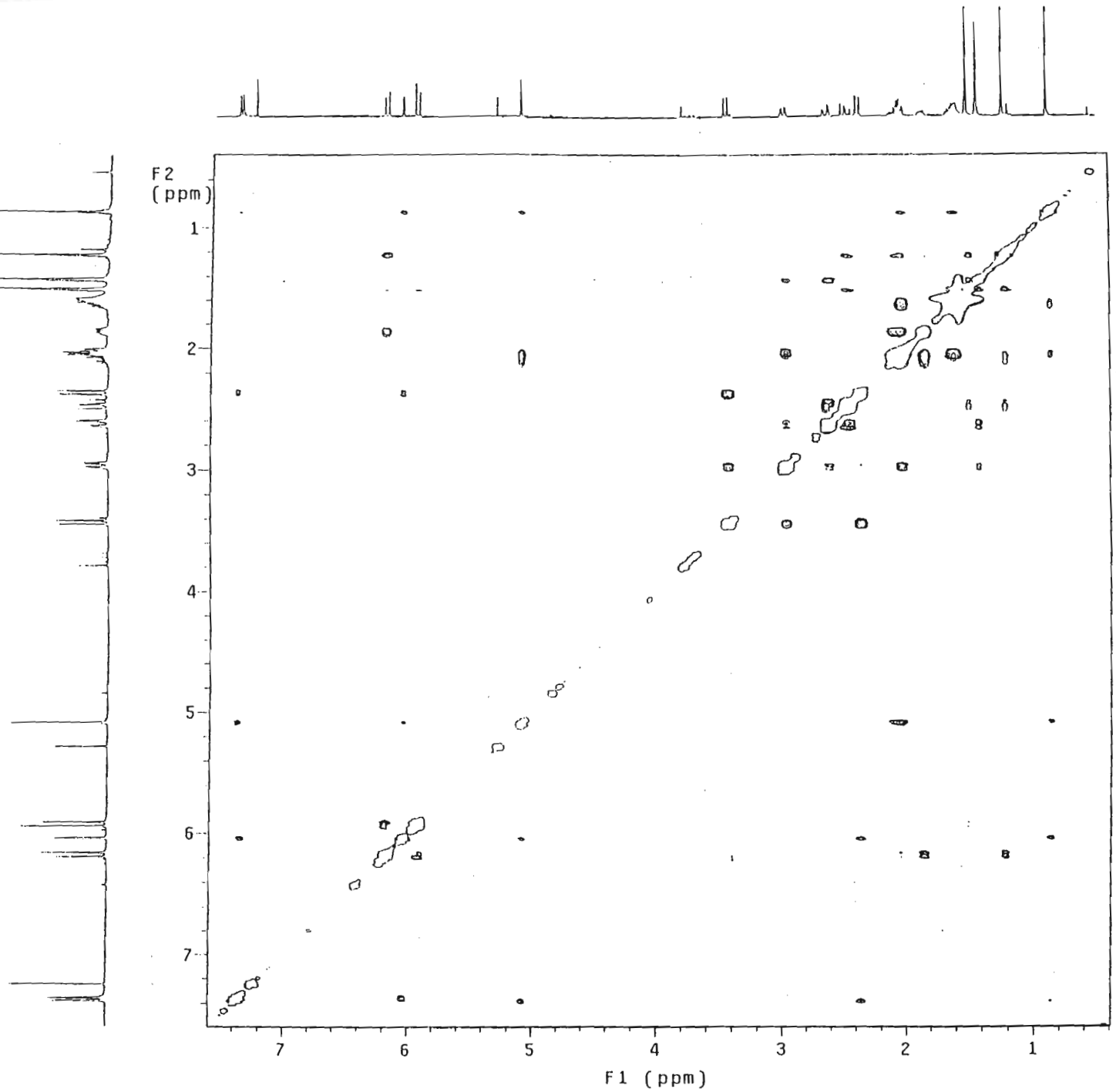

NOESY NMR spectrum of cedmiline (14)

β-Amyrin (15)

IR spectrum [15]

^{1}H NMR [16]

^{13}C NMR [17]

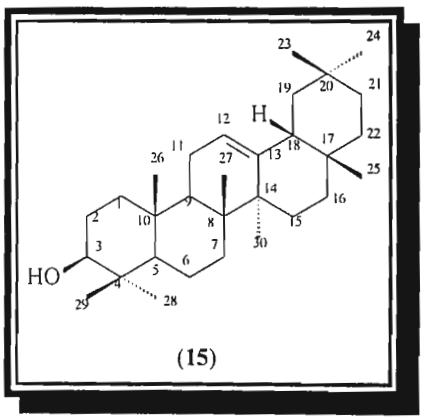

β-Amyrin (15)

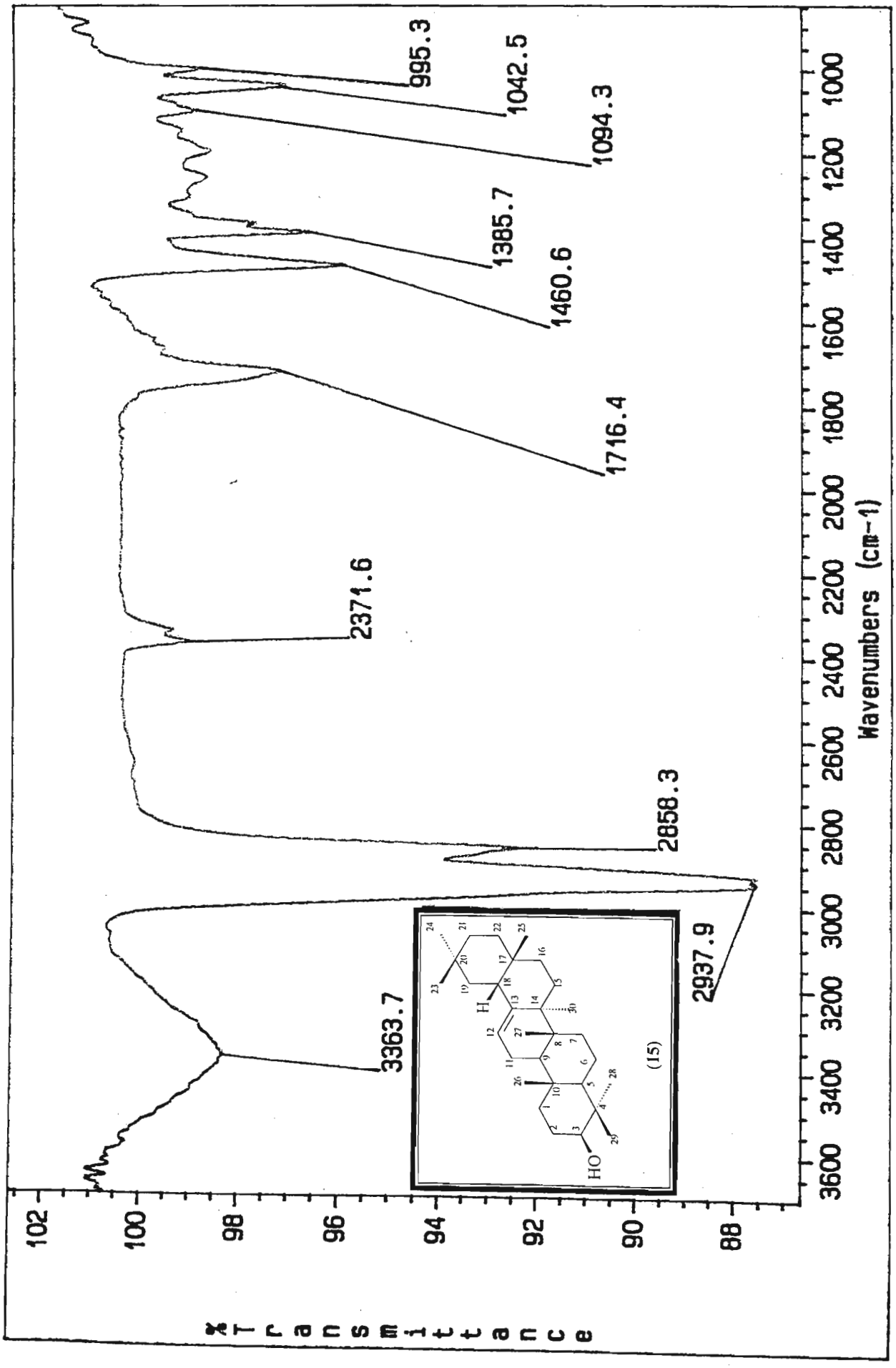

IR spectrum of β-amyrin (15)

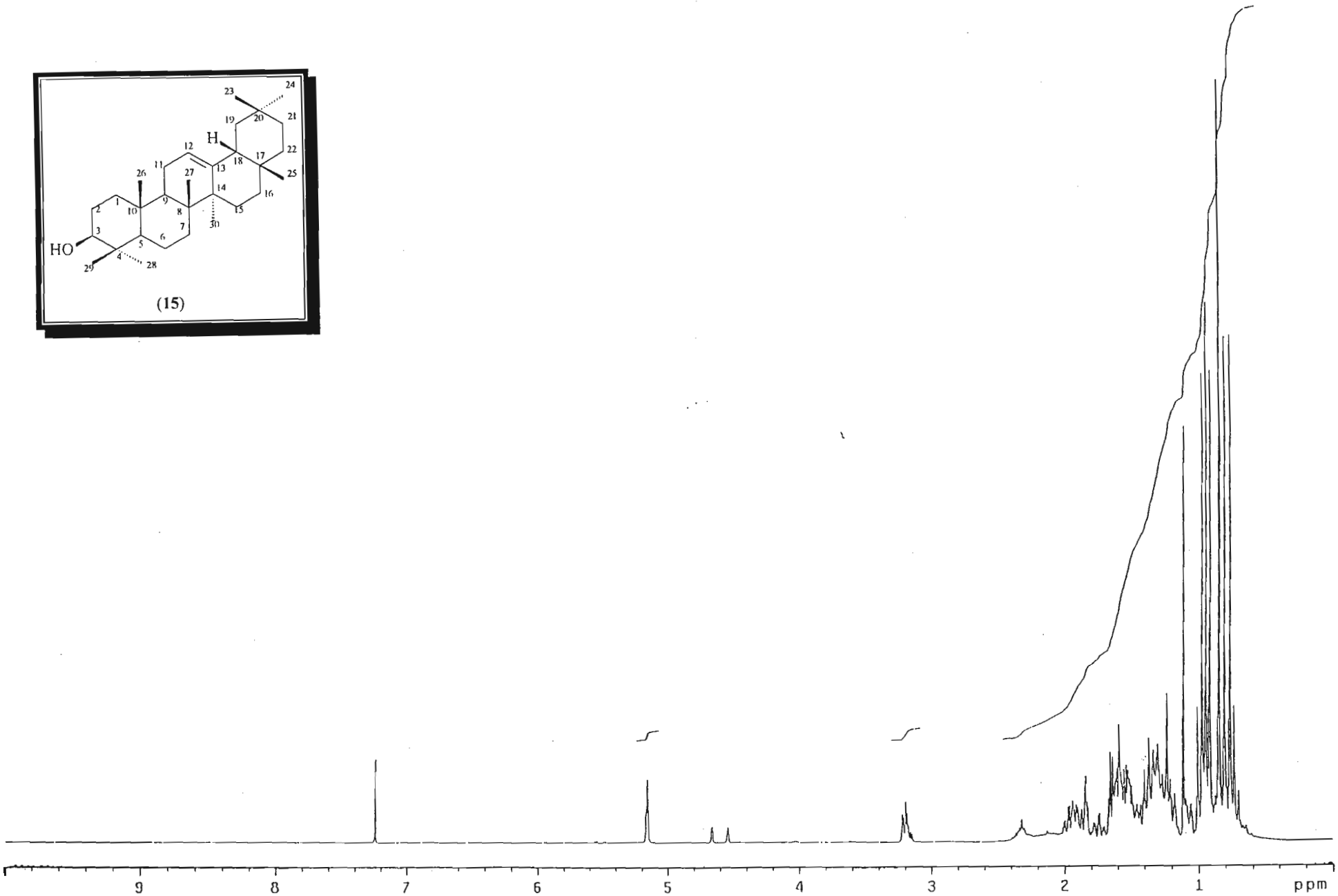

^{1}H NMR spectrum of β-amyrin (15)

cdm4.dn-4 in cdcl3
probe=3mmID

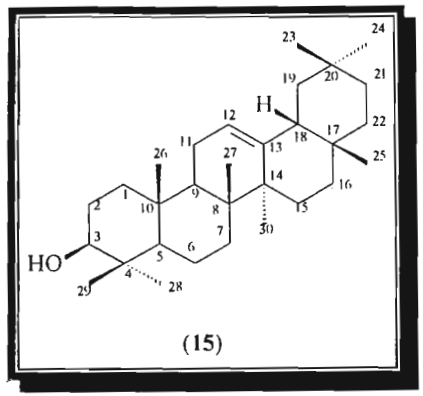

(15)

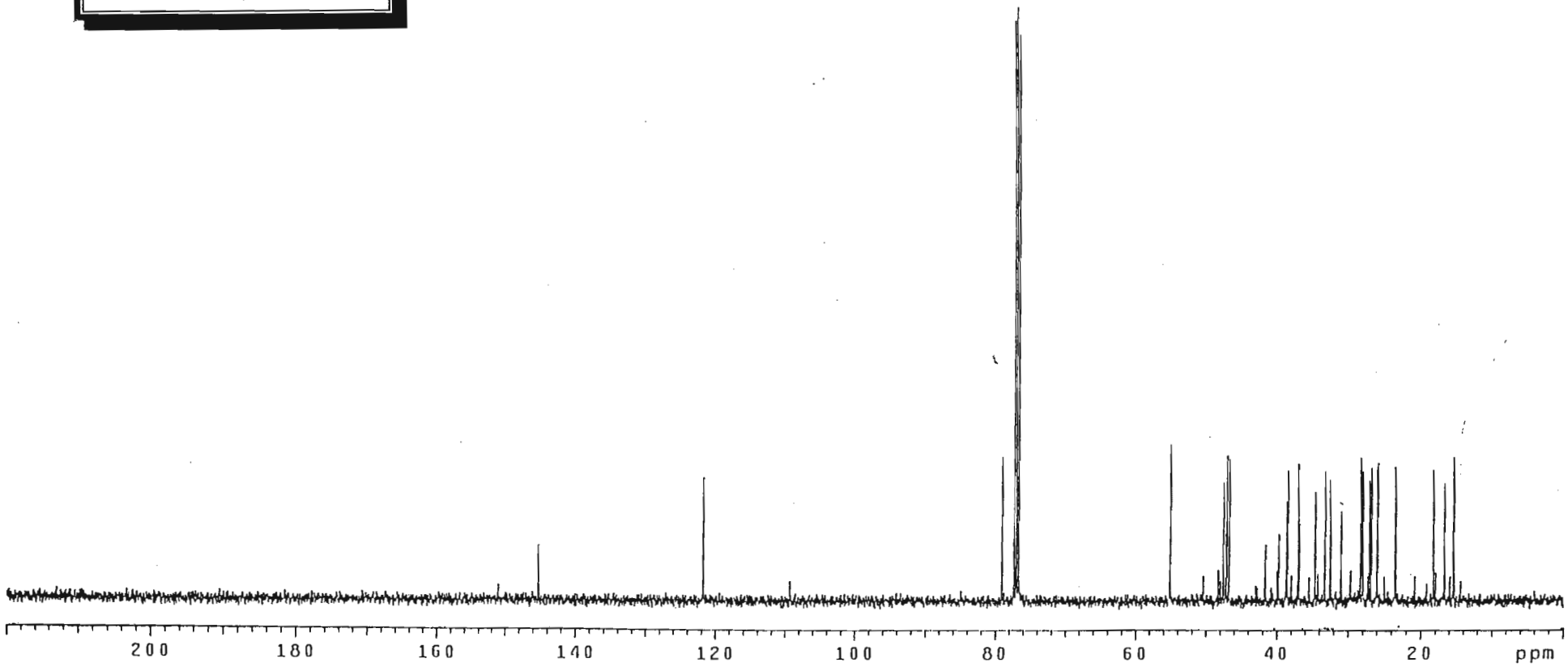

^{13}C NMR spectrum of β-amyrin (15)

Scoparone (16)

Mass spectrum	**[19]**
IR spectrum	**[20]**
UV spectrum	**[21]**
^{1}H NMR	**[22]**
^{13}C NMR	**[23]**
HSQC	**[24]**
HMBC	**[25]**
COSY	**[26]**
NOESY	**[27]**

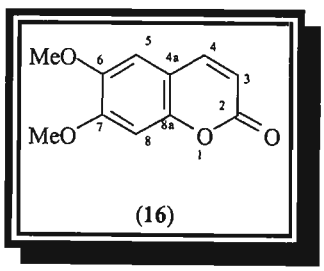

Scoparone (16)

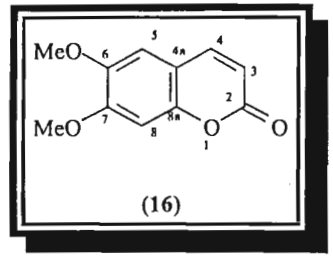

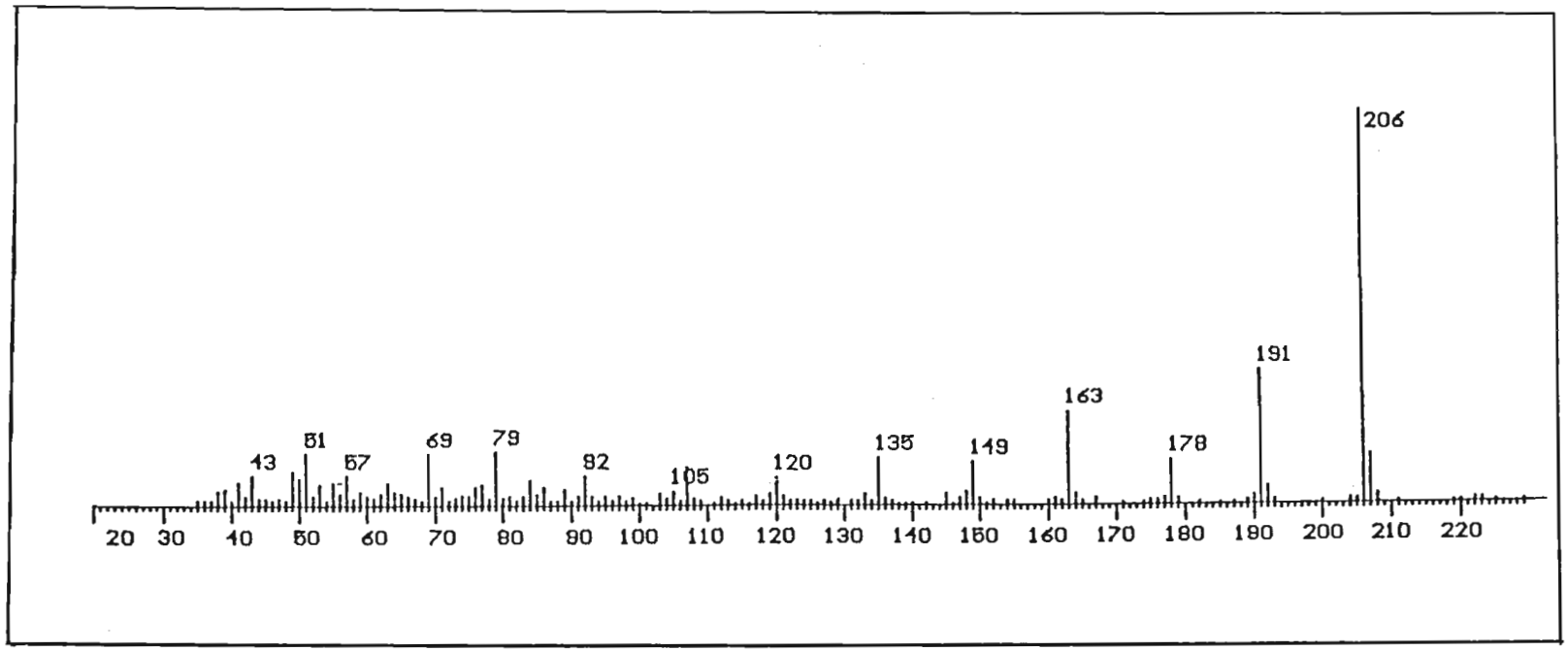

Mass spectrum of scoparone (16)

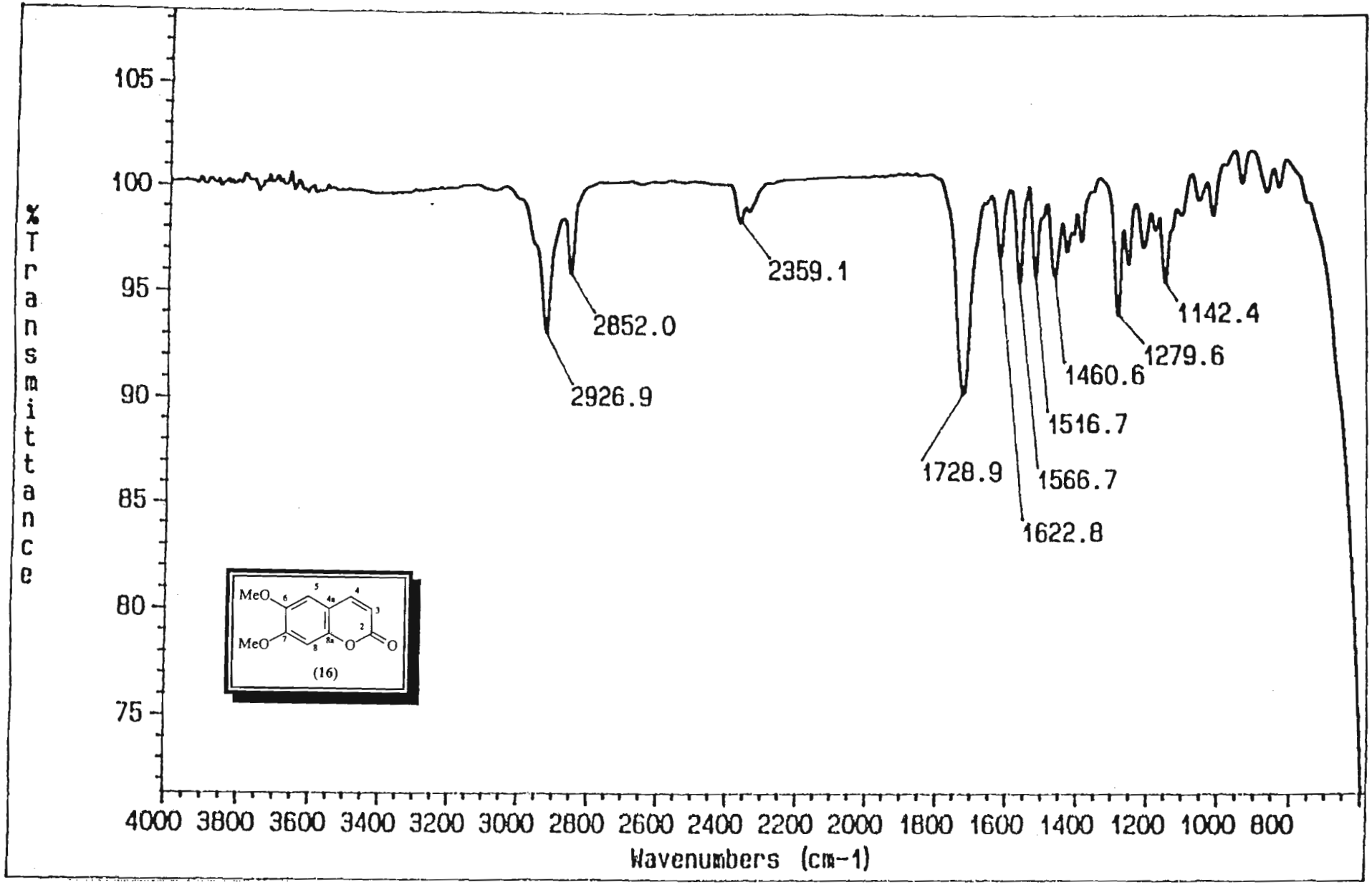

IR spectrum of scoparone (16)

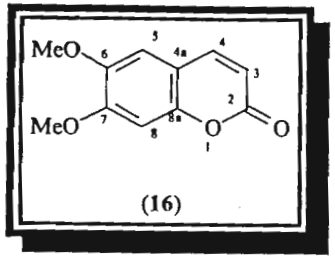

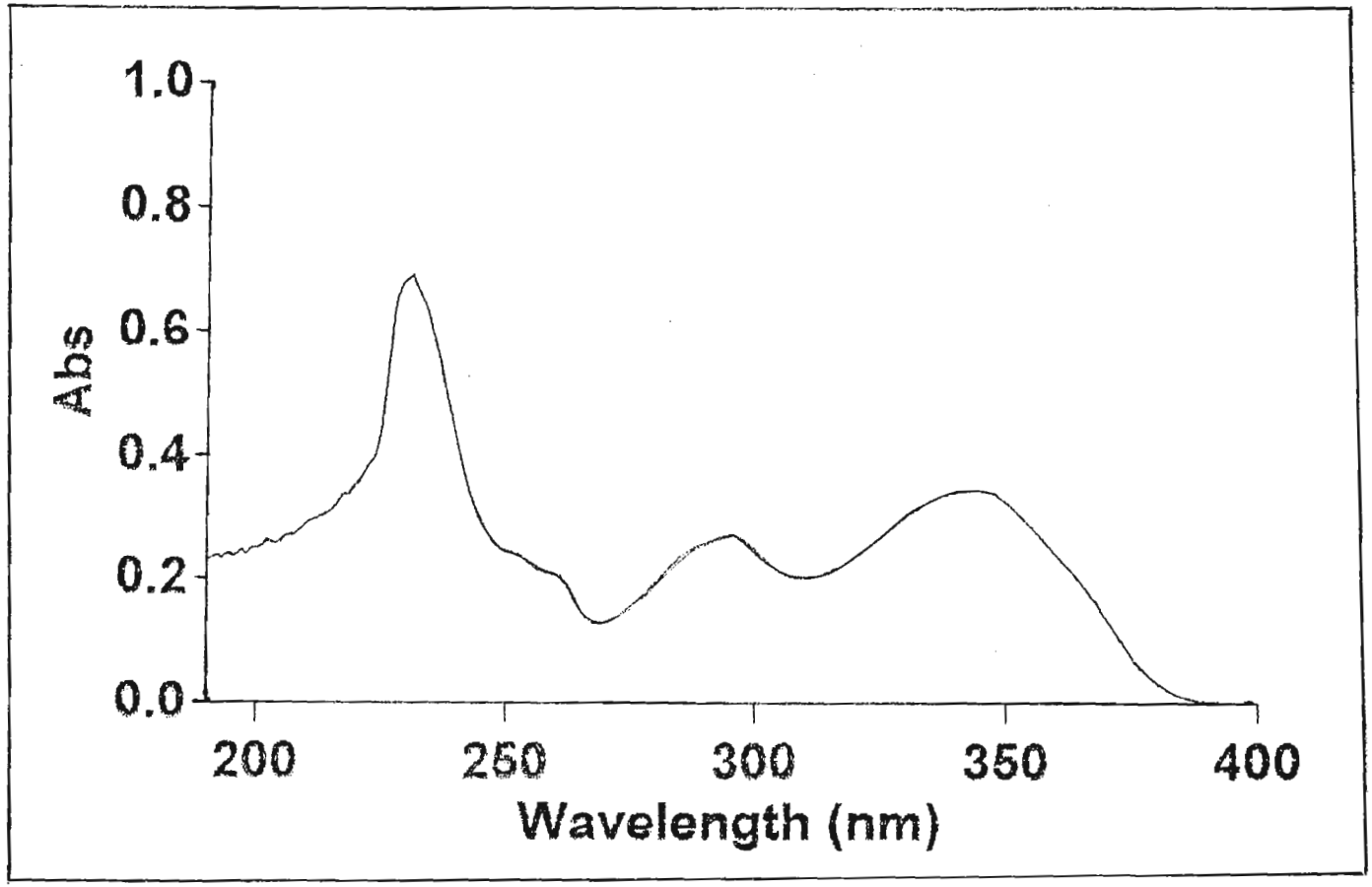

UV spectrum of scoparone (16)

dn 23-41 in cdcl3
probe=3mmID

(16)

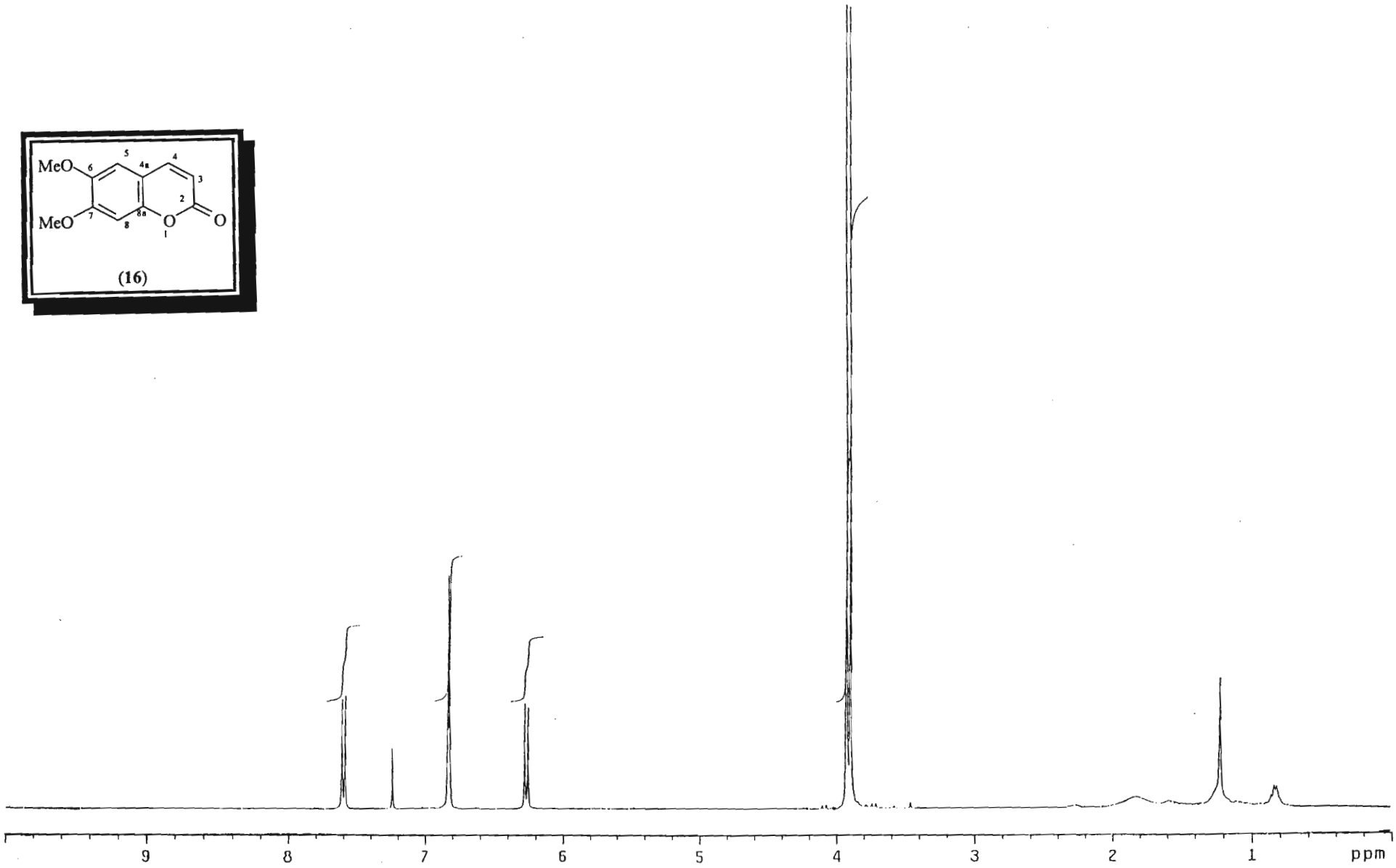

^{1}H NMR spectrum of scoparone (16)

dn 23-41 in cdcl3
probe=3mmID

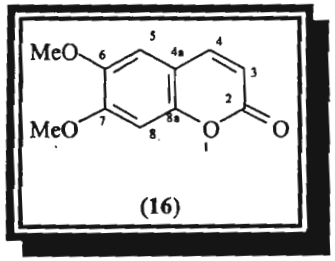

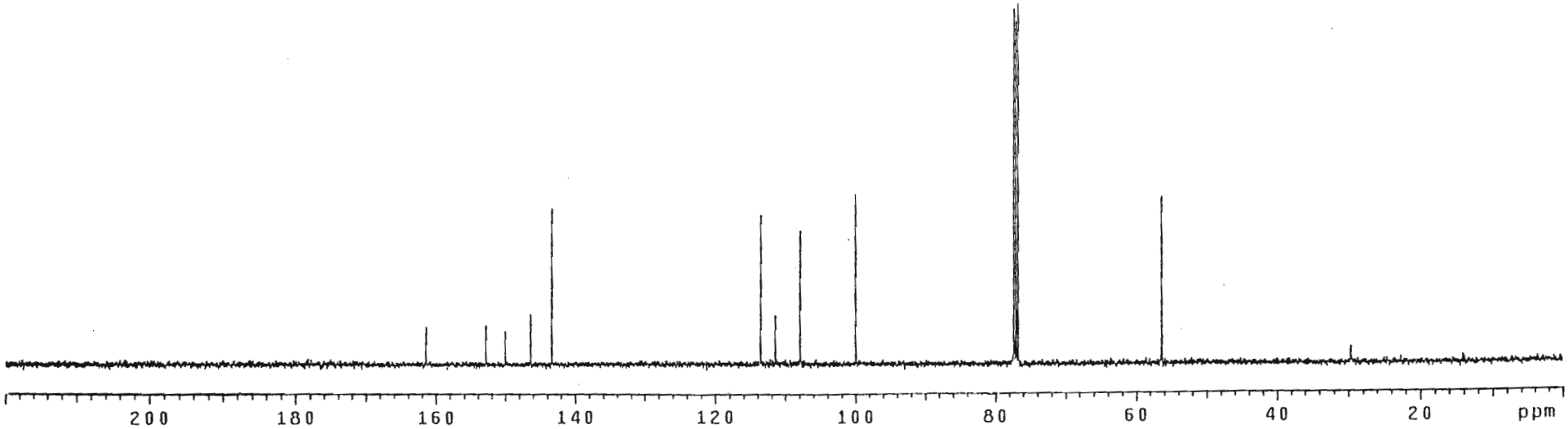

^{13}C NMR spectrum of scoparone (16)

dn 23-41 in cdcl3
Gradient HSQC expt.

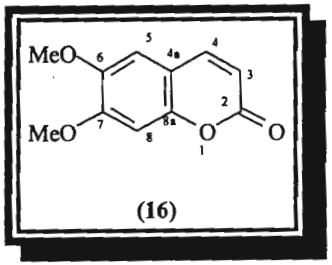

(16)

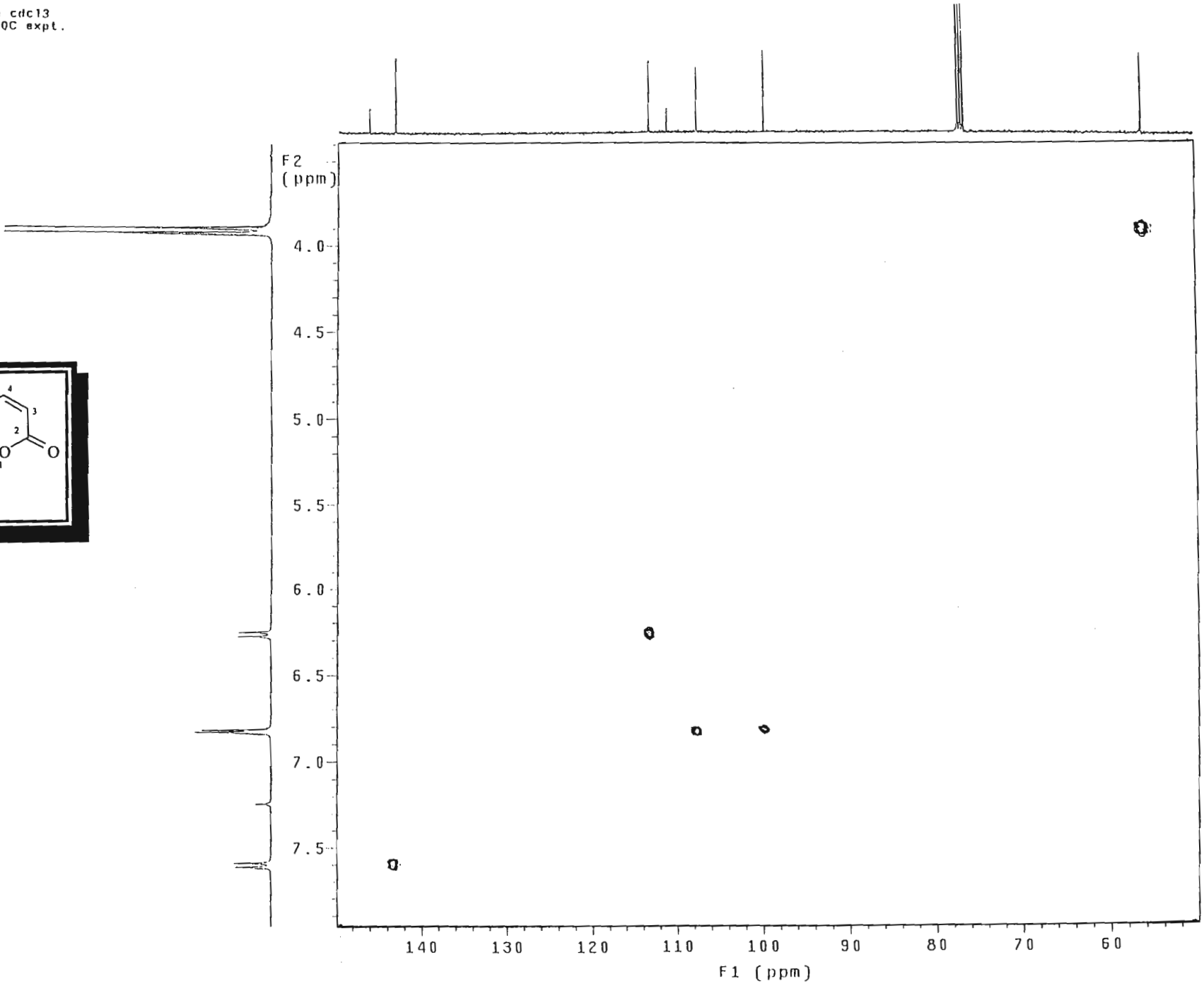

HSQC NMR spectrum of scoparone (16)

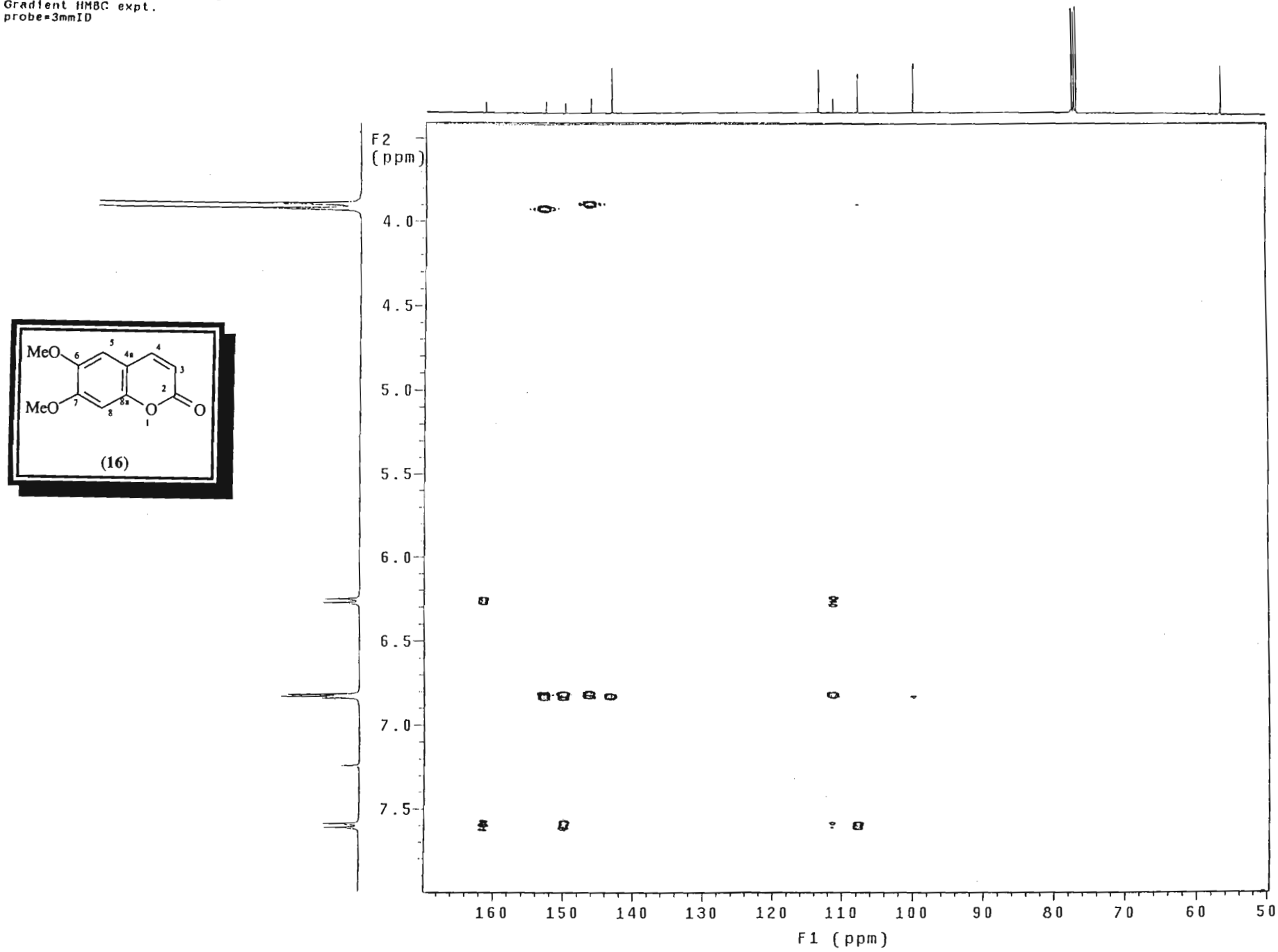

HMBC NMR spectrum of scoparone (16)

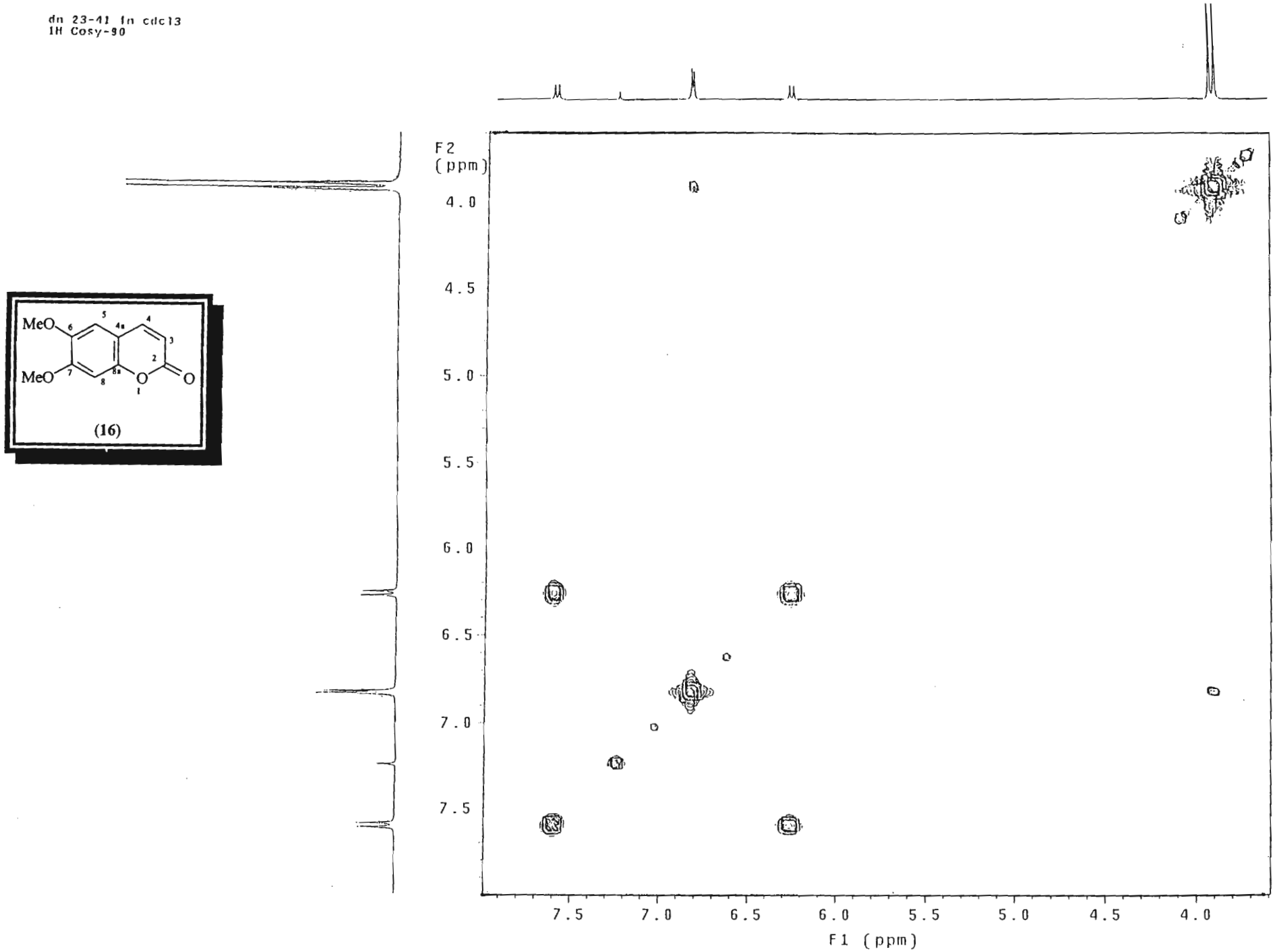

COSY NMR spectrum of scoparone (16)

dn 23-41 in cdcl3
NOESY expt.

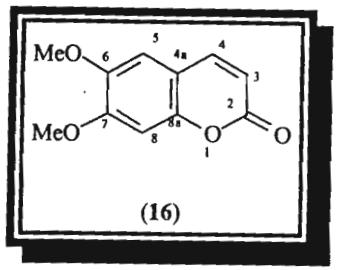

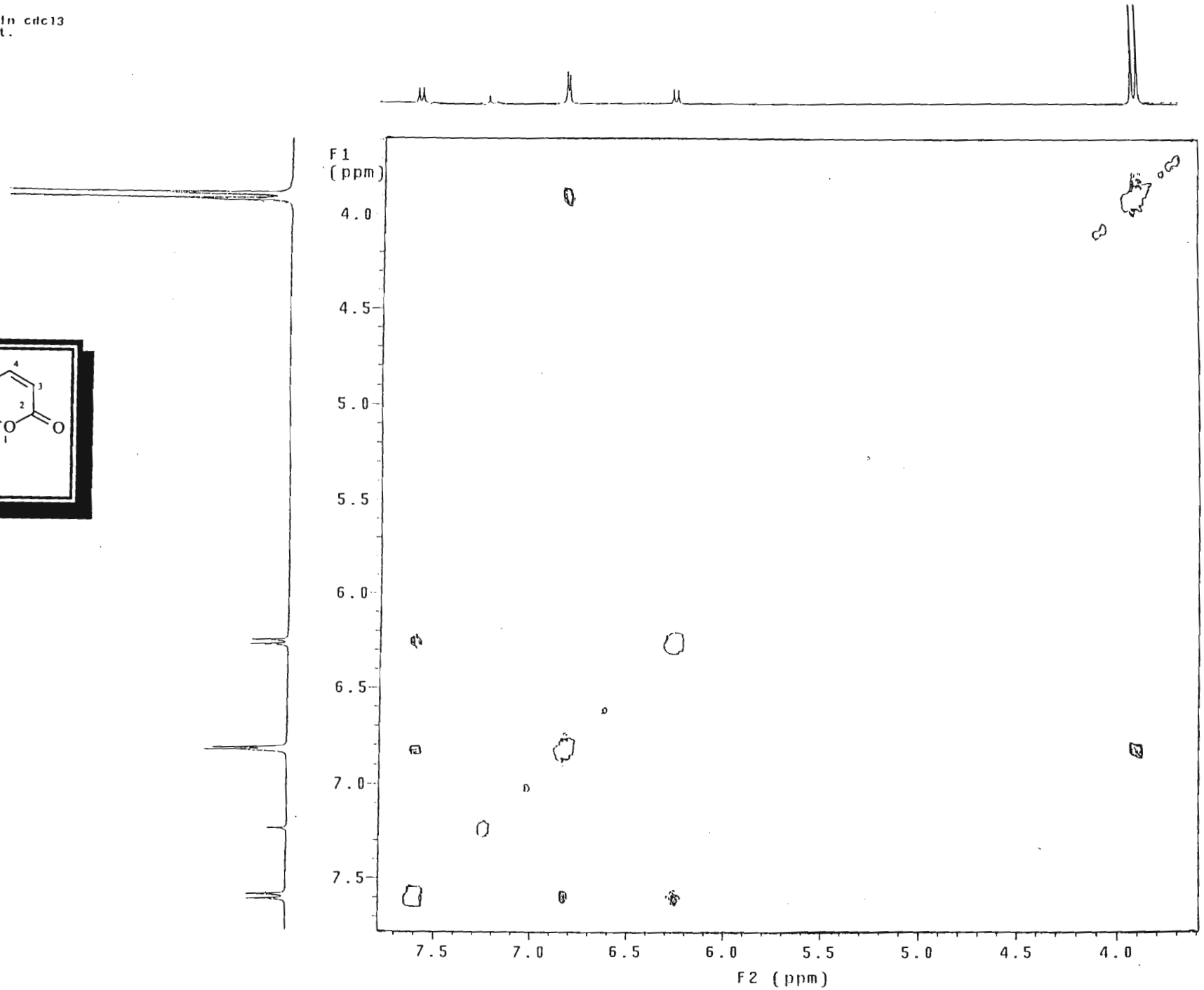

NOESY NMR spectrum of scoparone (16)

Cedashnine (17)

Mass spectrum	[29]
IR spectrum	[30]
^{1}H NMR	[31]
^{13}C NMR	[32]
HSQC	[33]
Expanded HSQC	[34]
HMBC	[35]
COSY	[36]
NOESY	[37]

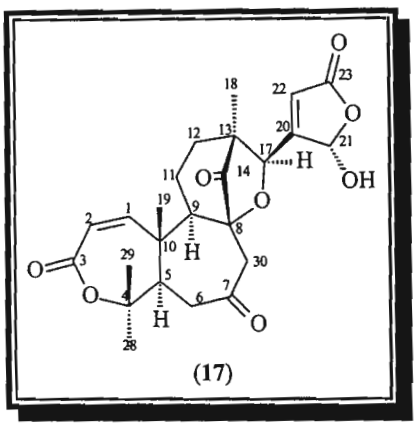

Cedashnine (17)

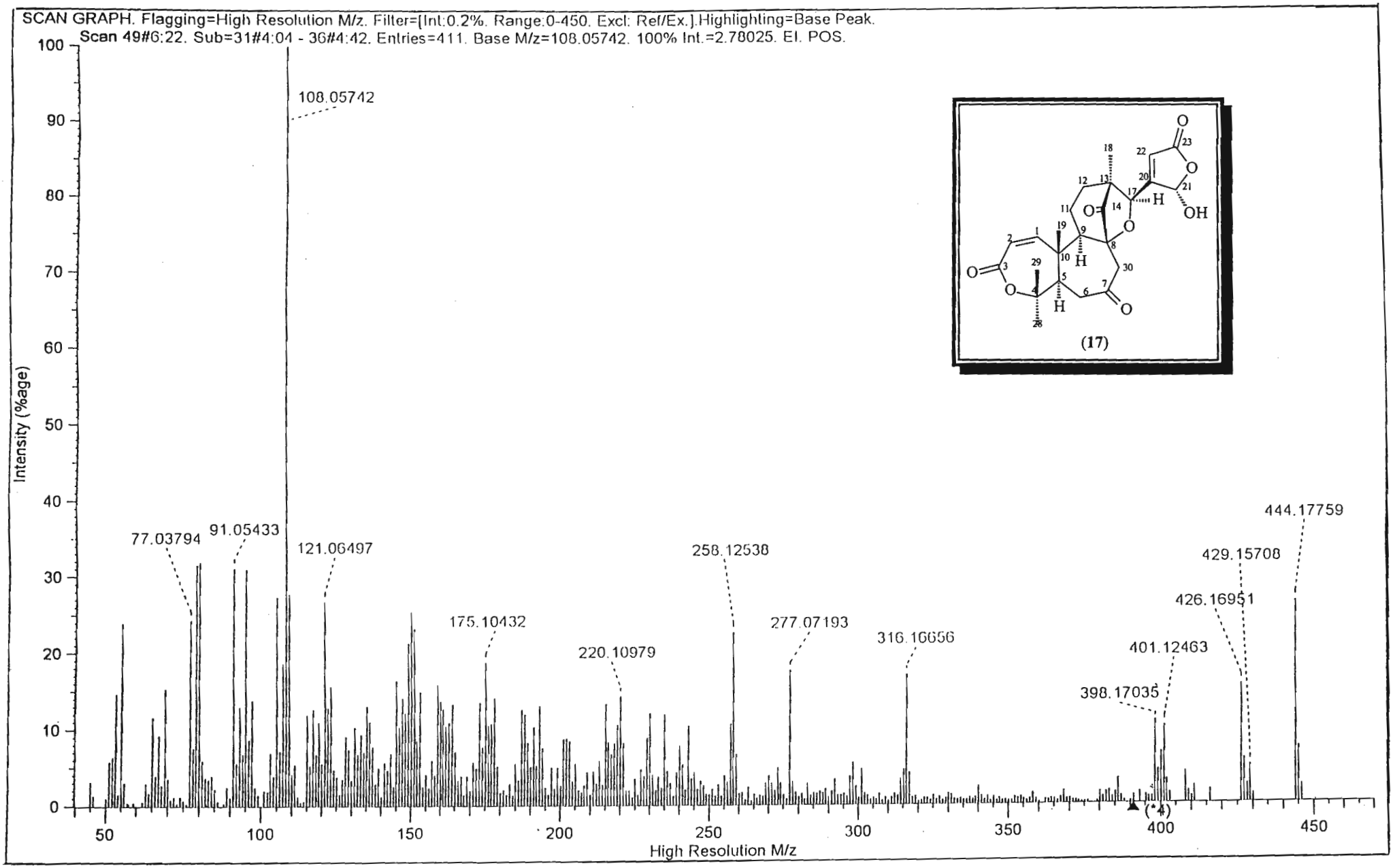

Mass spectrum of cedashnine (17)

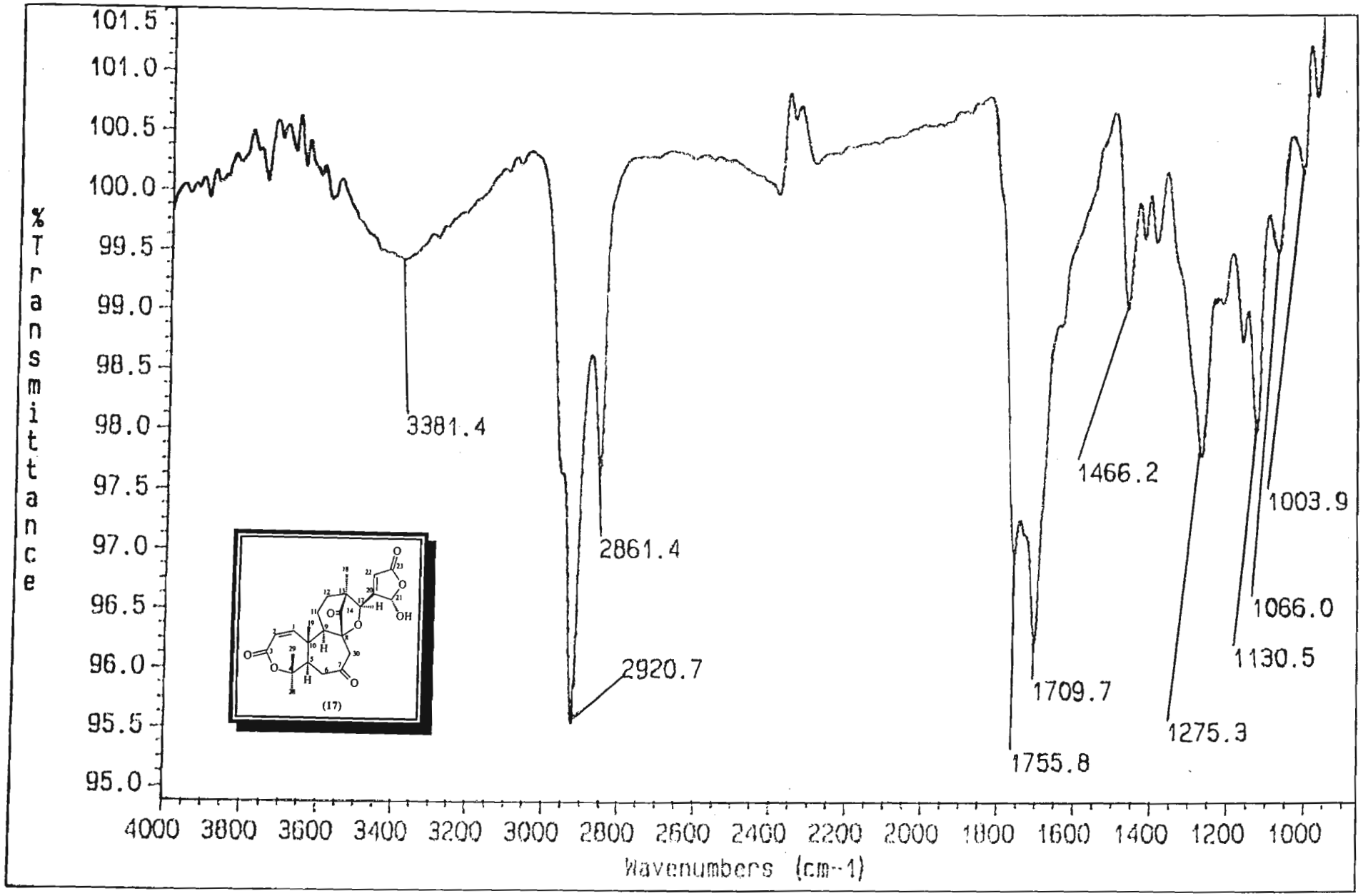

IR spectrum of cedashnine (17)

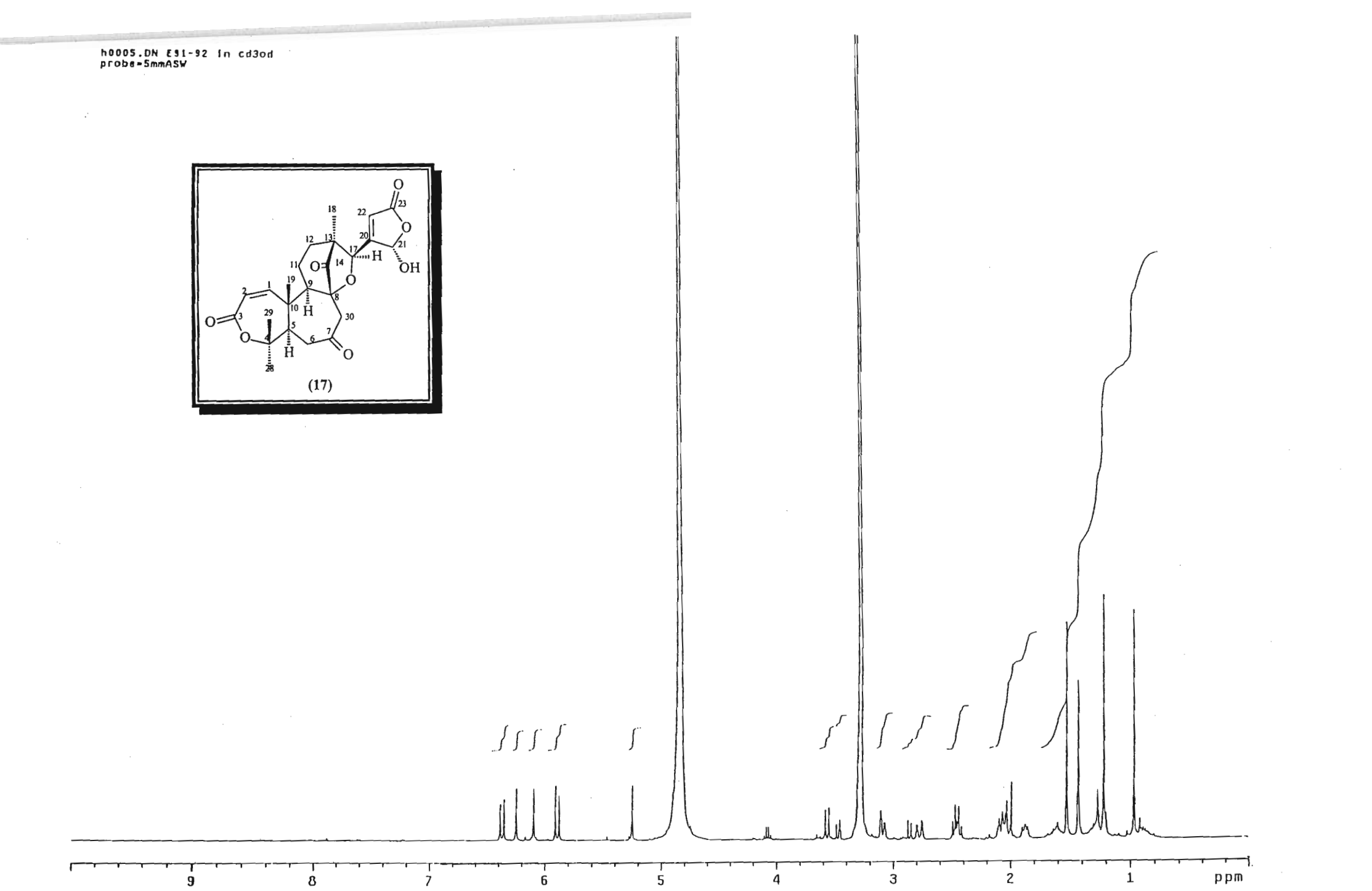

^{1}H NMR spectrum of cedashnine (17)

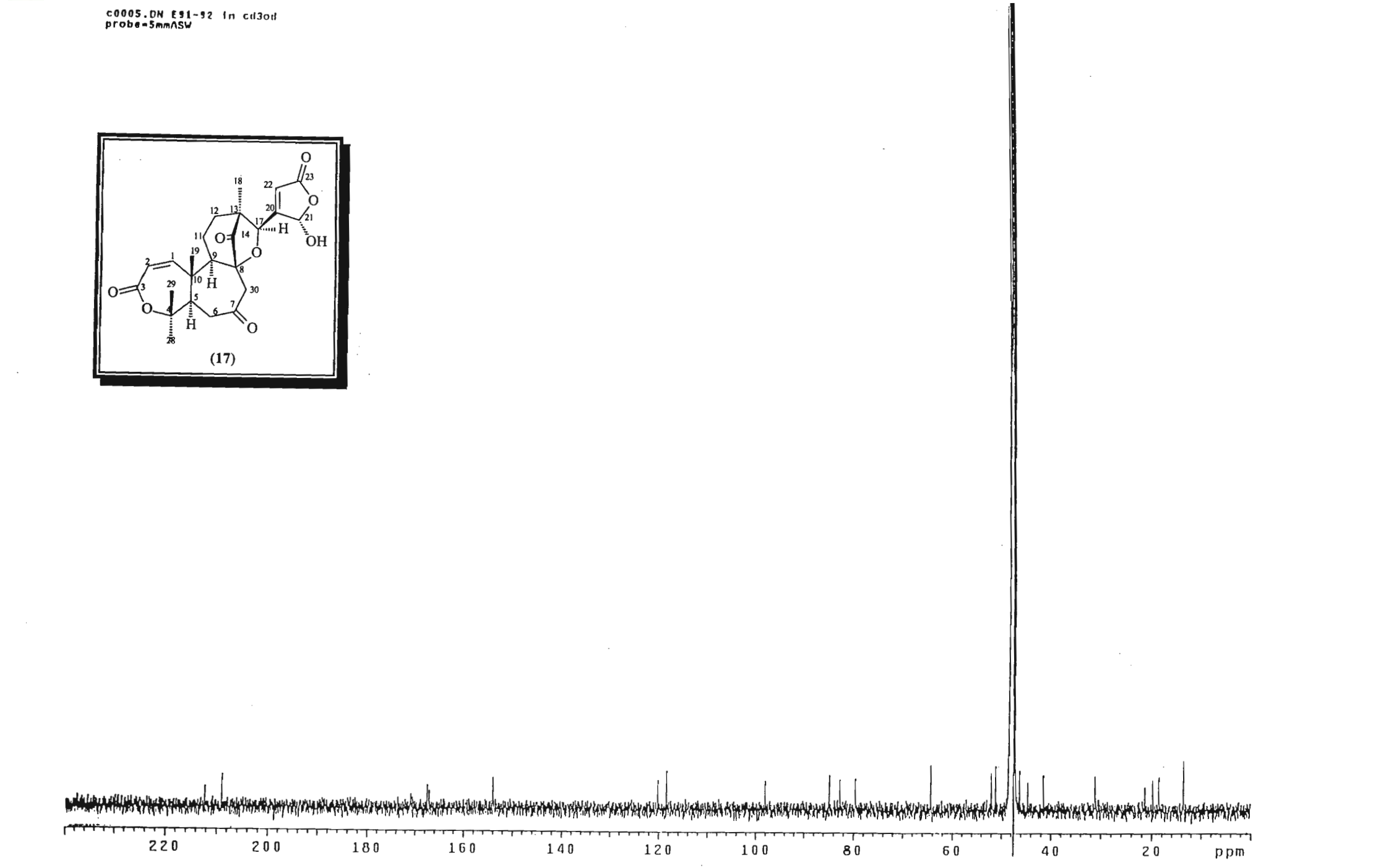

^{13}C NMR spectrum of cedashnine (17)

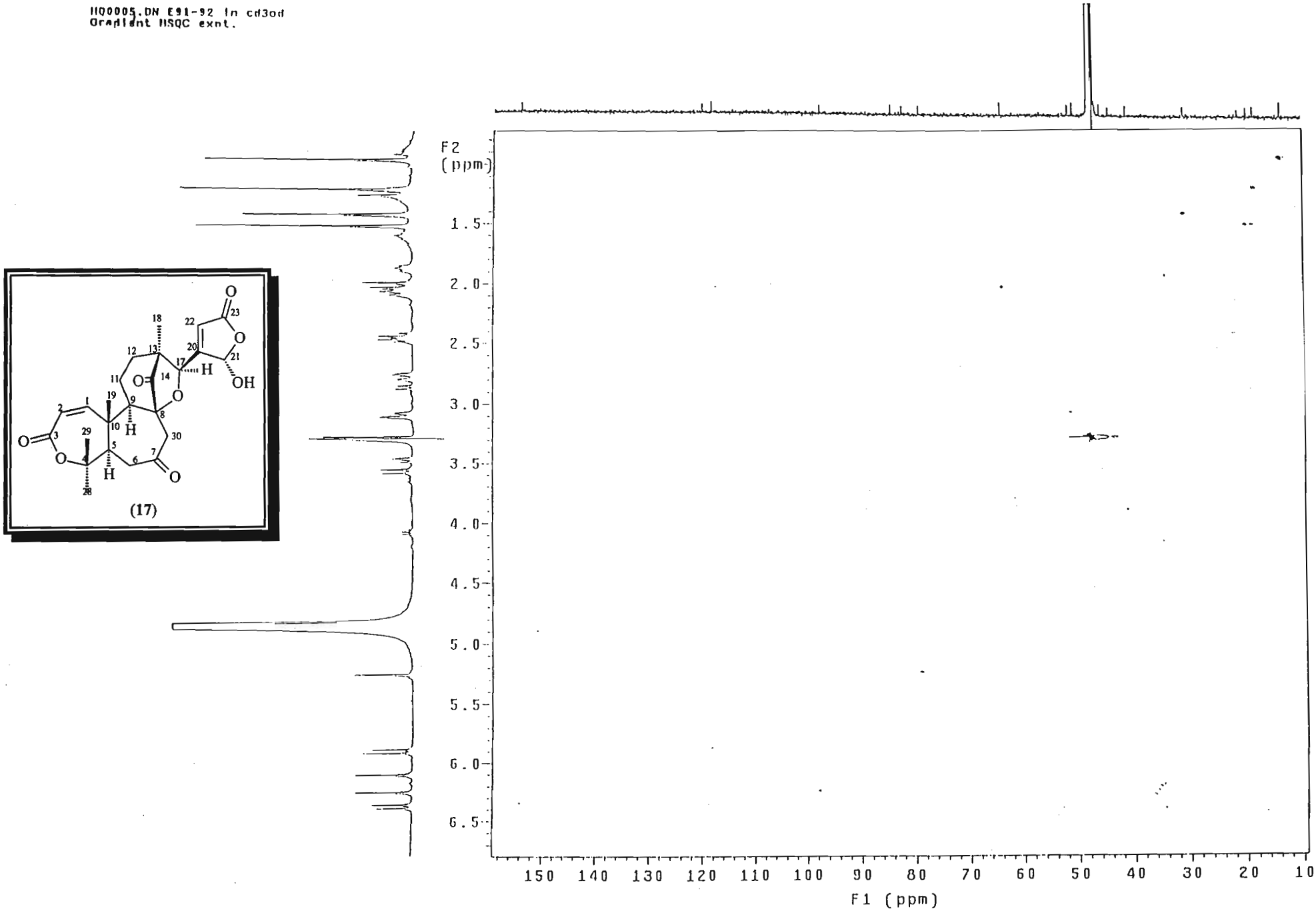

HSQC NMR spectrum of cedashnine (17)

HQ0005.ON E91-92 In cd3od
Gradient HSQC expt.

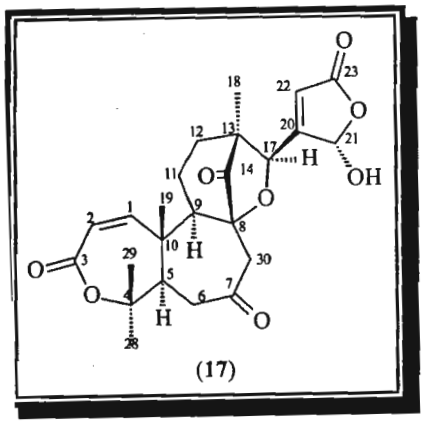

(17)

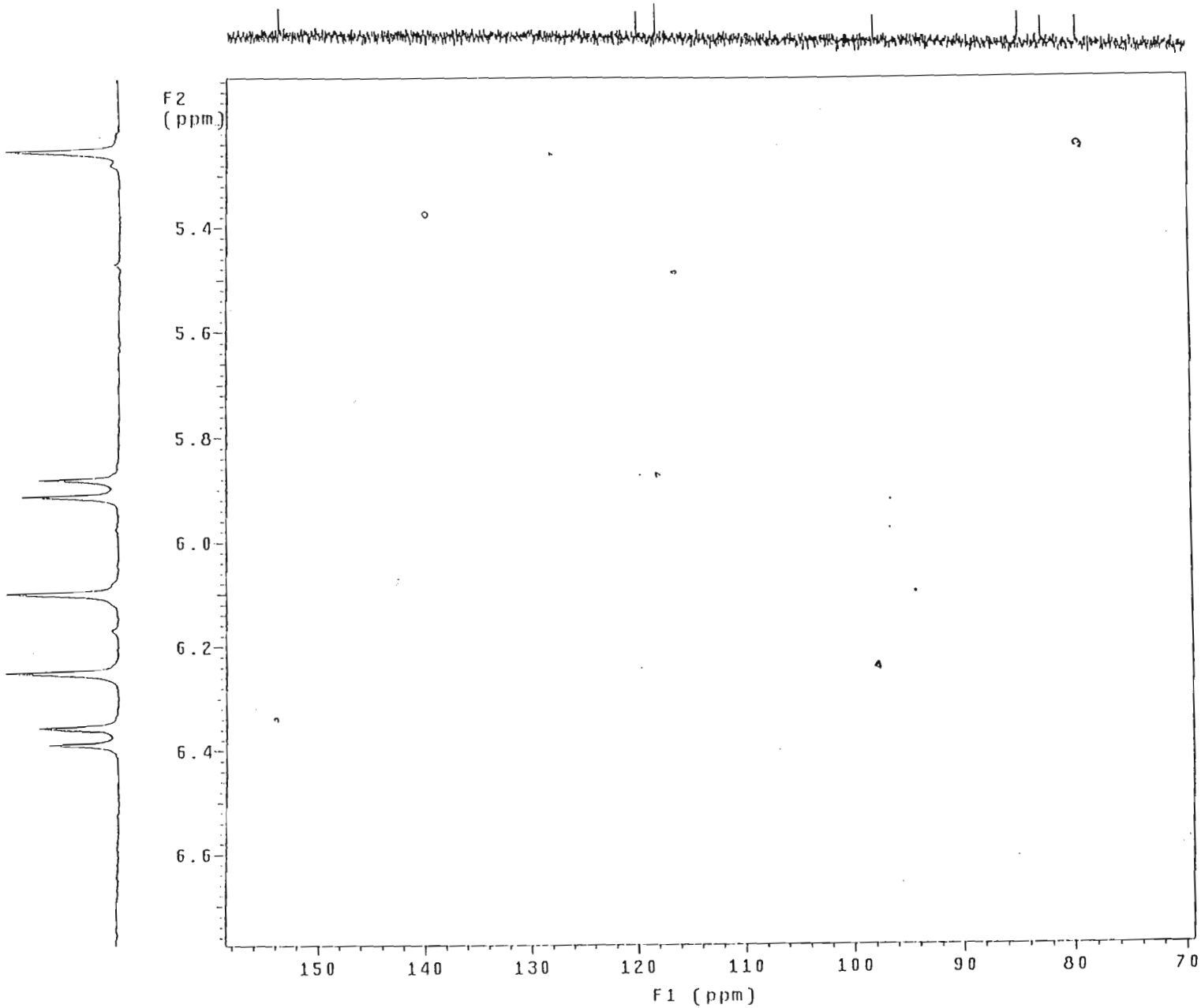

HSQC NMR spectrum of cedashnine (17)

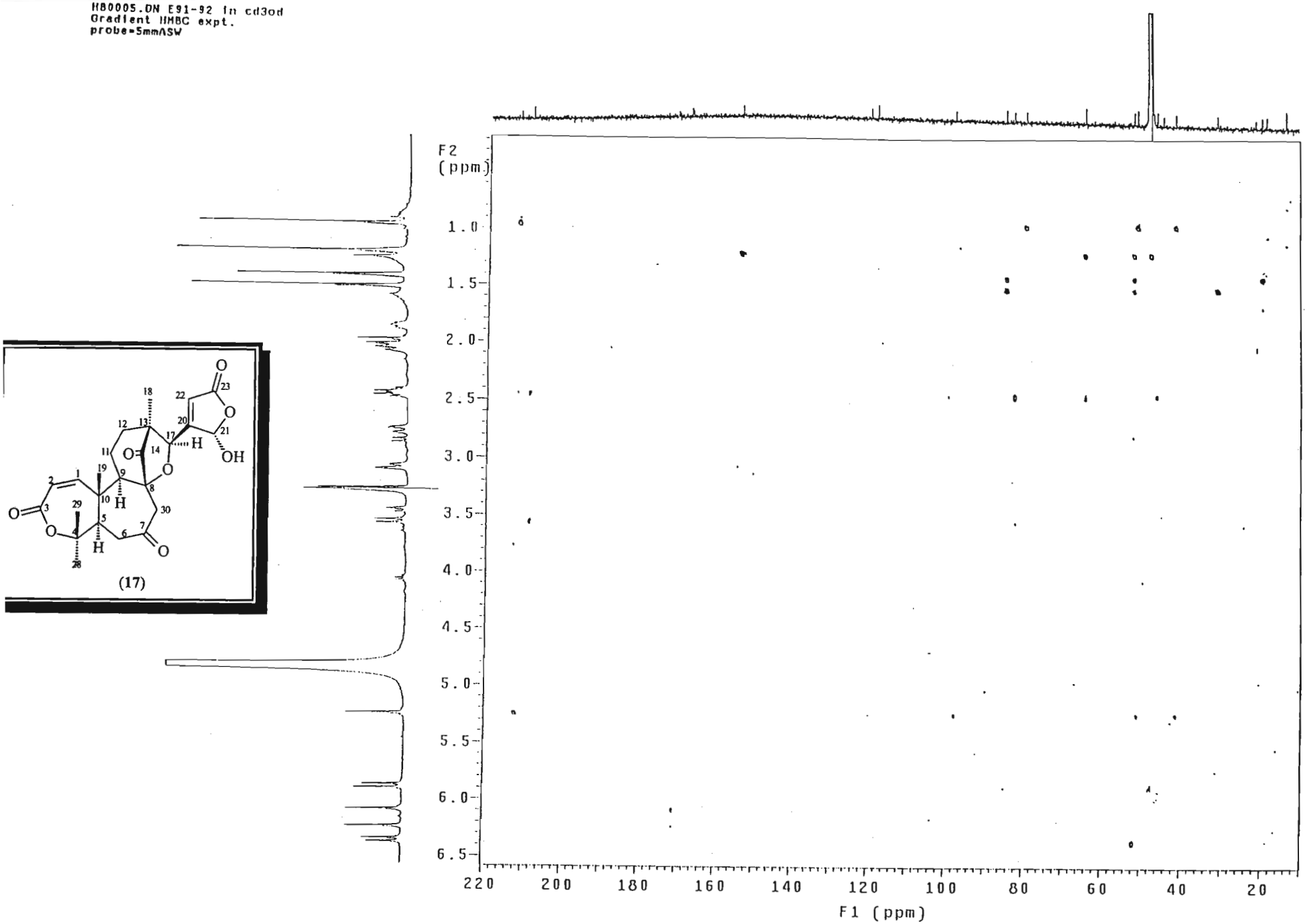

HMBC NMR spectrum of cedashnine (17)

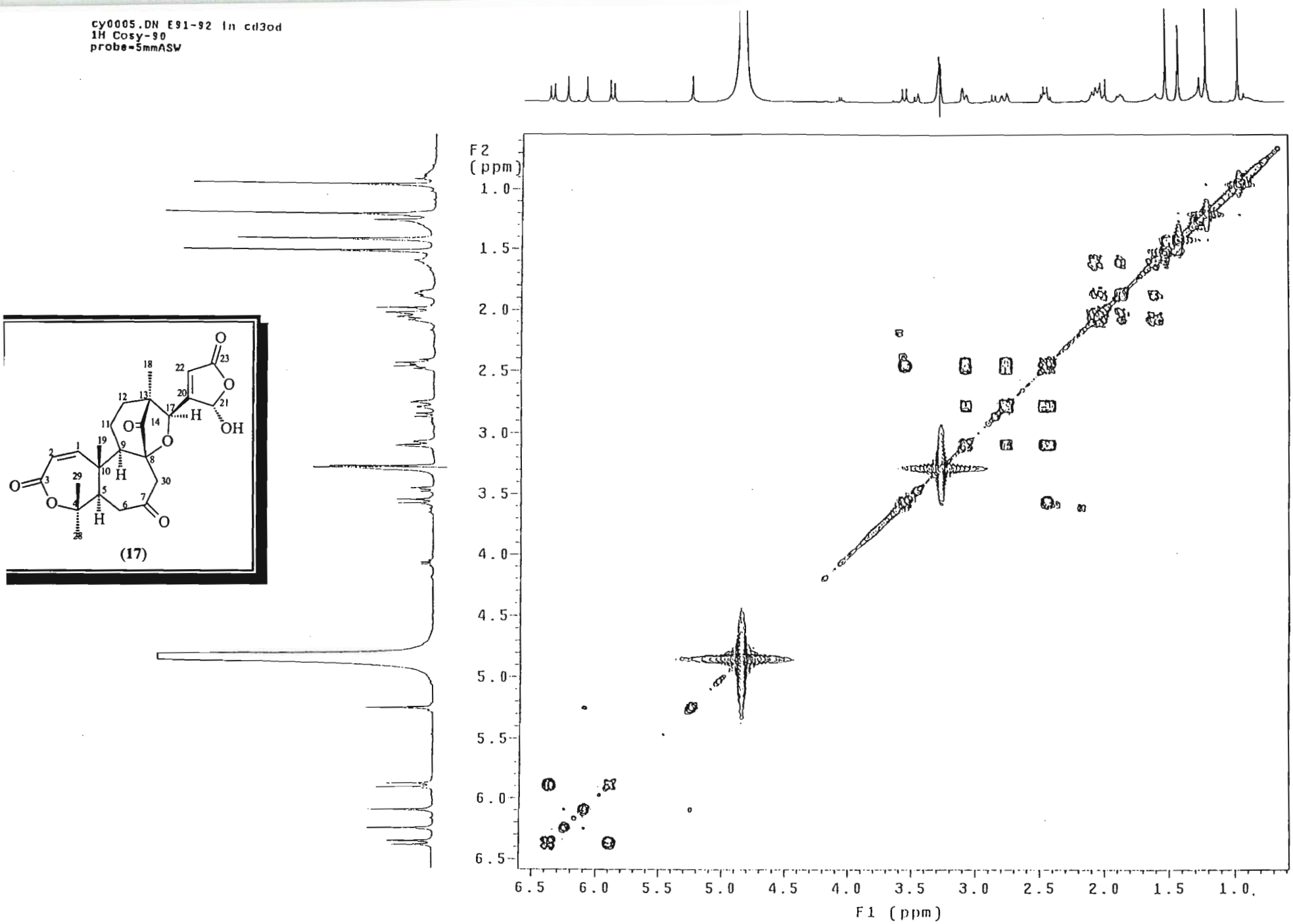

COSY NMR spectrum of cedashnine (17)

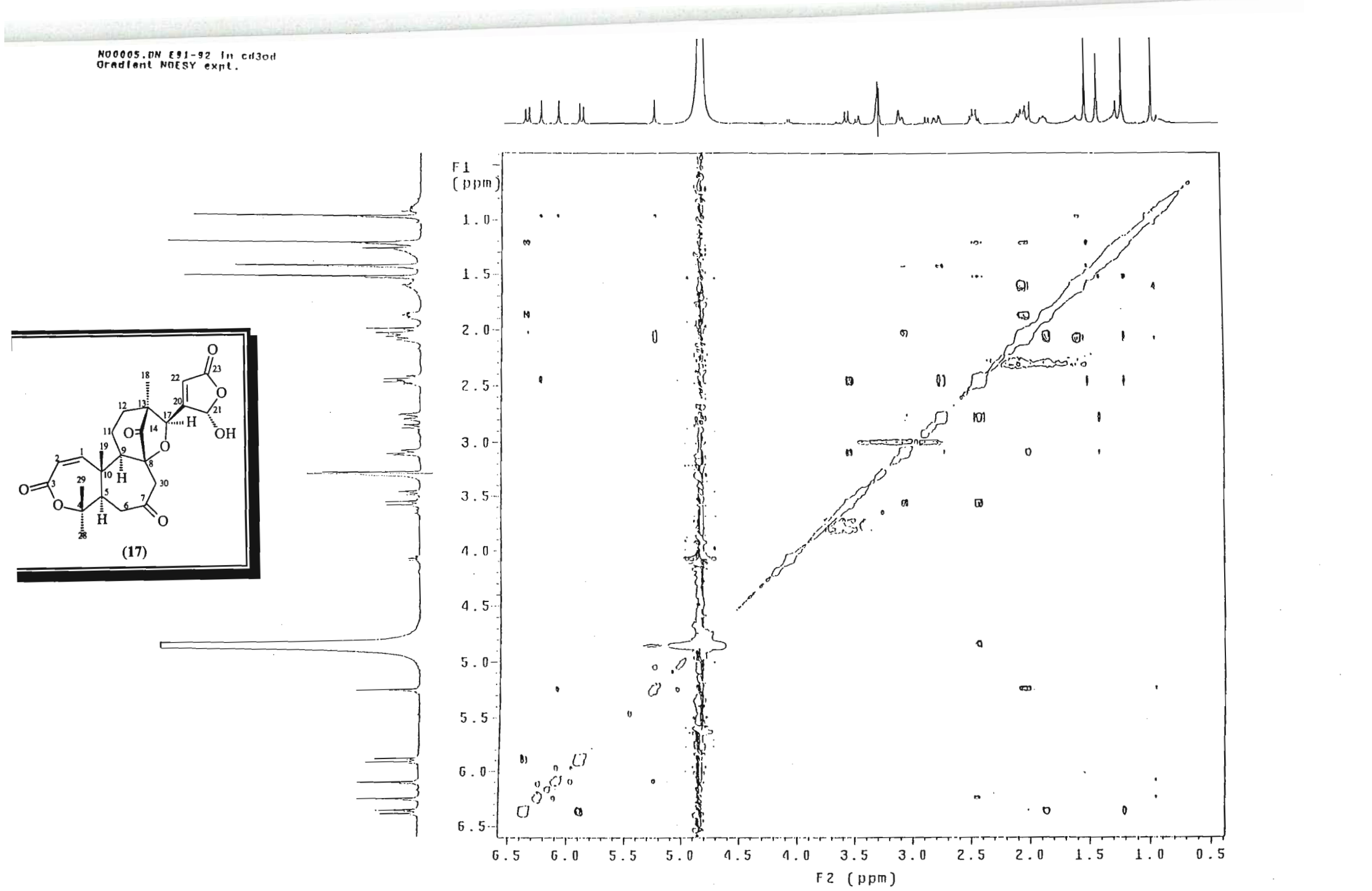

NOESY NMR spectrum of cedashnine (17)

Cedpetine (18)

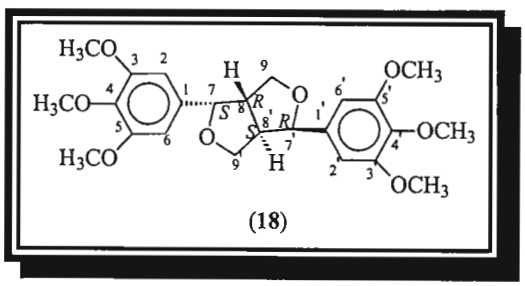

(18)

Cedpetine (18)

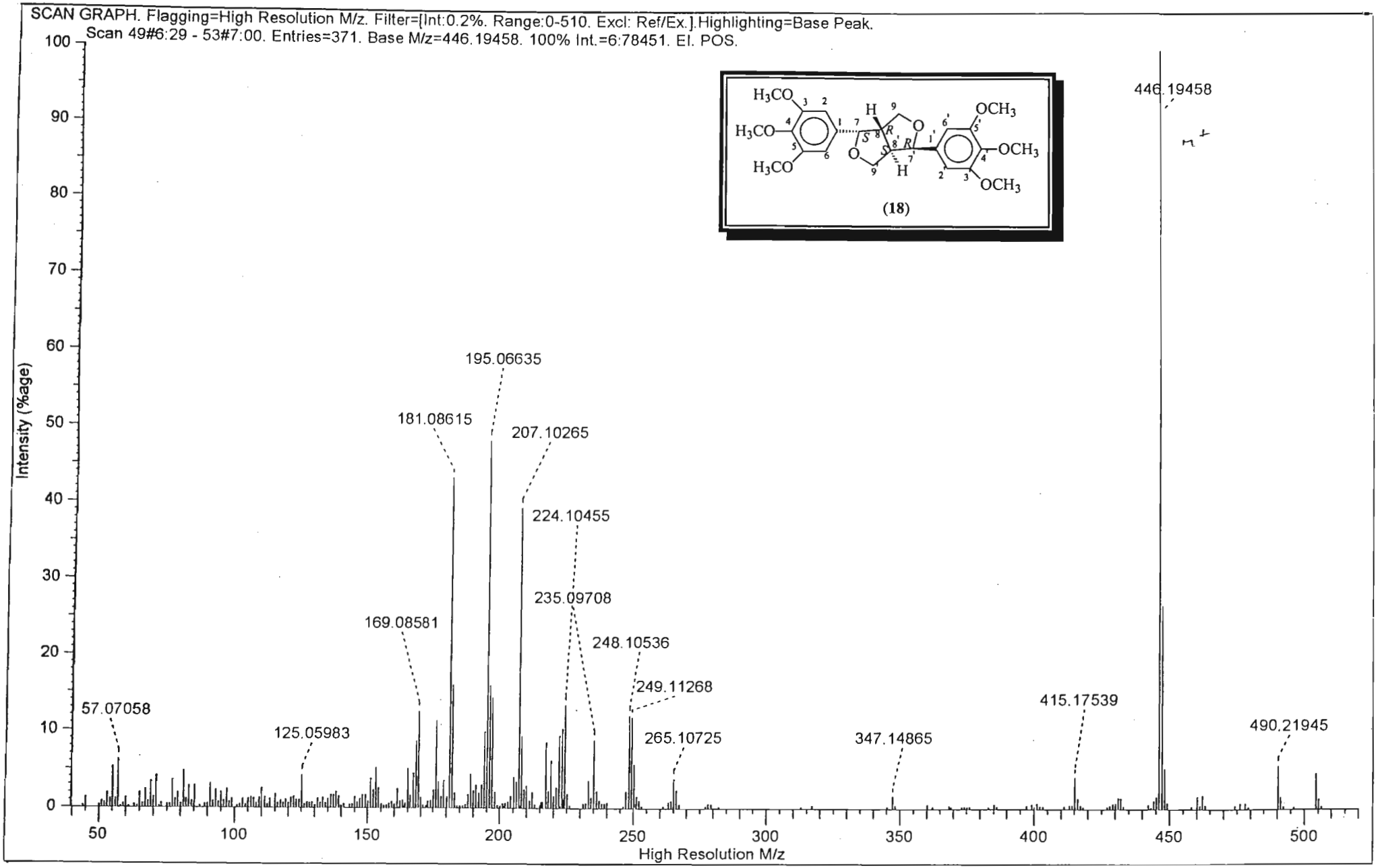

Mass spectrum of cedpetine (18)

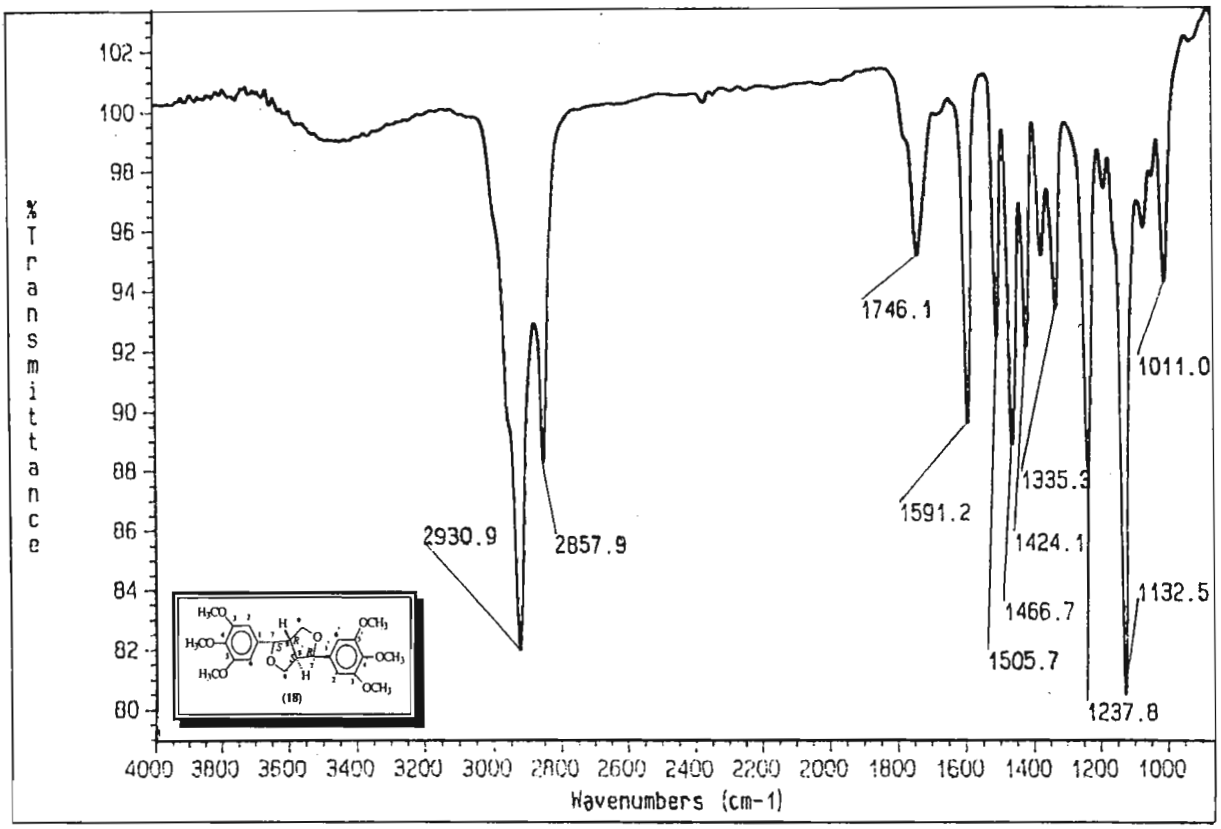

IR spectrum of cedpetine (18)

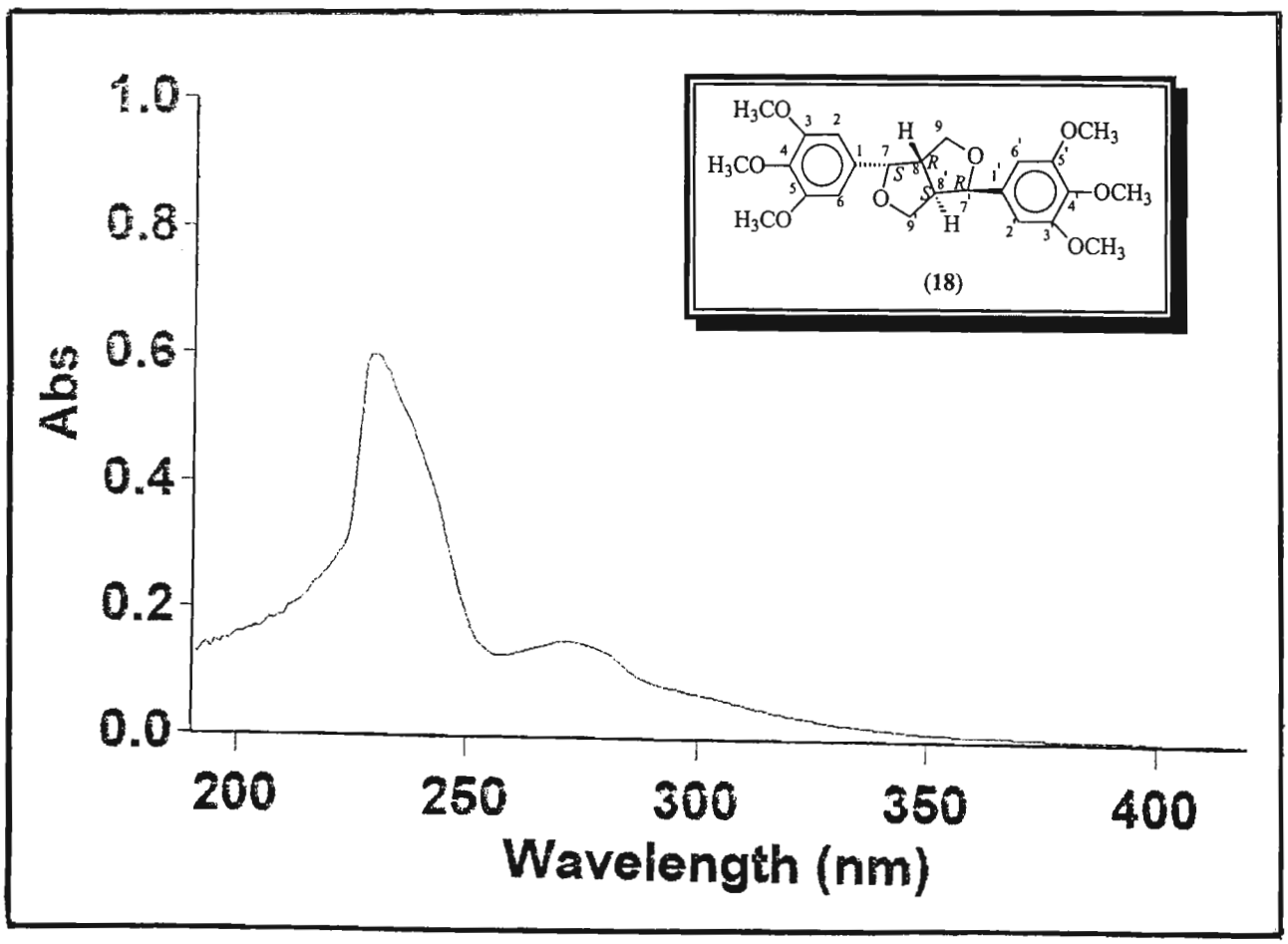

UV spectrum of cedpetine (18)

hdn30.dn23-30 in cdcl3
probe=5mmASW

Pulse Sequence: s2pul

(18)

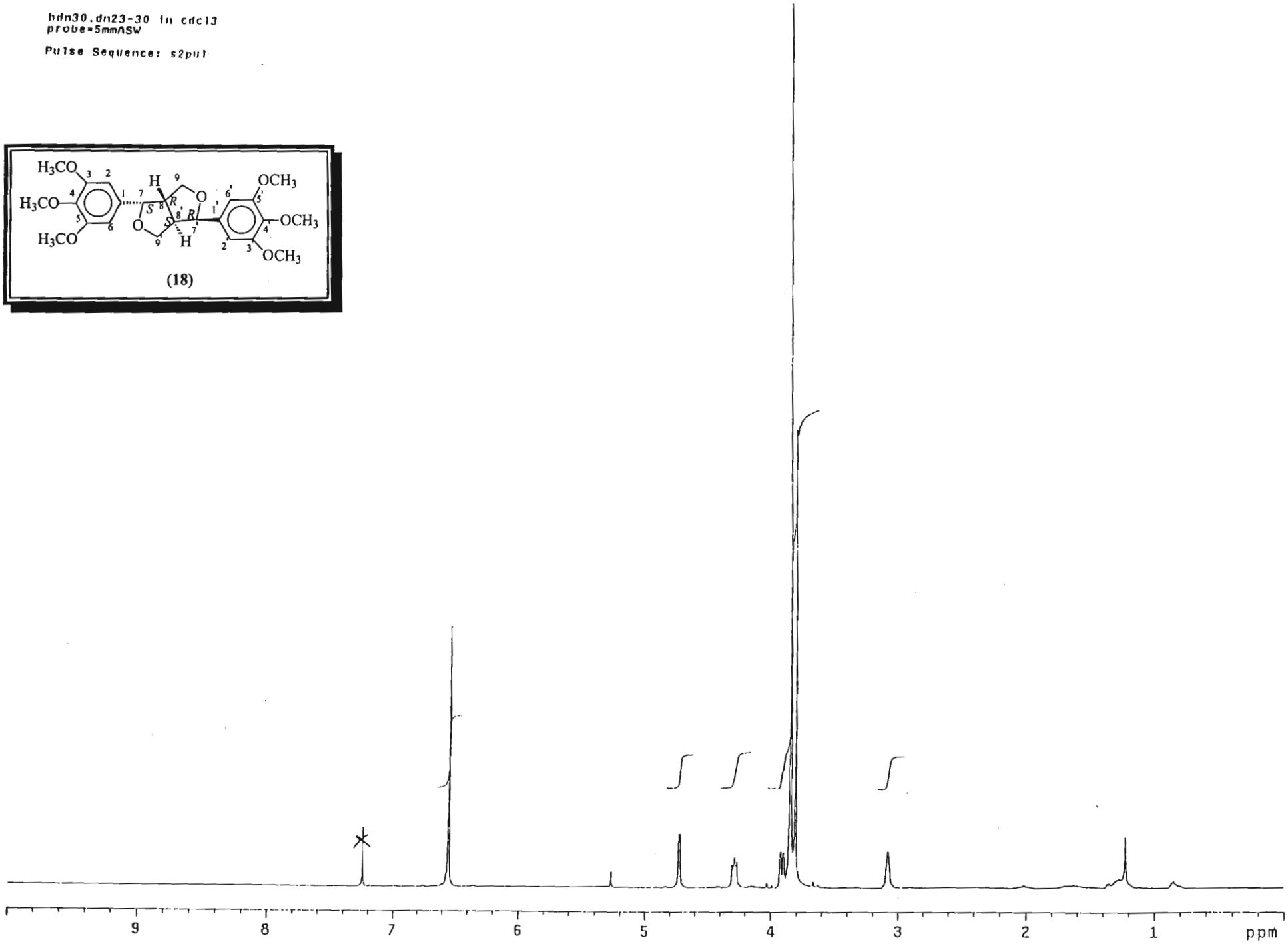

^{1}H NMR spectrum of cedpetine (18)

cdn30.dn23-30 in cdcl3
probe=5mmASV

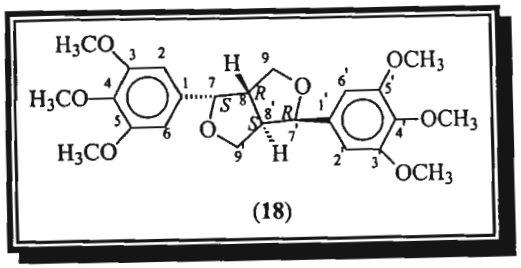

(18)

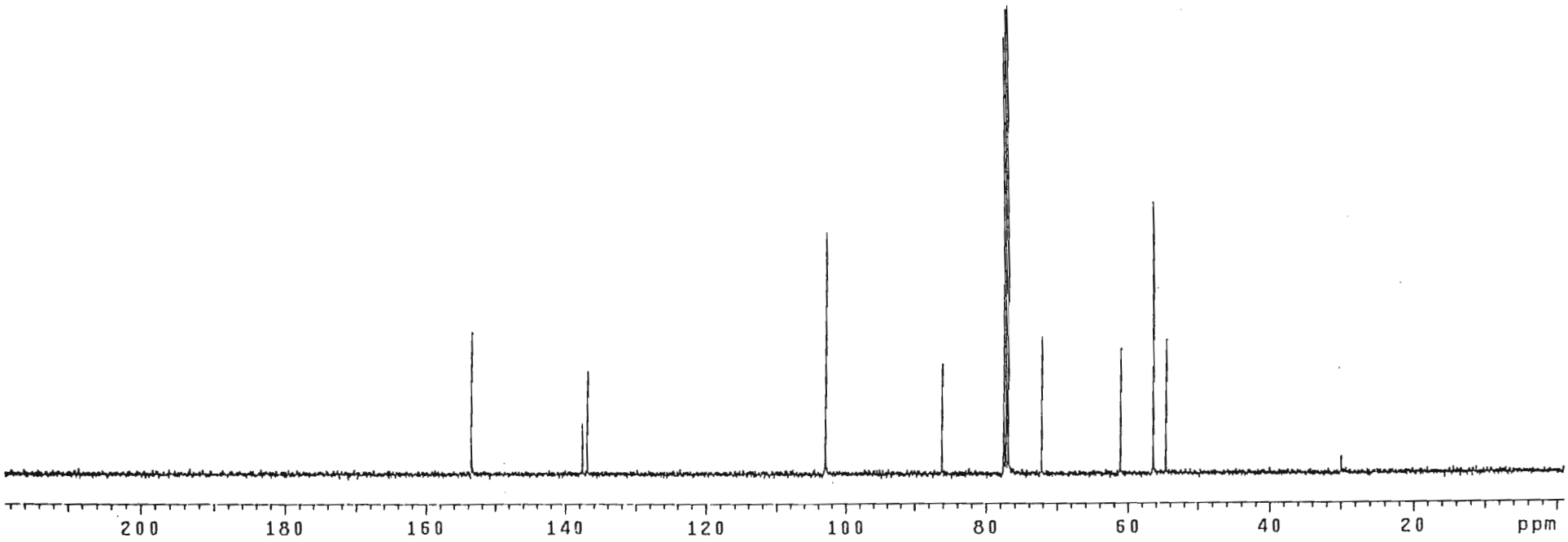

^{13}C NMR spectrum of cedpetine (18)

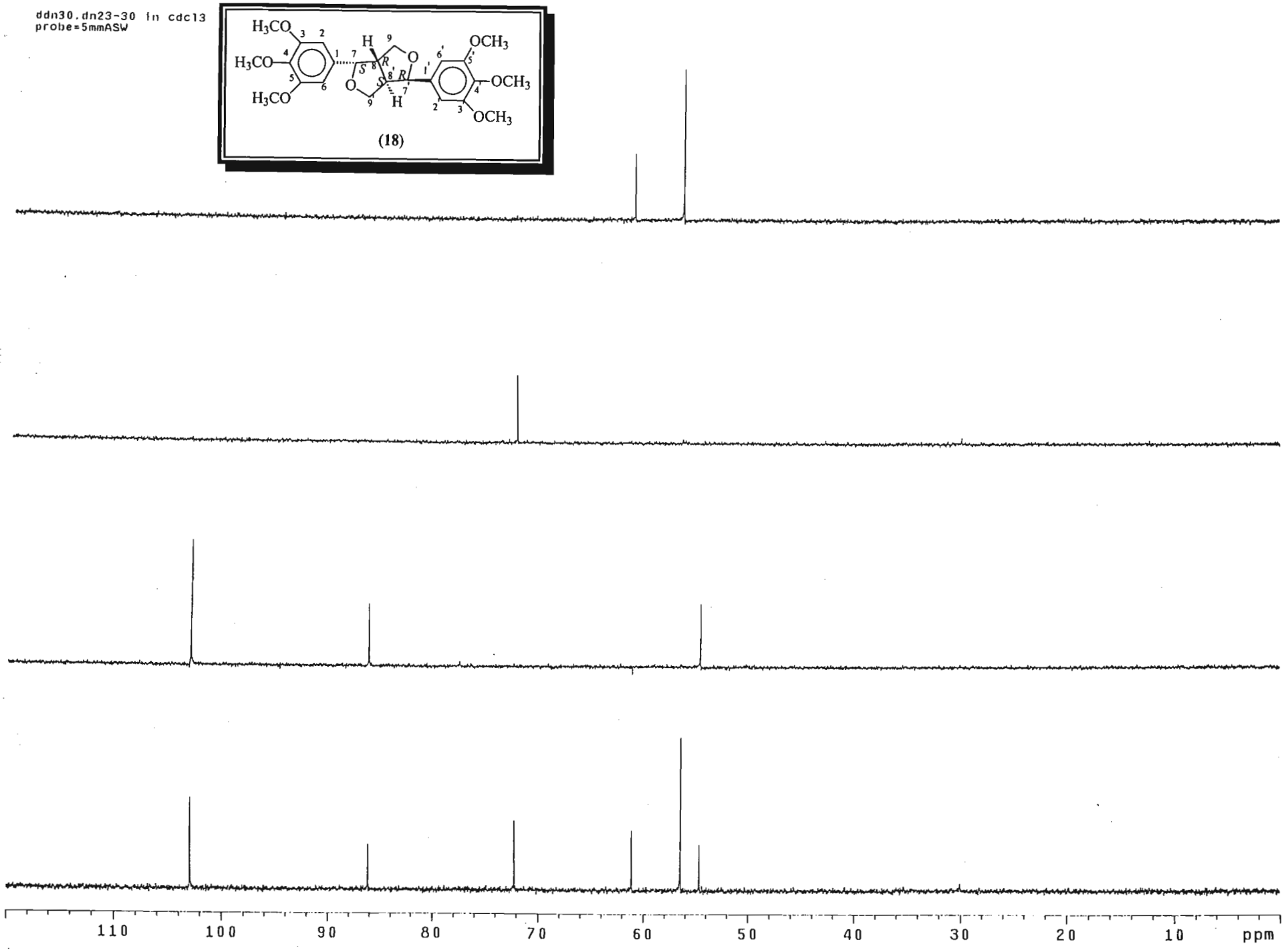

ADEPT NMR spectrum of cedpetine (18)

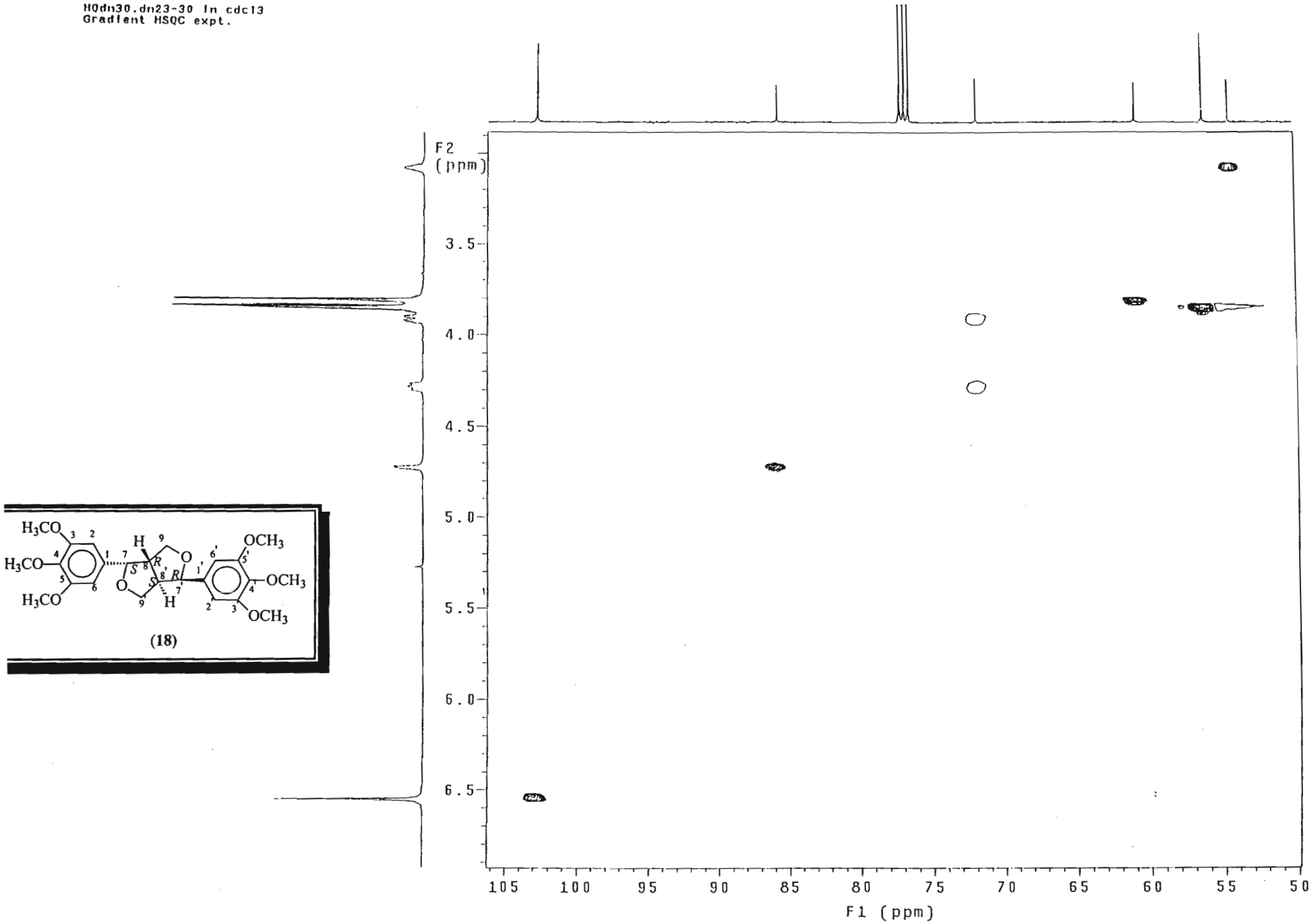

(18)

HSQC NMR spectrum of cedpetine (18)

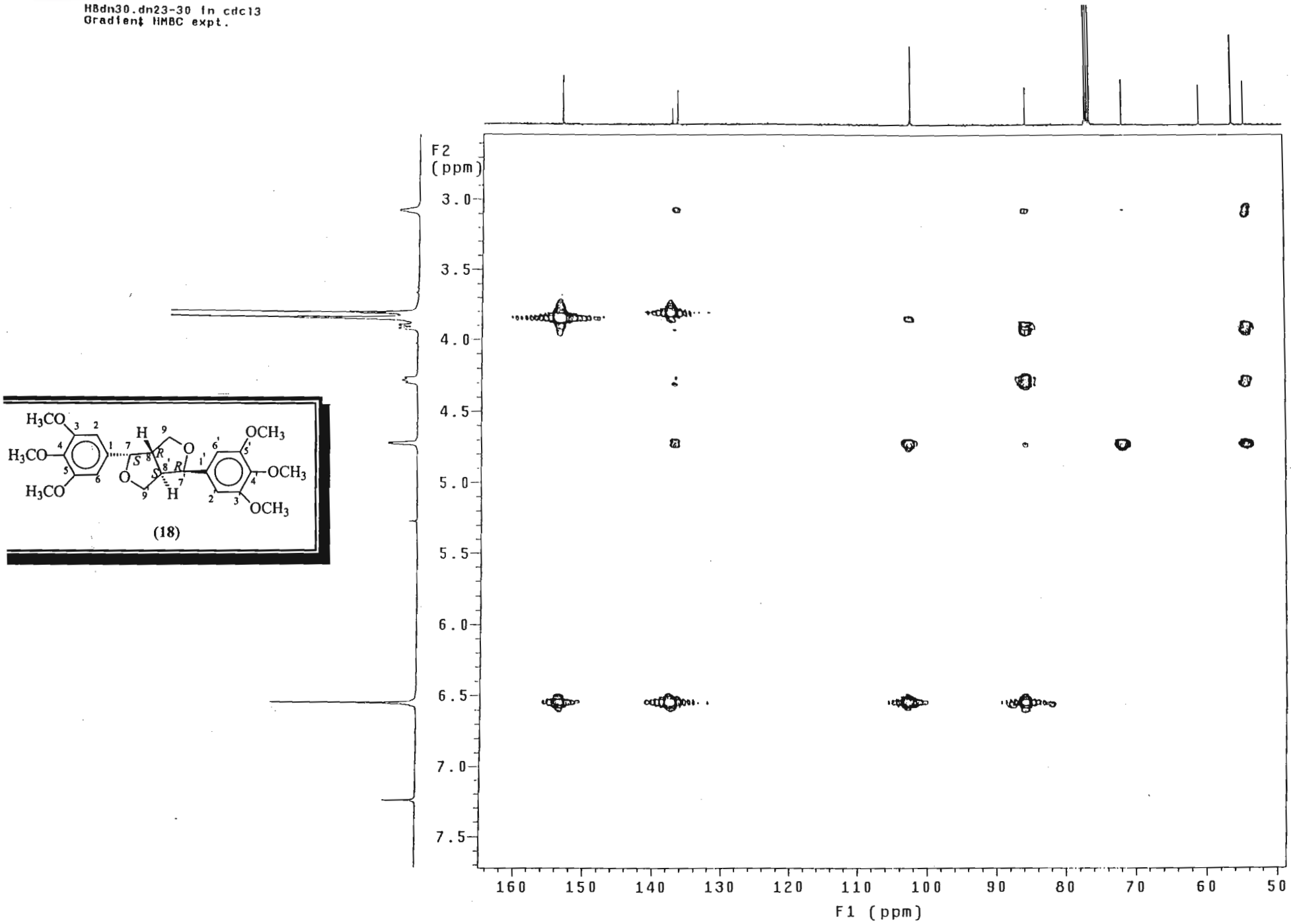

HMBC NMR spectrum of cedpetine (18)

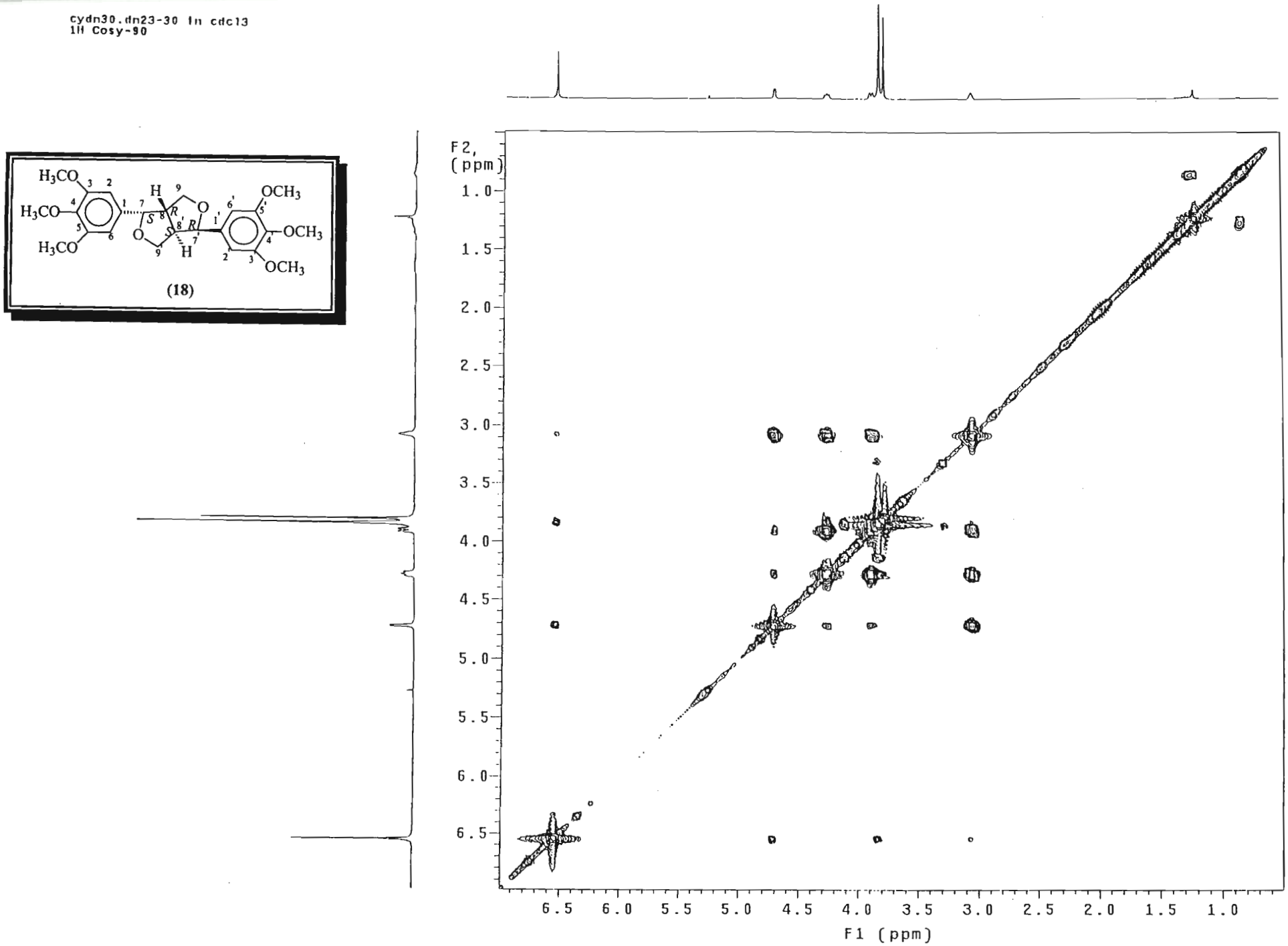

(18)

COSY NMR spectrum of cedpetine (18)

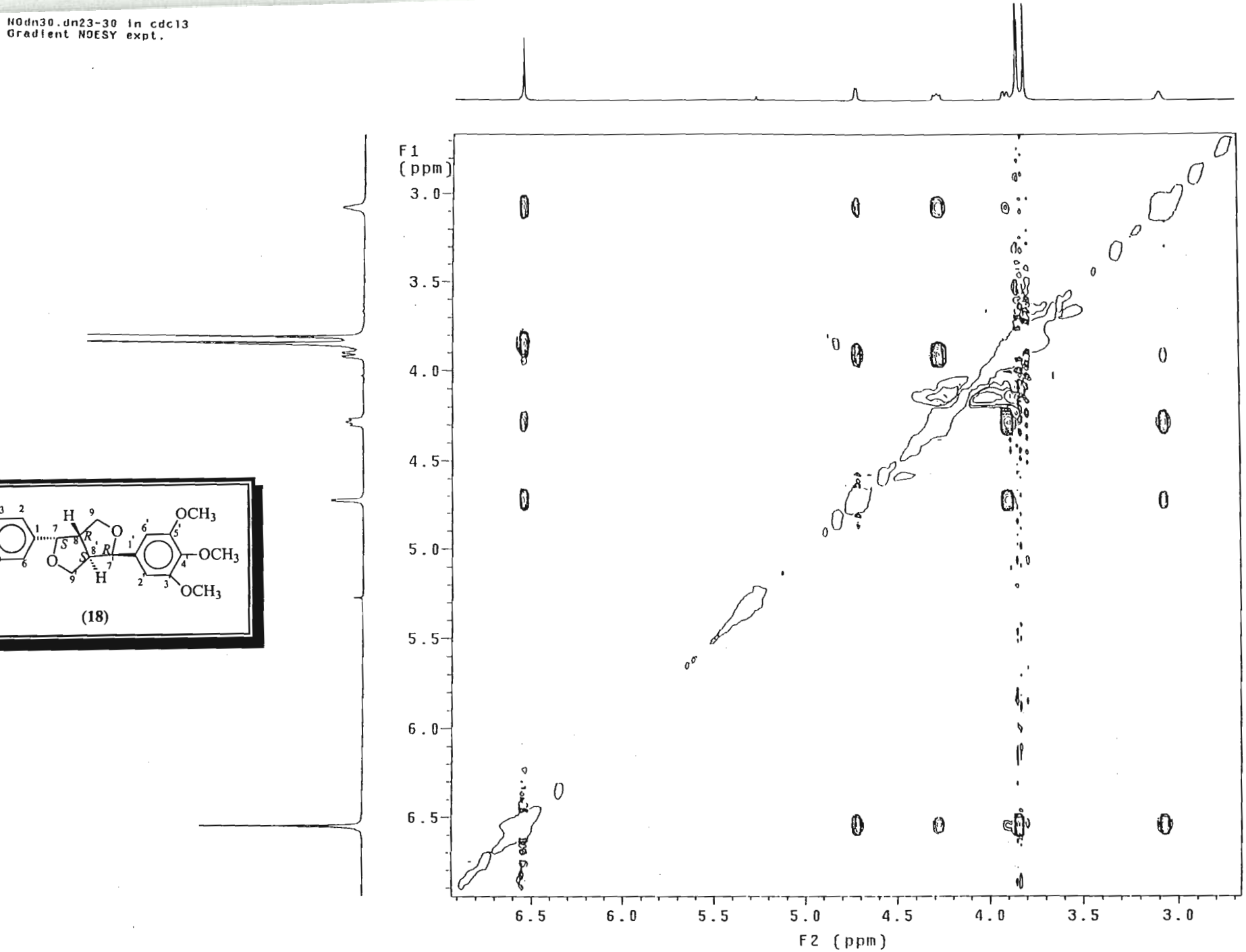

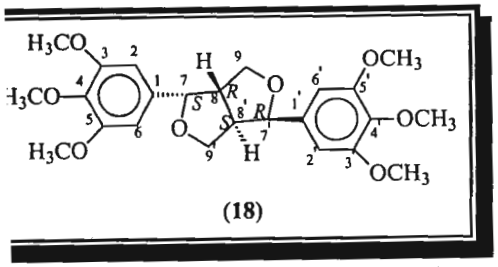

NOESY NMR spectrum of cedpetine (18)

Cedphiline (19)

Mass spectrum	**[49]**
IR spectrum	**[50]**
^{1}H NMR	**[51]**
^{13}C NMR	**[52]**
ADEPT	**[53]**
HSQC	**[55]**
Expanded HSQC	**[54]**
HMBC	**[56-57]**
COSY	**[58]**
NOESY	**[59]**

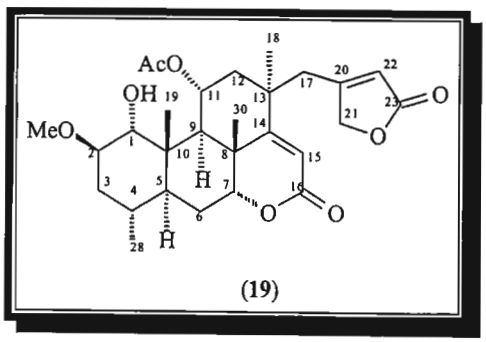

Cedphiline (19)

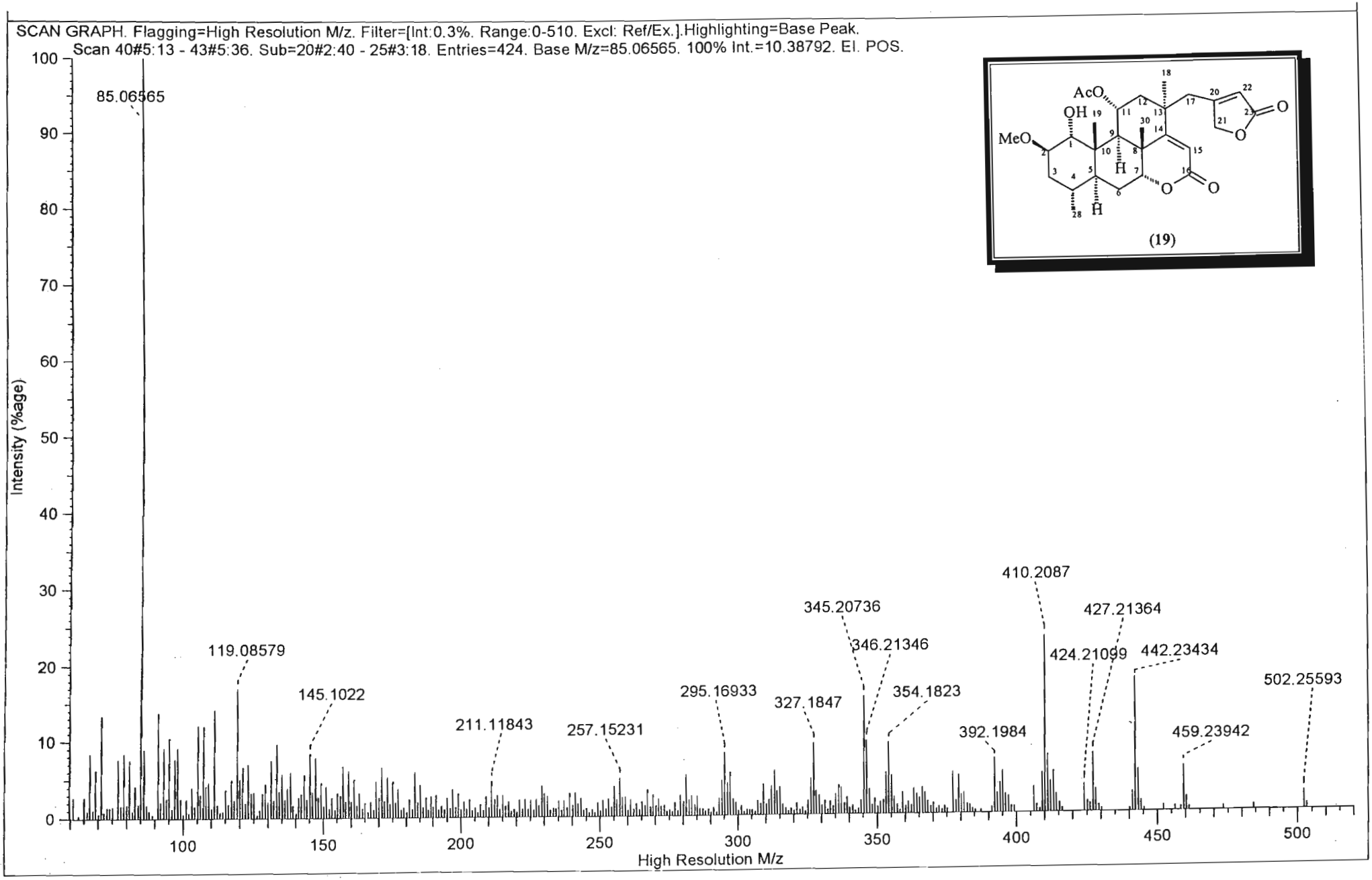

Mass spectrum of cedphiline (19)

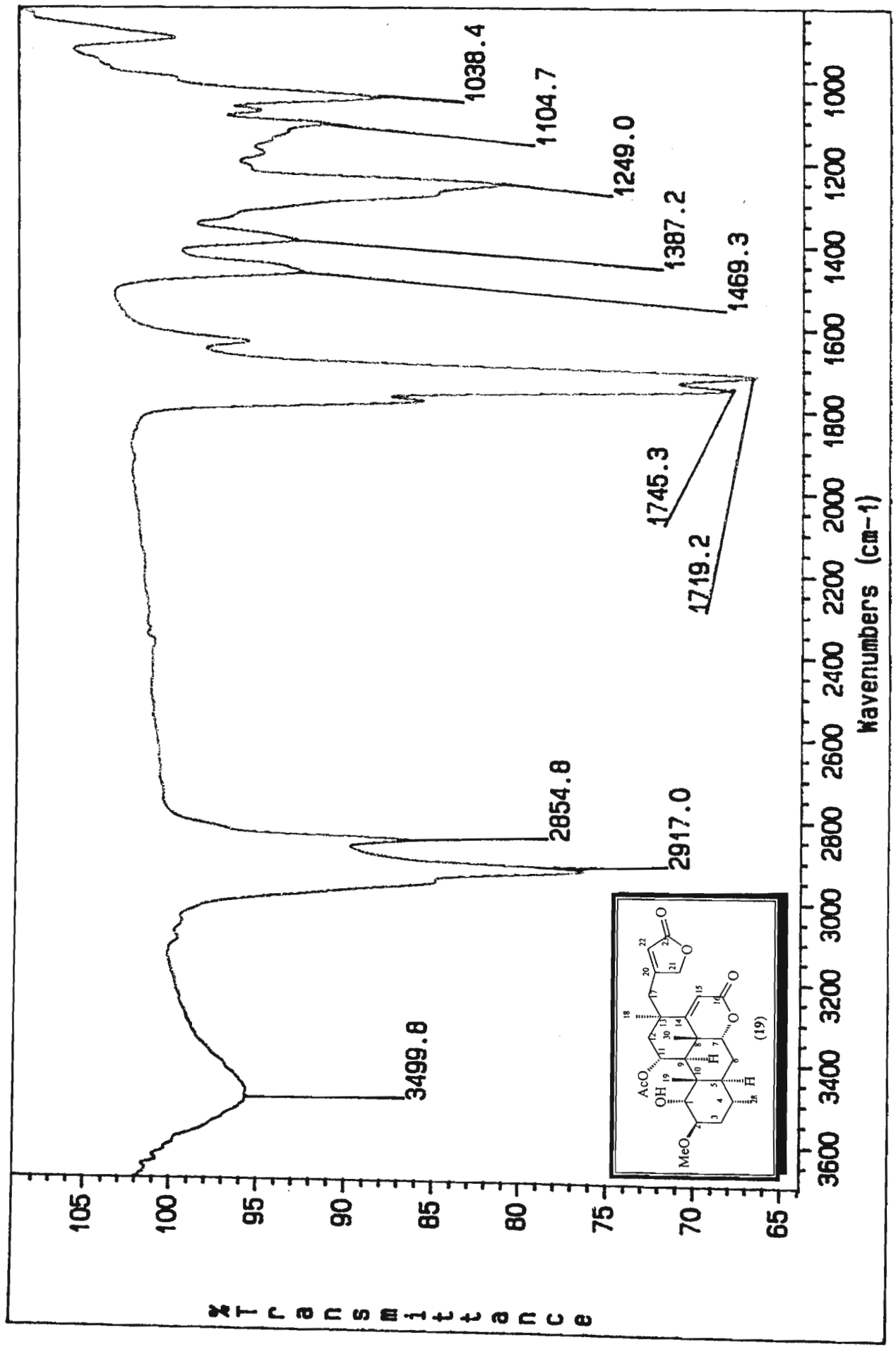

IR spectrum of cedphiline (19)

(19)

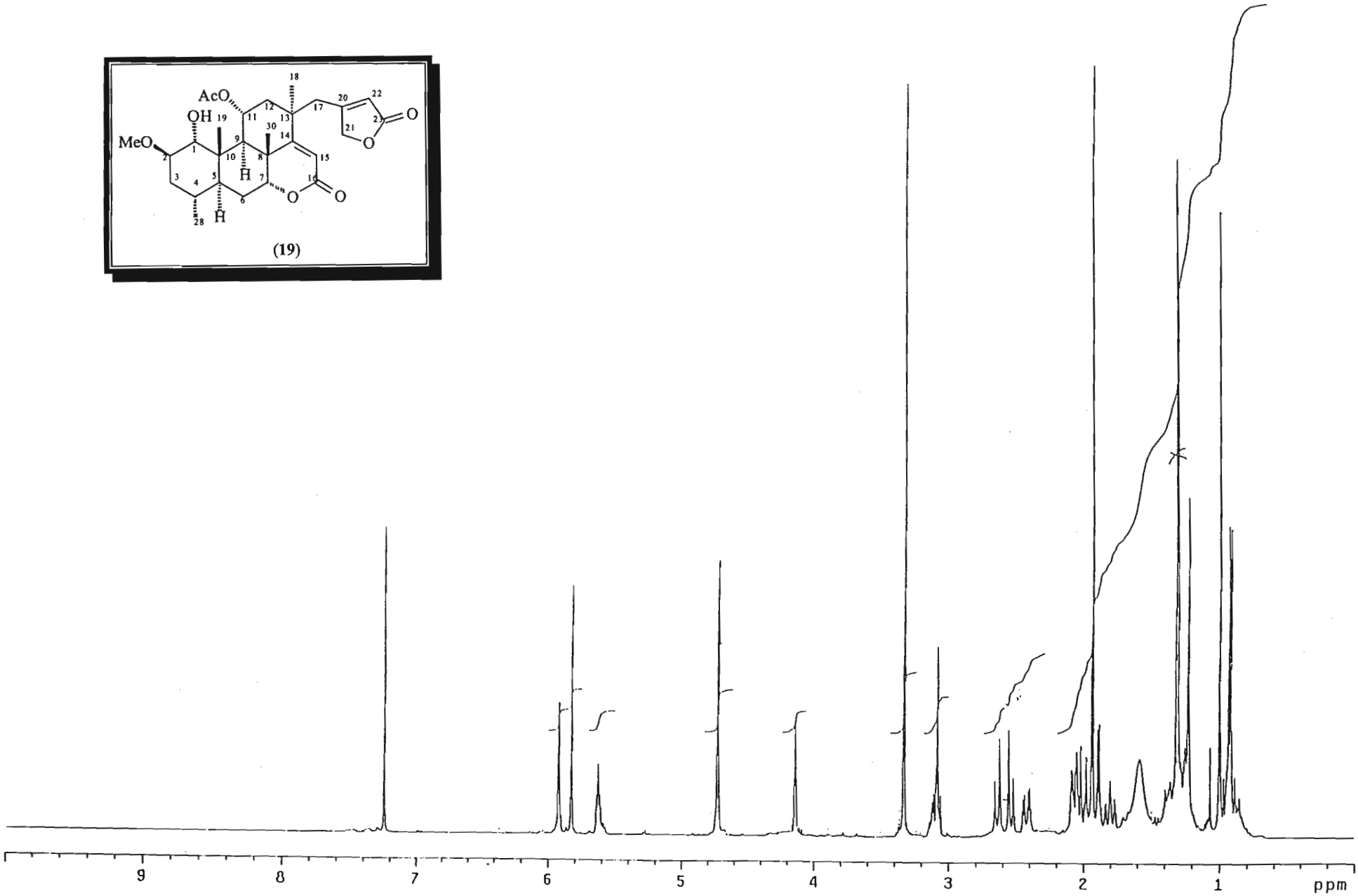

^{1}H NMR spectrum of cedphiline (19)

c0006.DN E 46-49 in cdc13
probe=5mmASW

(19)

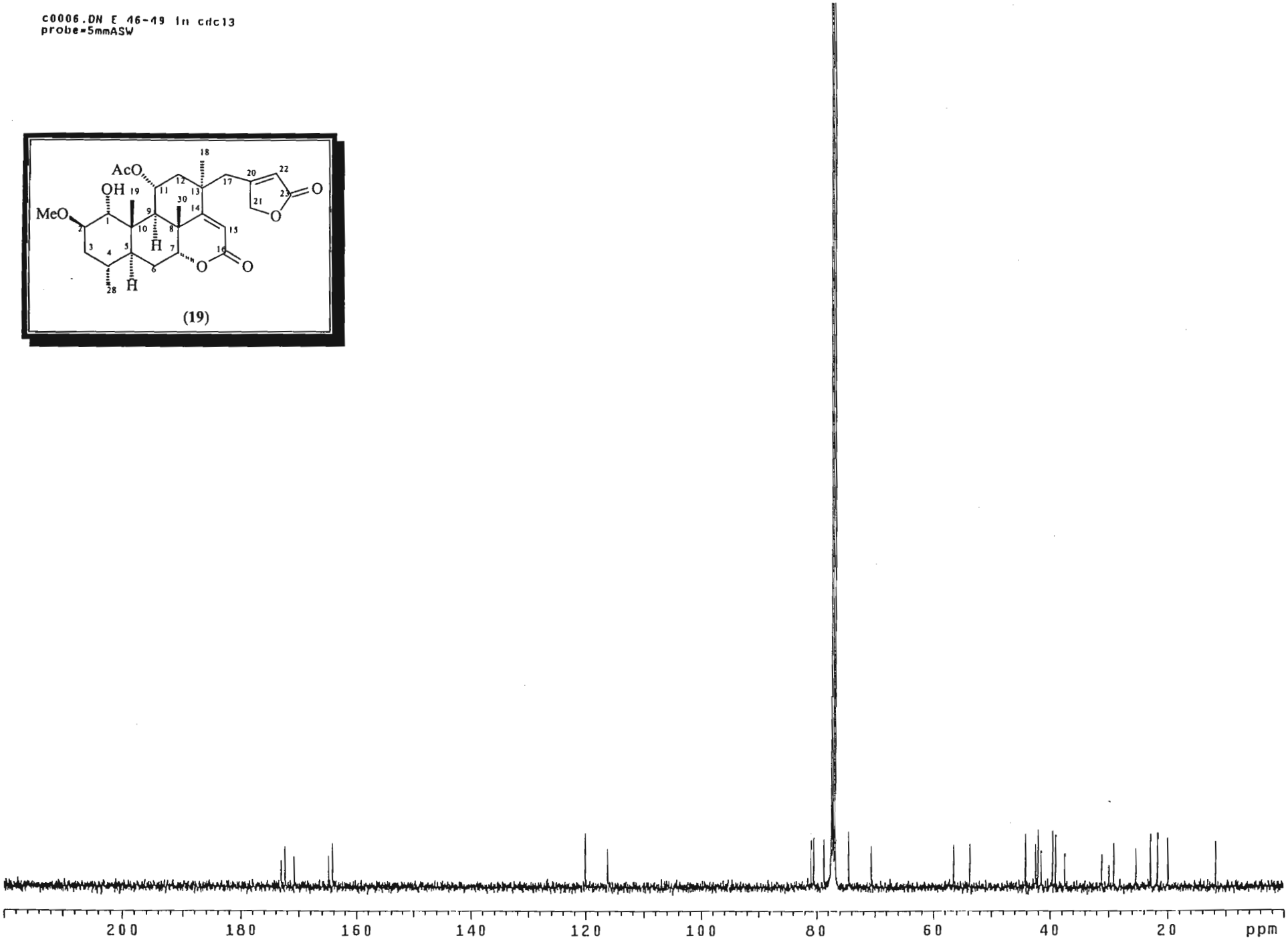

^{13}C NMR spectrum of cedphiline (19)

d0006.DN E16-19 in cdcl3
probe=5mmASW

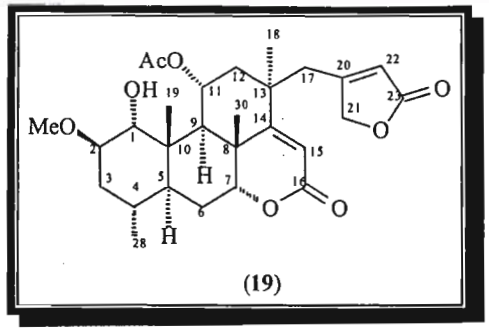

(19)

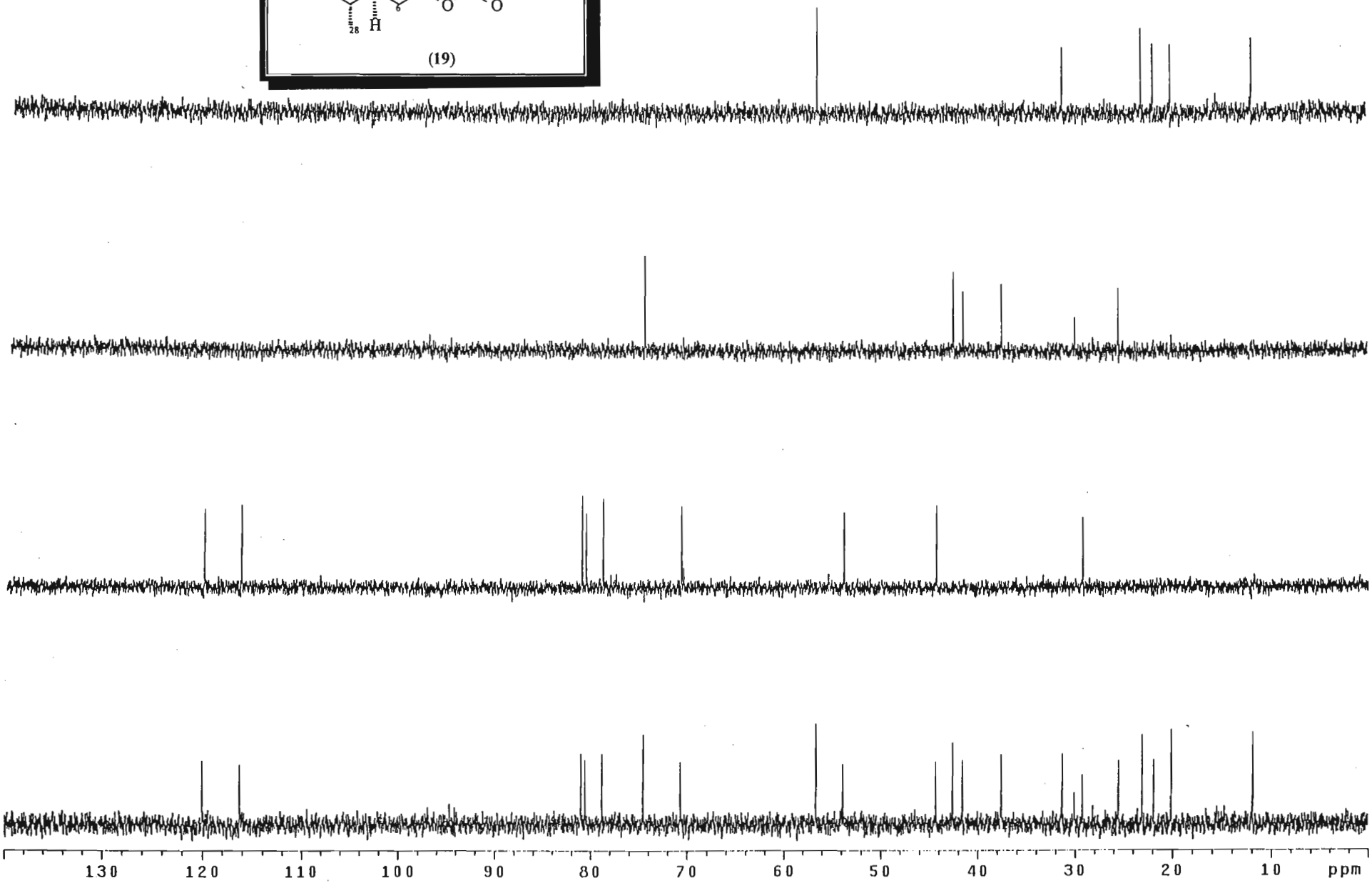

ADEPT NMR spectrum of cedphiline (19)

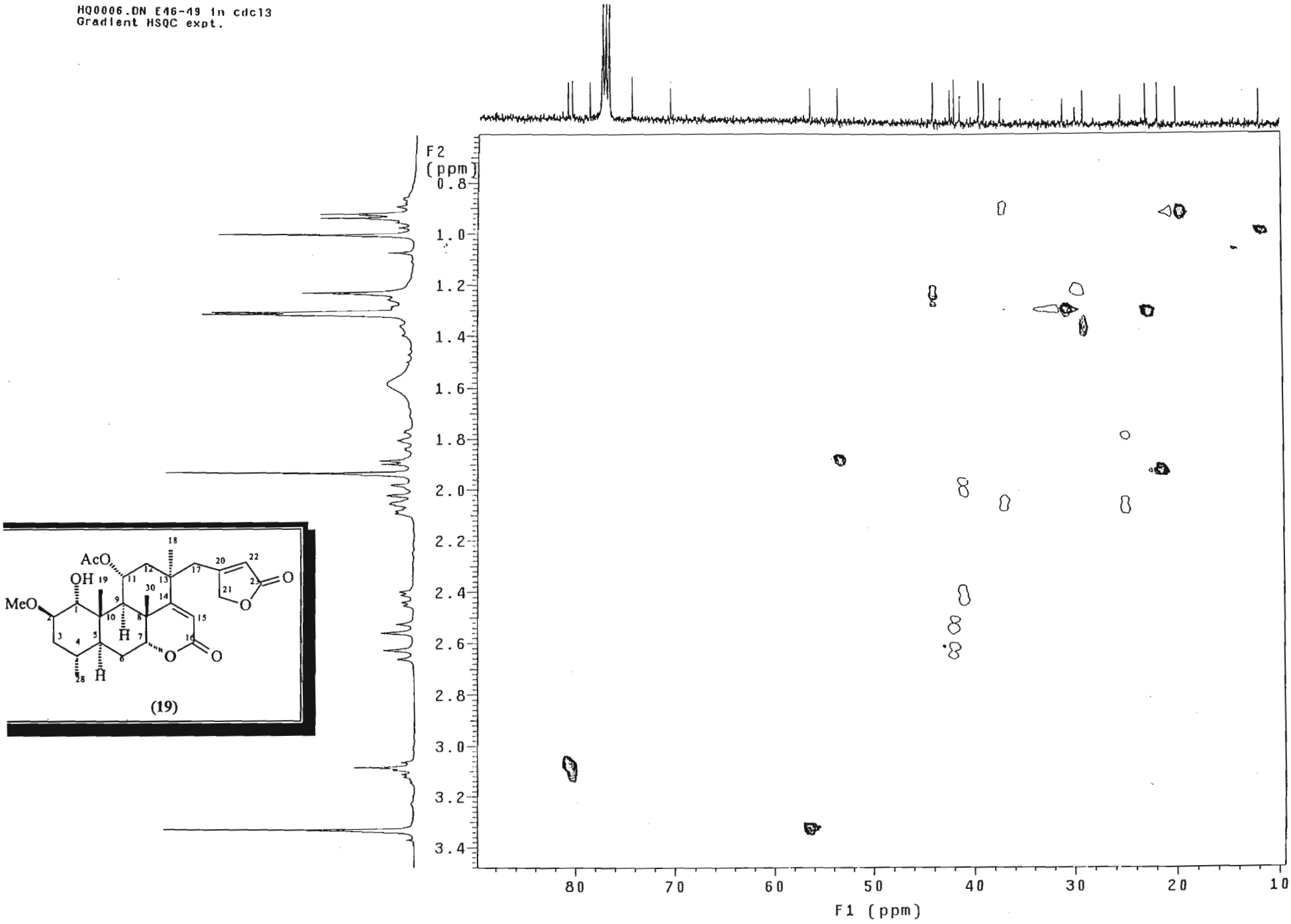

HSQC NMR spectrum of cedphiline (19)

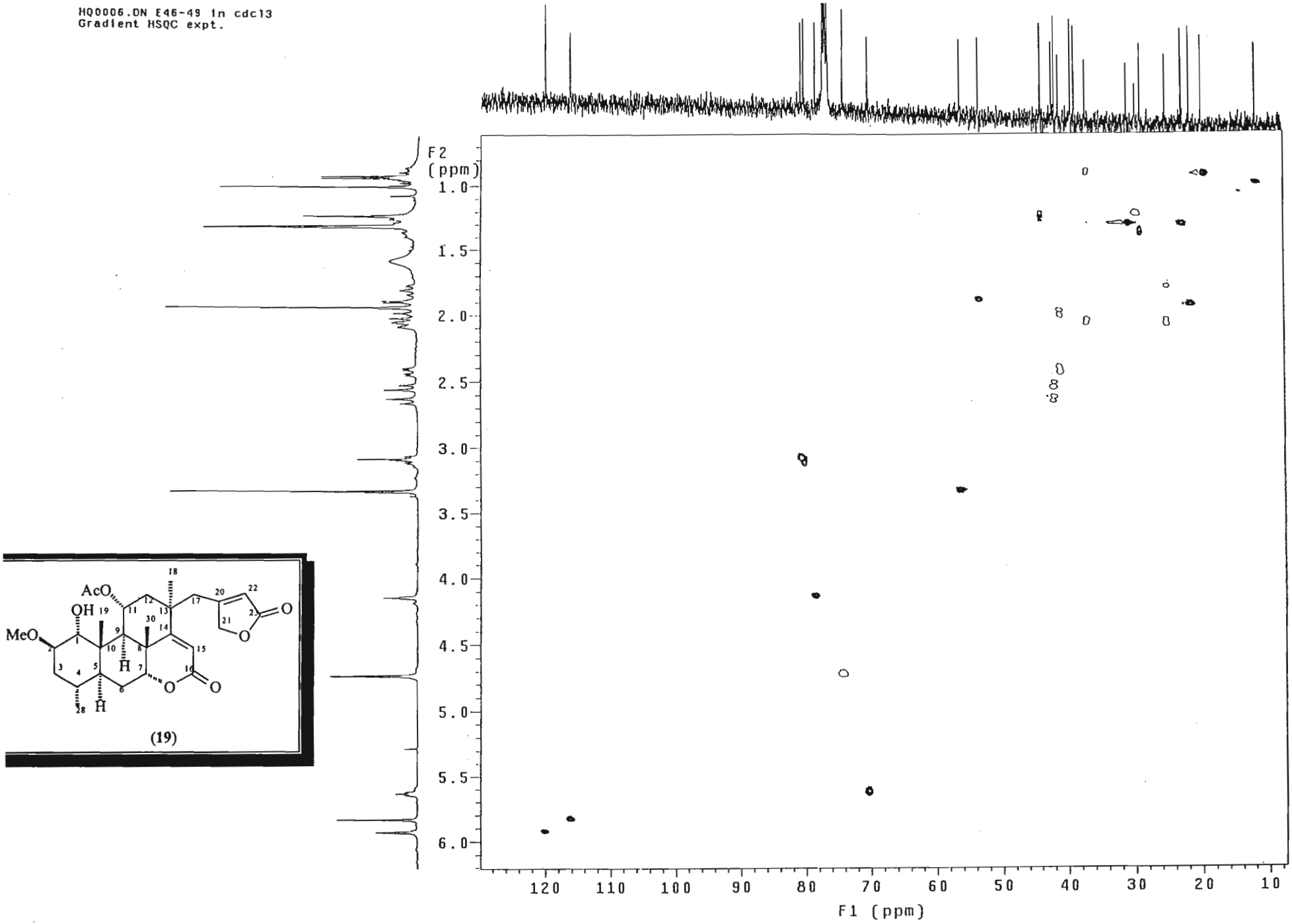

HSQC NMR spectrum of cedphiline (19)

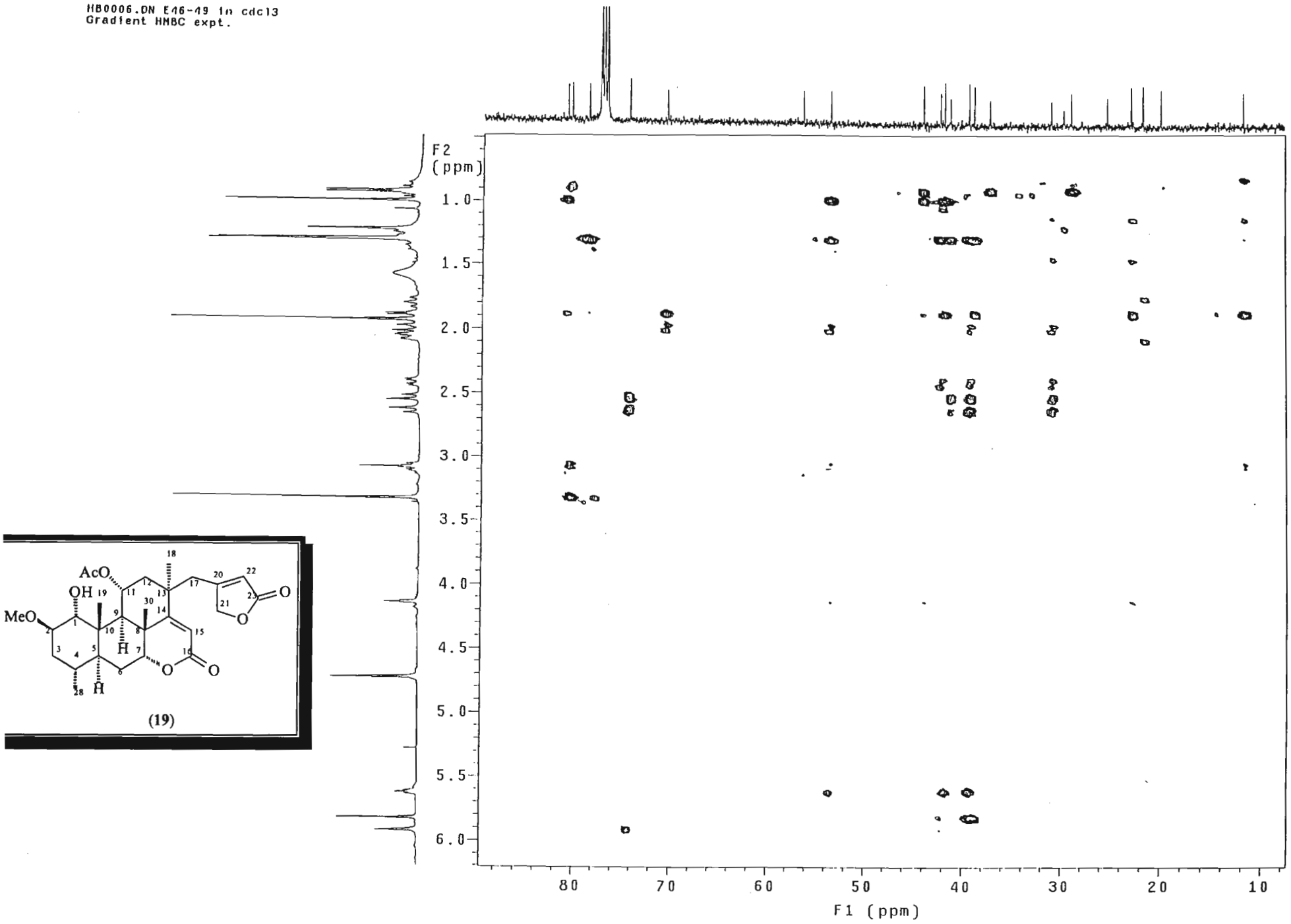

HMBC NMR spectrum of cedphiline (19)

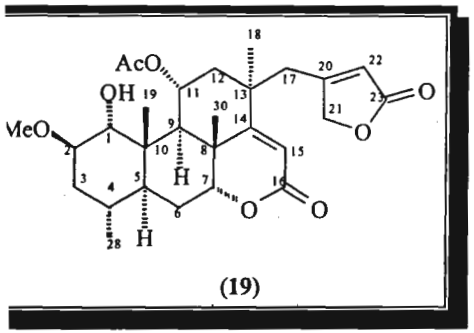

(19)

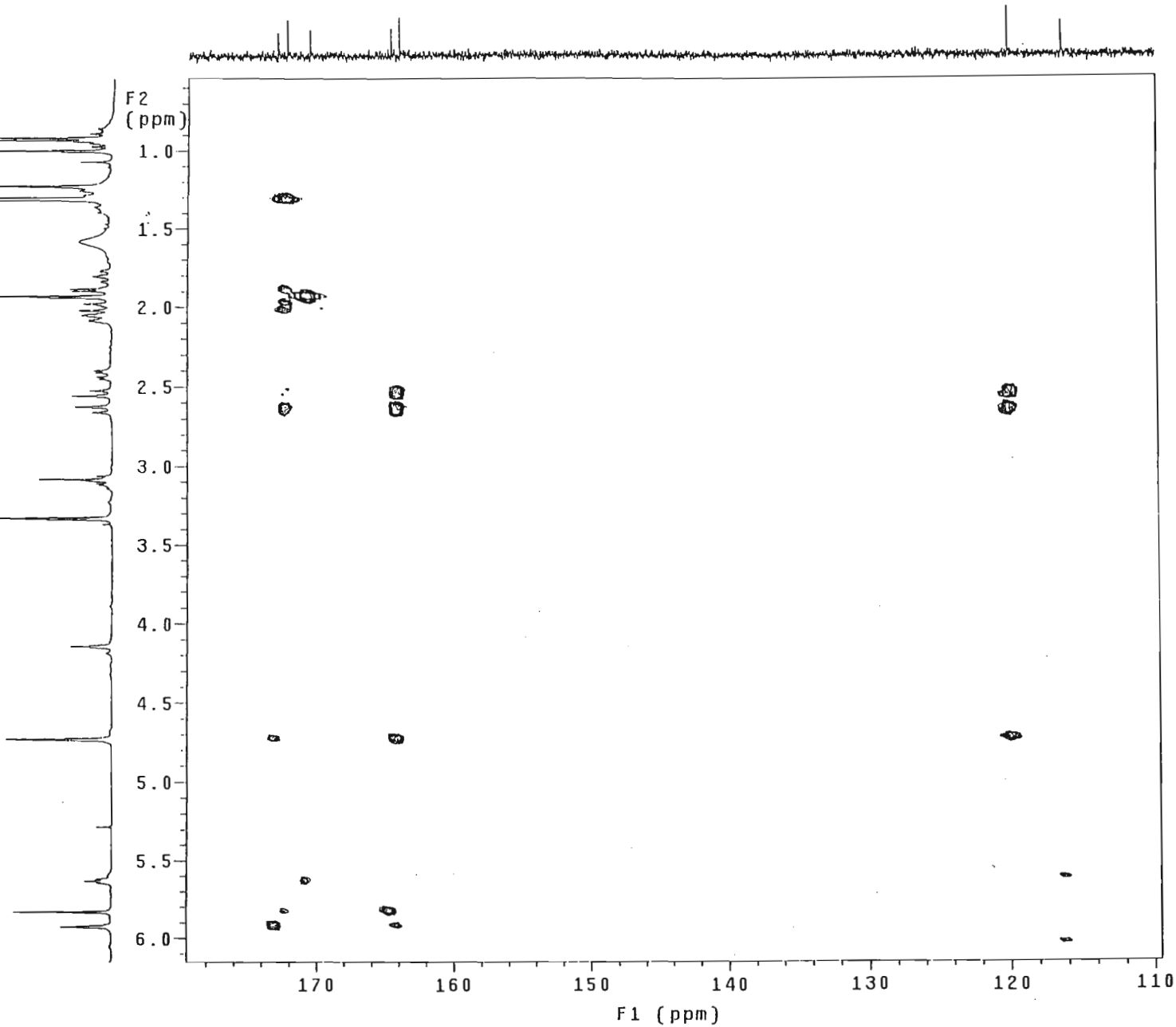

HMBC NMR spectrum of cedphiline (19)

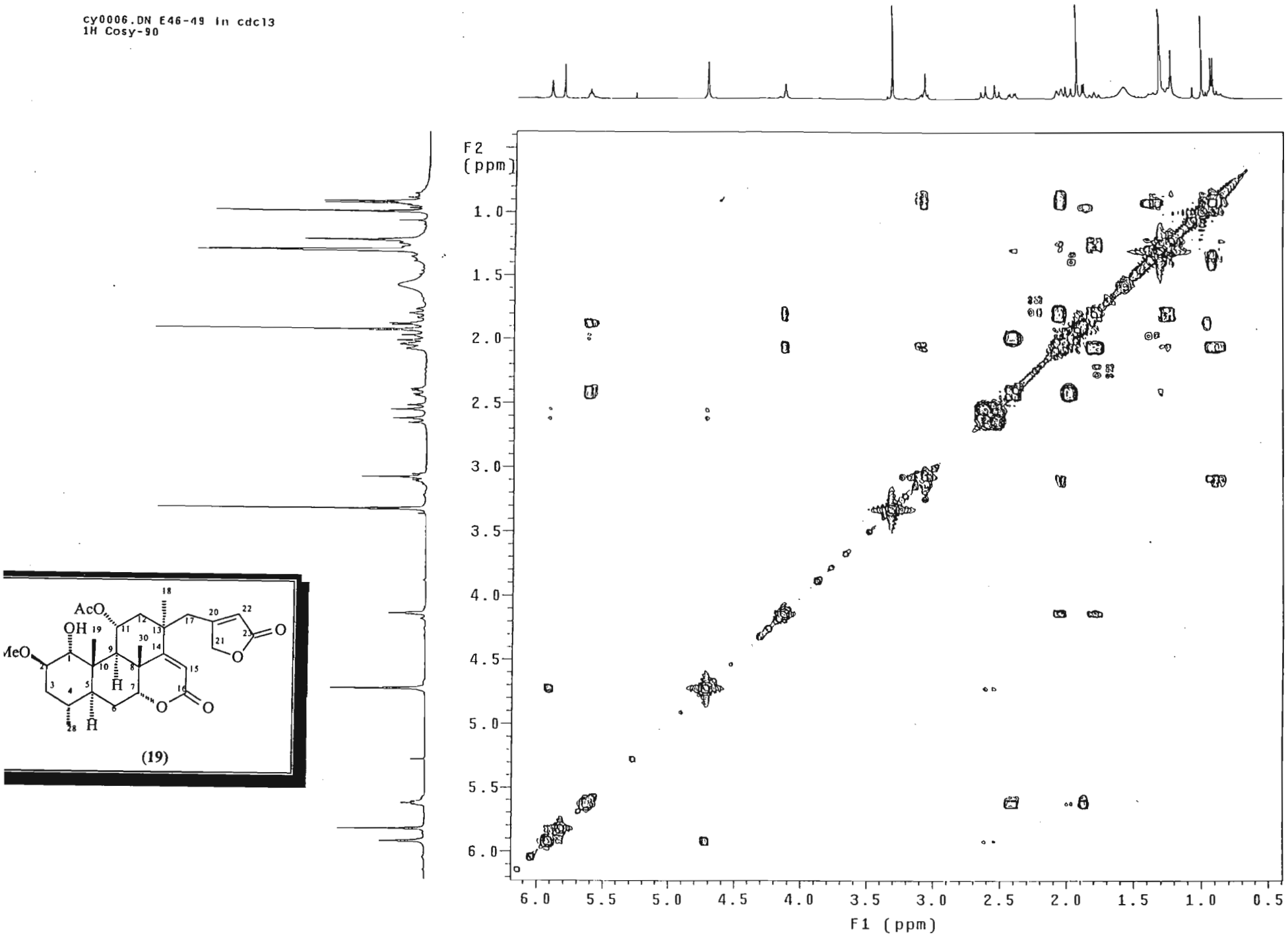

COSY NMR spectrum of cedphiline (19)

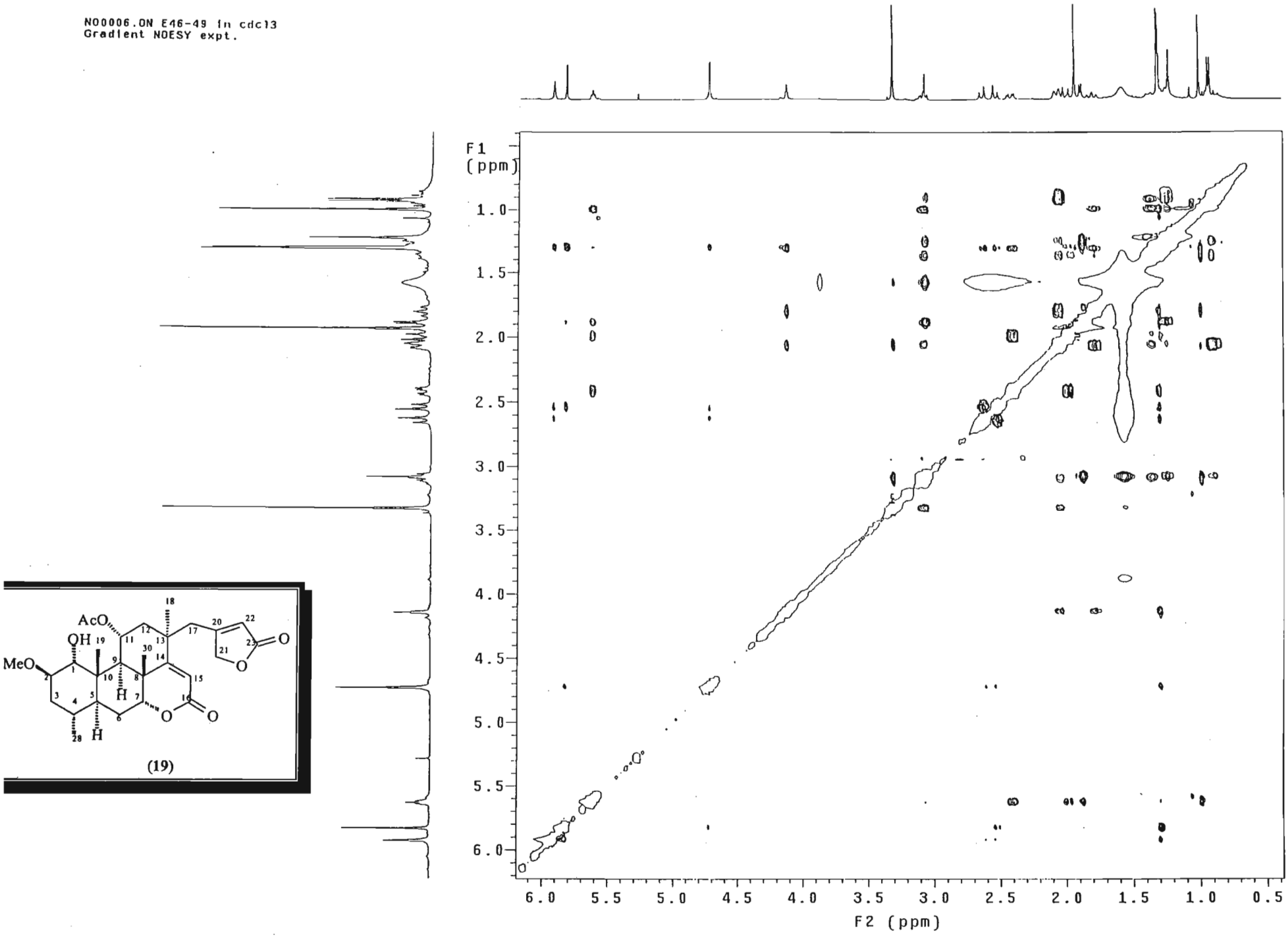

(19)

NOESY NMR spectrum of cedphiline (19)

Sitosteryl β-D-glucopyranoside tetra-acetate (21)

IR spectrum [61]

^{1}H NMR [62]

^{13}C NMR [63]

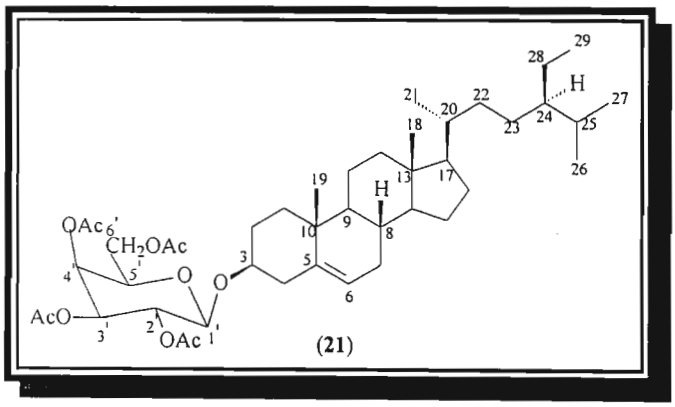

Sitosteryl β-D-glucopyranoside tetra-acetate (21)

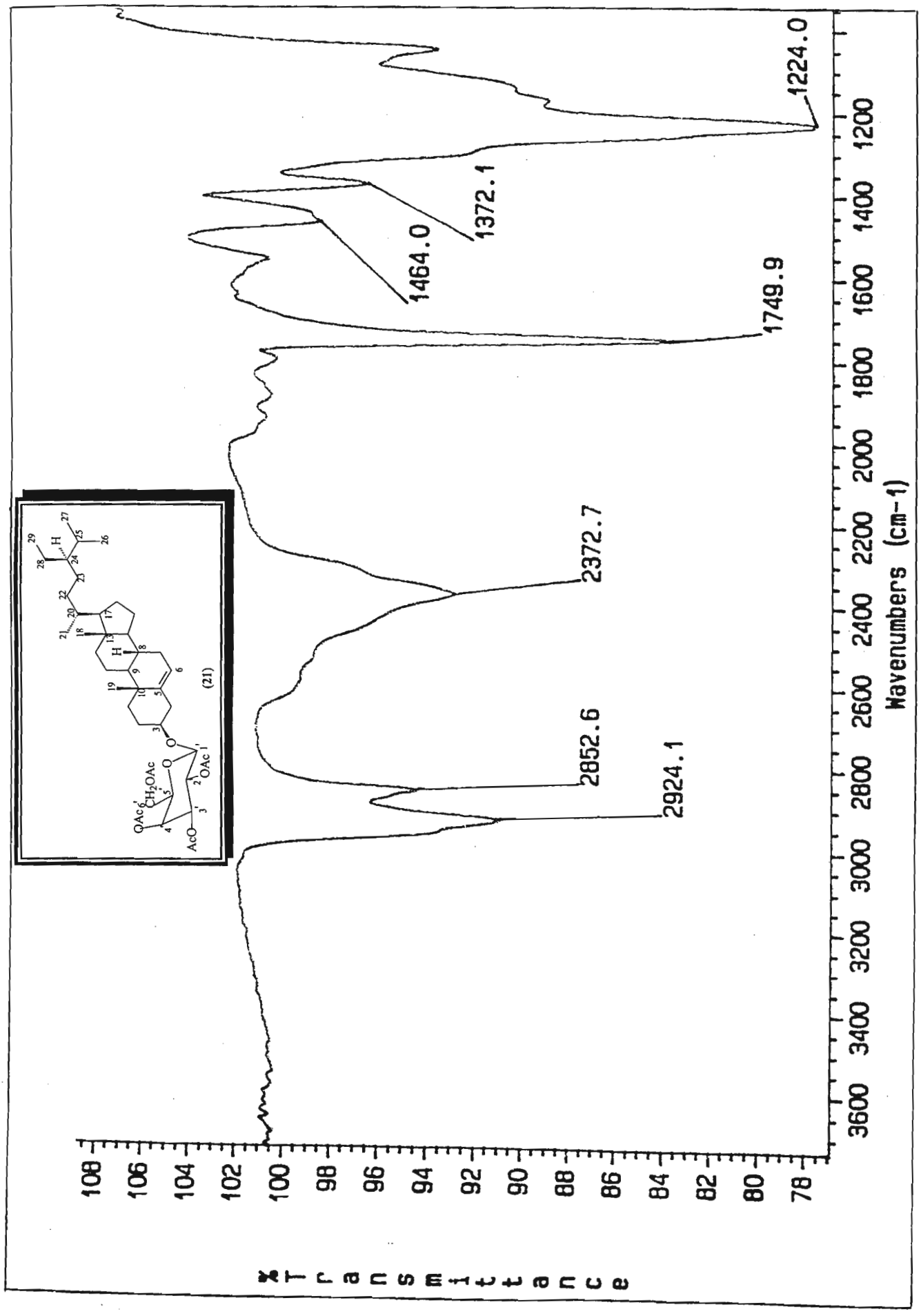

IR spectrum of sitosteryl β-D-glucopyranoside tetra-acetate (21)

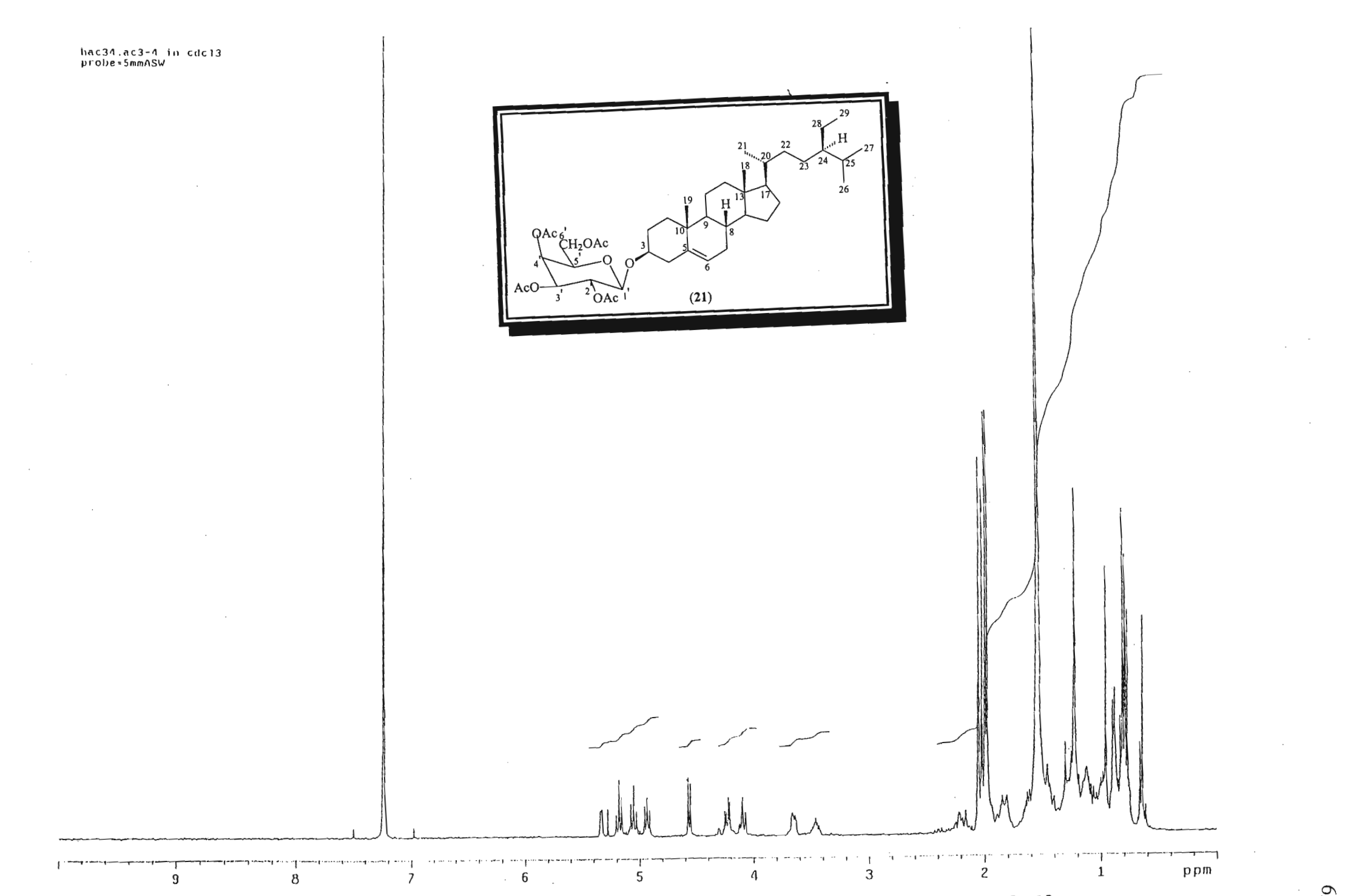

^{1}H NMR spectrum of sitosteryl β-D-glucopyranoside tetra-acetate (21)

cac34.ac3-4 in cdcl3
probe=5mmASW

(21)

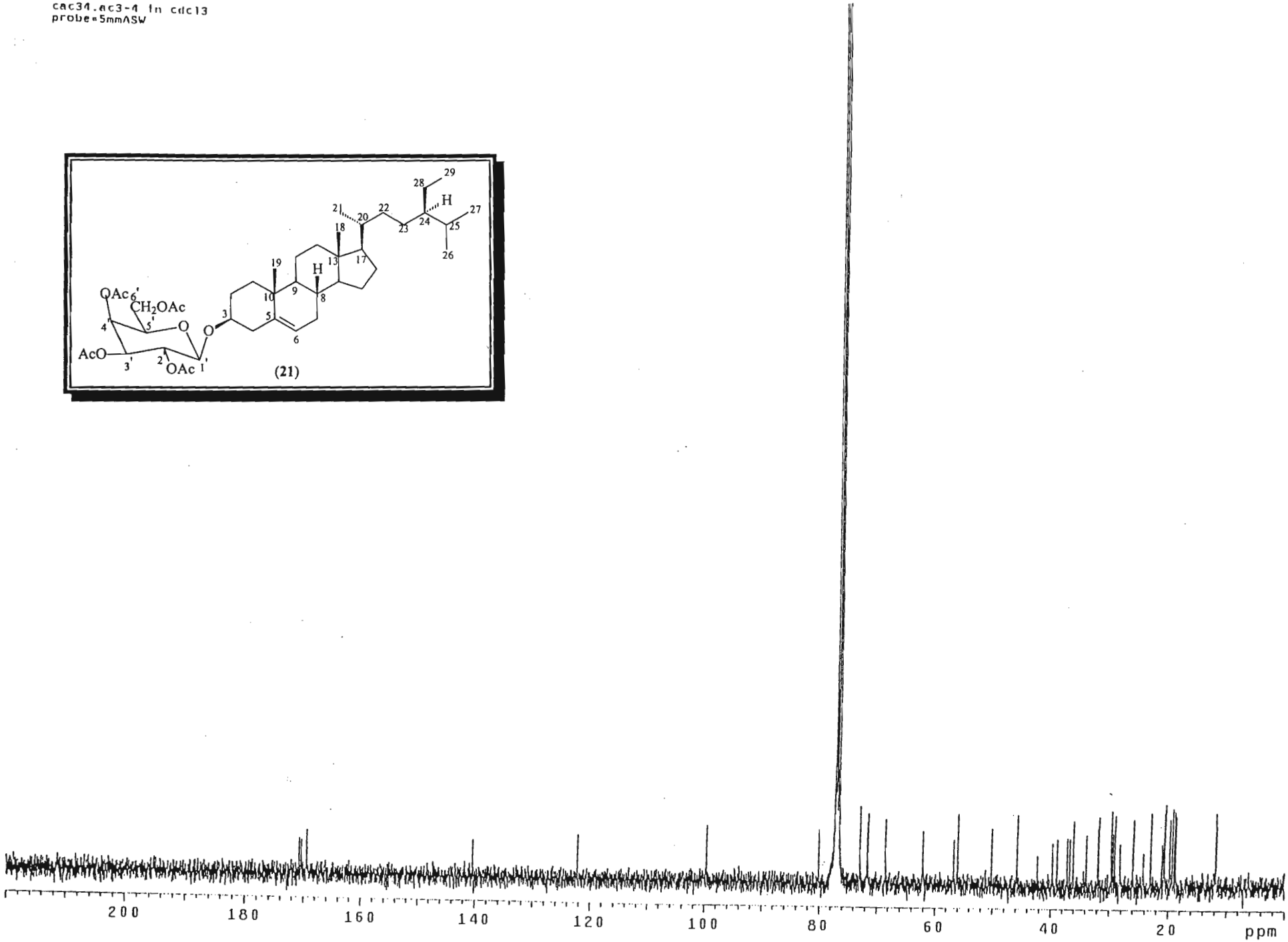

^{13}C NMR spectrum of sitosteryl β-D-glucopyranoside tetra-acetate (21)

Extractives from *Neobeguea mahafalensis* seeds

Photograph by Dr. Milijaona Randrianarivelojosia

Methyl angolensate (5)

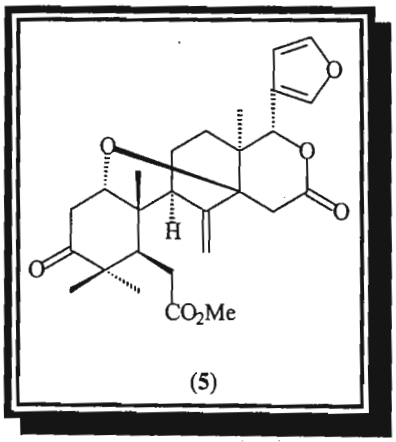

(5)

Methyl angolensate (5)

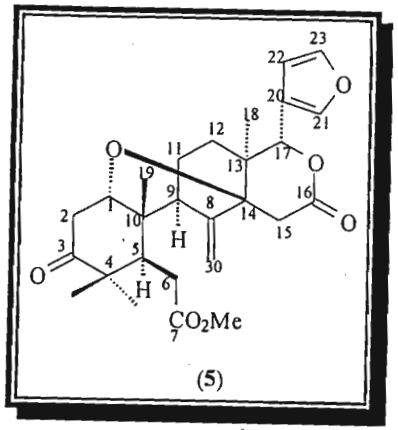

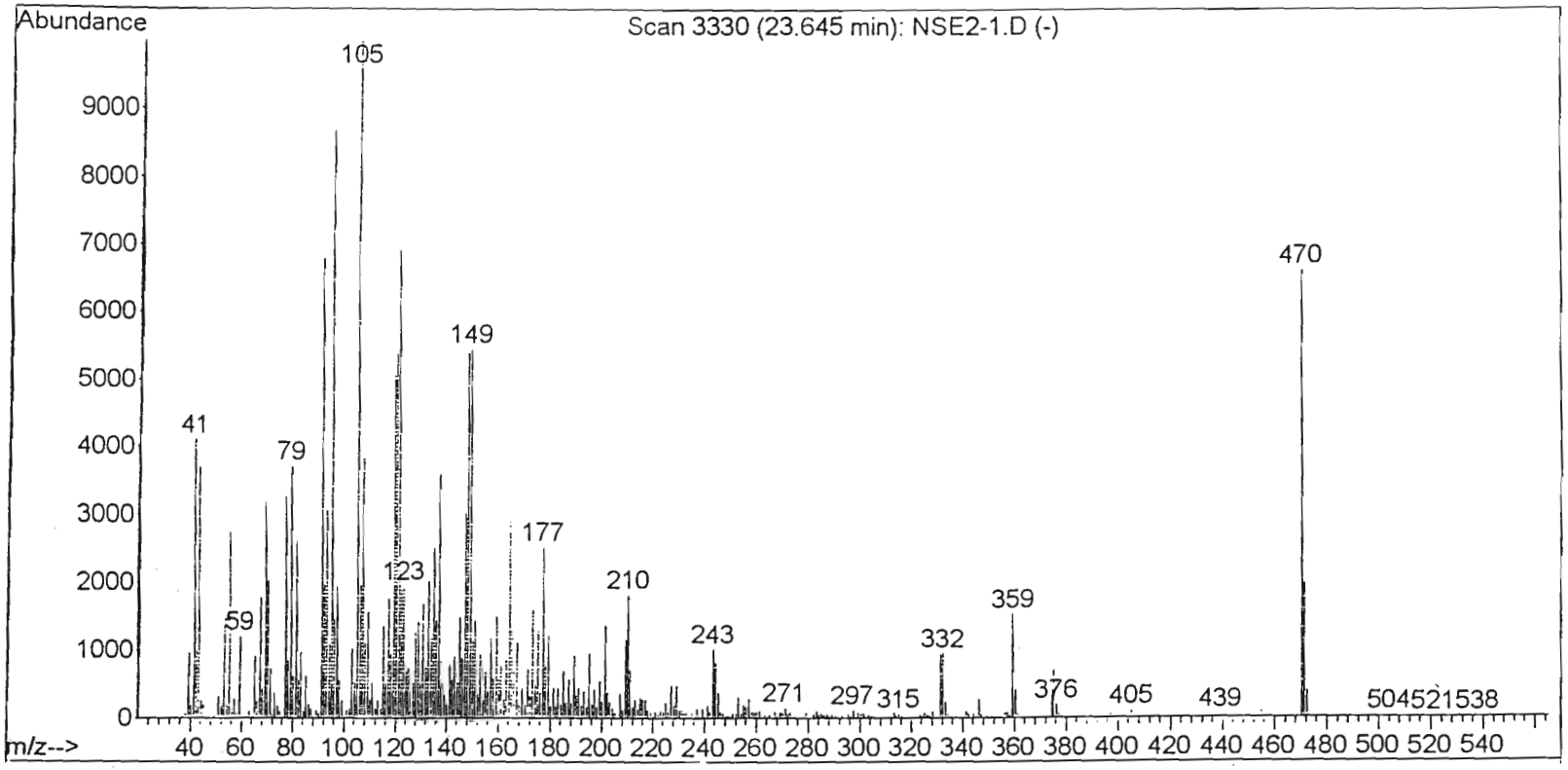

Mass spectrum of methyl angolensate (5)

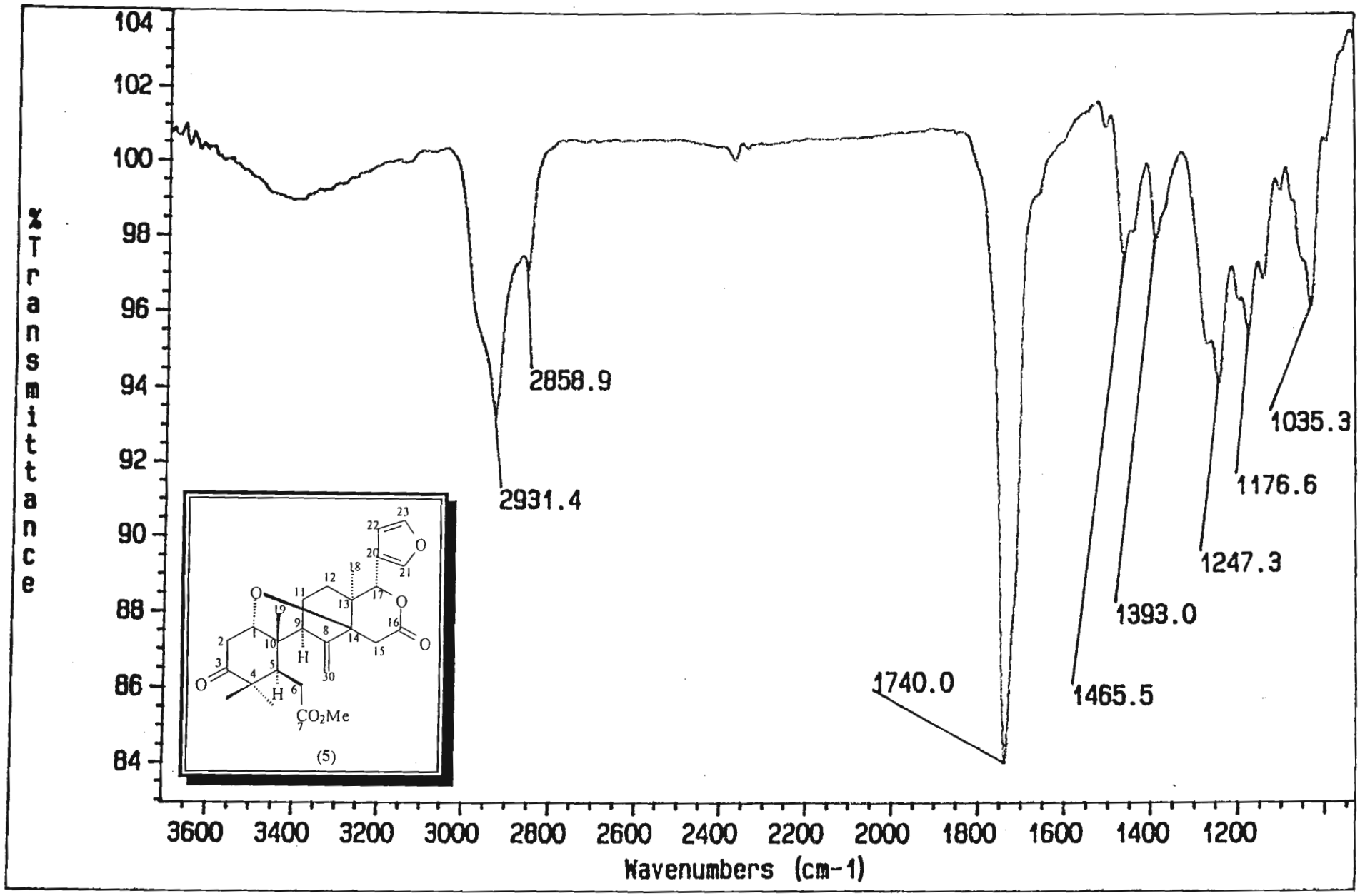

IR spectrum of methyl angolensate (5)

hnse41.nse 2-4 1 in cdcl3
probe=5mmASW

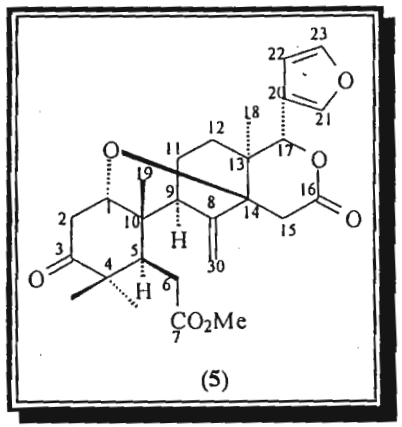

(5)

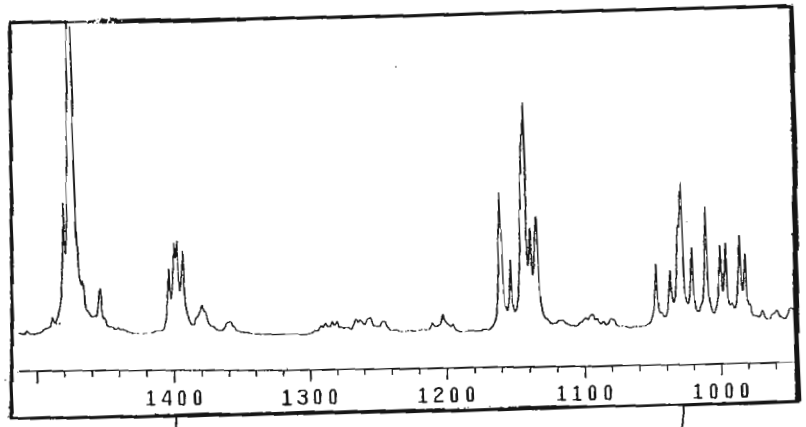

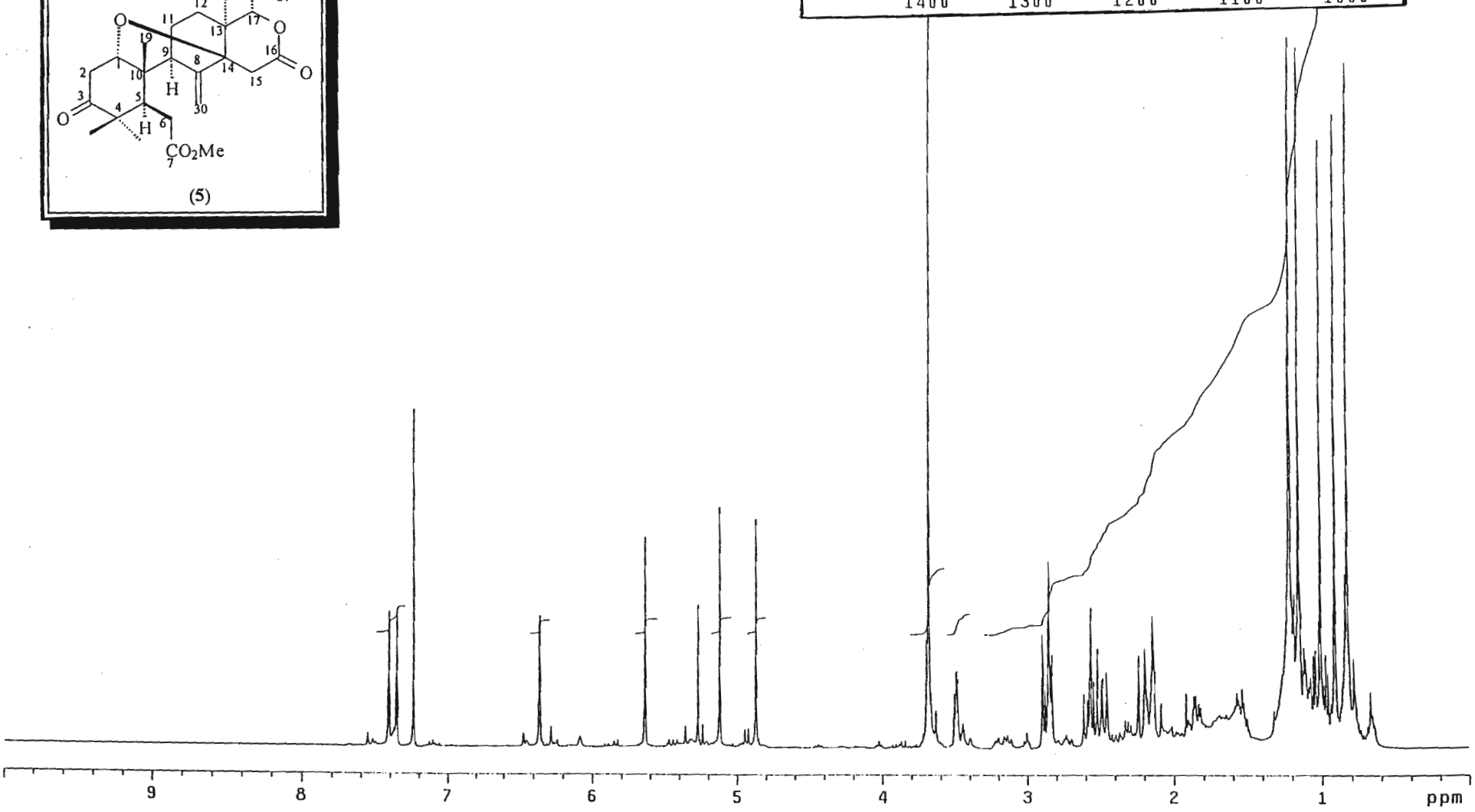

^{1}H NMR spectrum of methyl angolensate (5)

cnse41.nse 2-4 1 in cdcl3
probe=5mmASW

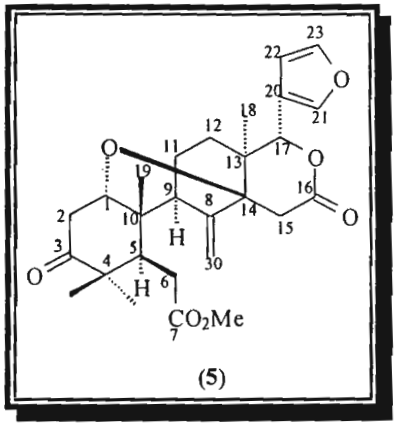

(5)

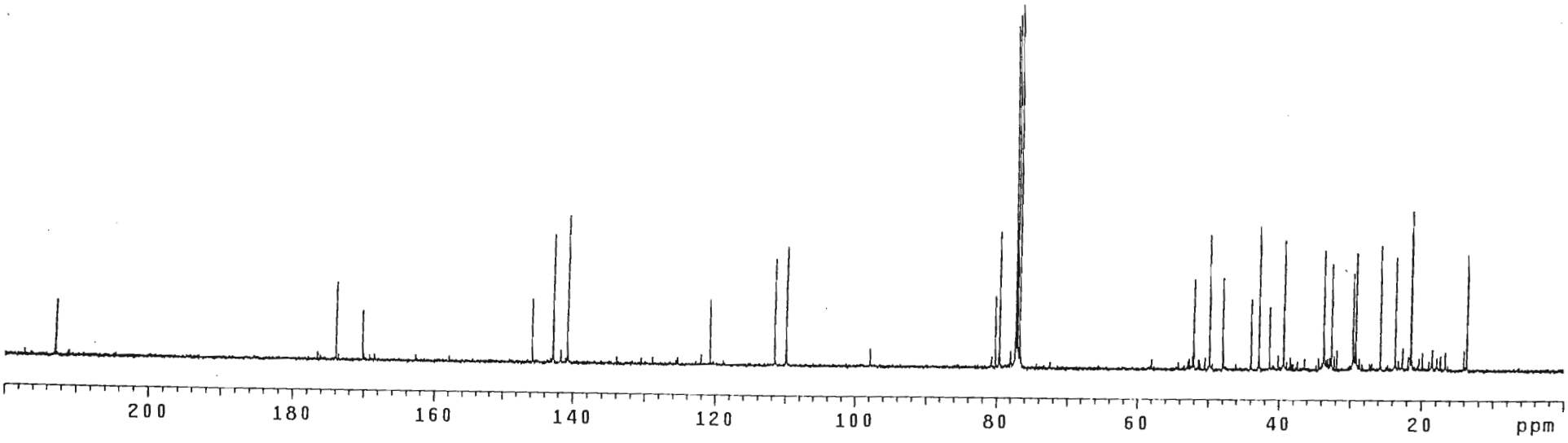

^{13}C NMR spectrum of methyl angolensate (5)

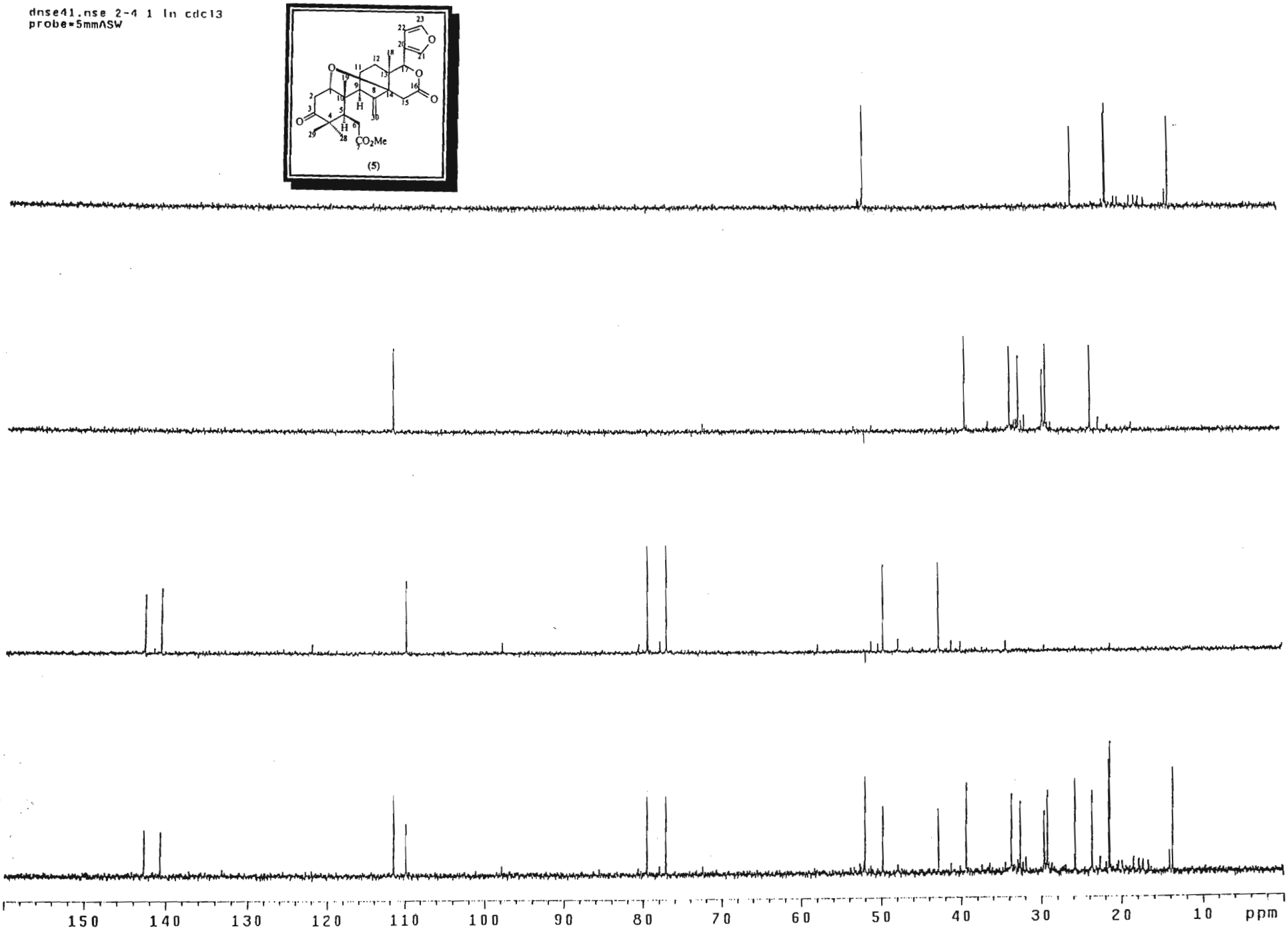

ADEPT NMR spectrum of methyl angolensate (5)

HQnse41.nse 2-4 1 in cdcl3
Gradient HSQC expt.

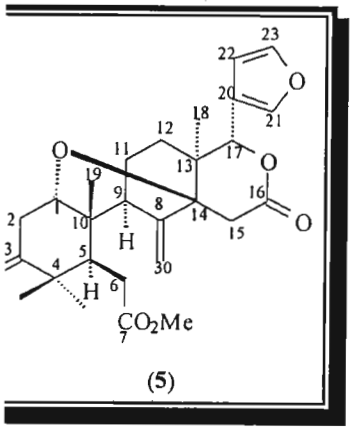

(5)

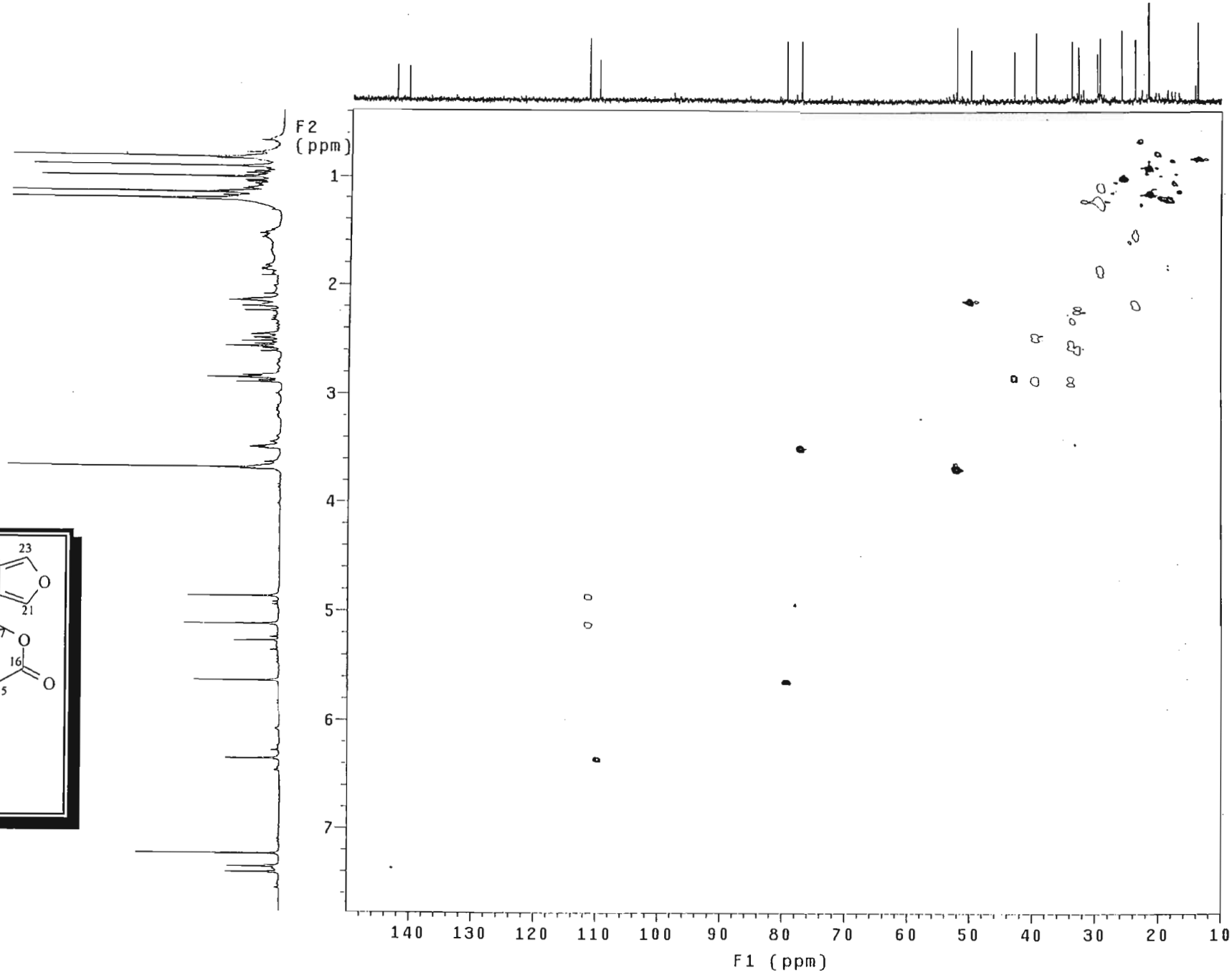

HSQC NMR spectrum of methyl angolensate (5)

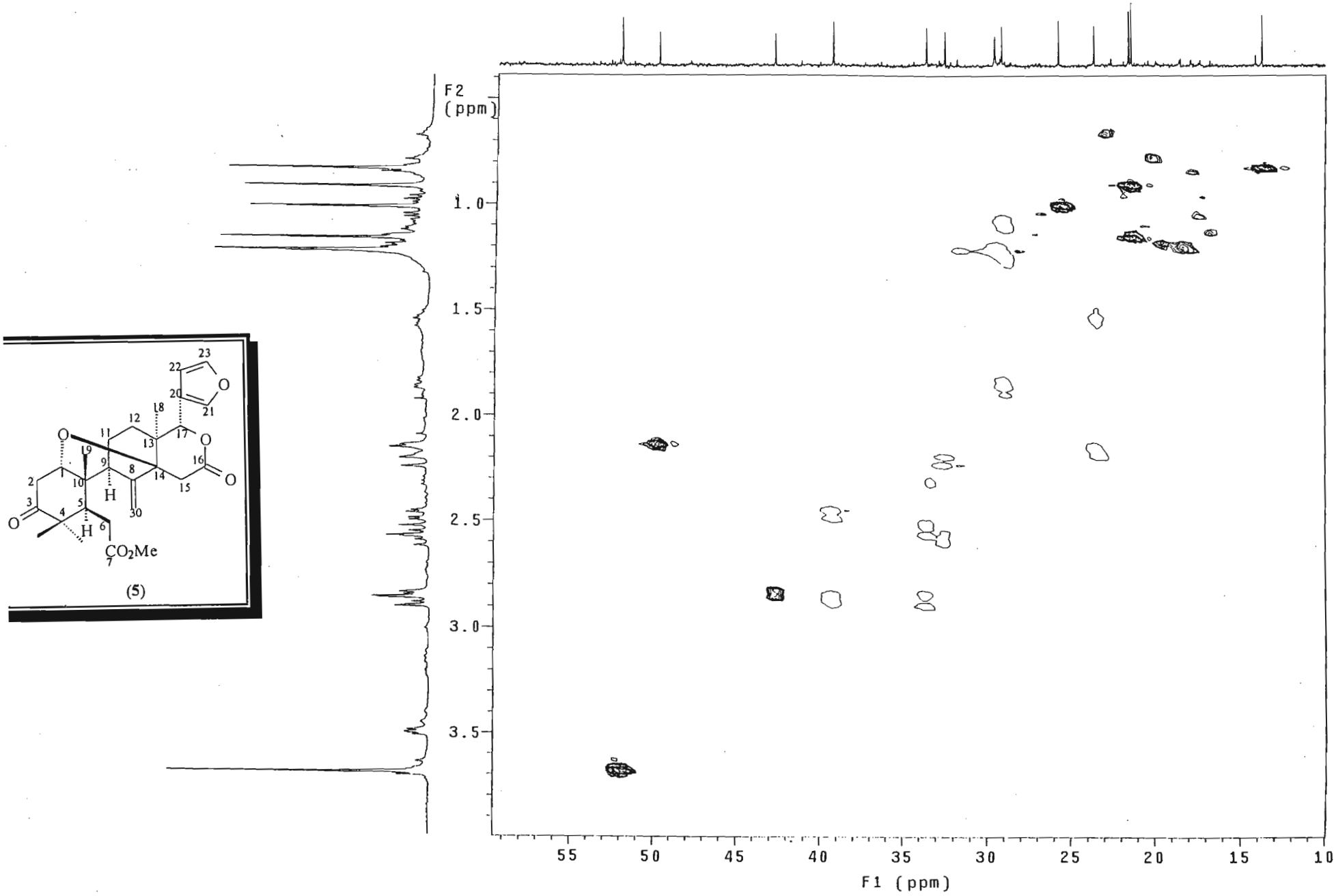

HSQC NMR spectrum of methyl angolensate (5)

HQnse41.nse 2-4 1 in cdcl3
Gradient HSQC expt.

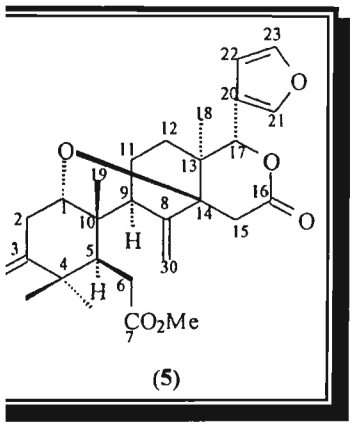

(5)

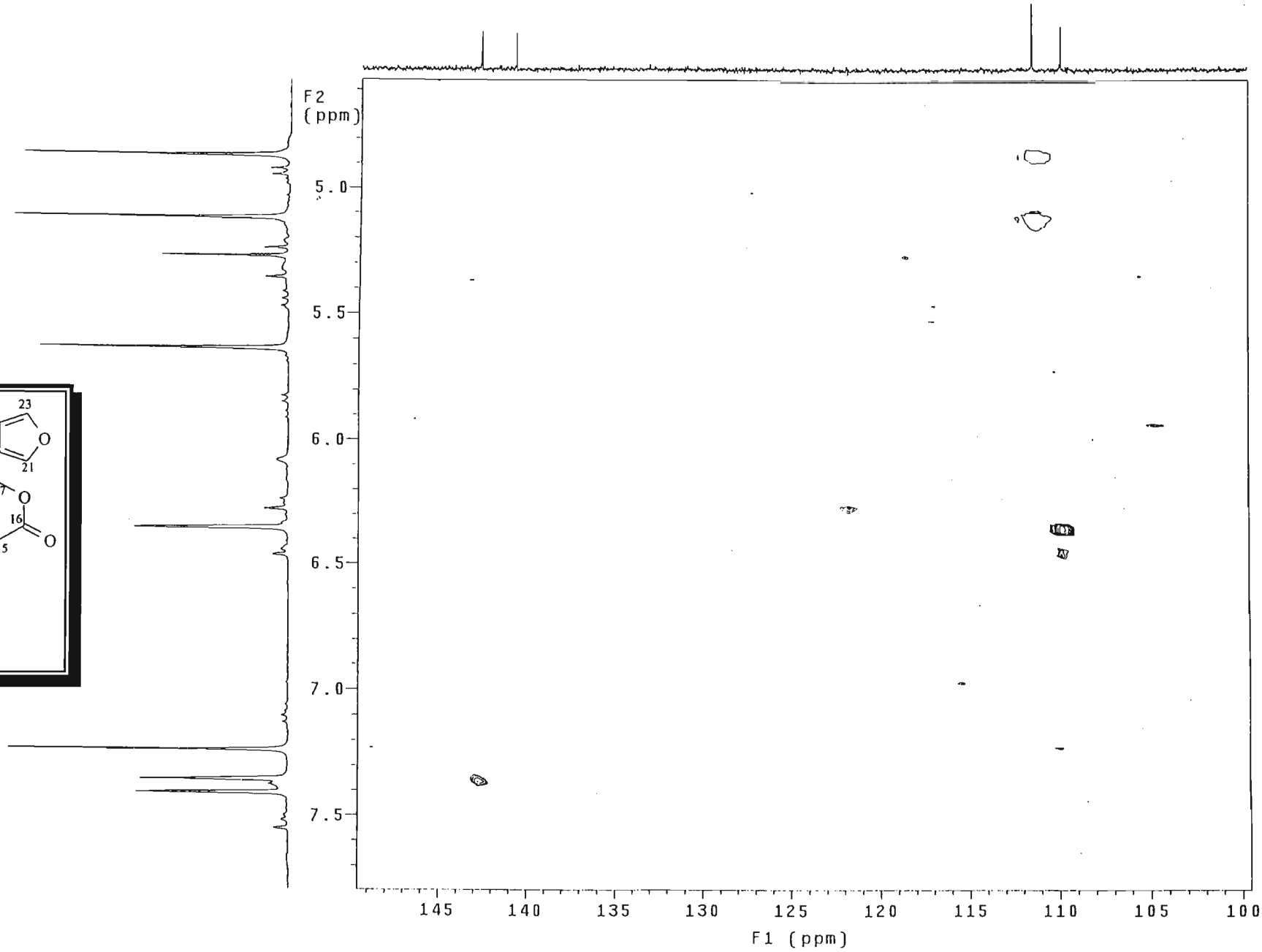

HSQC NMR spectrum of methyl angolensate (5)

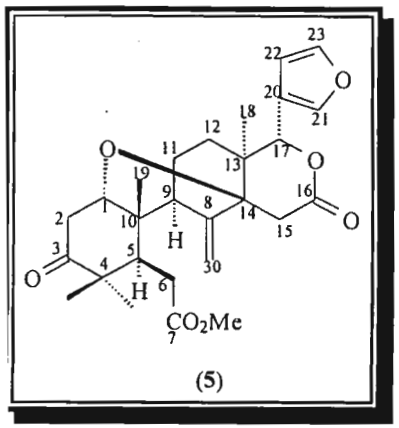

HBnse41.nse 2-4 1 in cdcl3
Gradient HMBC expt.

F2 (ppm)

1.0
1.5
2.0
2.5
3.0
3.5
4.0

80 70 60 50 40 30 20 10

F1 (ppm)

HMBC NMR spectrum of methyl angolensate (5)

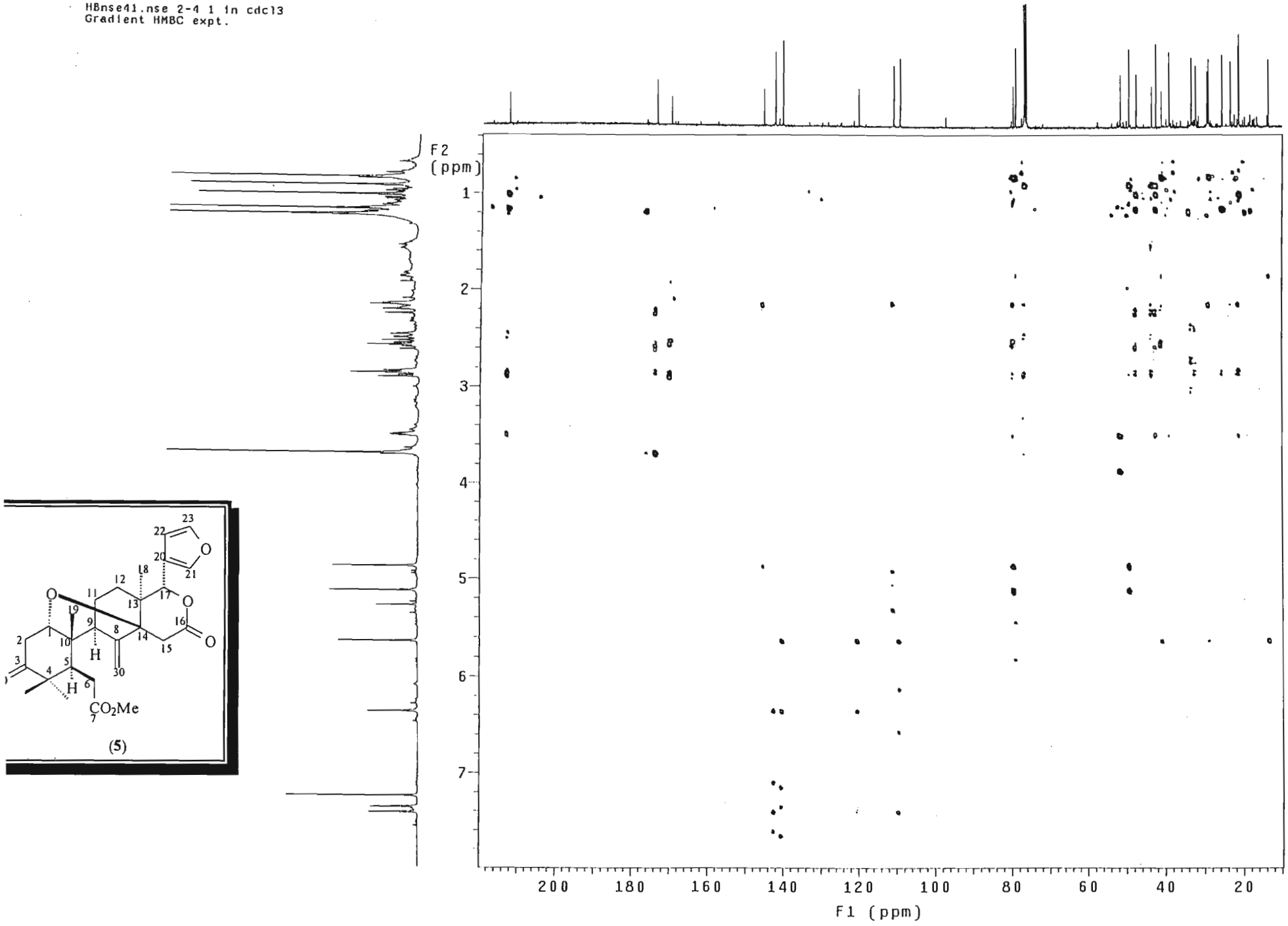

HMBC NMR spectrum of methyl angolensate (5)

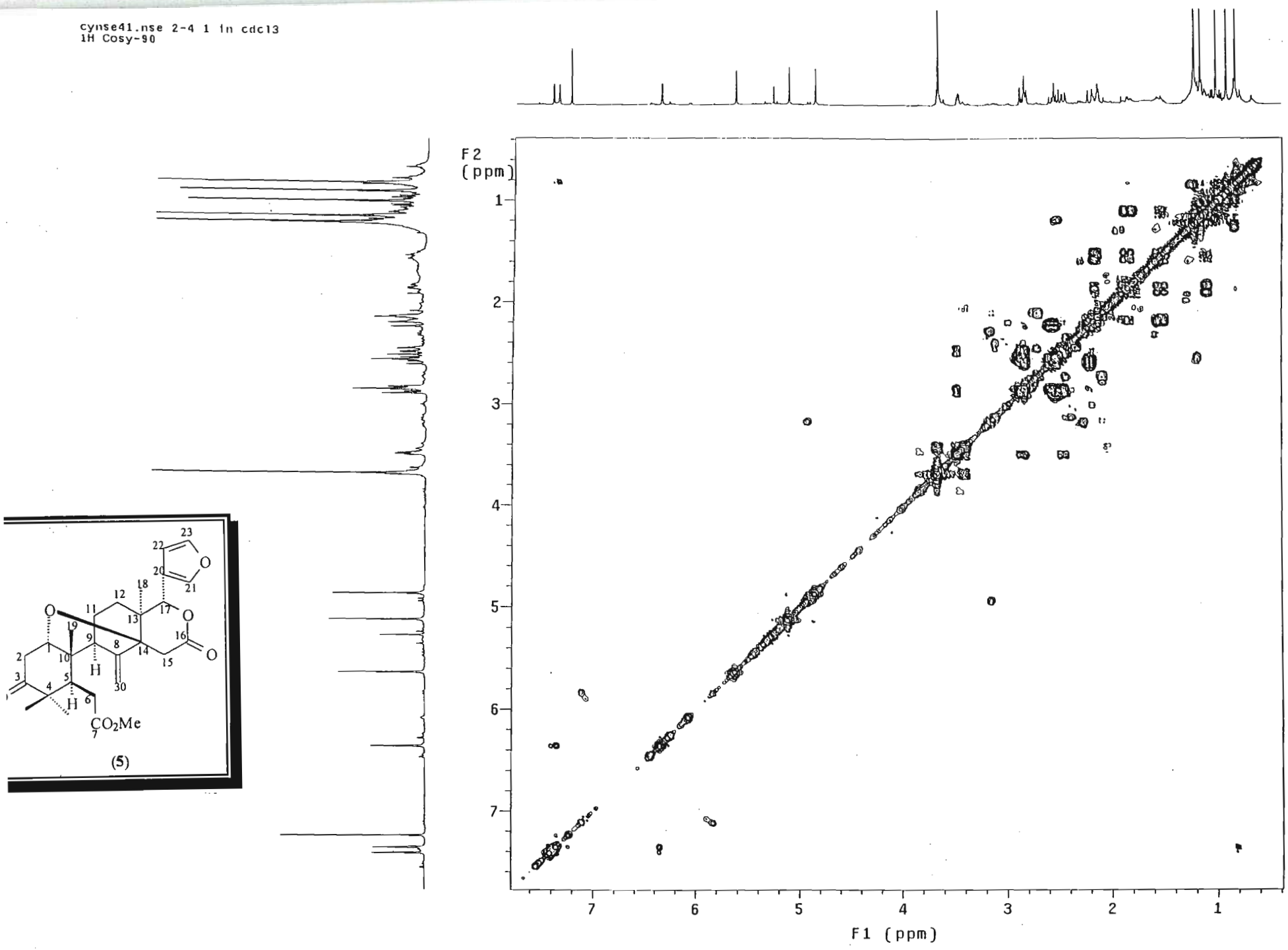

COSY NMR spectrum of methyl angolensate (5)

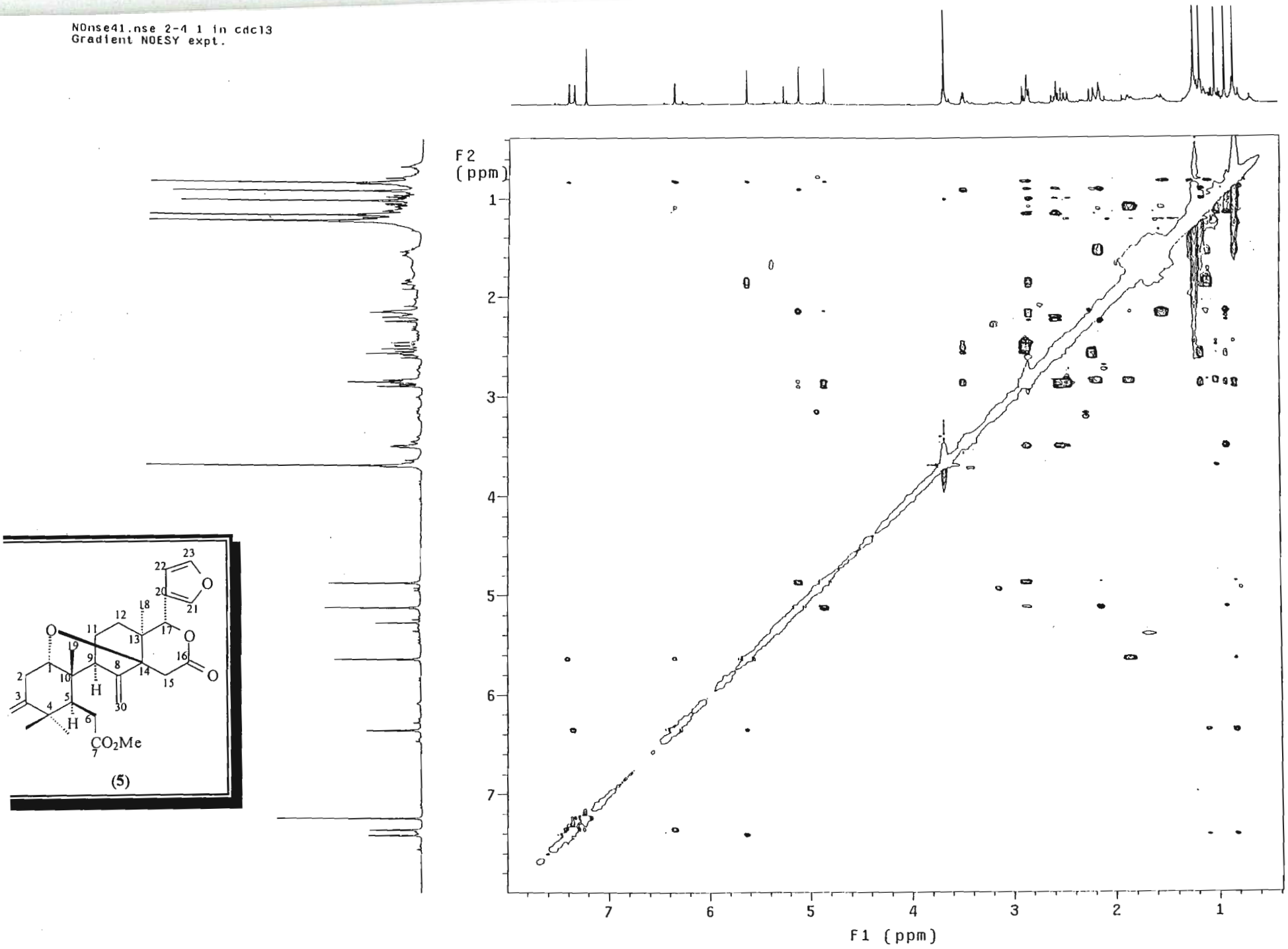

NOESY NMR spectrum of methyl angolensate (5)

Mexicanolide (6)

Mass spectrum	**[79]**
IR spectrum	**[80]**
^{1}H NMR	**[81]**
^{13}C NMR	**[82]**
ADEPT	**[83]**
HSQC	**[84]**
Expanded HSQC	**[85-86]**
HMBC	**[87-89]**
COSY	**[90]**
NOESY	**[91]**

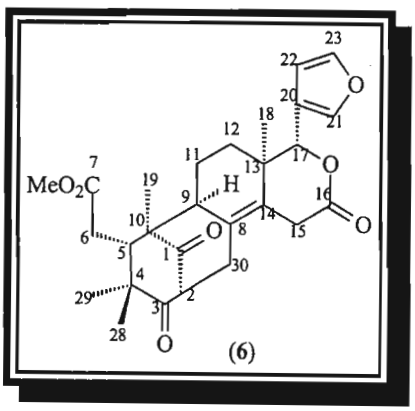

Mexicanolide (6)

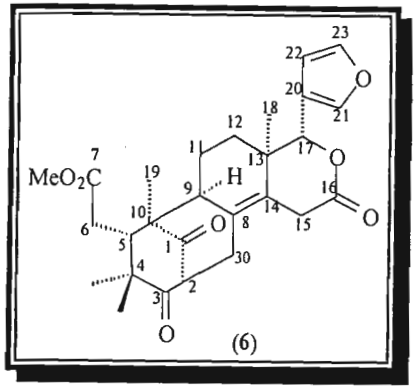

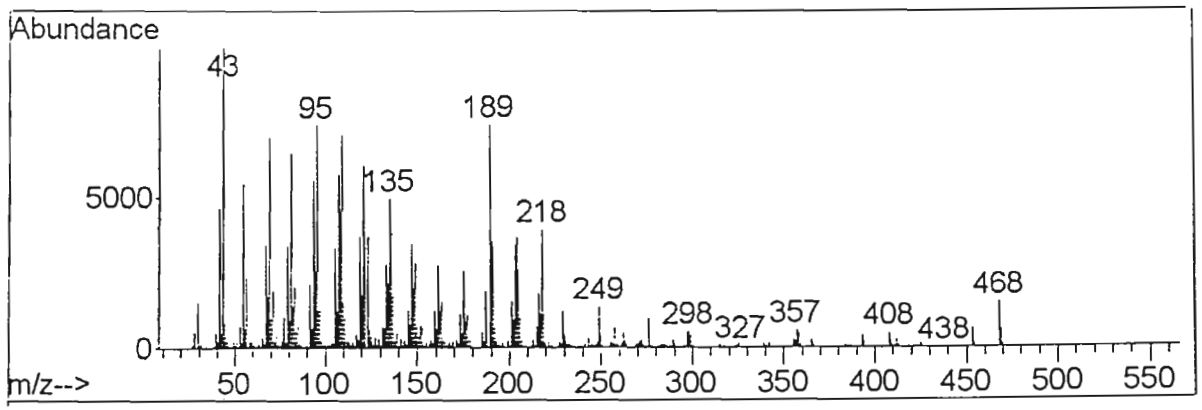

Mass spectrum of mexicanolide (6)

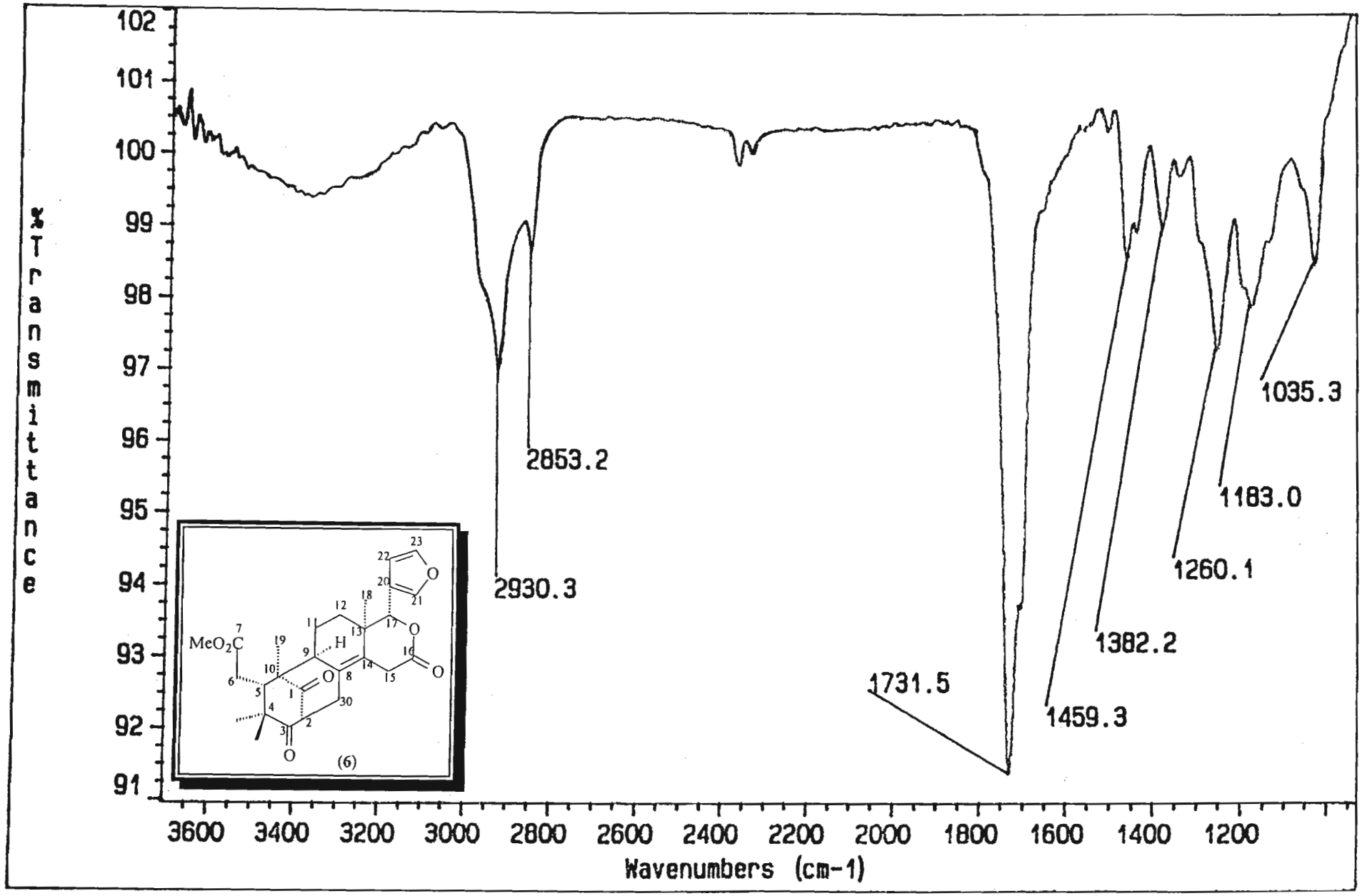

IR spectrum of mexicanolide (6)

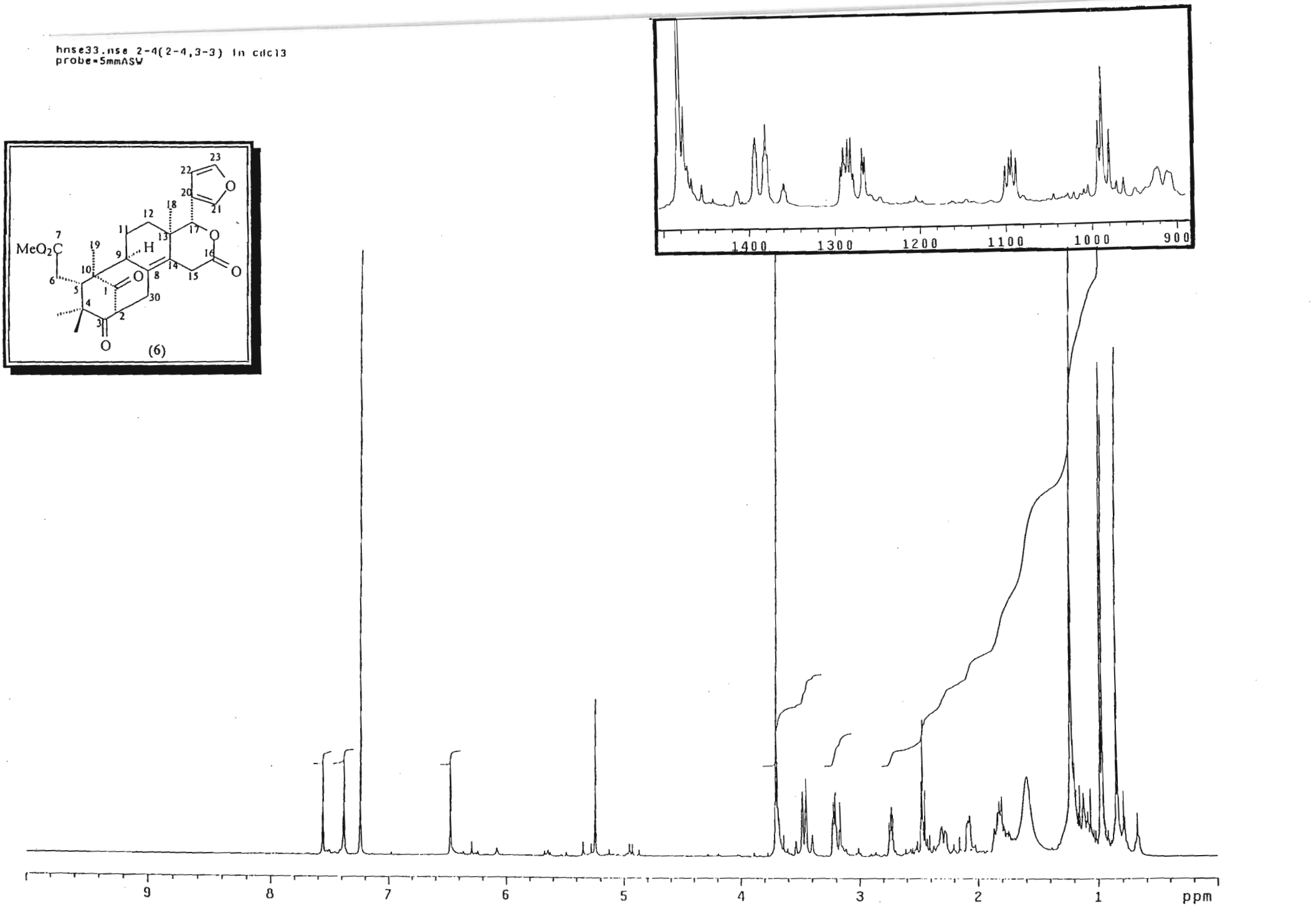

^{1}H NMR spectrum of mexicanolide (6)

cnse33.nse 2-4(2-4,3-3) in cdcl3
probe=5mmASW

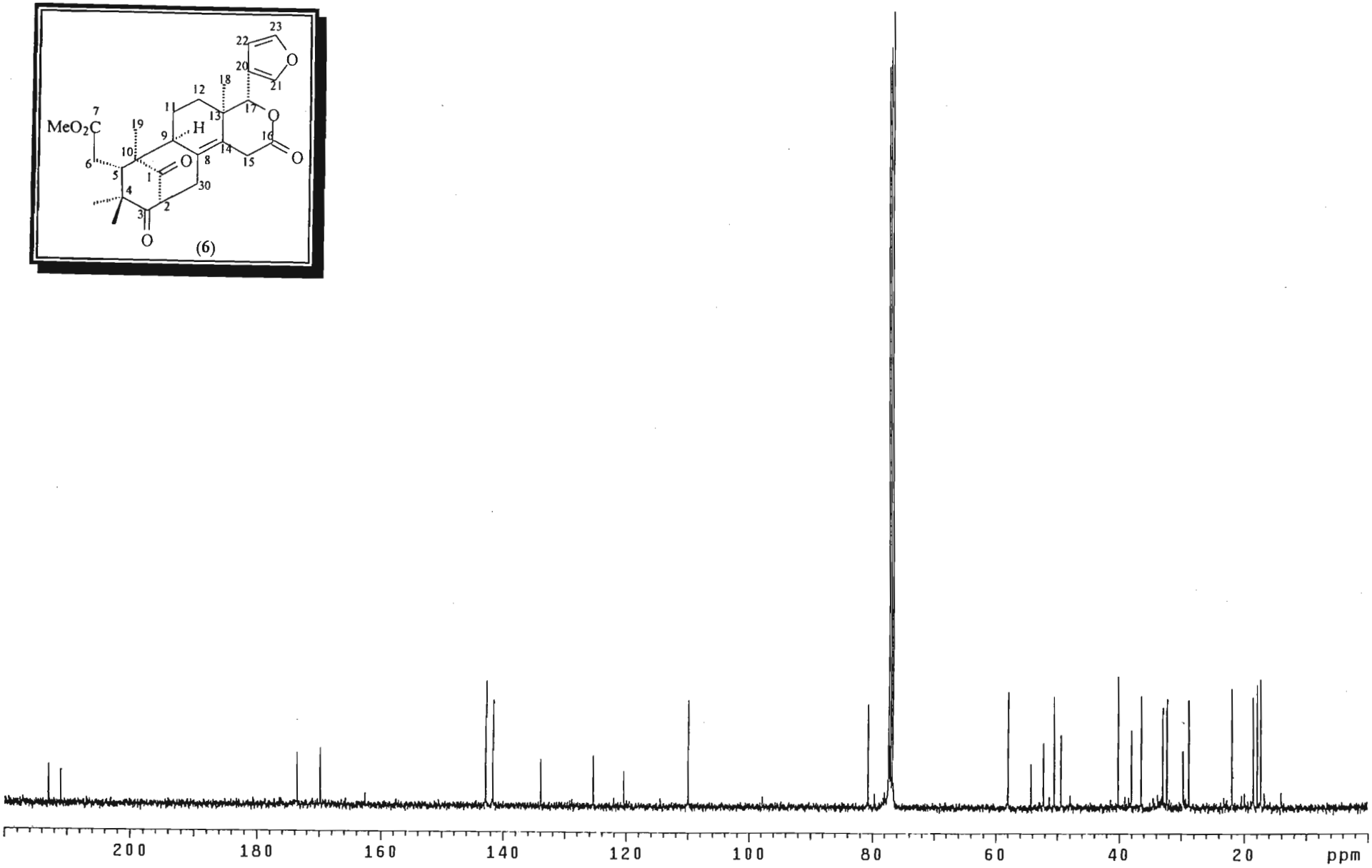

^{13}C NMR spectrum of mexicanolide (6)

dnse33.nse 2-4(2-4,3-3) in cdcl3
probe=5mmASW

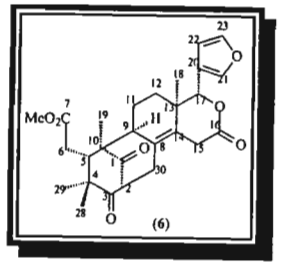

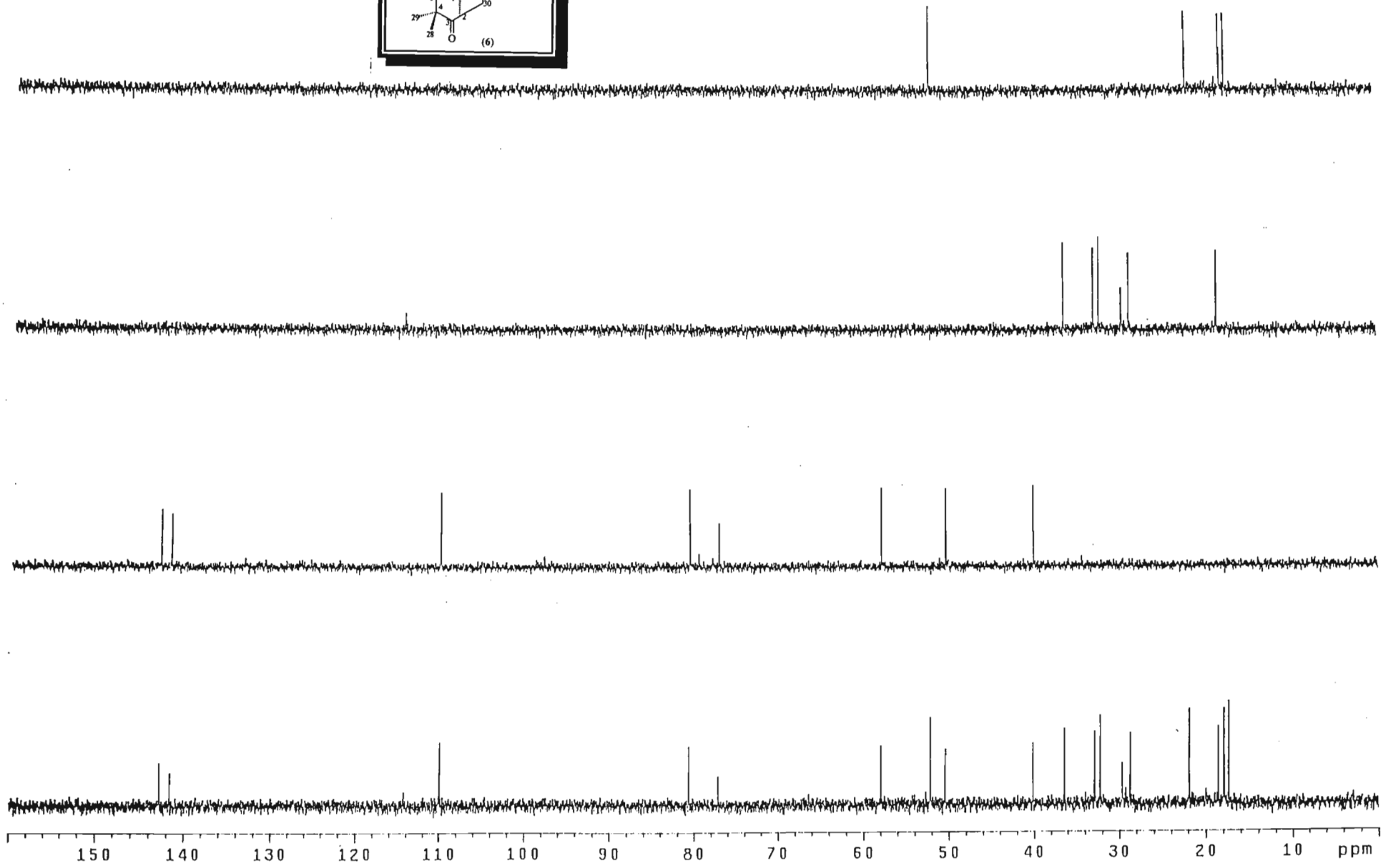

ADEPT NMR spectrum of mexicanolide (6)

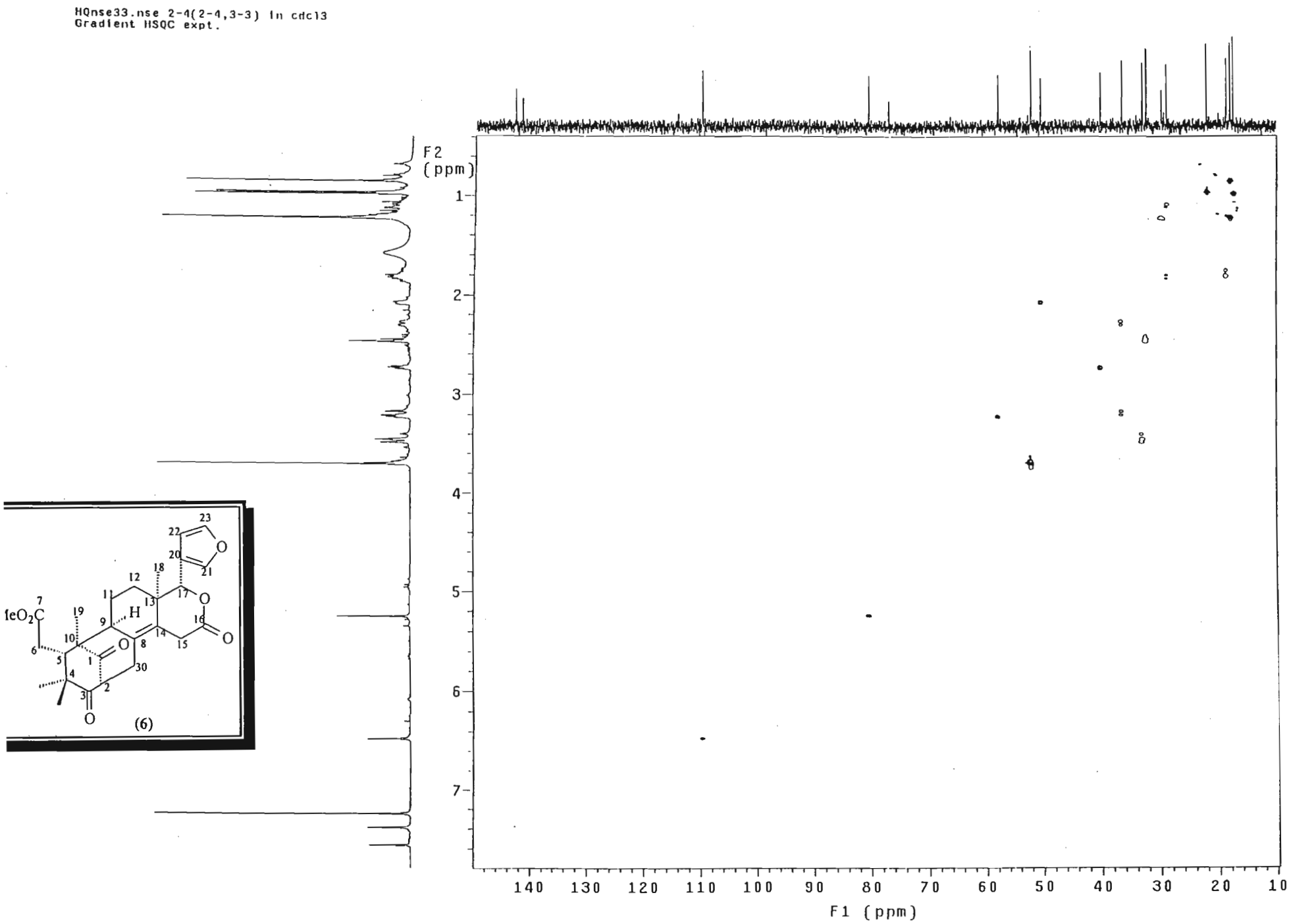

HSQC NMR spectrum of mexicanolide (6)

HQnse33.nse 2-4(2-4,3-3) In cdcl3
Gradient HSQC expt.

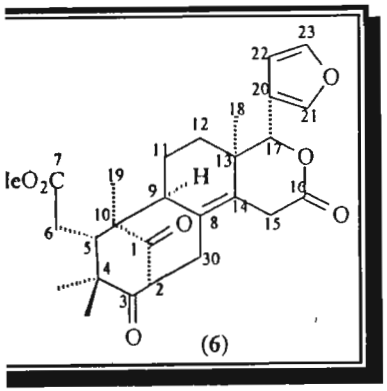

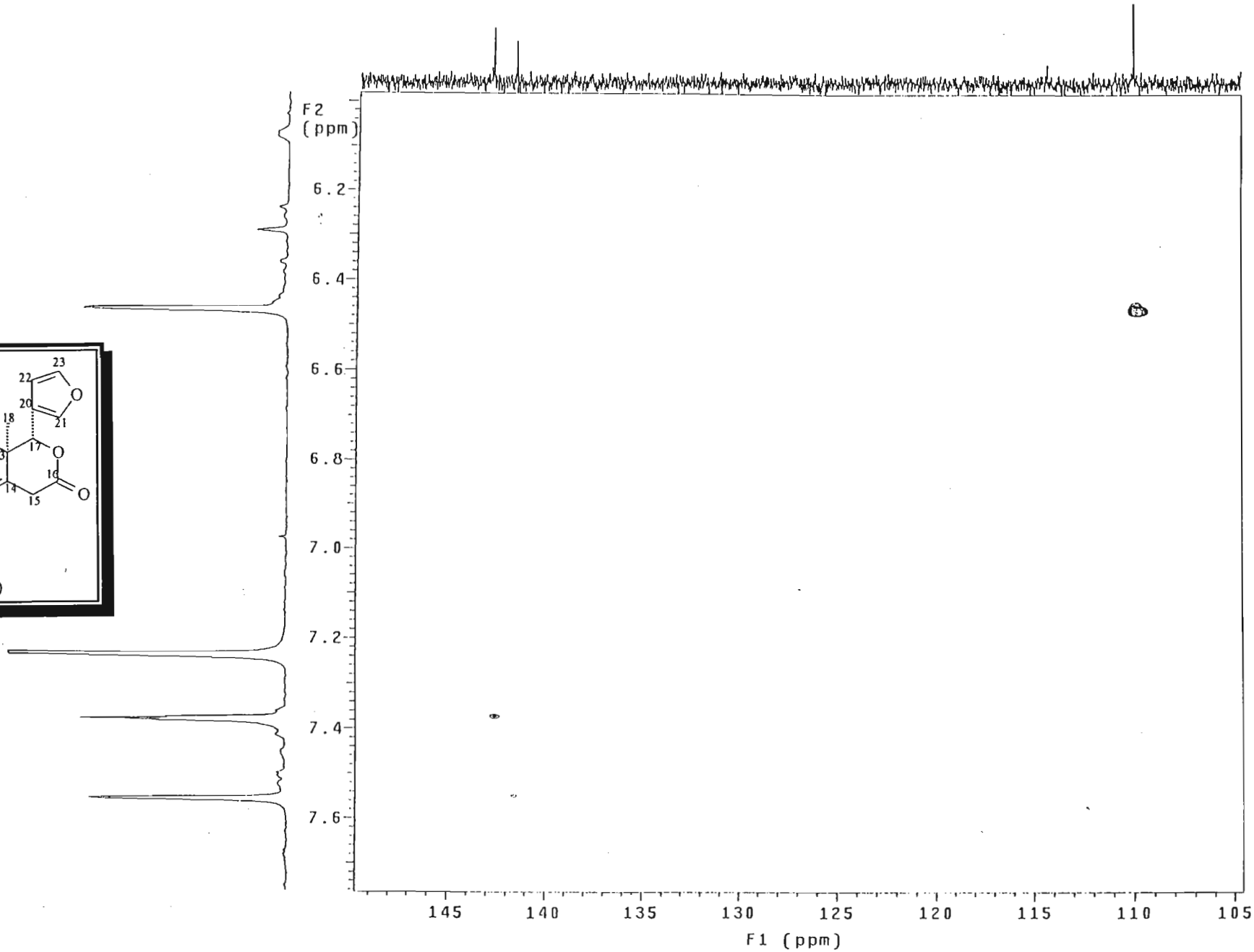

HSQC NMR spectrum of mexicanolide (6)

HQnse33.nse 2-4(2-4,3-3) In cdcl3
Gradient HSQC expt.

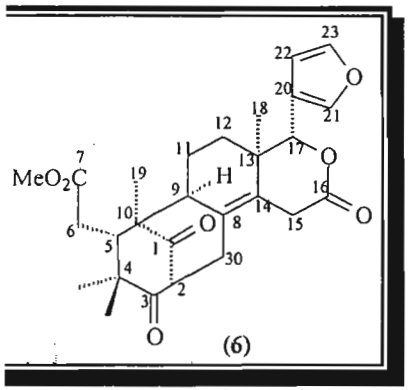

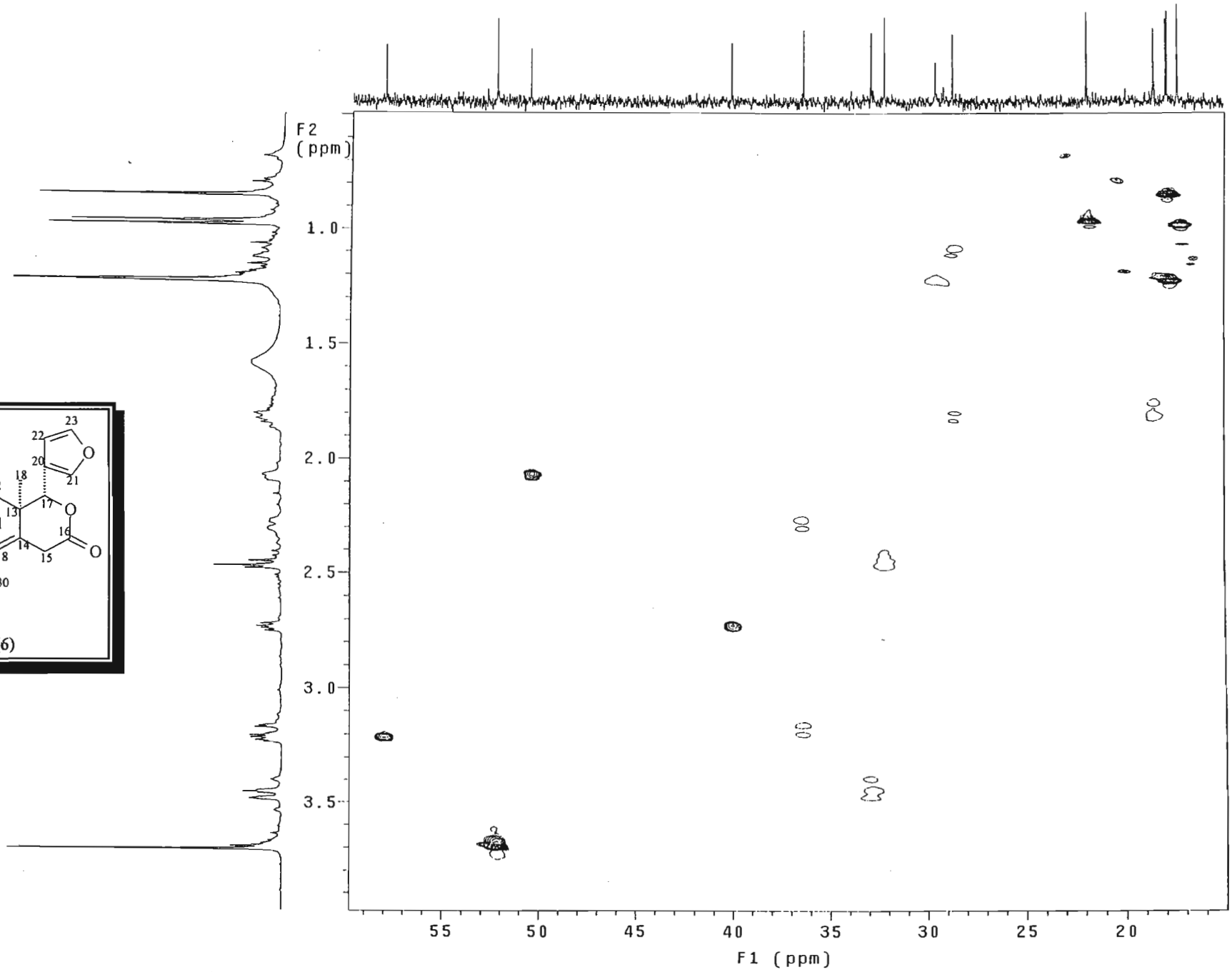

HSQC NMR spectrum of mexicanolide (6)

HBnse33.nse 2-4(2-4,3-3) in cdcl3
Gradient HMBC expt.

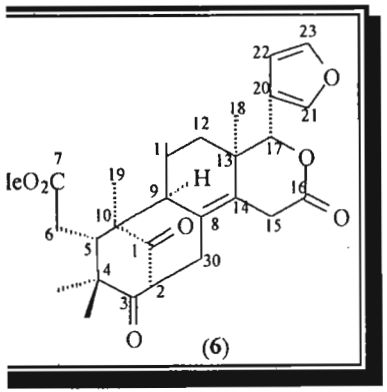

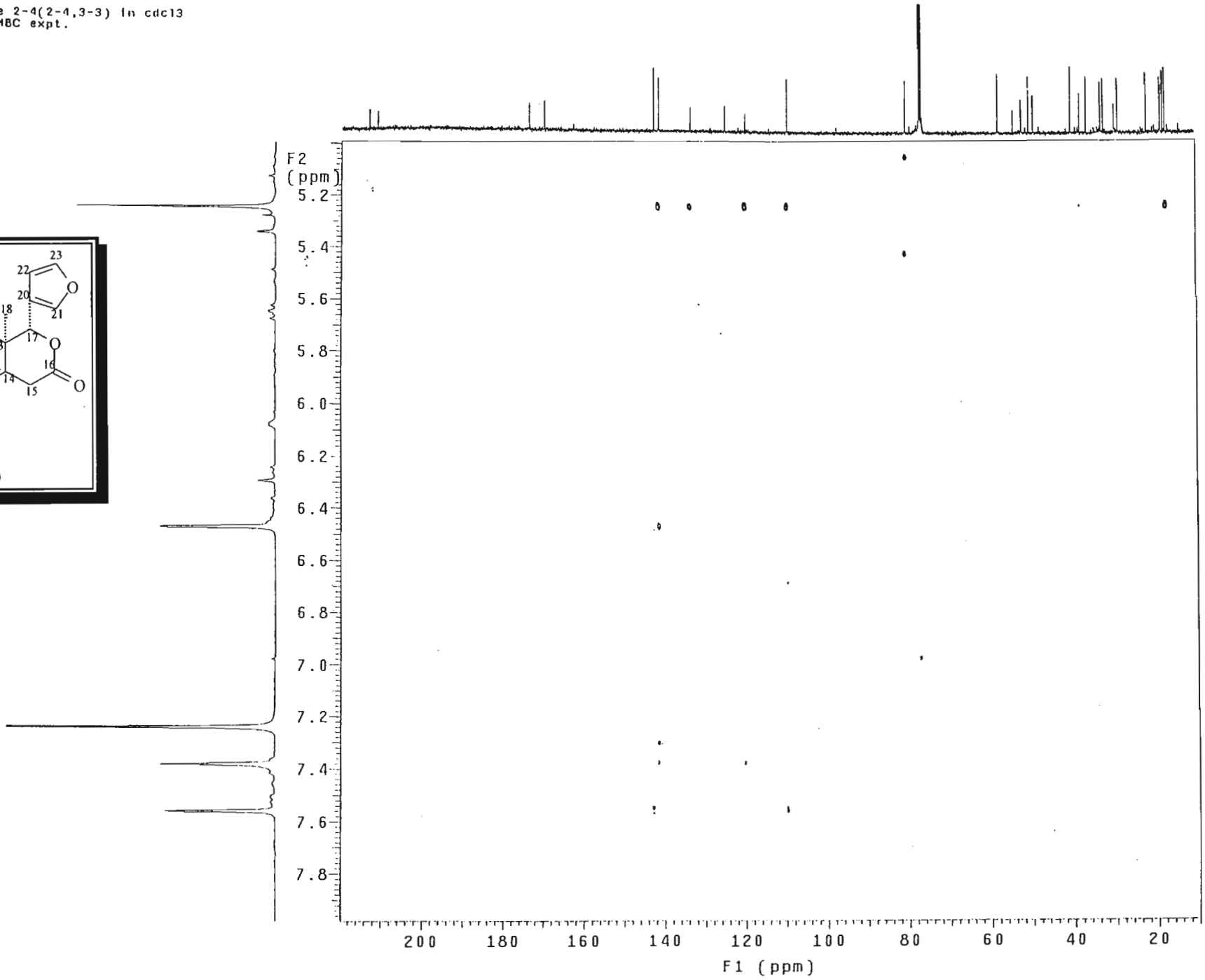

HMBC NMR spectrum of mexicanolide (6)

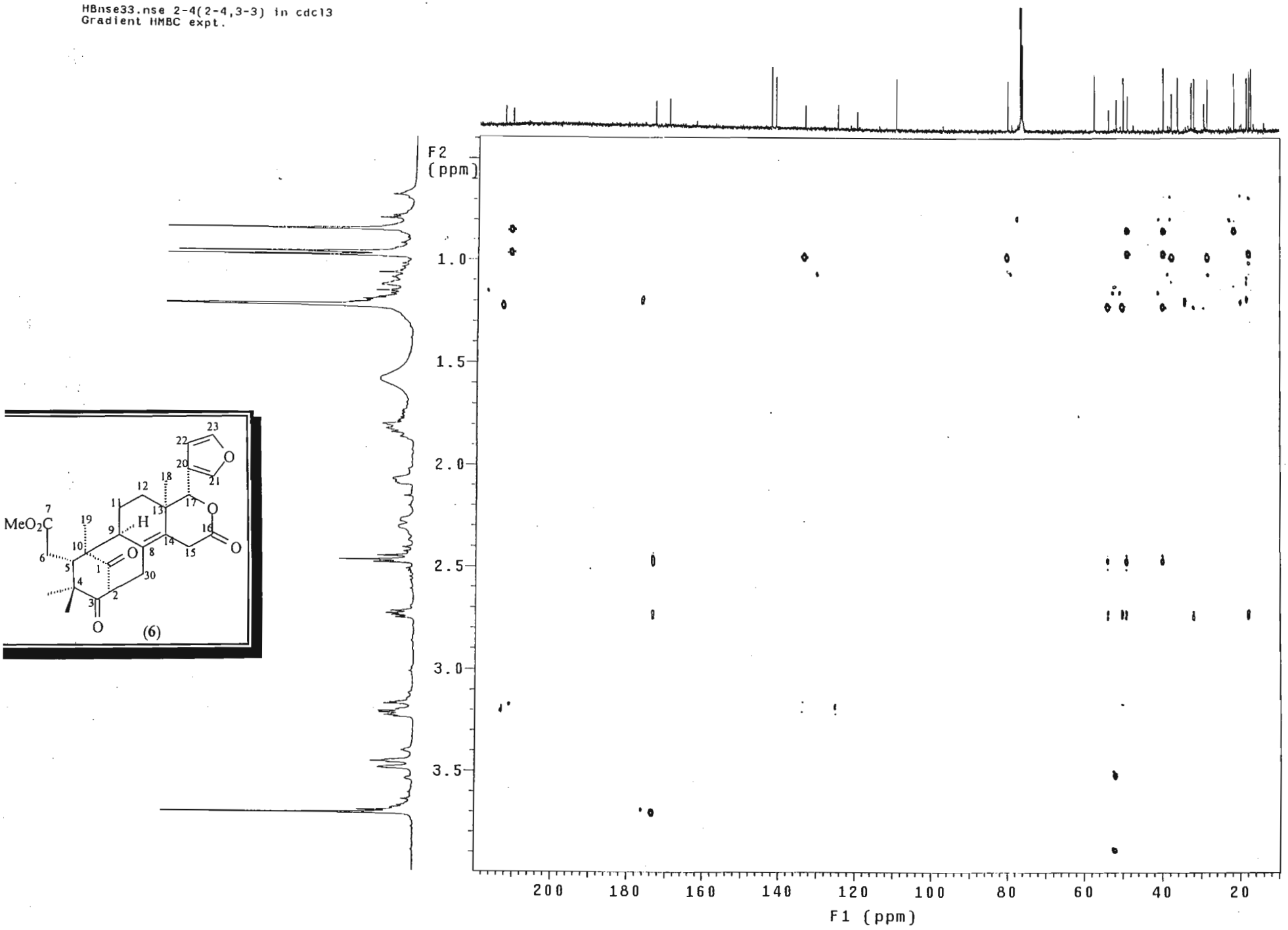

HMBC NMR spectrum of mexicanolide (6)

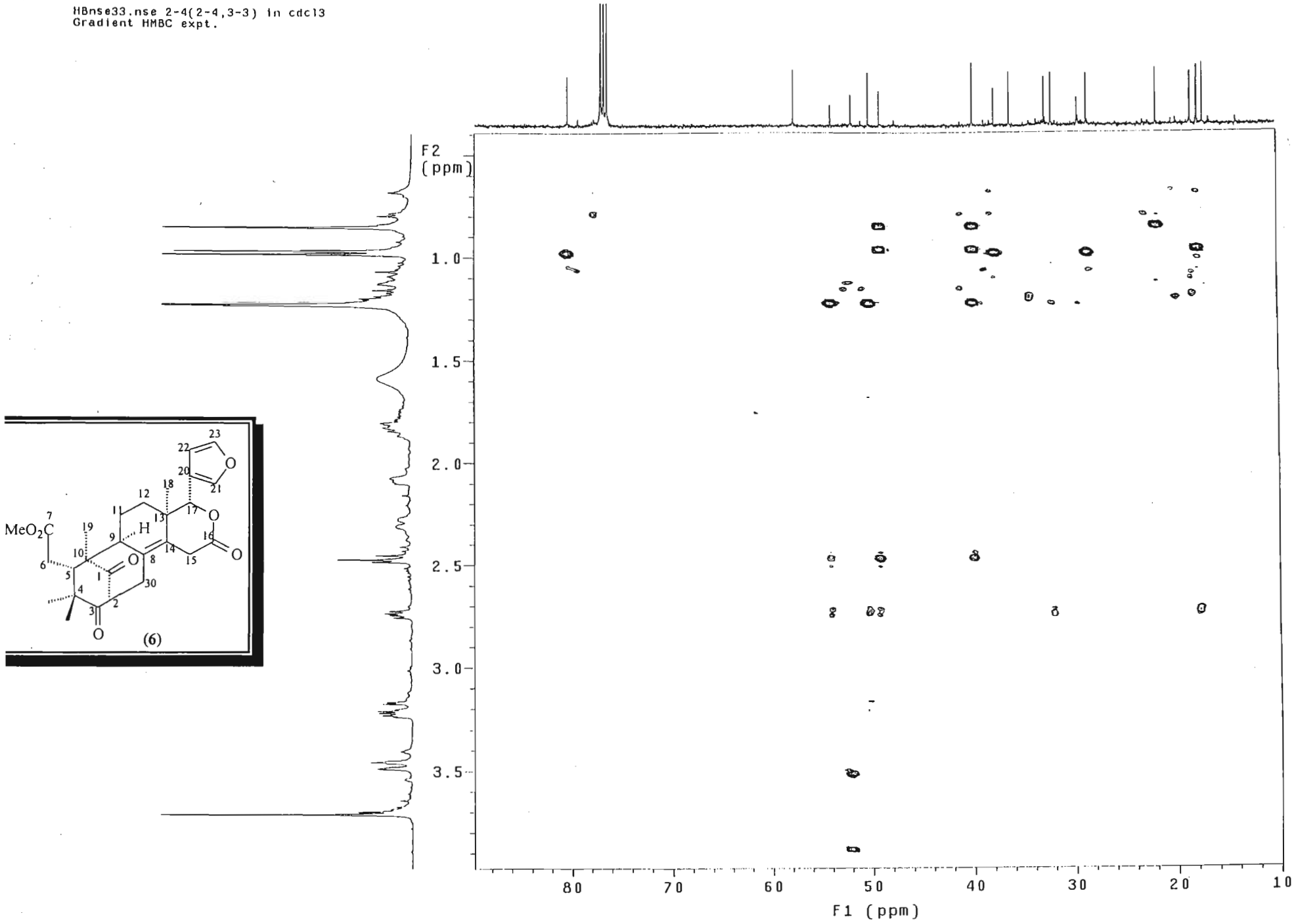

HMBC NMR spectrum of mexicanolide (6)

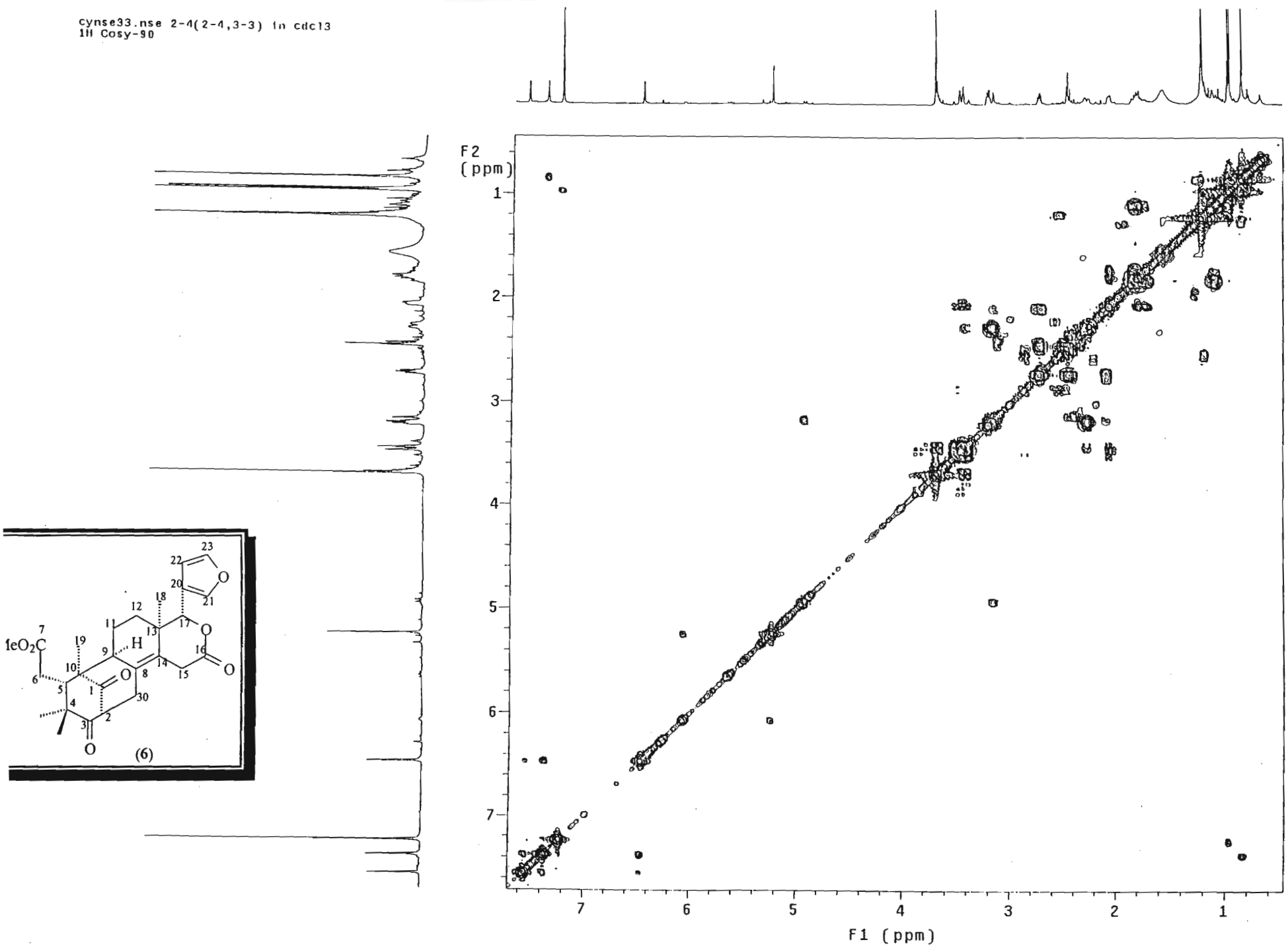

COSY NMR spectrum of mexicanolide (6)

NOnse33.nse 2-4(2-4,3-3) in cdcl3
Gradient NOESY expt.

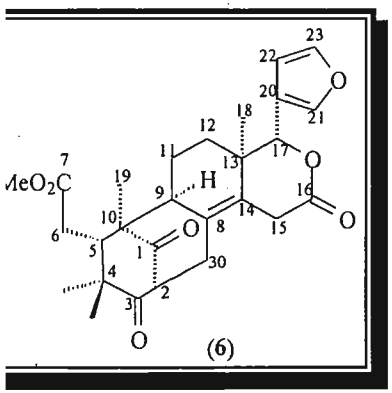

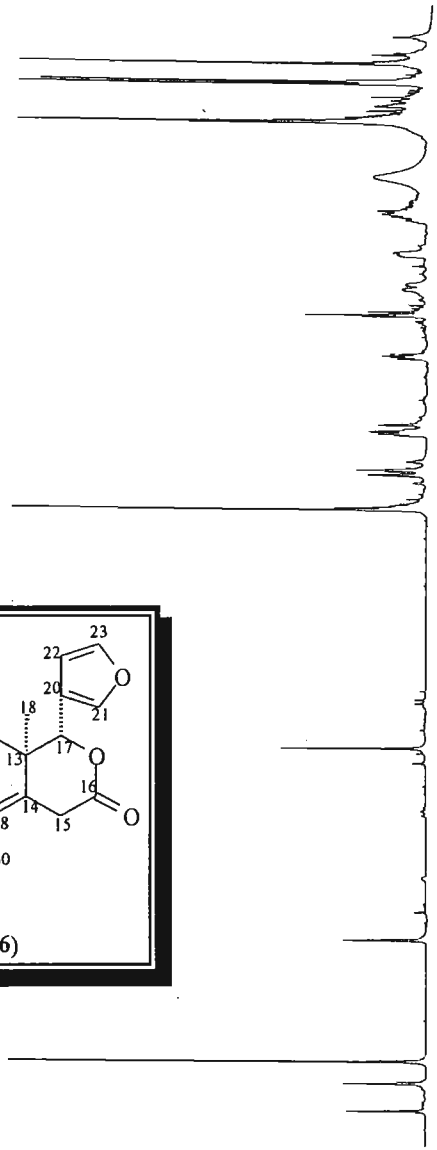

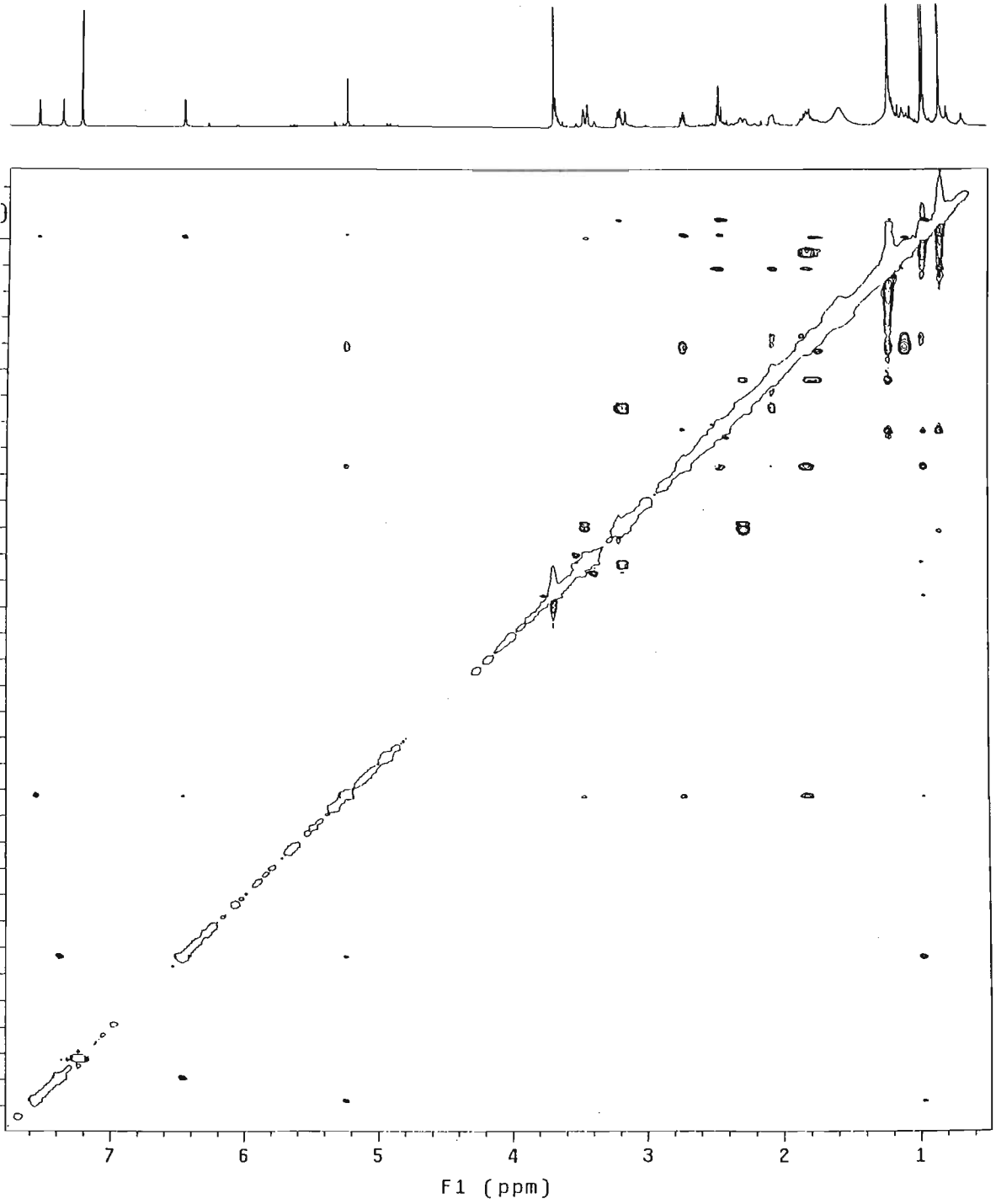

NOESY NMR spectrum of mexicanolide (6)

Khayasin (7)

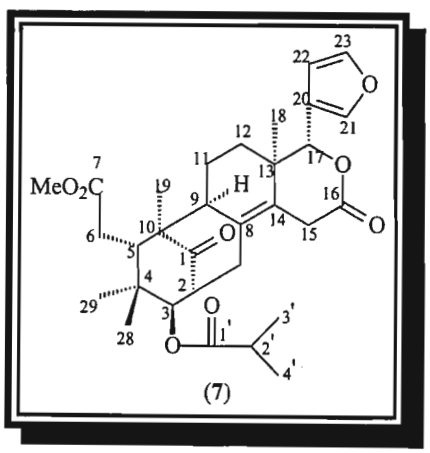

Khayasin (7)

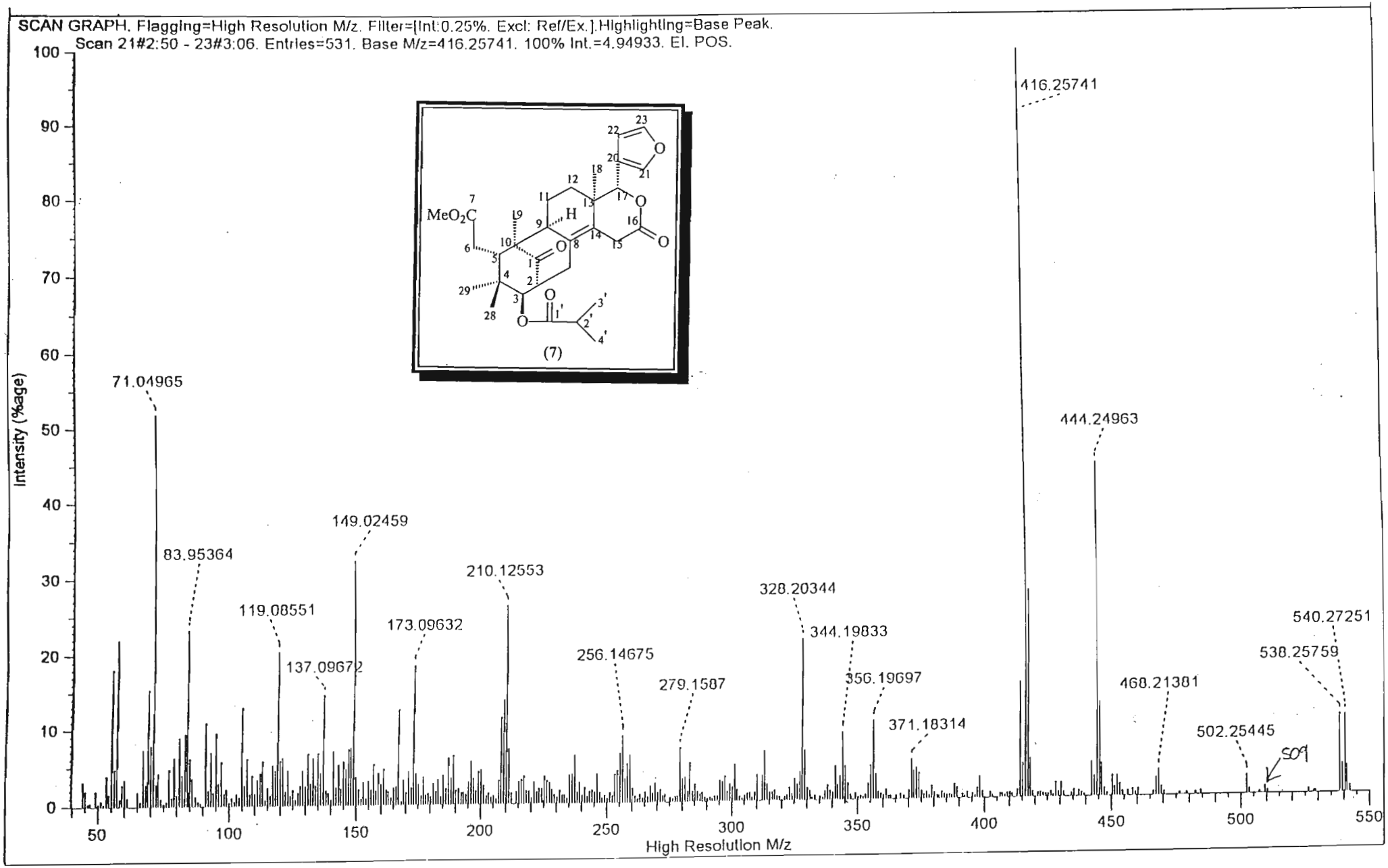

Mass spectrum of khayasin (7)

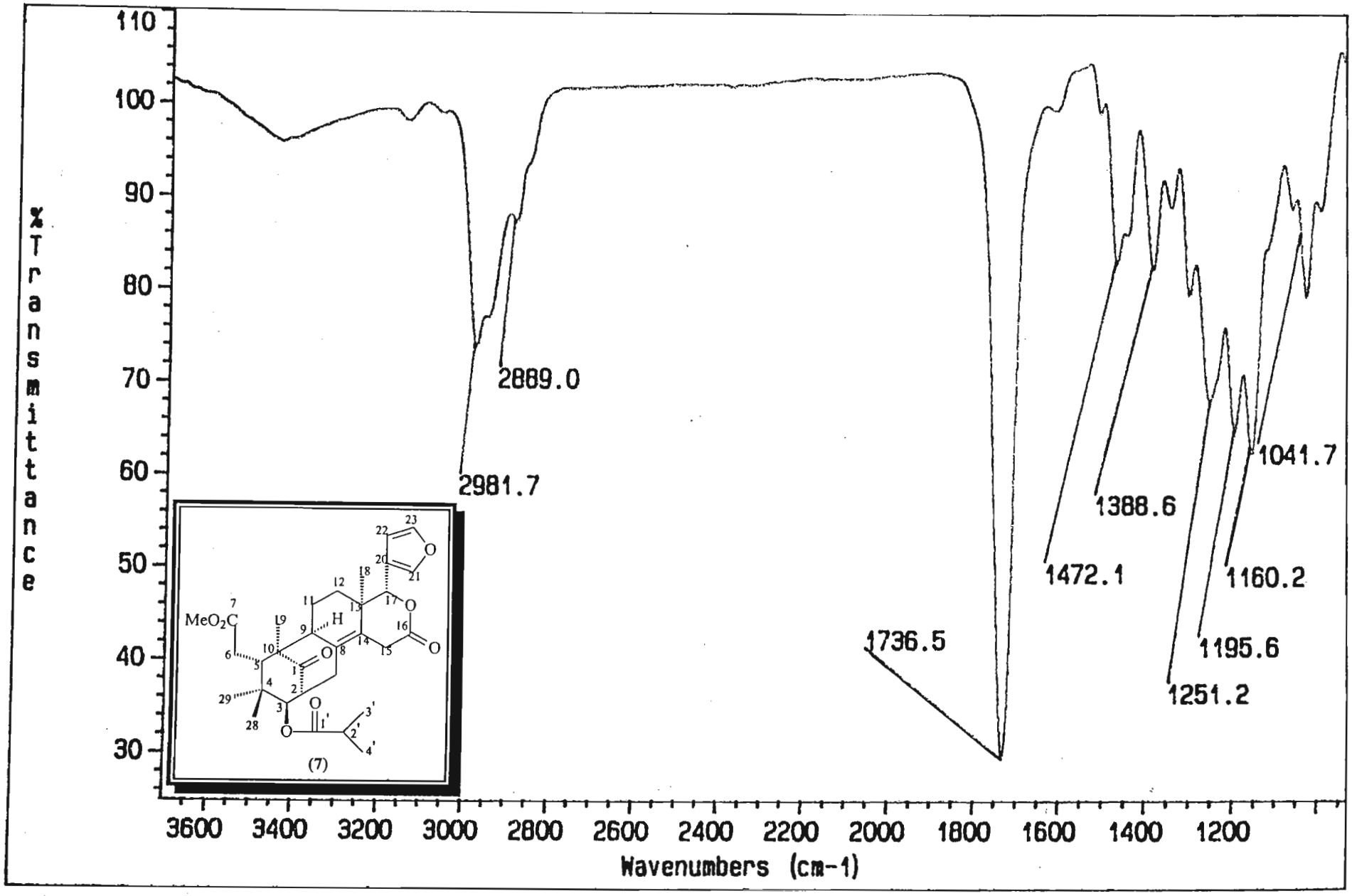

IR spectrum of khayasin (7)

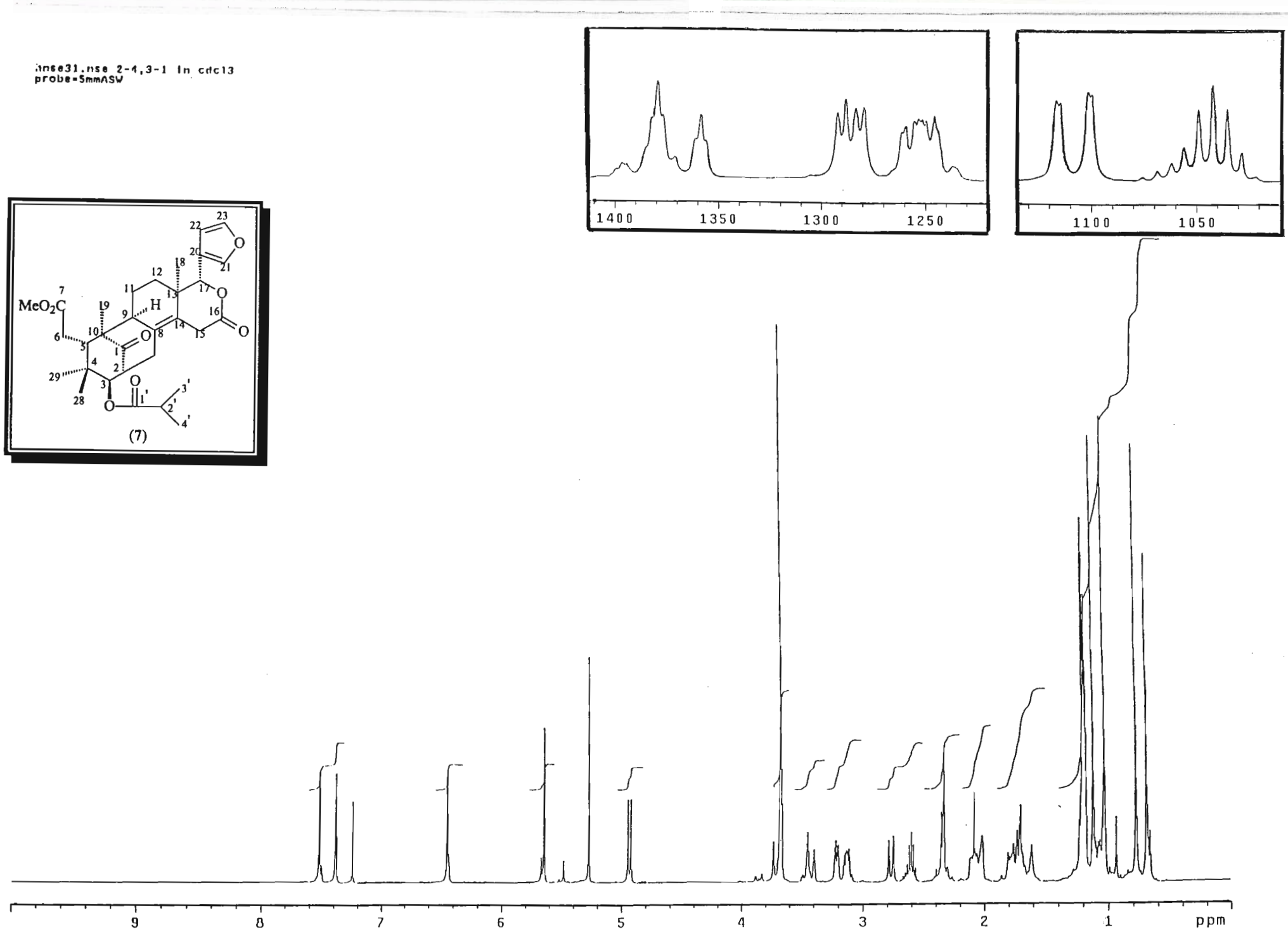

^{1}H NMR spectrum of khayasin (7)

cnse31.nse 2-4,3-1 in cdcl3
probe=5mmASW

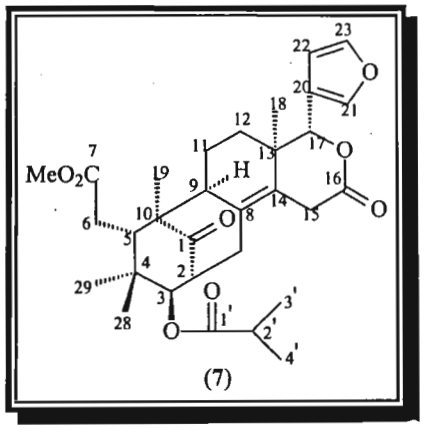

(7)

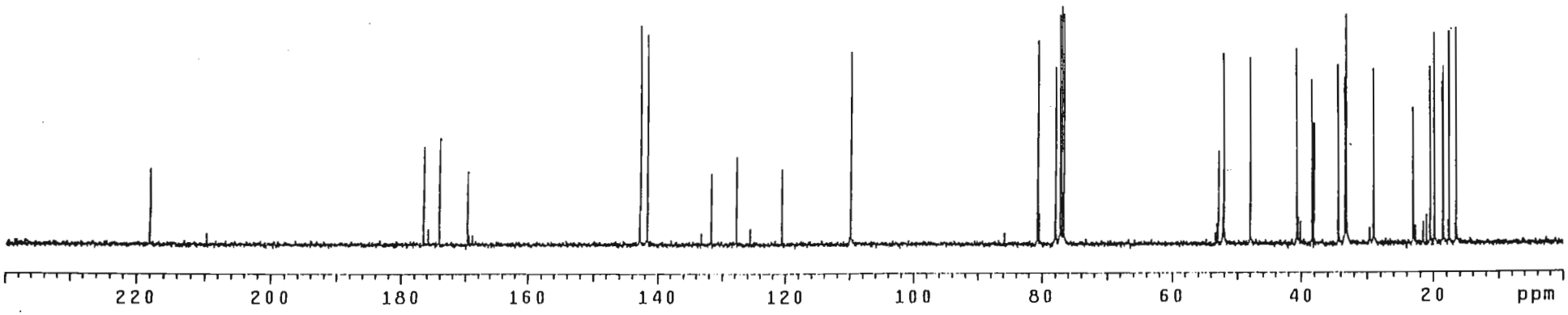

^{13}C NMR spectrum of khayasin (7)

dnse31.nse 2-4,3-1 in cdcl3
probe=5mmASW

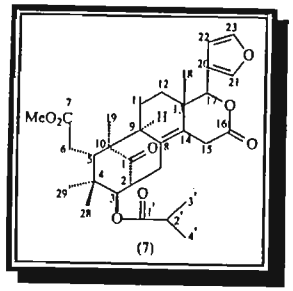

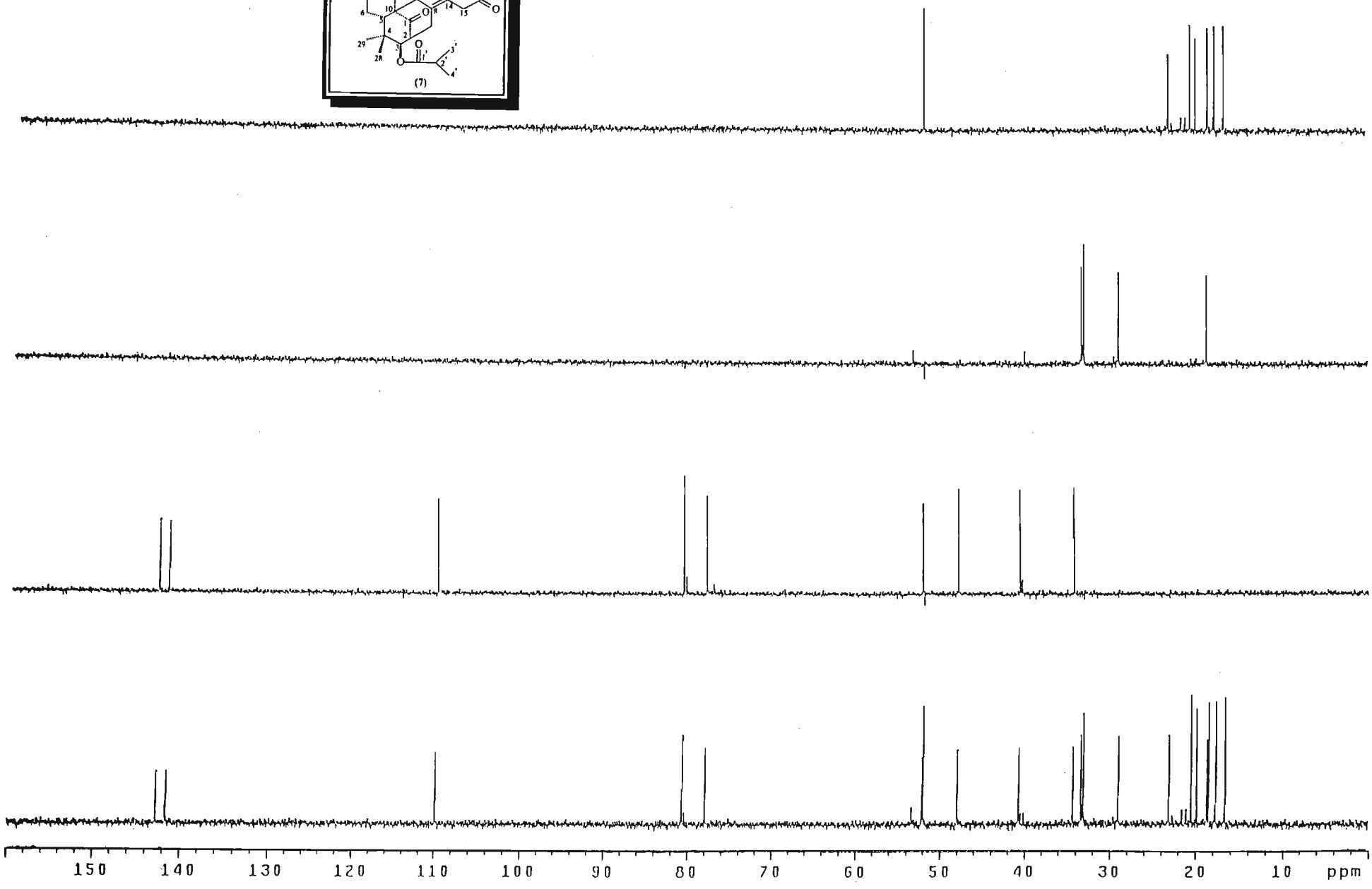

ADEPT NMR spectrum of khayasin (7)

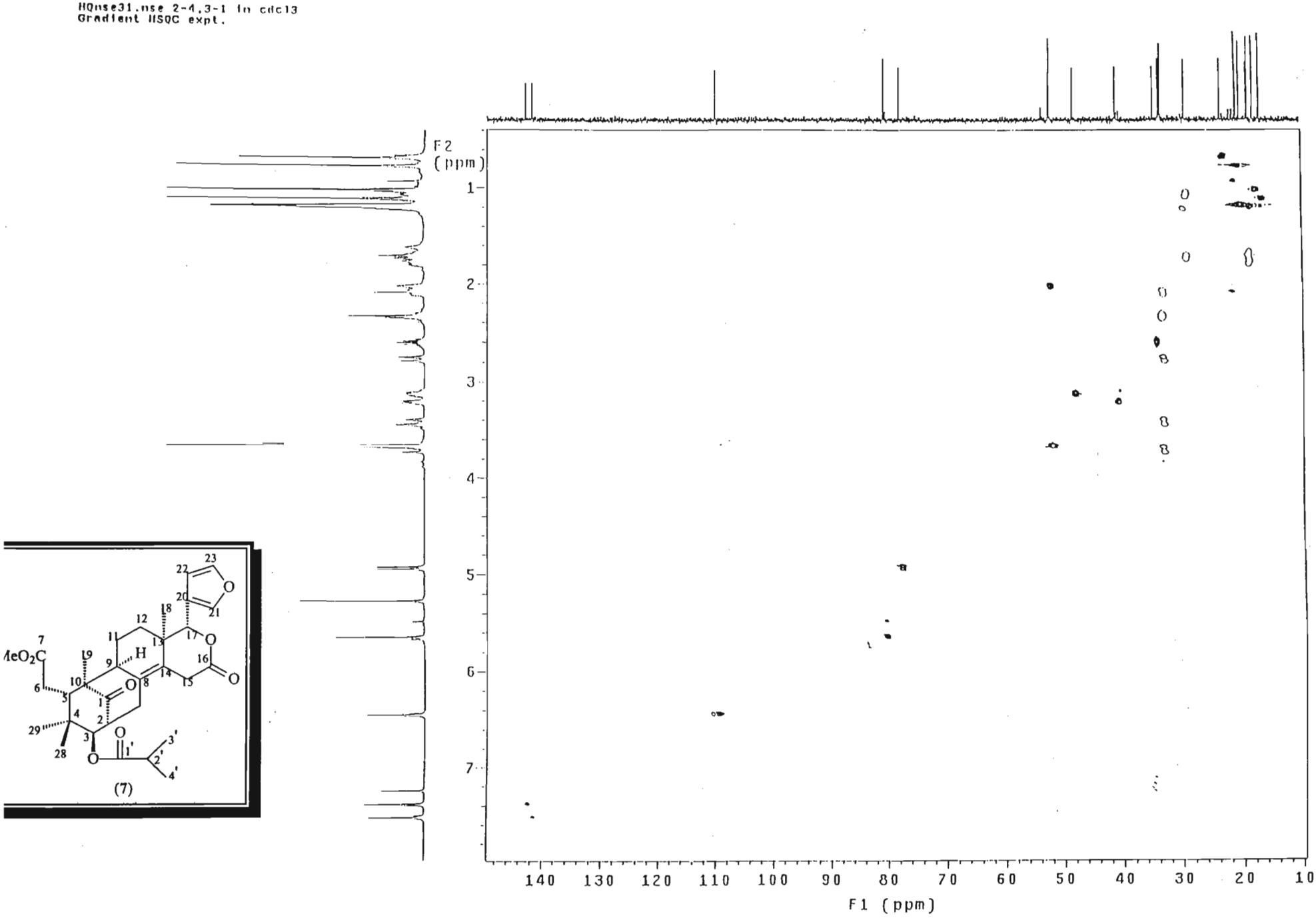

HSQC NMR spectrum of khayasin (7)

HQnse31.nse 2-4,3-1 in cdcl3
Gradient HSQC expt.

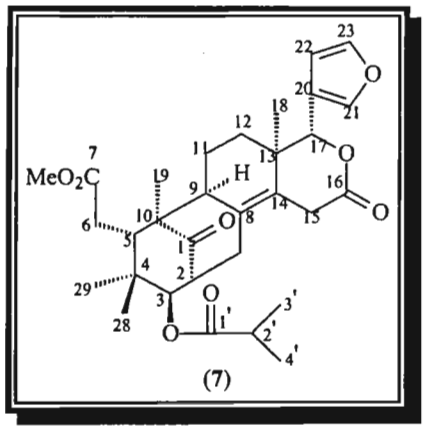

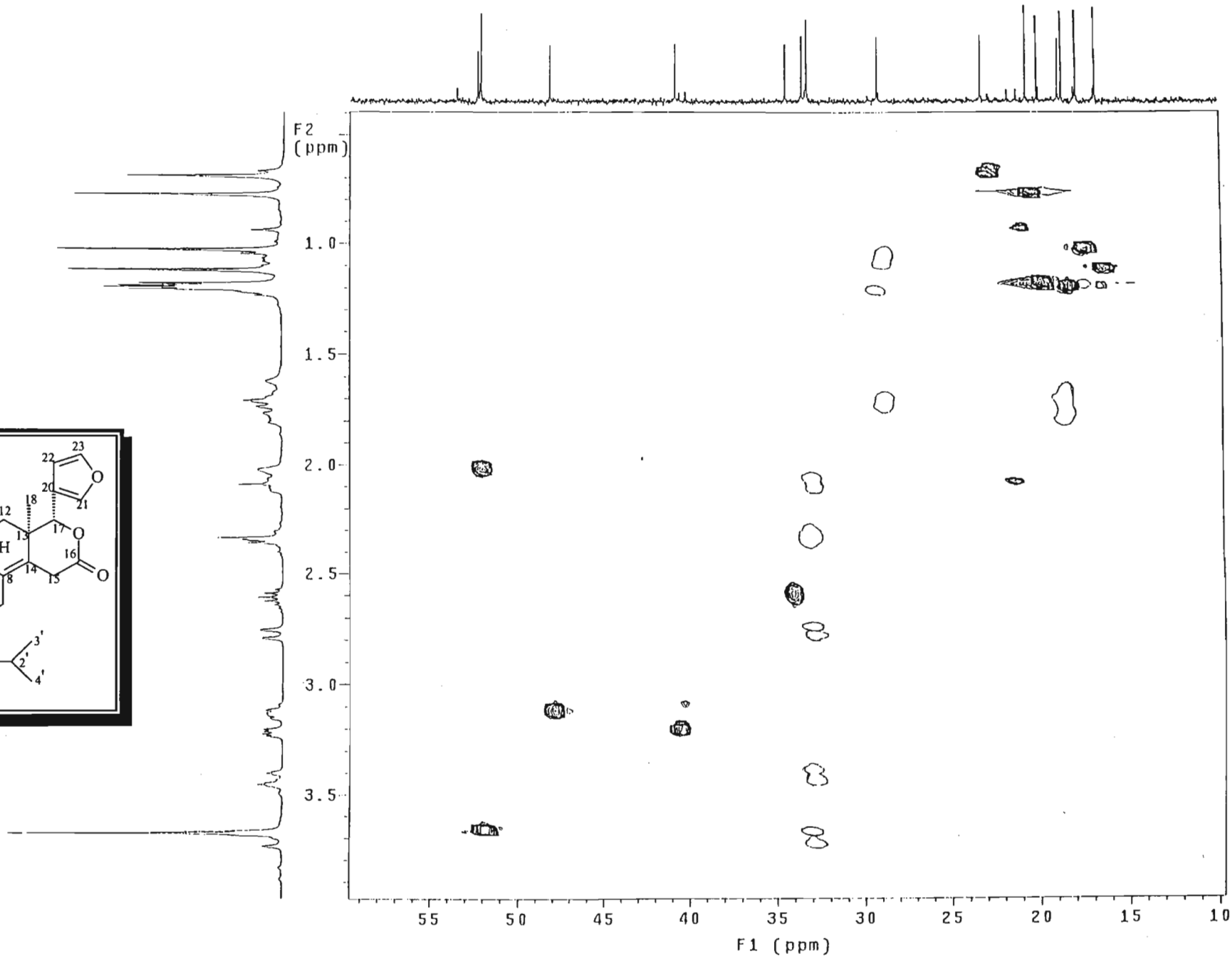

HSQC NMR spectrum of khayasin (7)

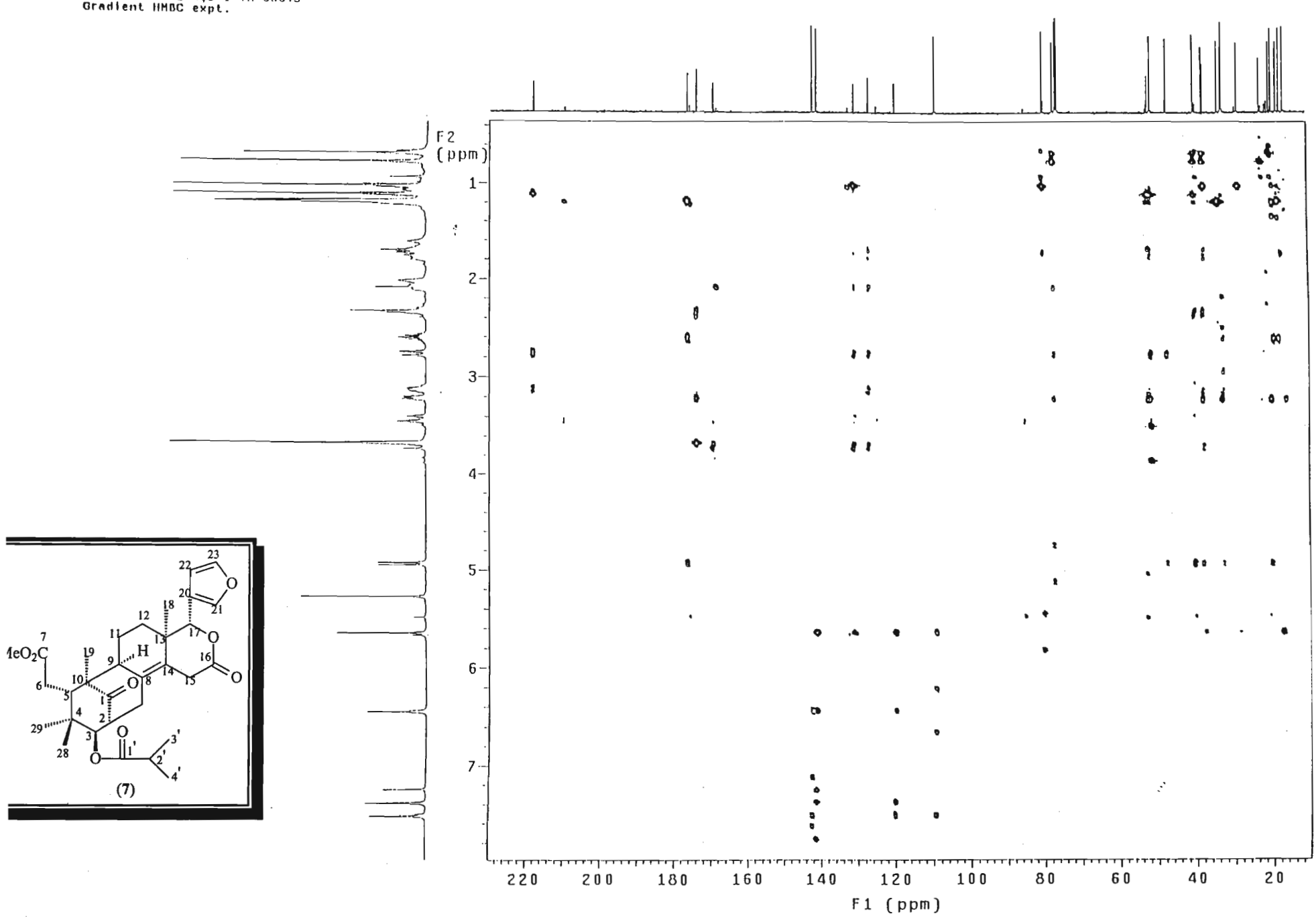

HMBC NMR spectrum of khayasin (7)

HMBC NMR spectrum of khayasin (7)

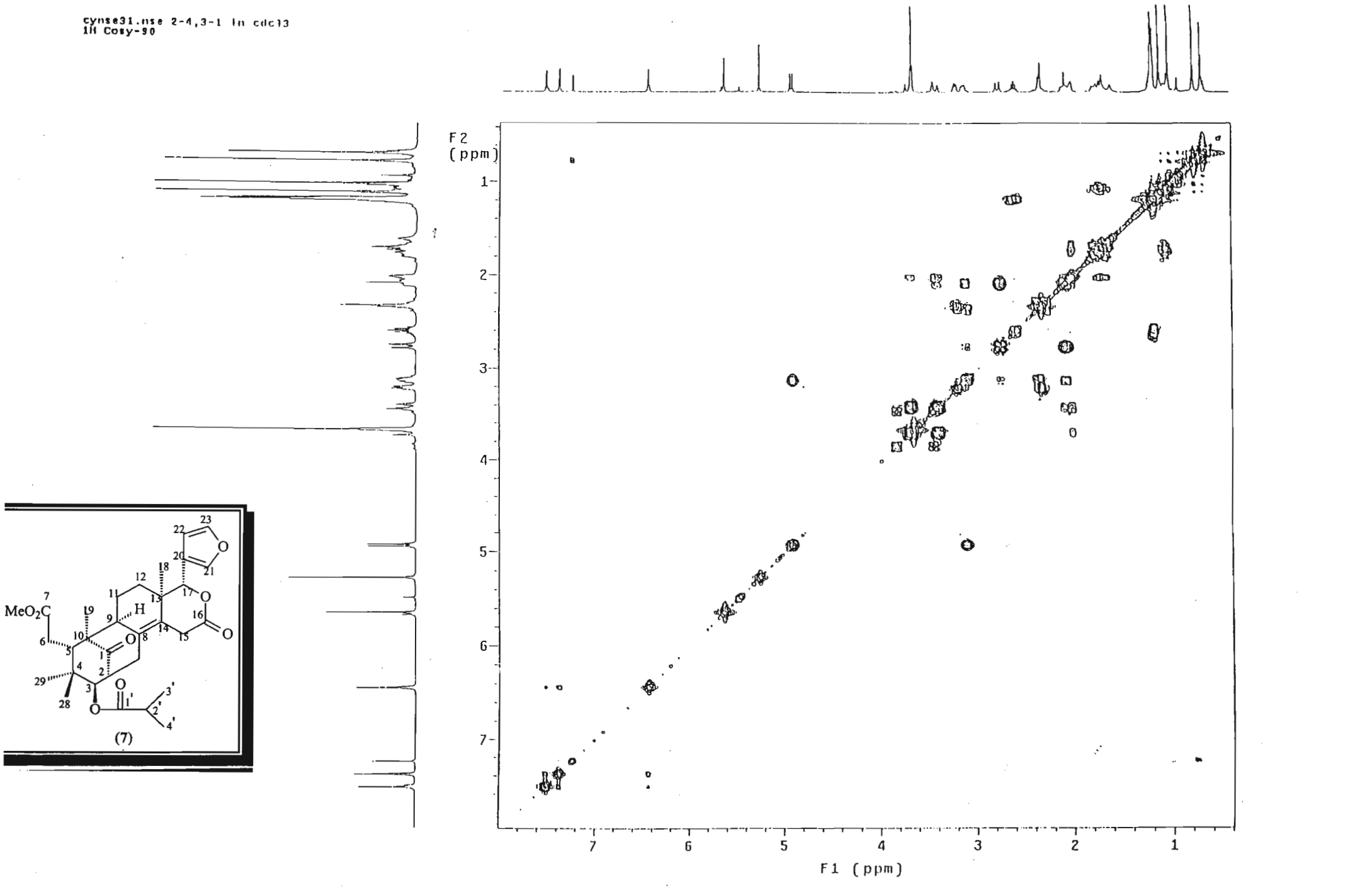

COSY NMR spectrum of khayasin (7)

NOnse31.nse 2-4,3-1 in cdcl3
Gradient NOESY expt.

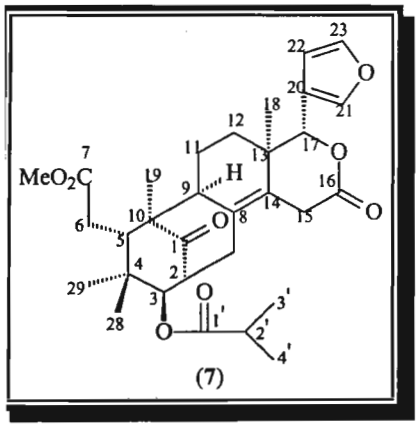

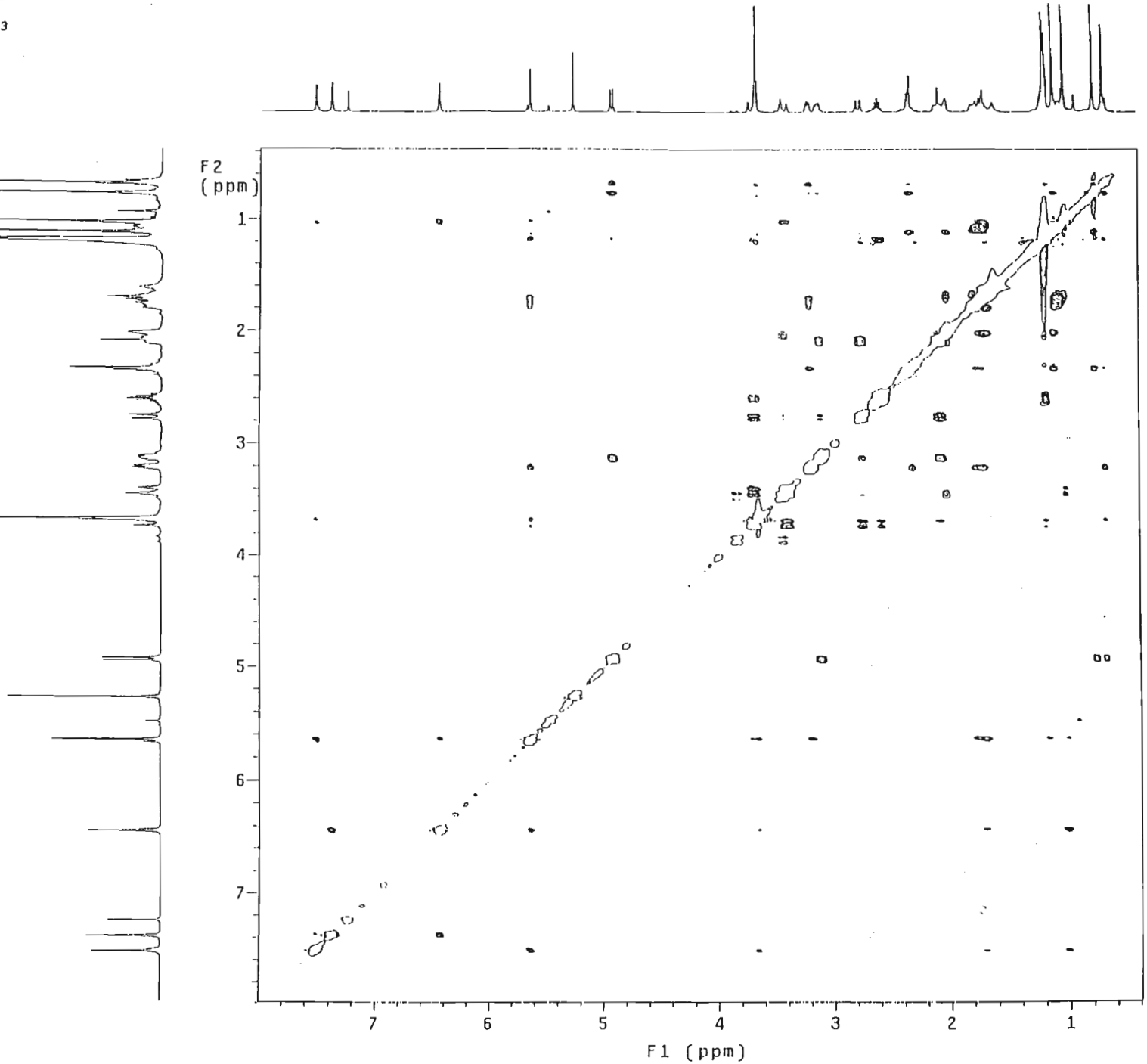

NOESY NMR spectrum of khayasin (7)

Sapelin E acetate (8)

Mass spectrum	**[105]**
IR spectrum	**[106]**
^{1}H NMR	**[107]**
^{13}C NMR	**[108]**
ADEPT	**[109]**
HSQC	**[110-111]**
HMBC	**[112-114]**
COSY	**[115]**
NOESY	**[116]**

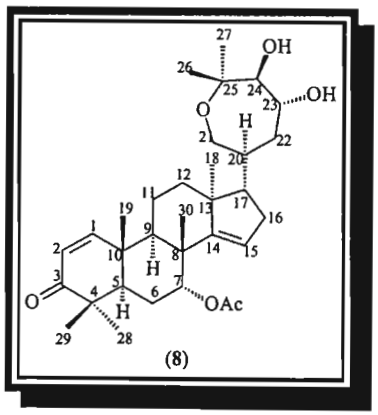

Sapelin E acetate (8)

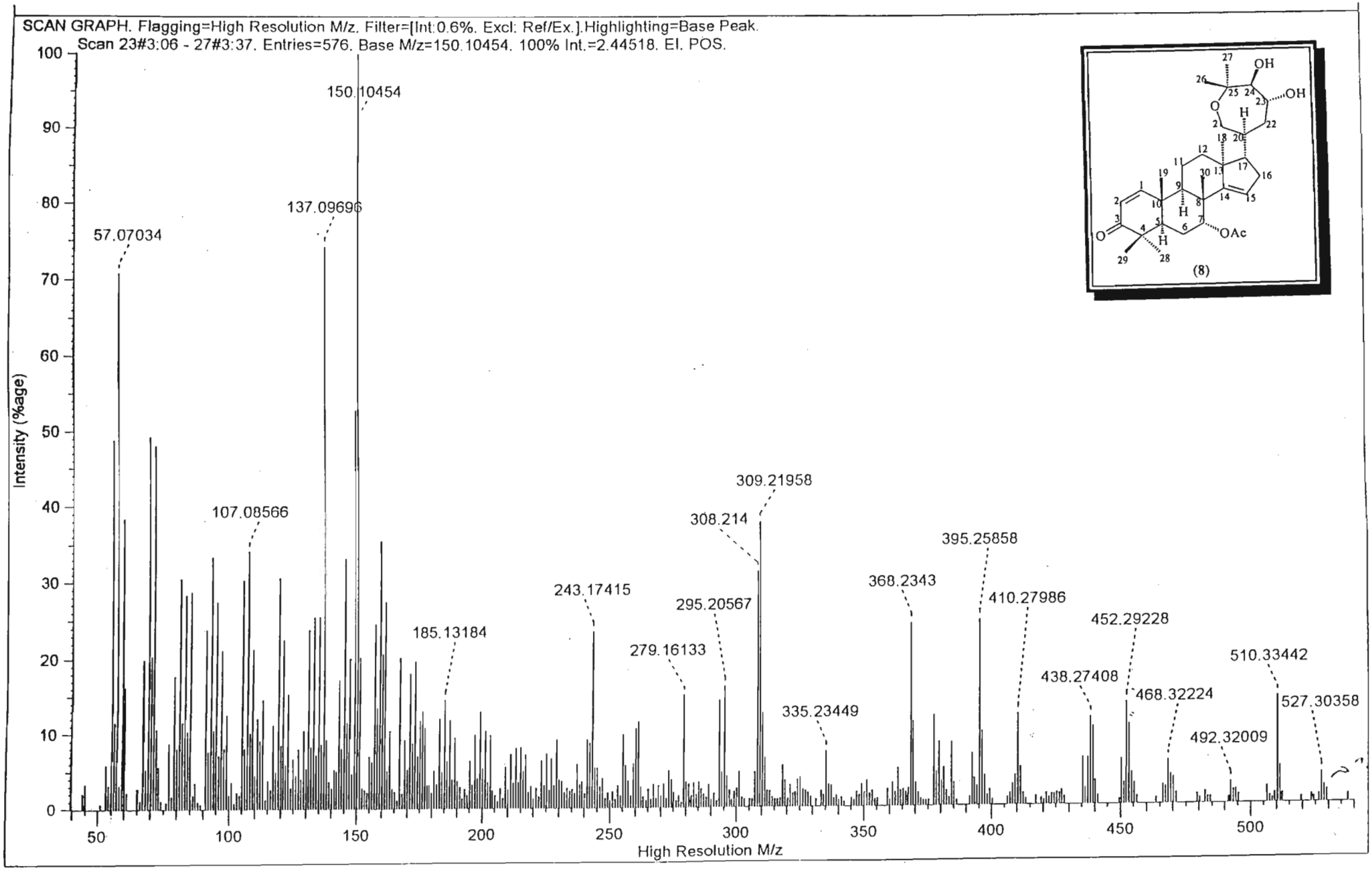

Mass spectrum of sapelin E acetate (8)

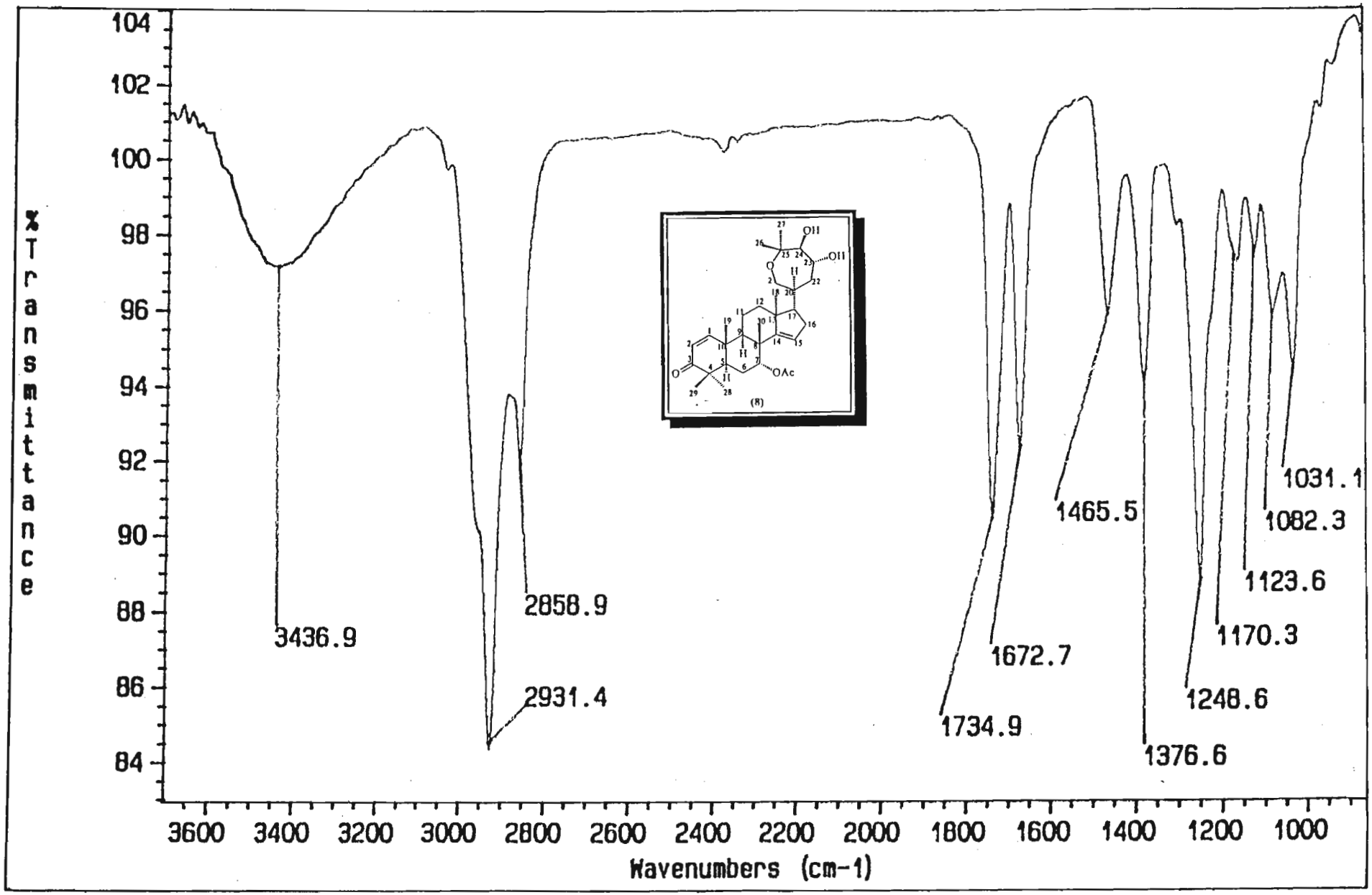

IR spectrum of sapelin E acetate (8)

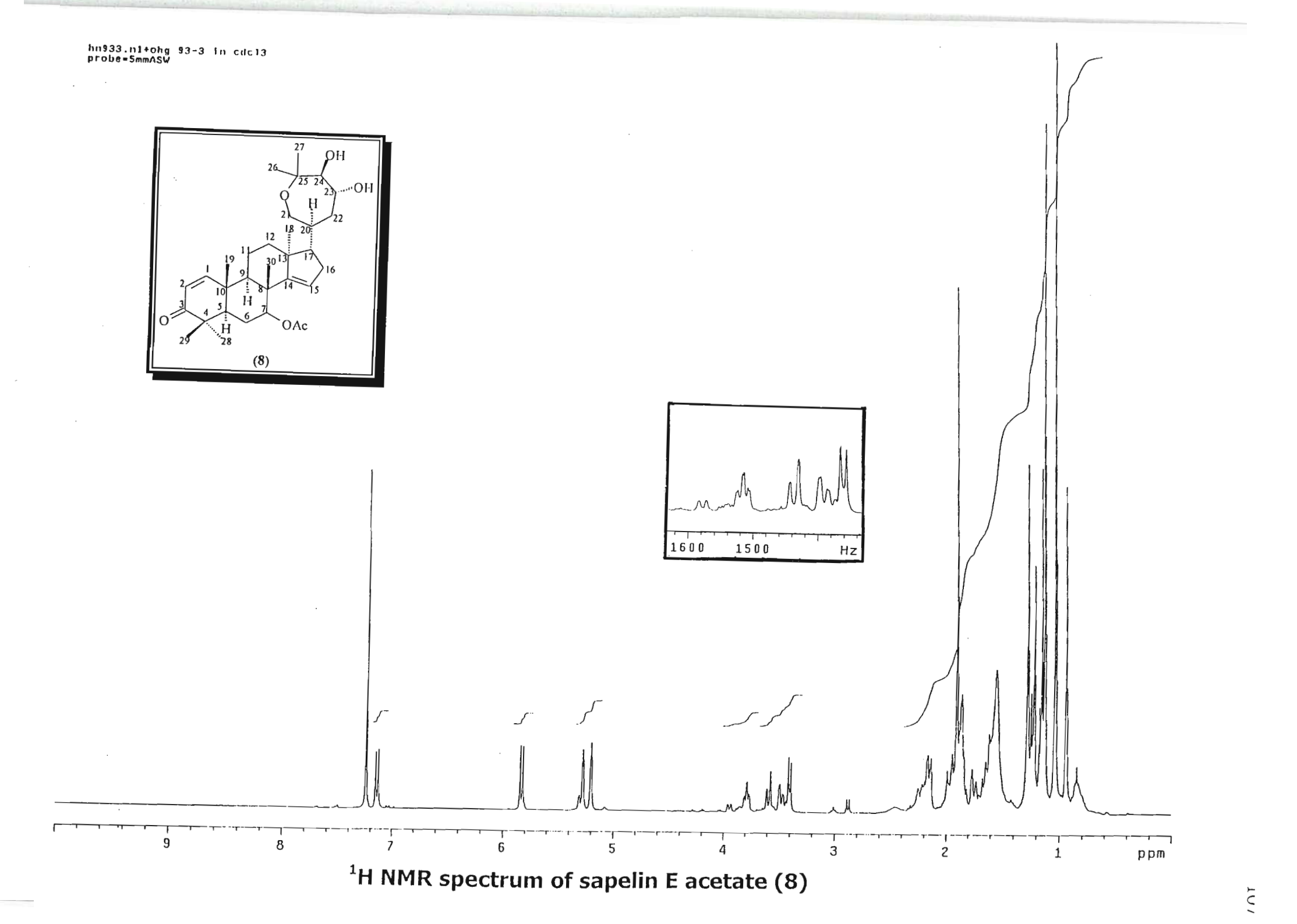

^{1}H NMR spectrum of sapelin E acetate (8)

cn933.n1+ohg 93-3 in cdcl3
probe=5mmASW

(8)

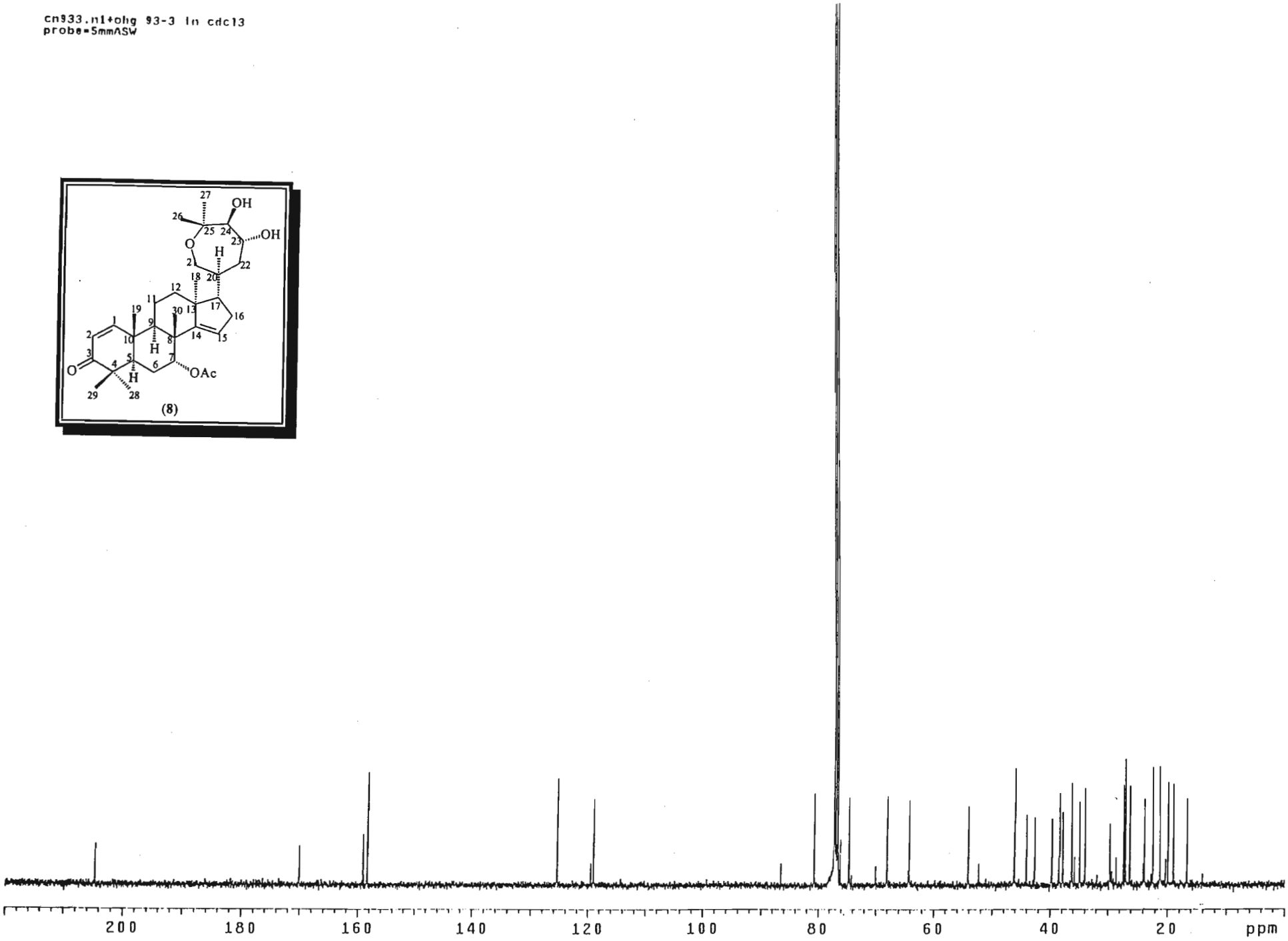

^{13}C NMR spectrum of sapelin E acetate (8)

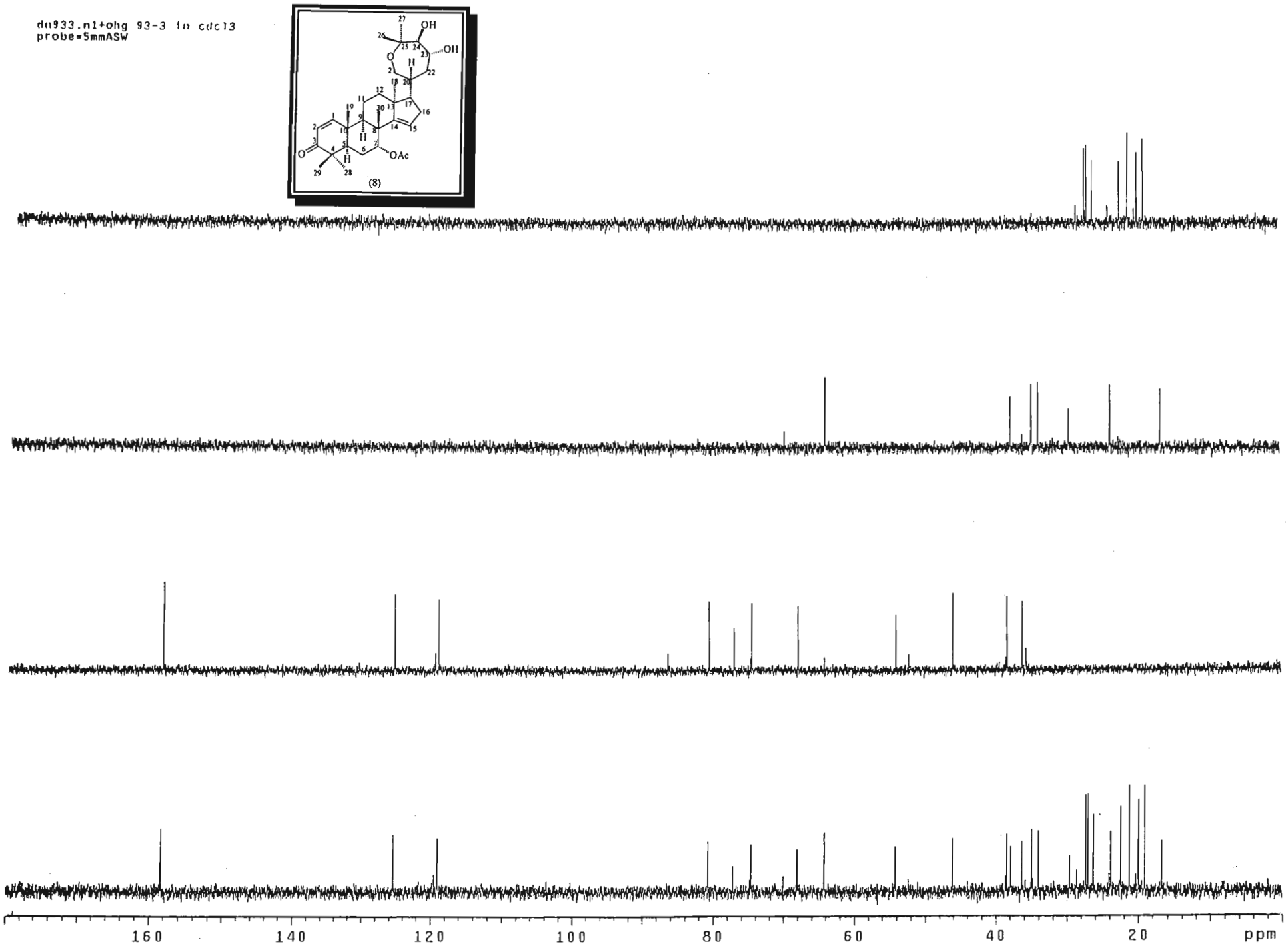

ADEPT NMR spectrum of sapelin E acetate (8)

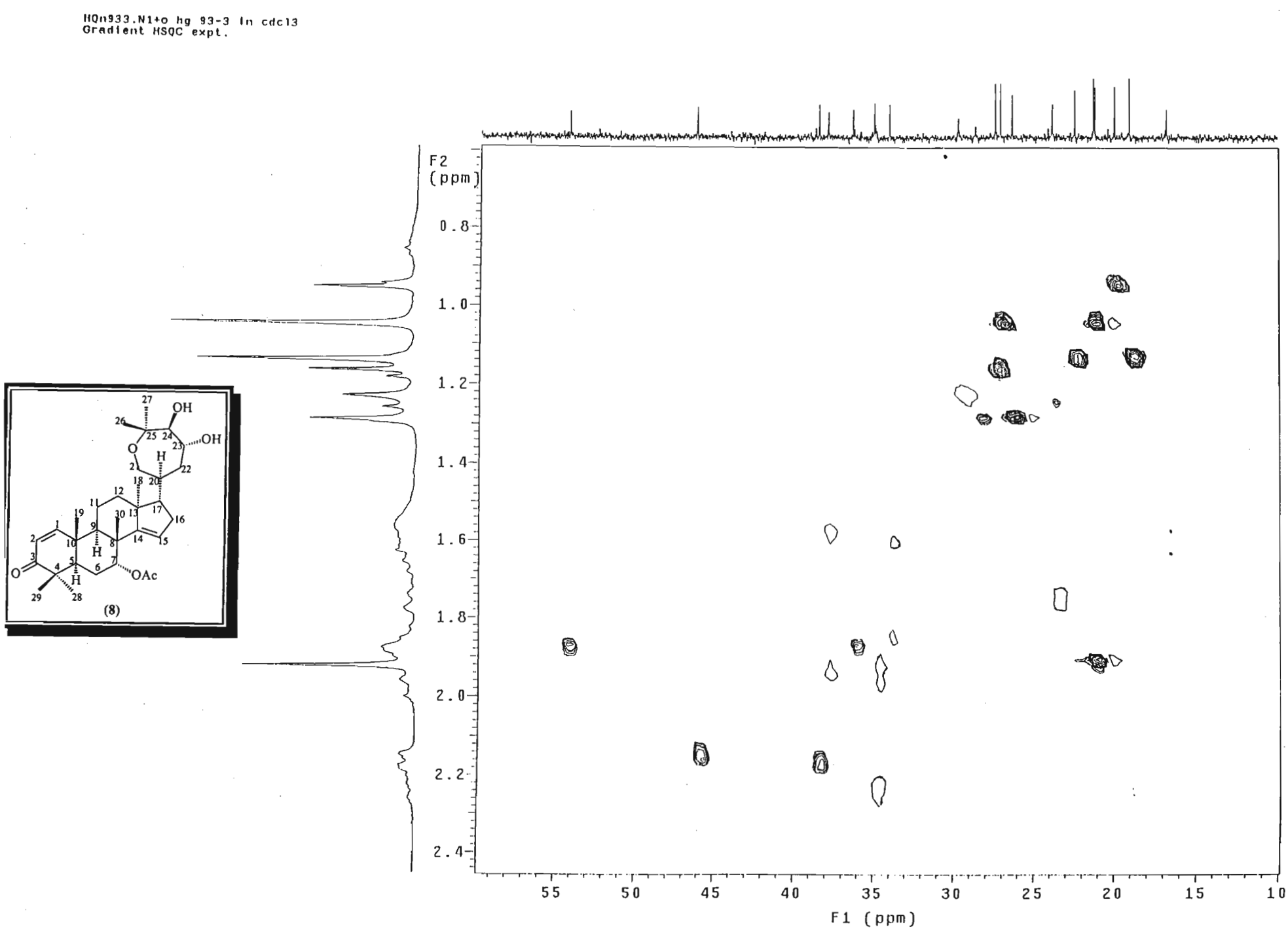

HSQC NMR spectrum of sapelin E acetate (8)

HQn933.N1+o hg 93-3 in cdcl3
Gradient HSQC expt.

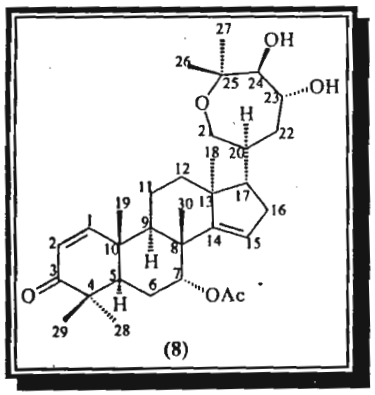

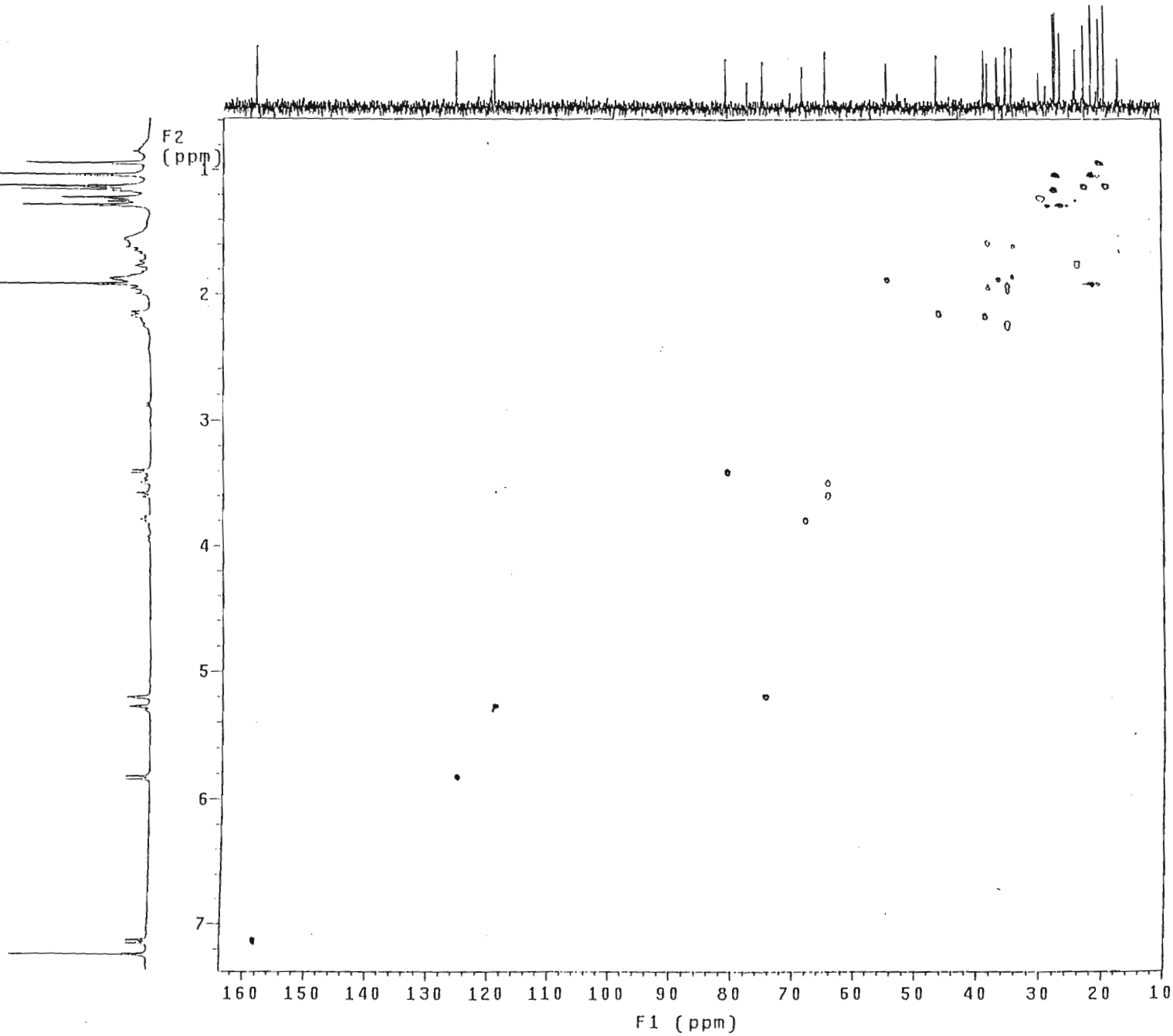

HSQC NMR spectrum of sapelin E acetate (8)

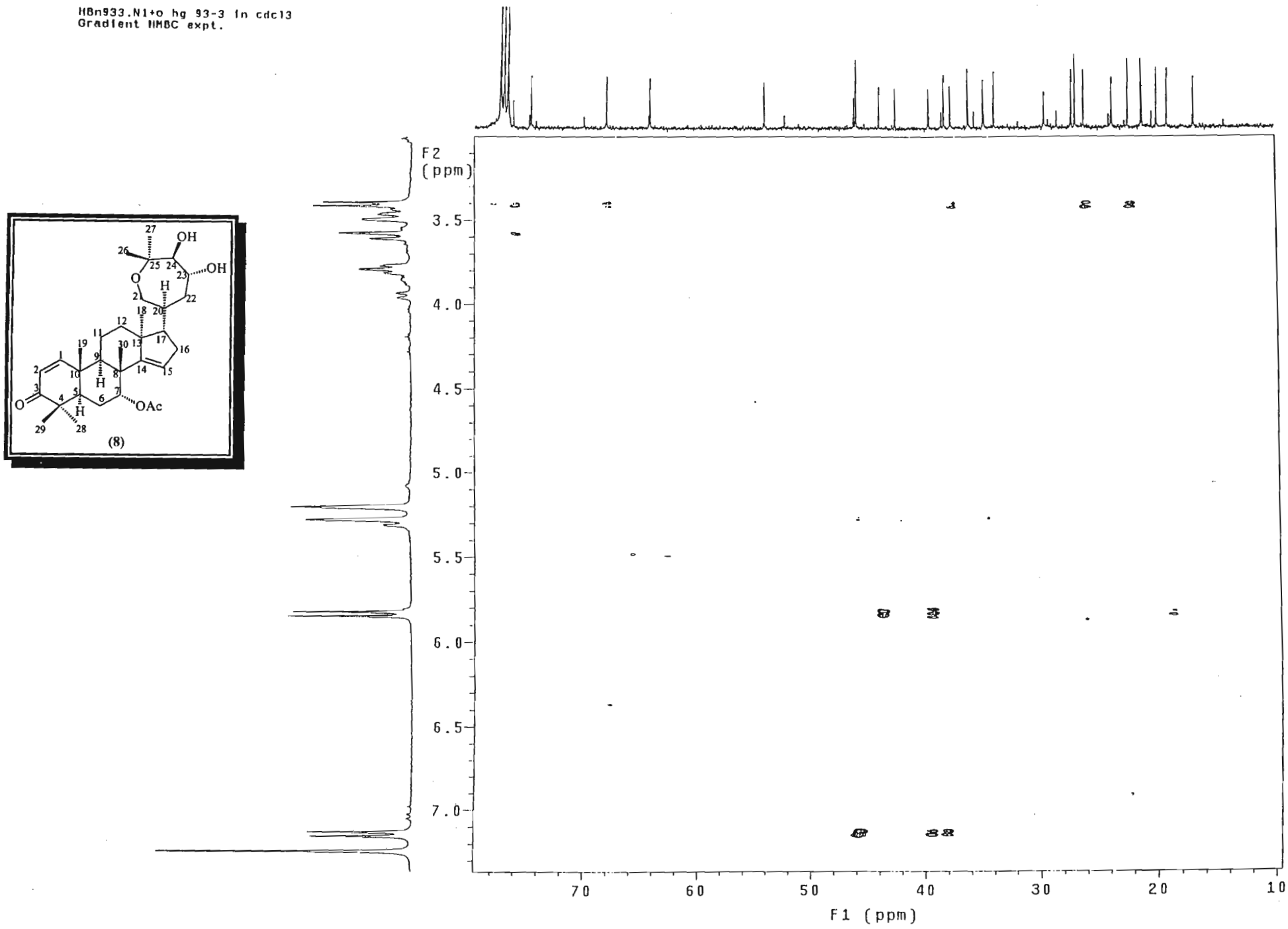

HMBC NMR spectrum of sapelin E acetate (8)

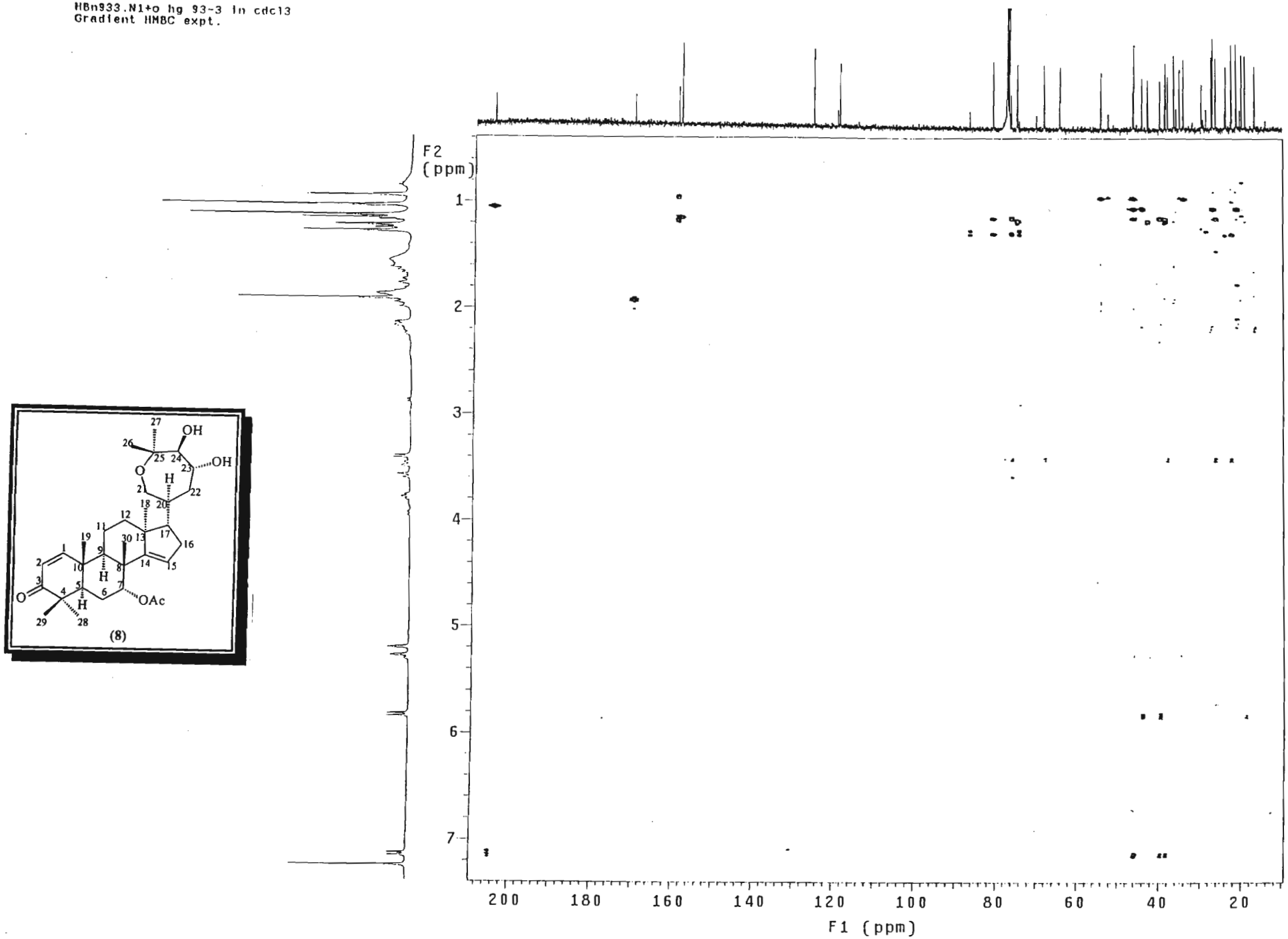

HMBC NMR spectrum of sapelin E acetate (8)

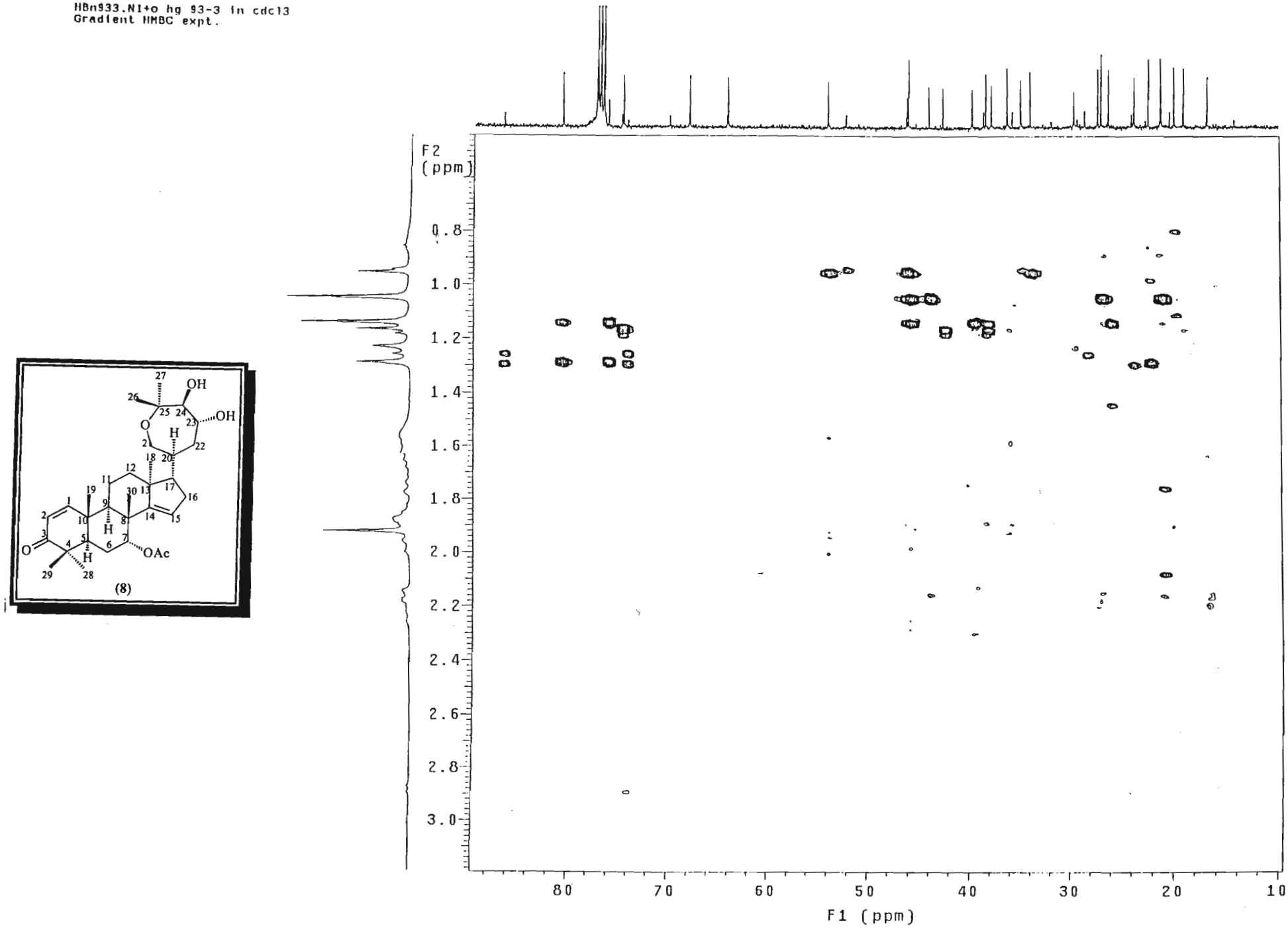

HMBC NMR spectrum of sapelin E acetate (8)

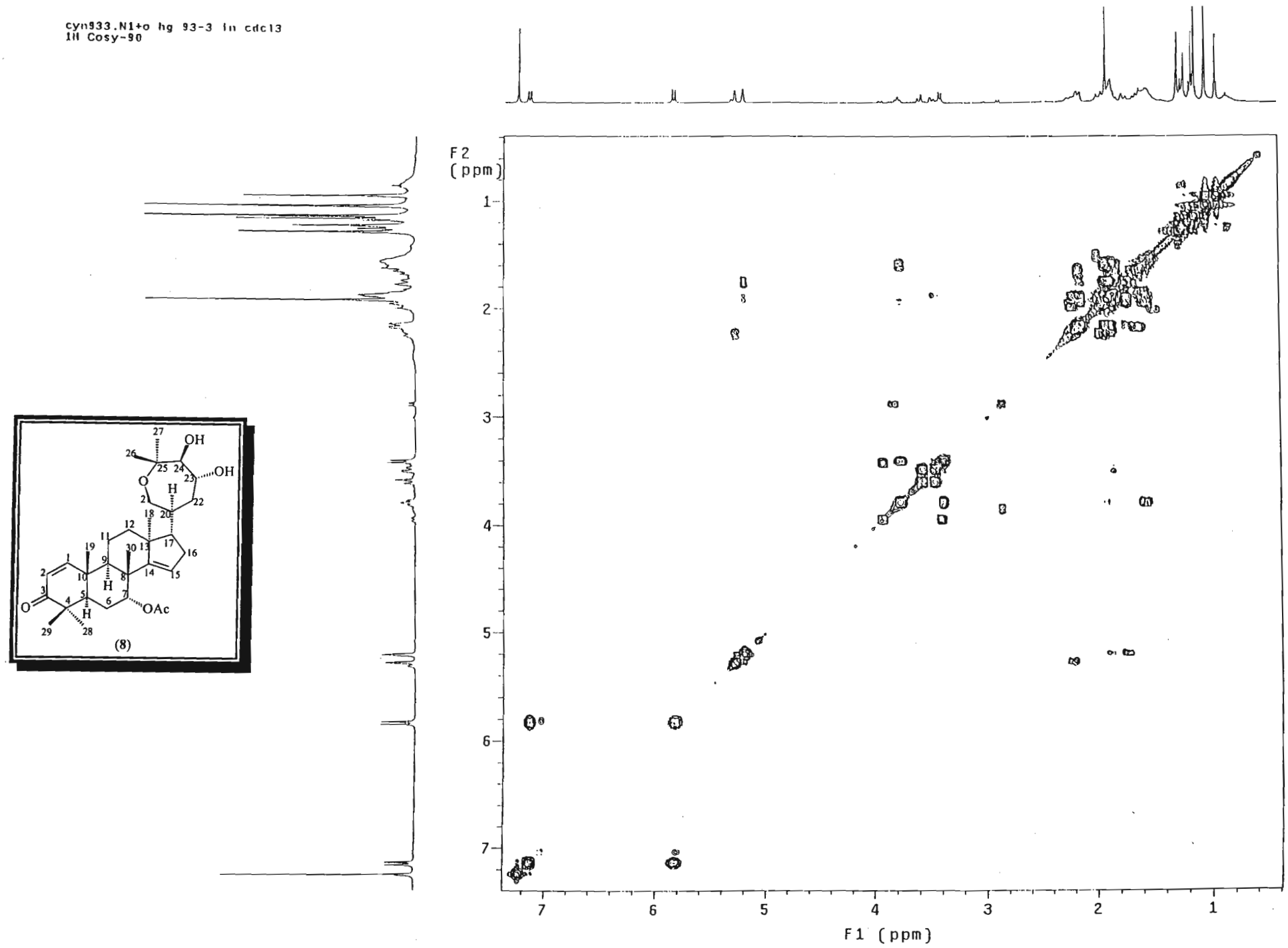

COSY NMR spectrum of sapelin E acetate (8)

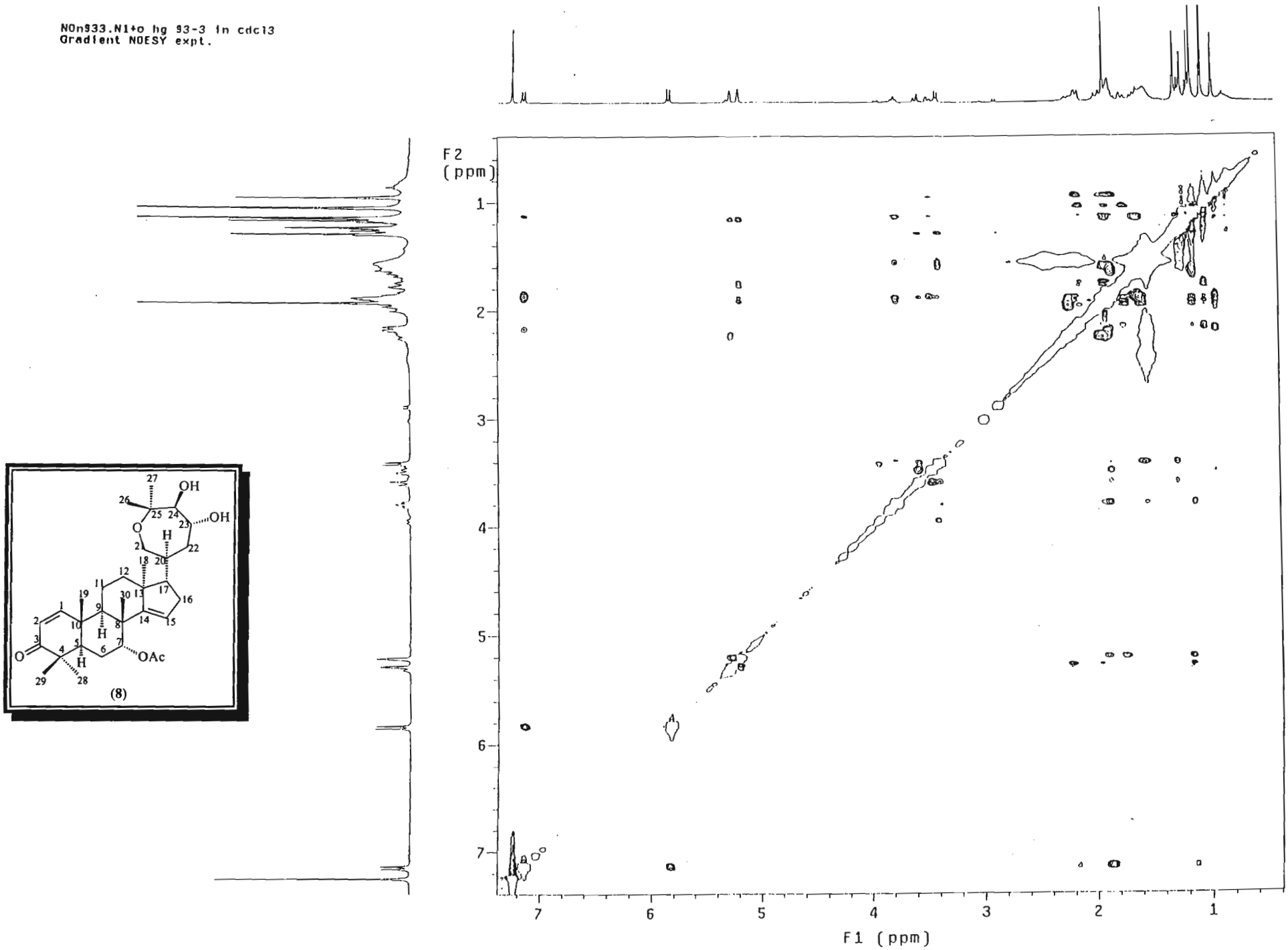

NOESY NMR spectrum of sapelin E acetate (8)

Sapelin C (9)

Mass spectrum	[118]
IR spectrum	[119]
^{1}H NMR	[120]
^{13}C NMR	[121]
HSQC	[122-123]
COSY	[124]
NOESY	[125]

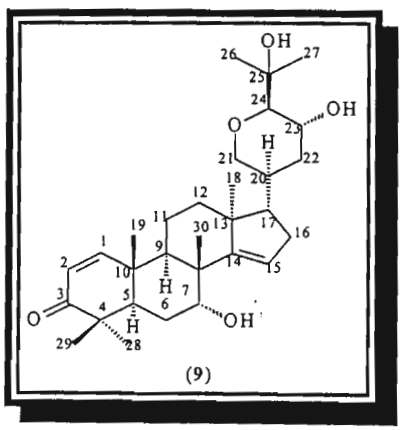

Sapelin C (9)

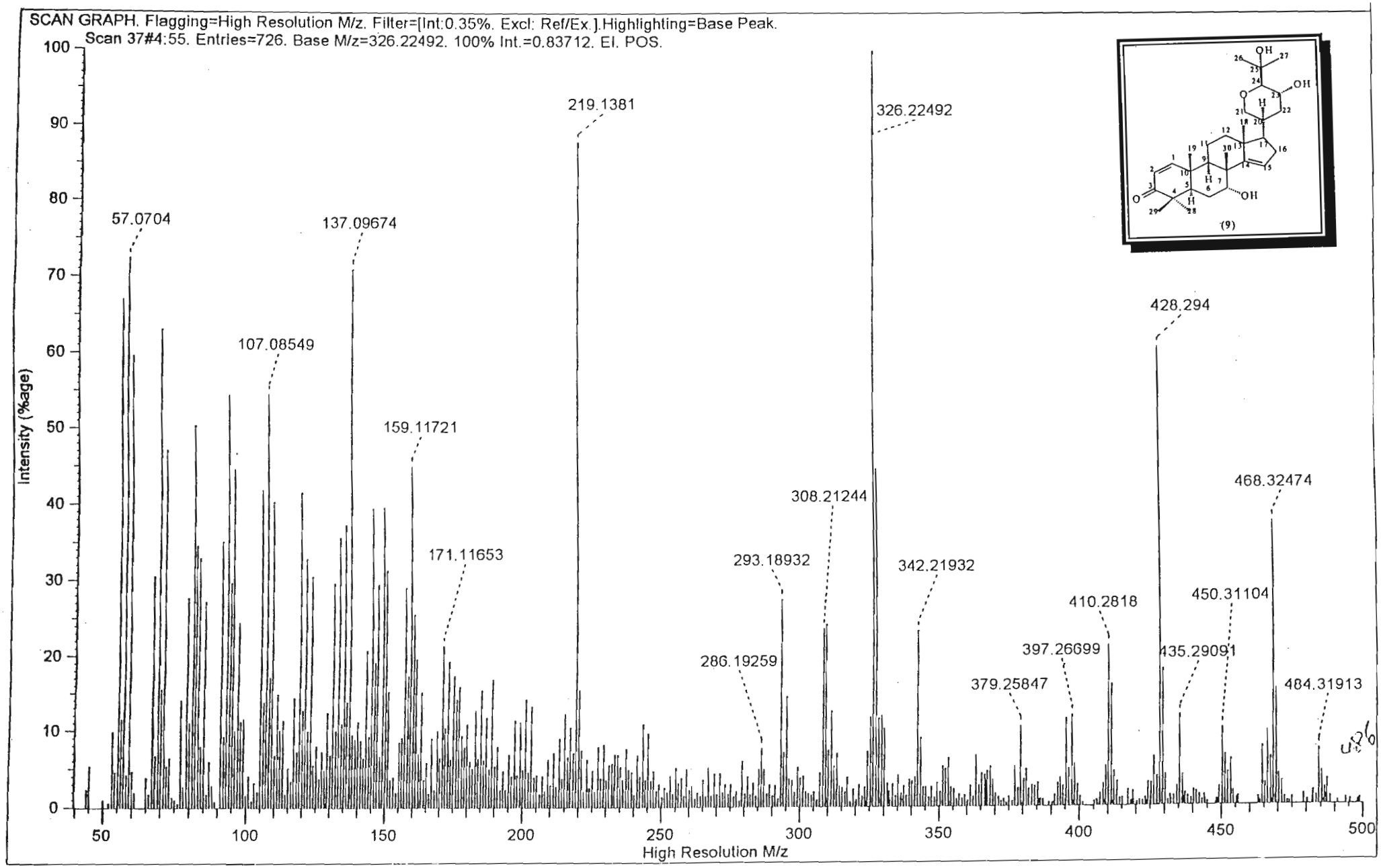

Mass spectrum of sapelin C (9)

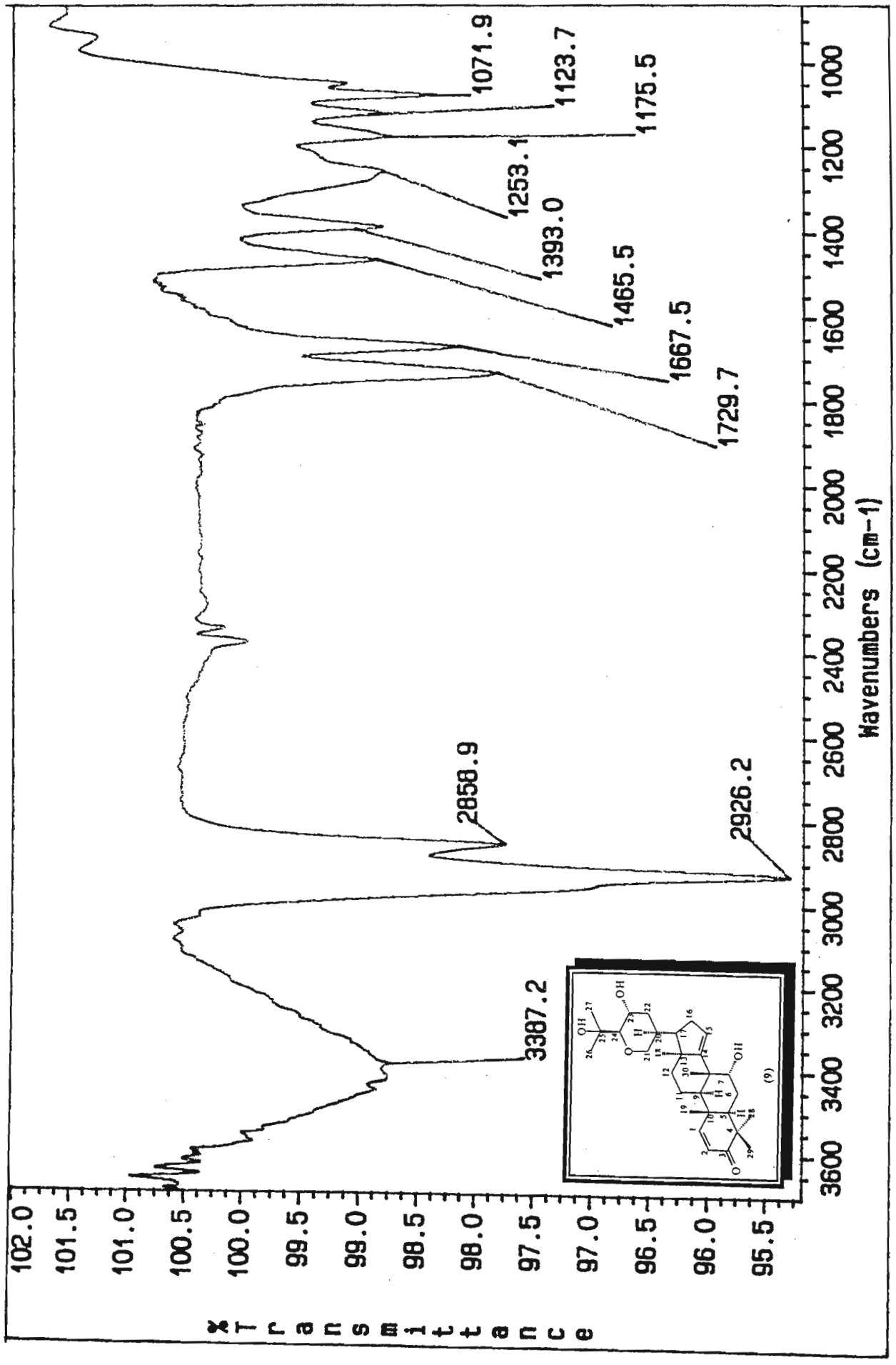

IR spectrum of sapelin C (9)

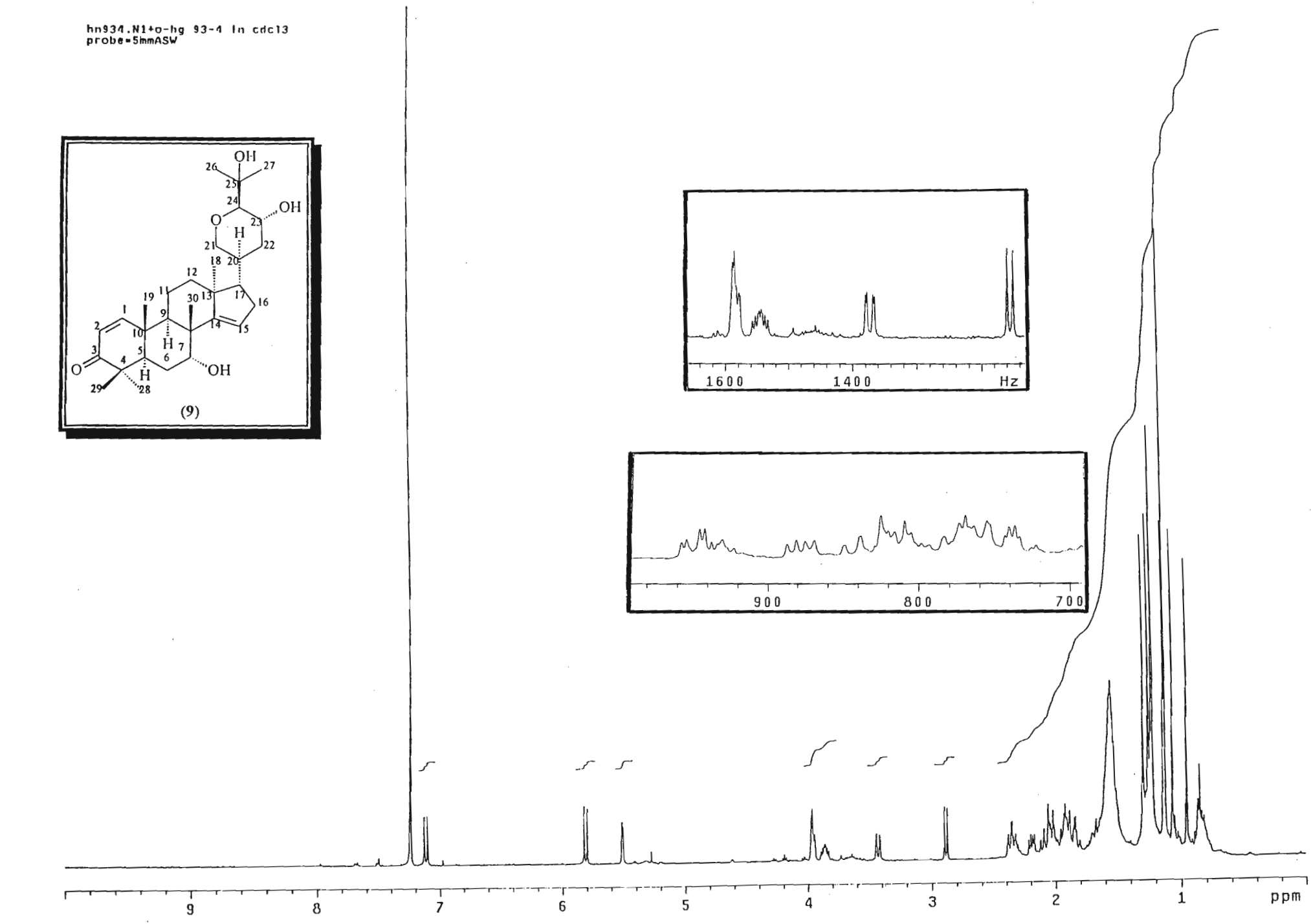

(9)

^{1}H NMR spectrum of sapelin C (9)

cn934.N1+o-hg 93-4 in cdcl3
probe=5mmASW

(9)

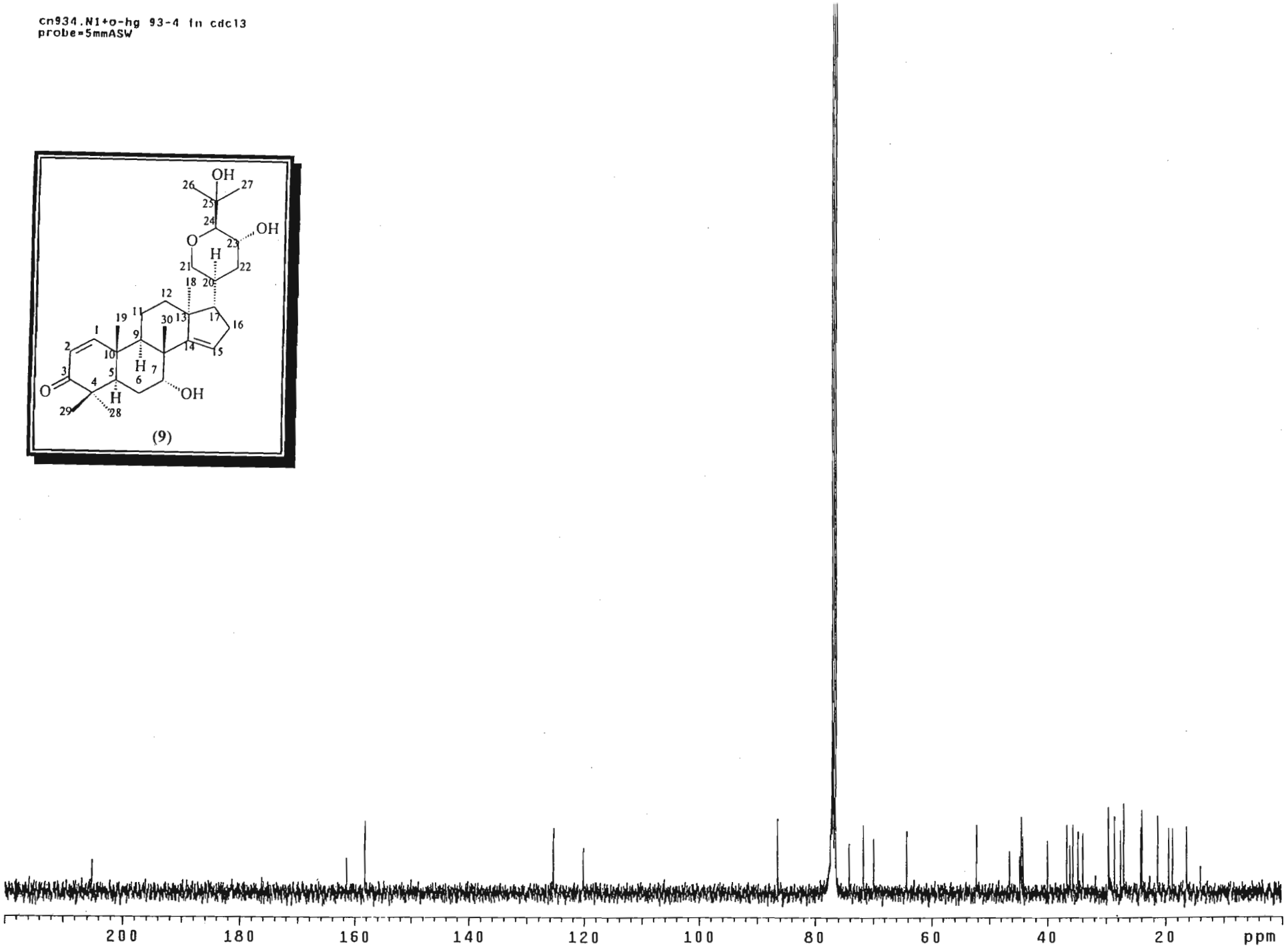

^{13}C NMR spectrum of sapelin C (9)

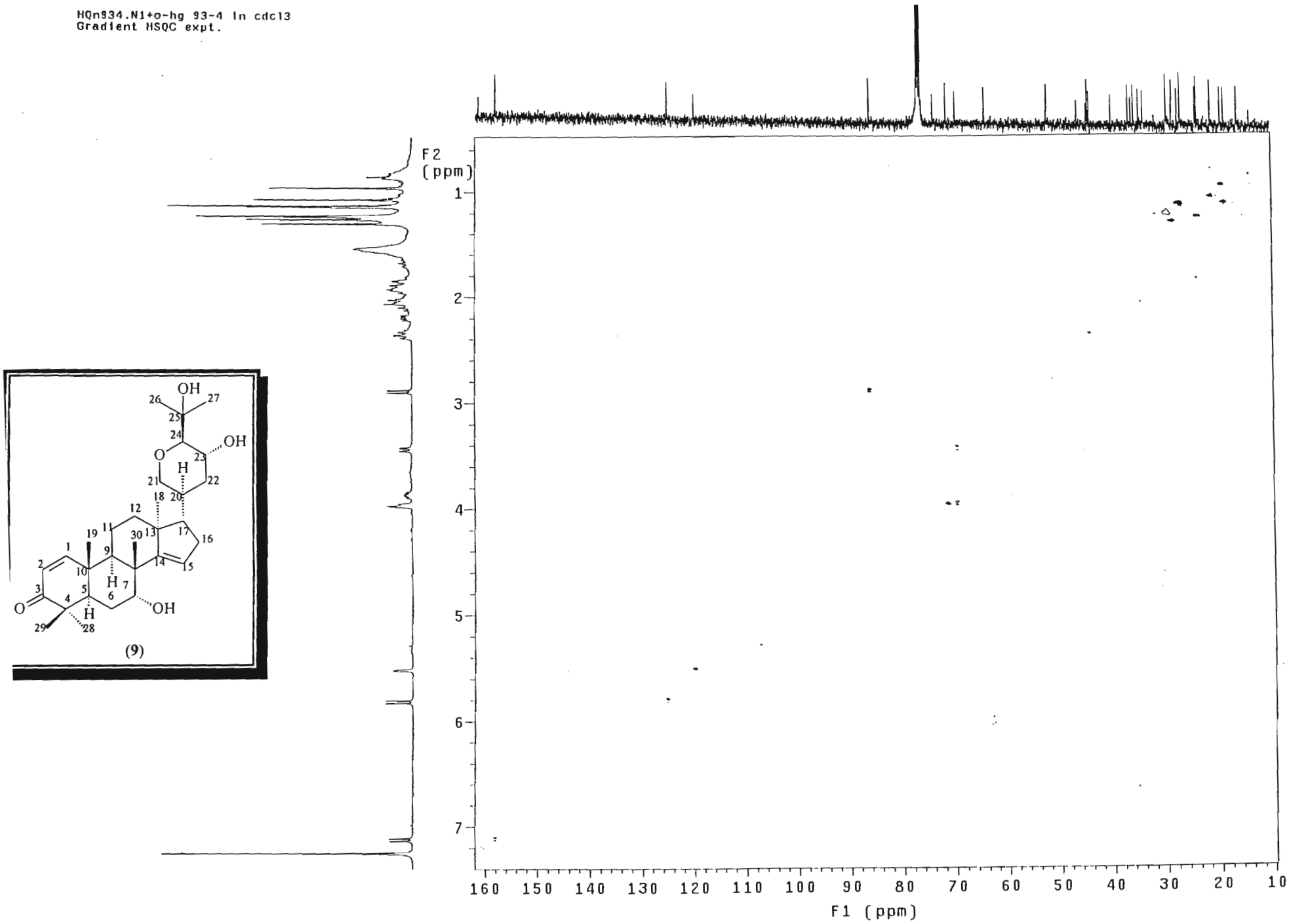

HSQC NMR spectrum of sapelin C (9)

HQn934.N1+o-hg 93-4 in cdcl3
Gradient HSQC expt.

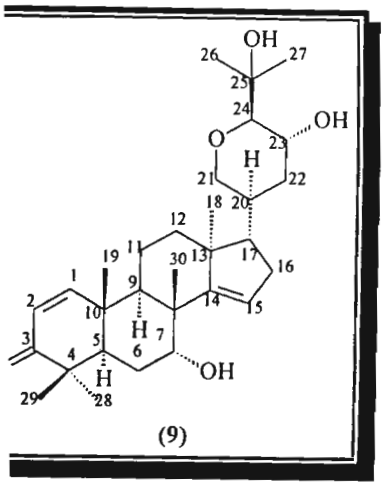

(9)

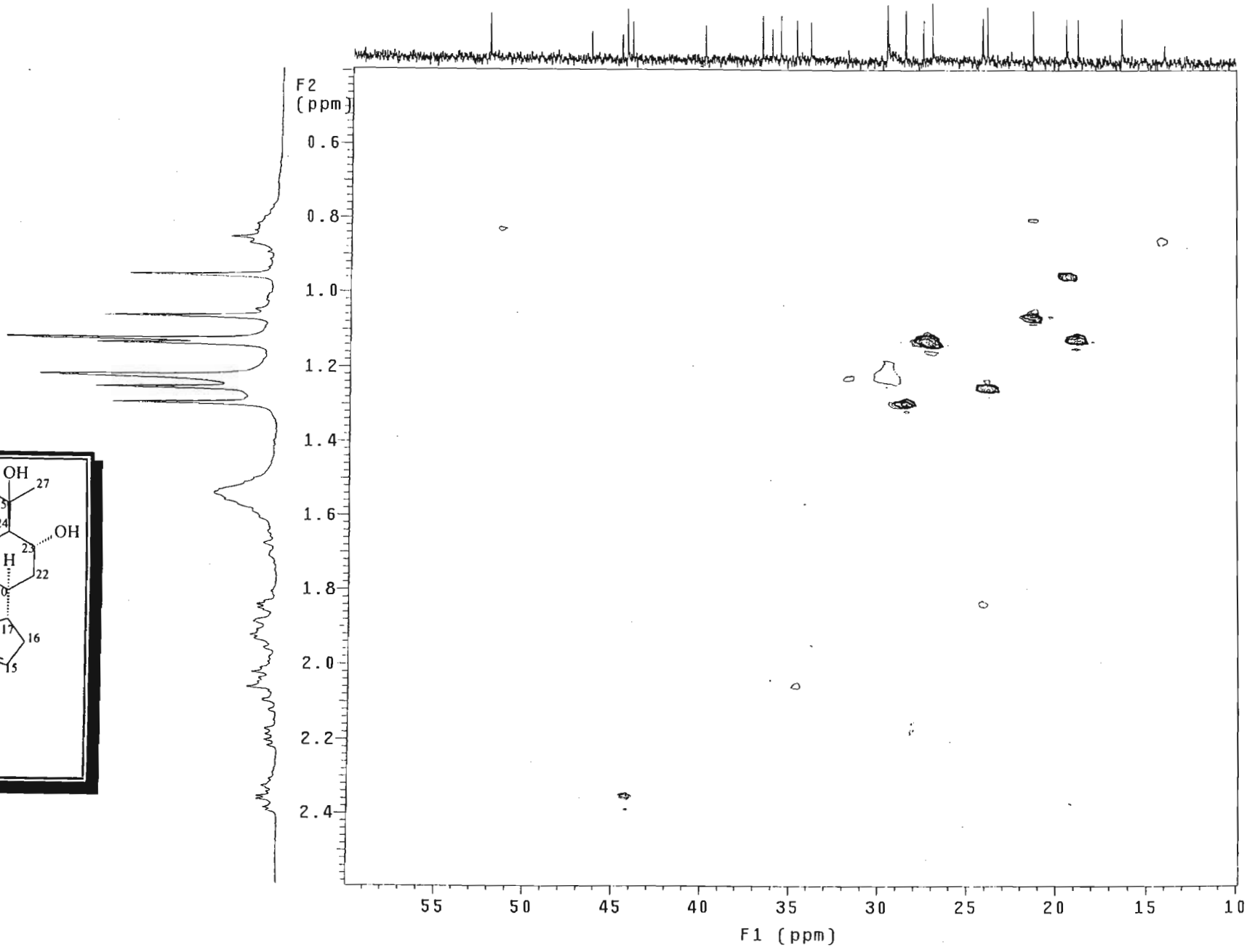

HSQC NMR spectrum of sapelin C (9)

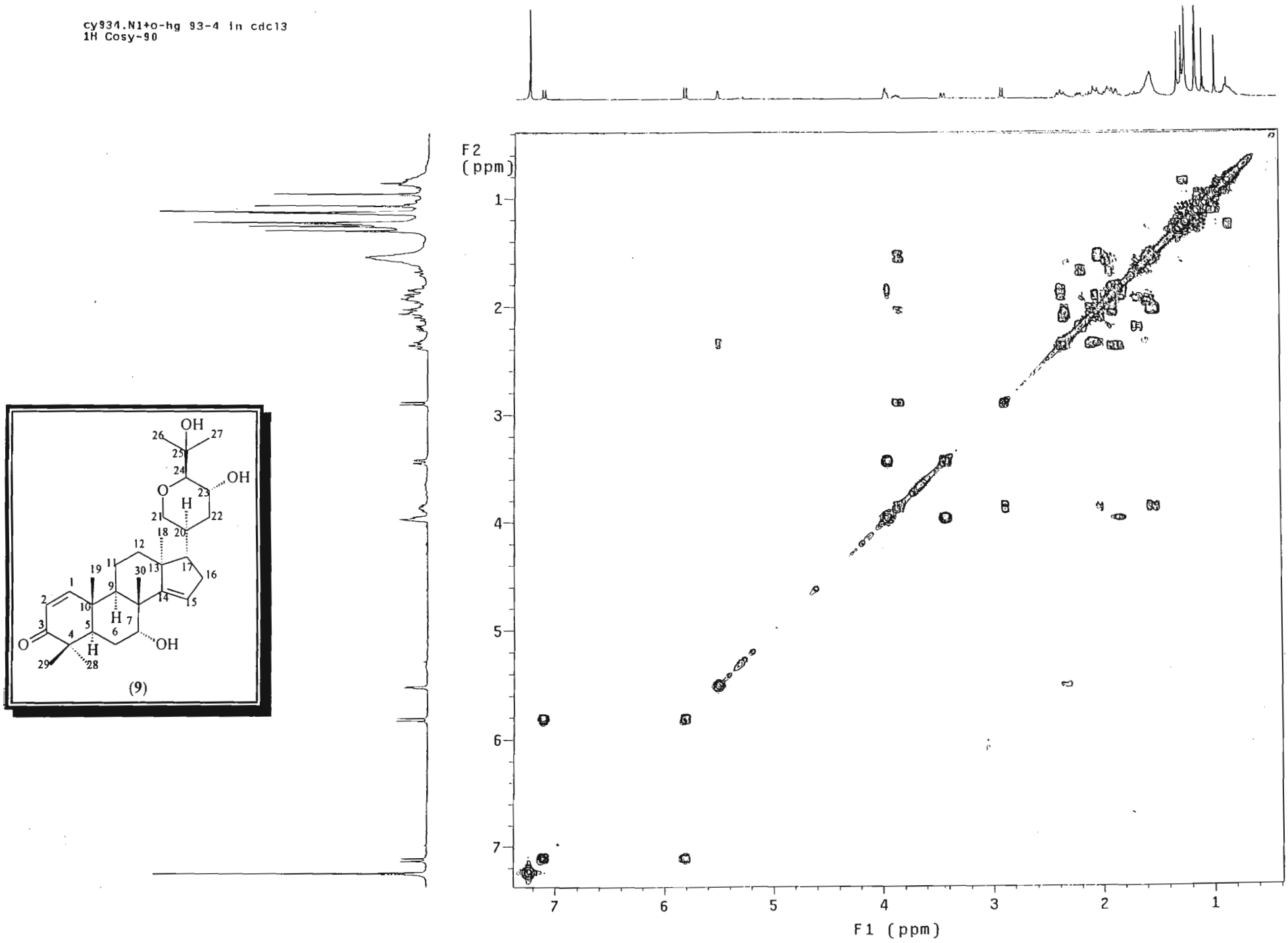

COSY NMR spectrum of sapelin C (9)

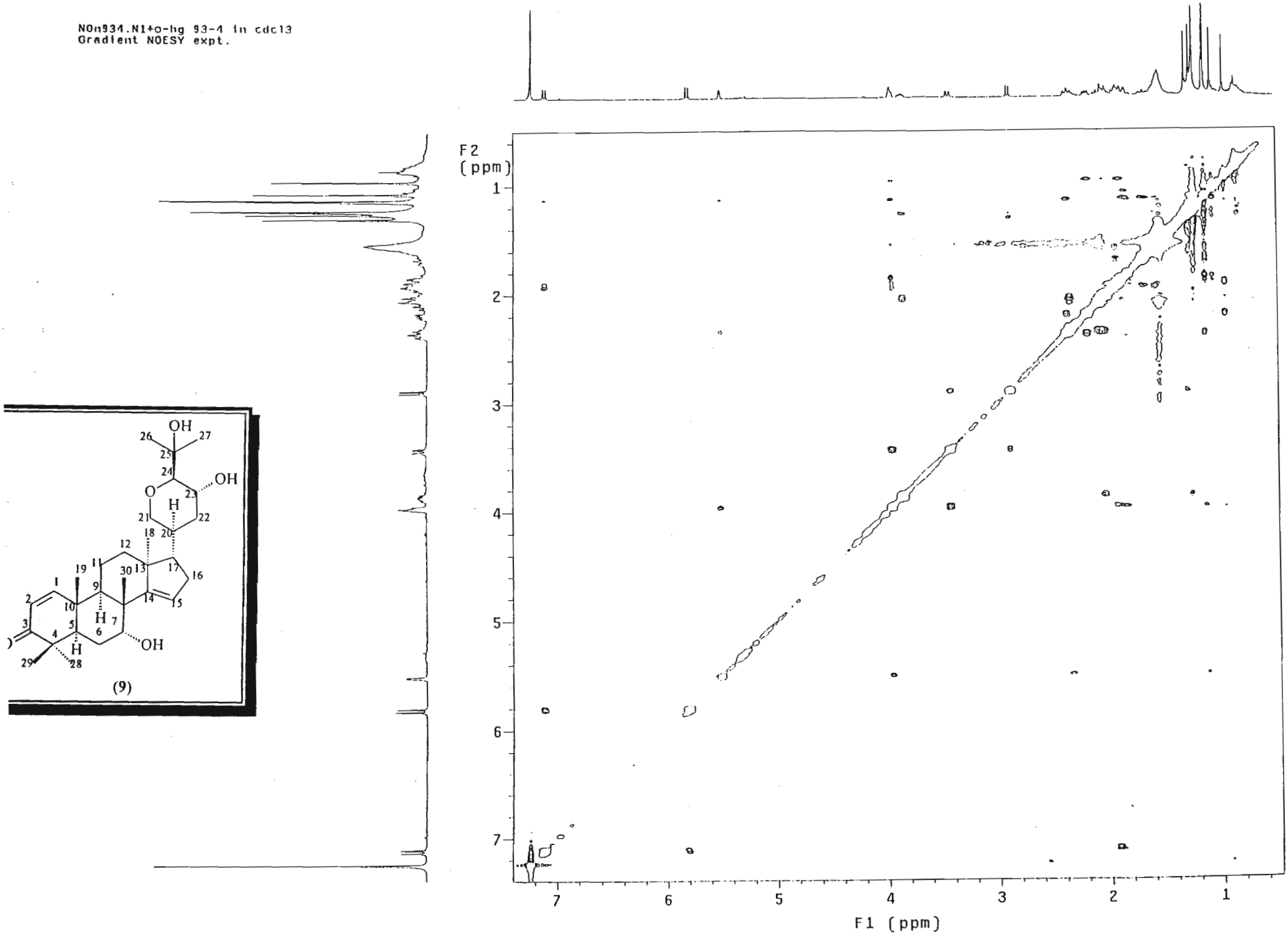

NOESY NMR spectrum of sapelin C (9)

Grandifoliolenone (10)

Mass spectrum	**[127]**
IR spectrum	**[128]**
^{1}H NMR	**[129]**
^{13}C NMR	**[130]**
ADEPT	**[131]**
HSQC	**[132-133]**
COSY	**[134]**
NOESY	**[135]**

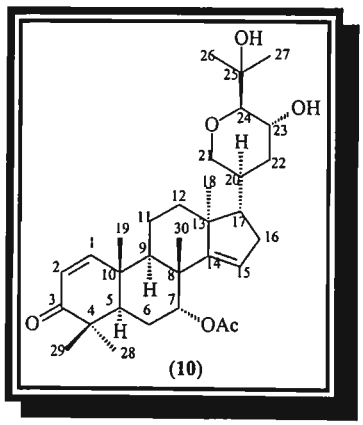

Grandifoliolenone (10)

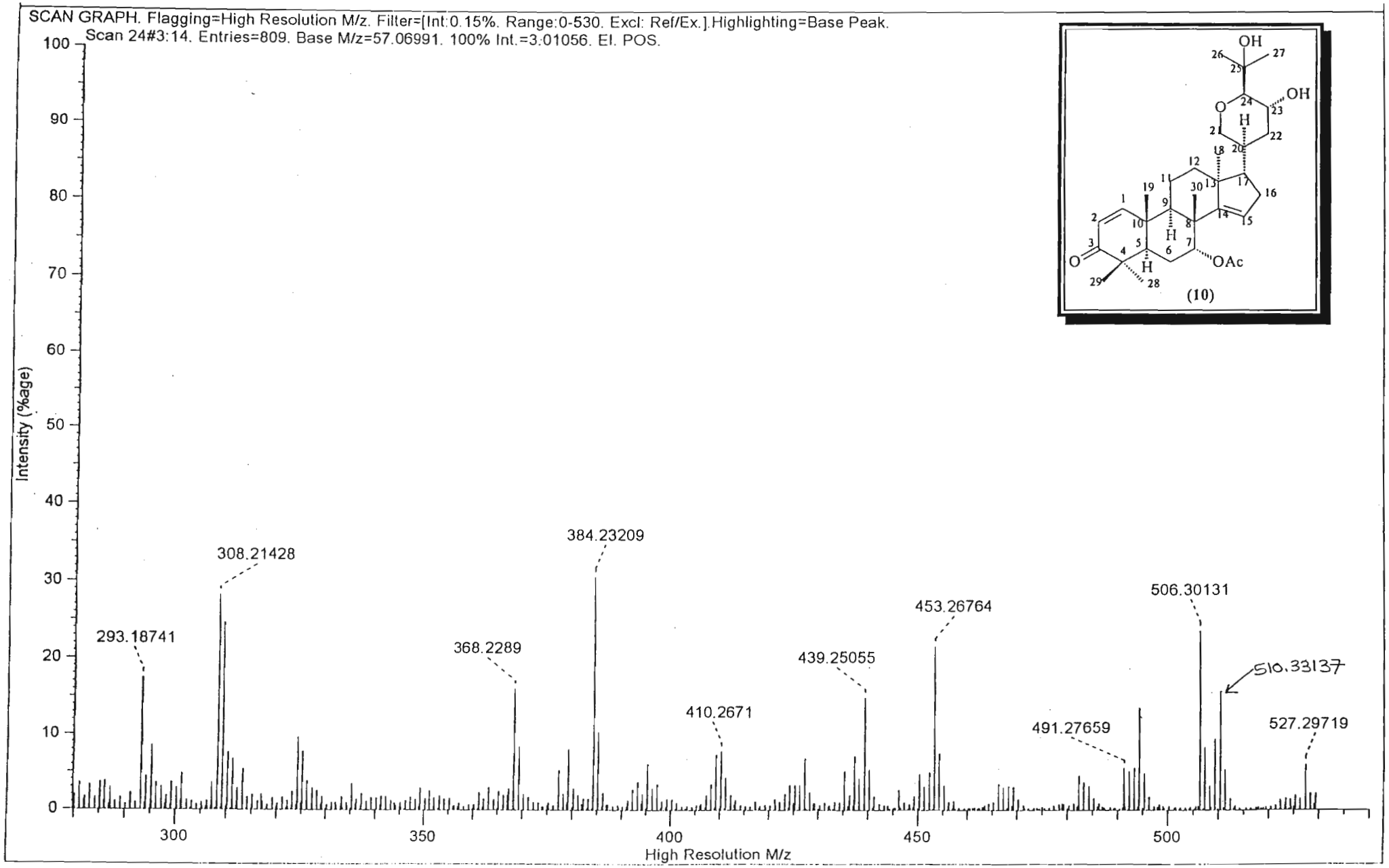

Mass spectrum of grandifoliolenone (10)

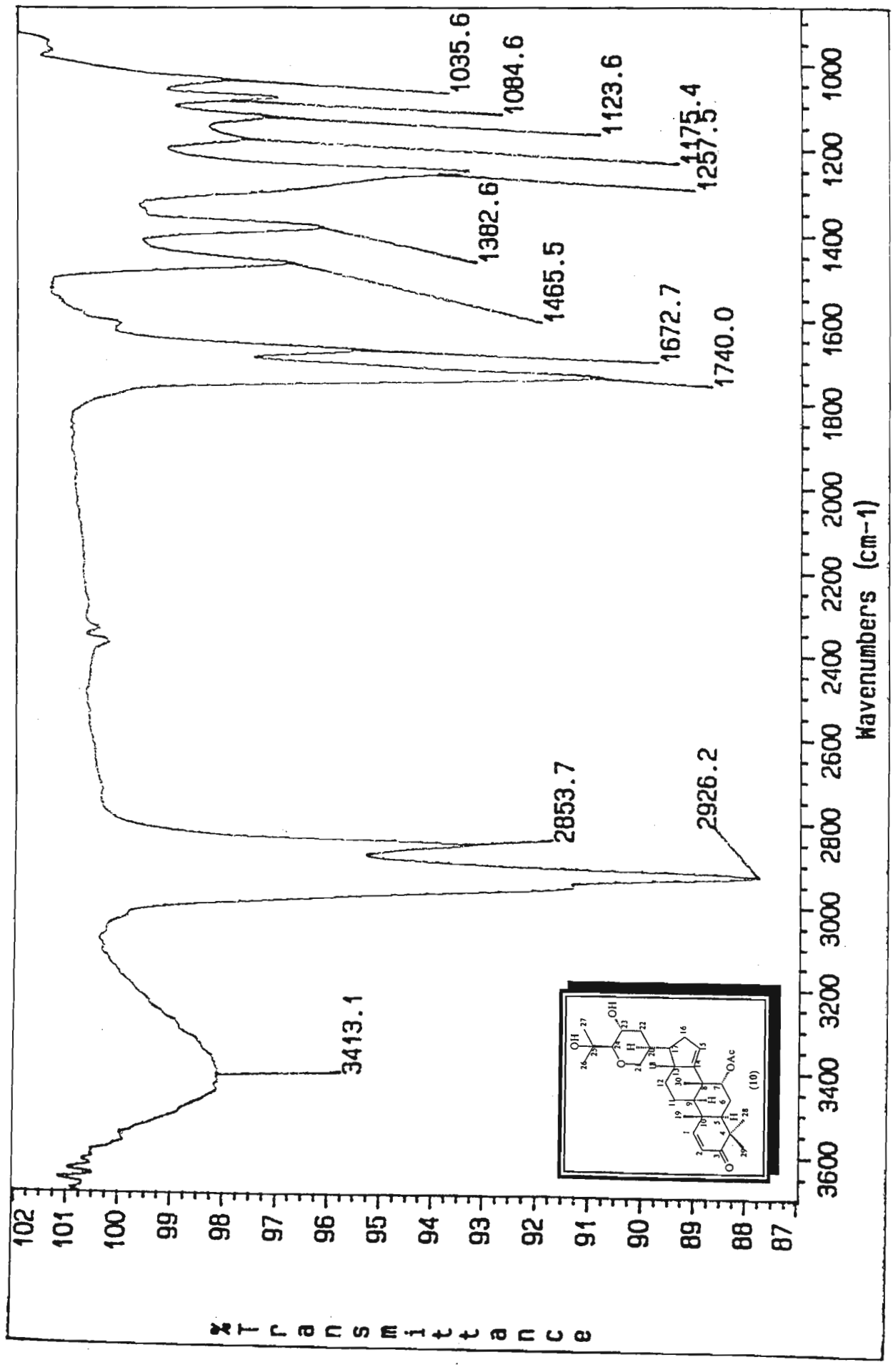

IR spectrum of grandifoliolenone (10)

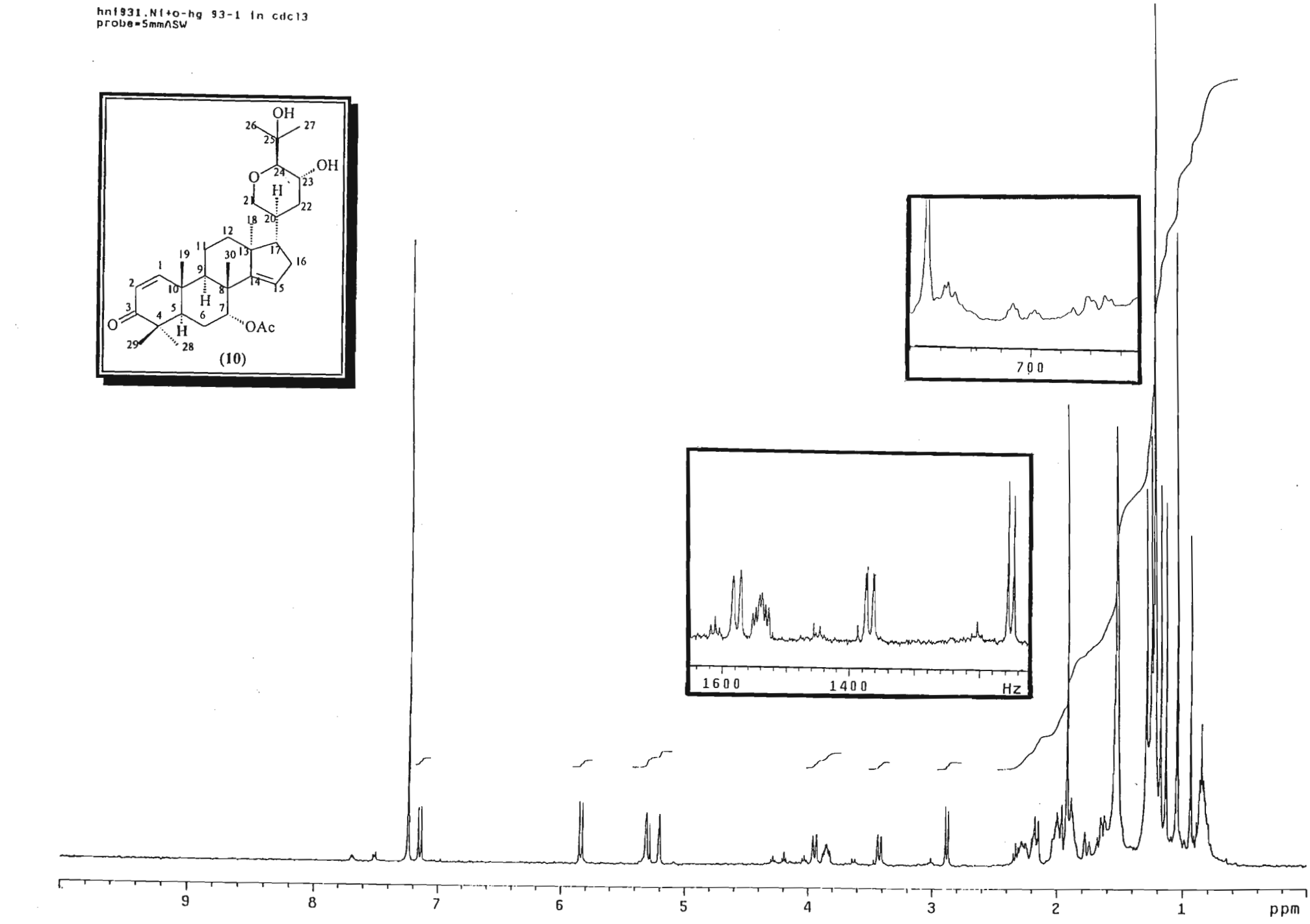

^{1}H NMR spectrum of grandifoliolenone (10)

cnl931.Nl+o-hg 93-1 in cdcl3
probe=5mmASW

(10)

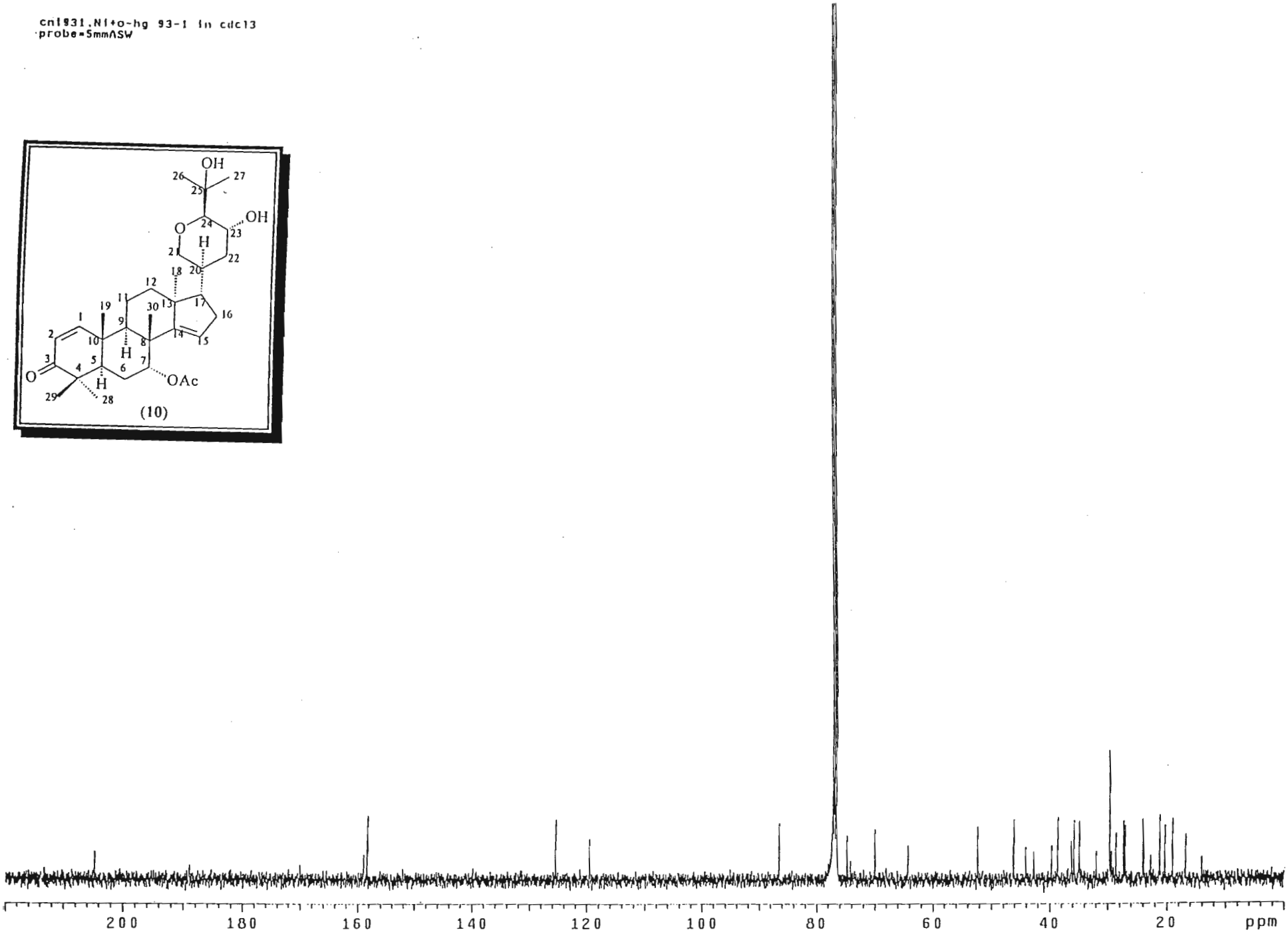

^{13}C NMR spectrum of grandifoliolenone (10)

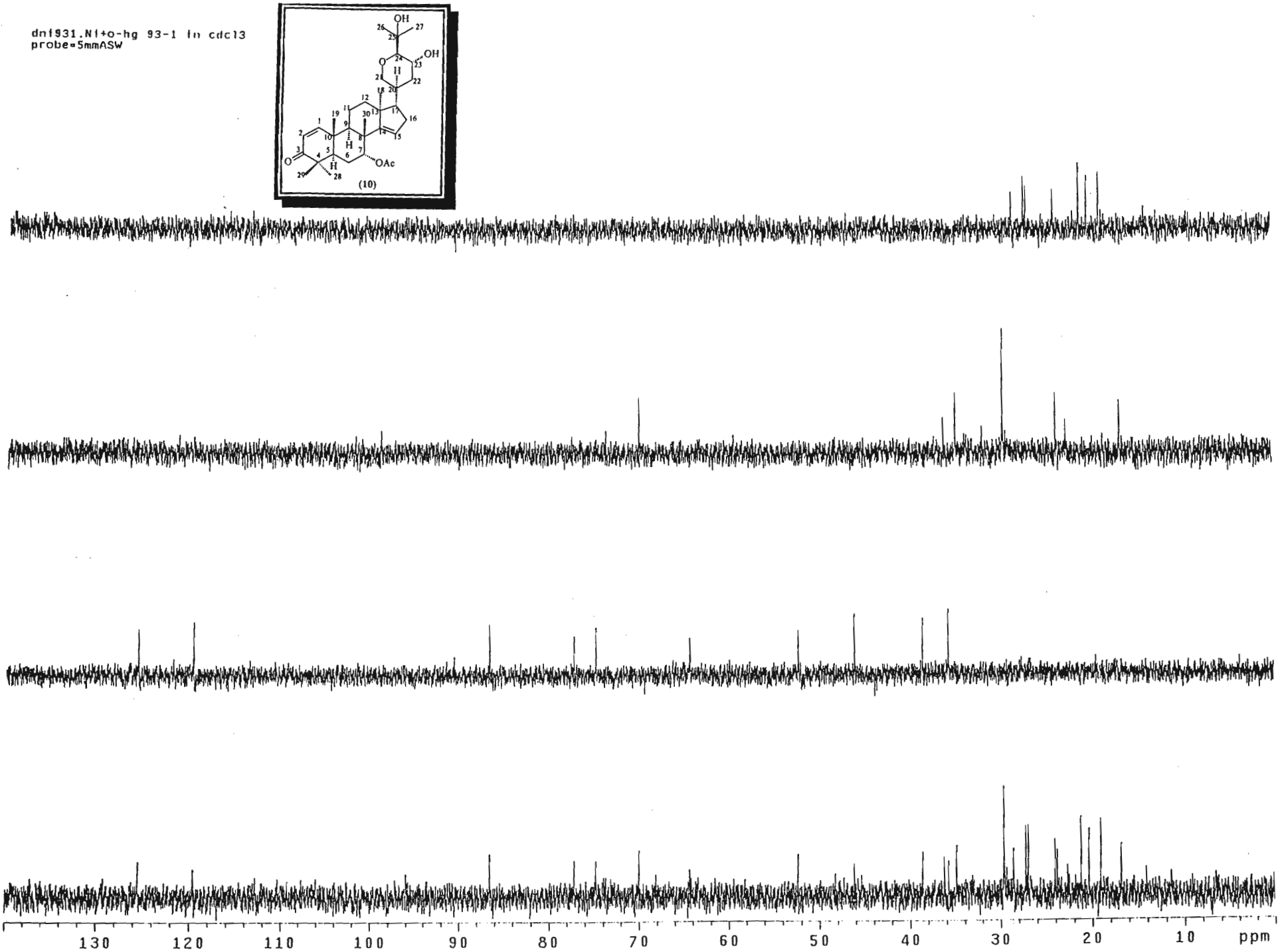

ADEPT NMR spectrum of grandifoliolenone (10)

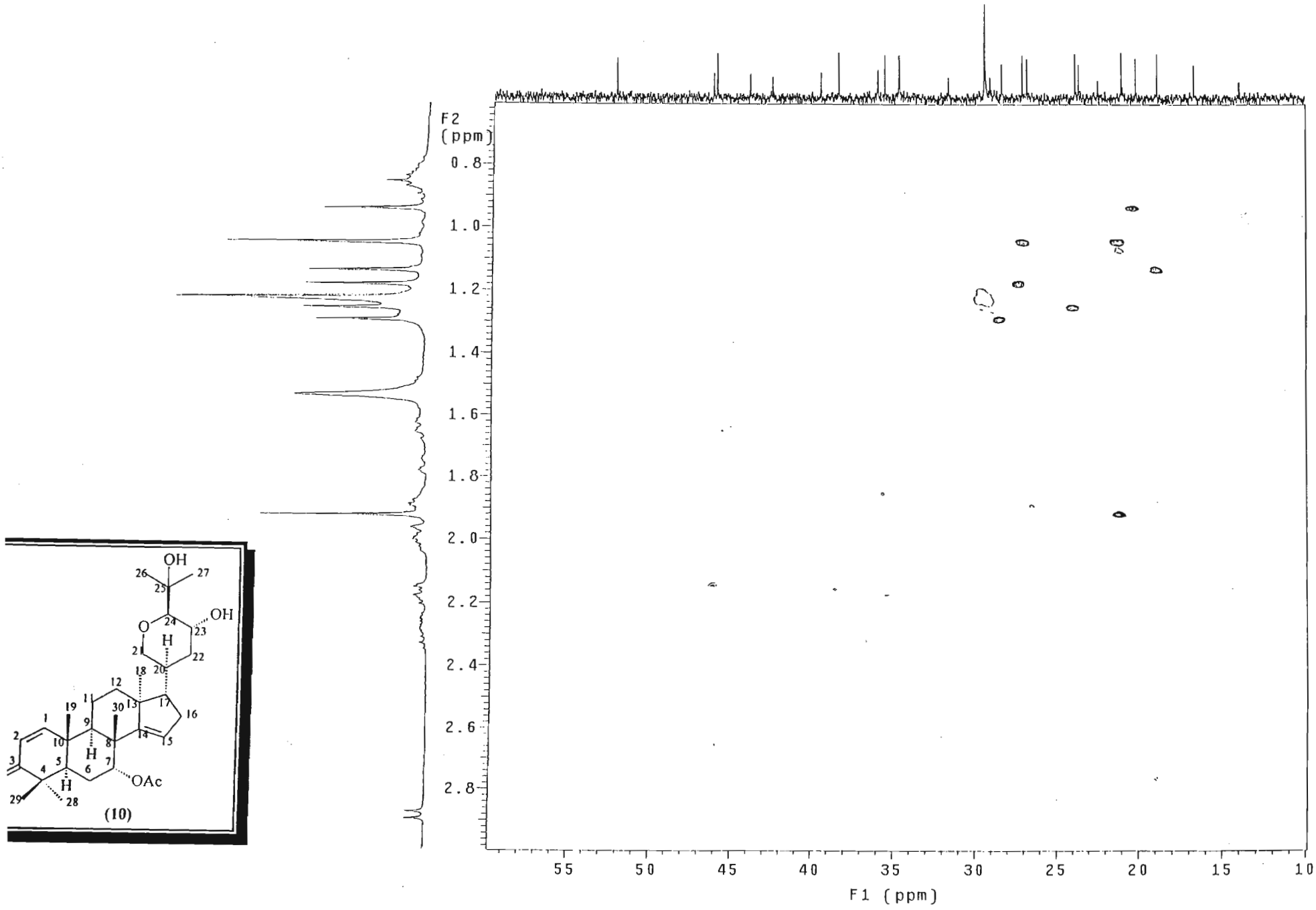

HSQC NMR spectrum of grandifoliolenone (10)

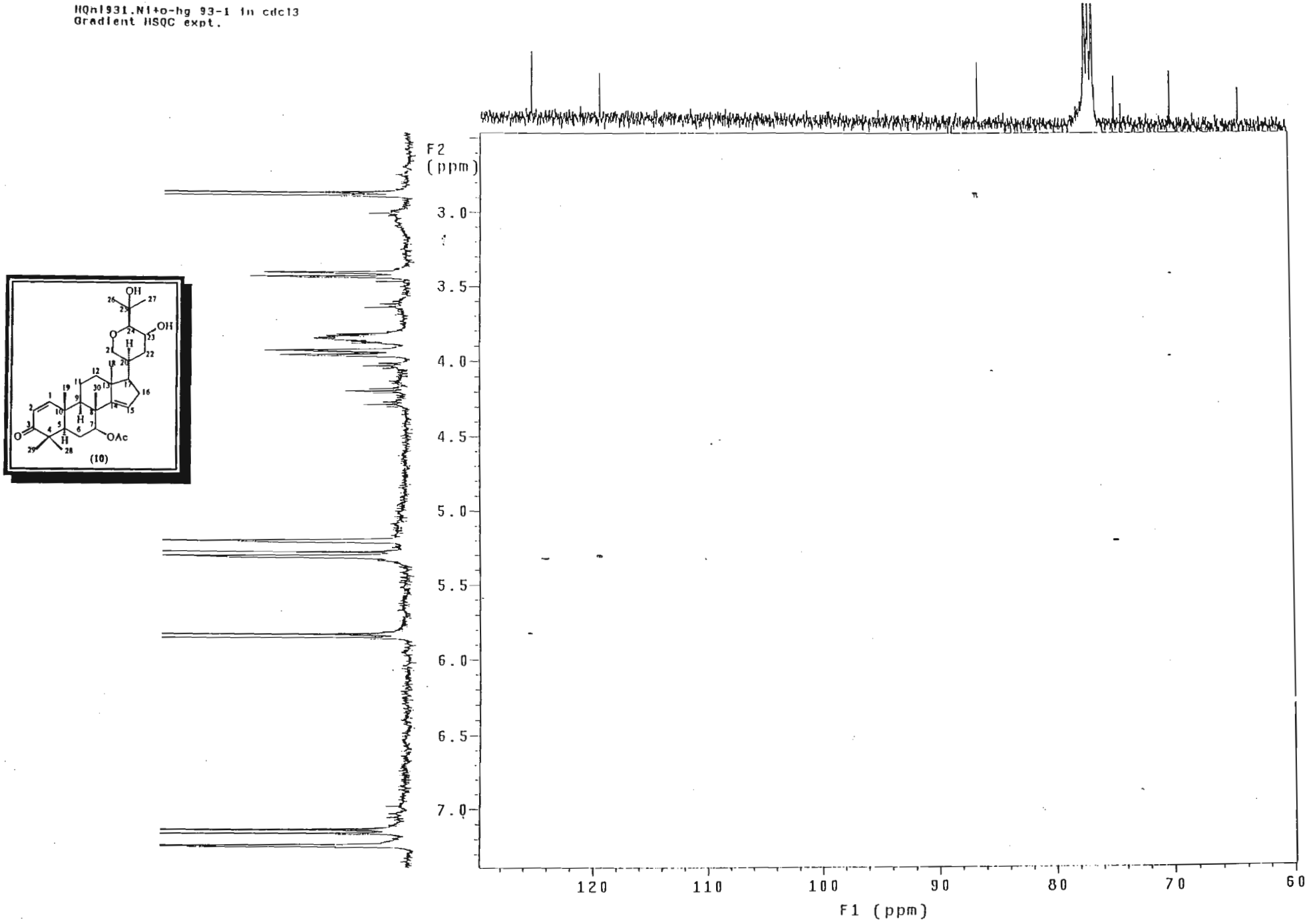

HSQC NMR spectrum of grandifoliolenone (10)

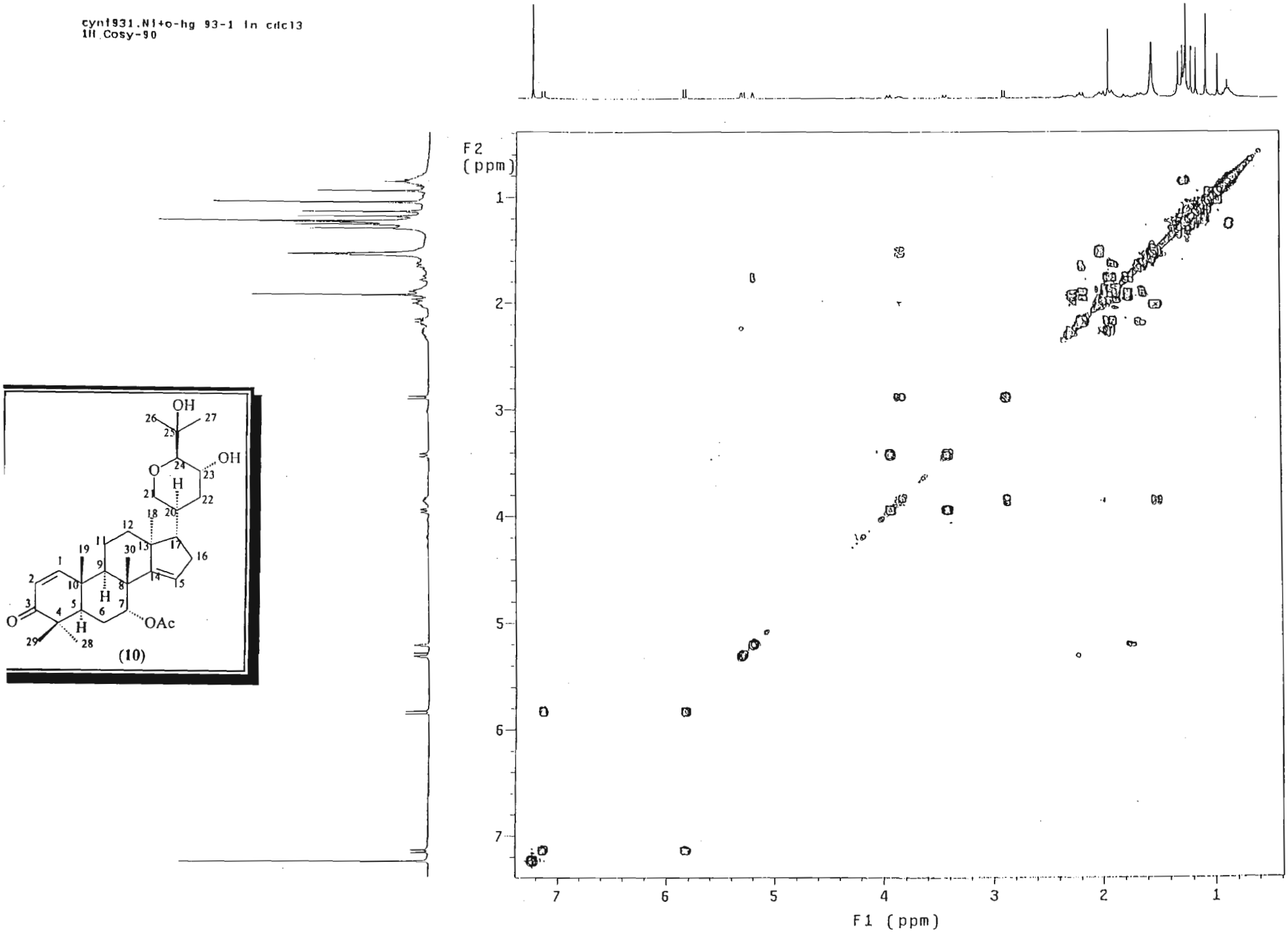

COSY NMR spectrum of grandifoliolenone (10)

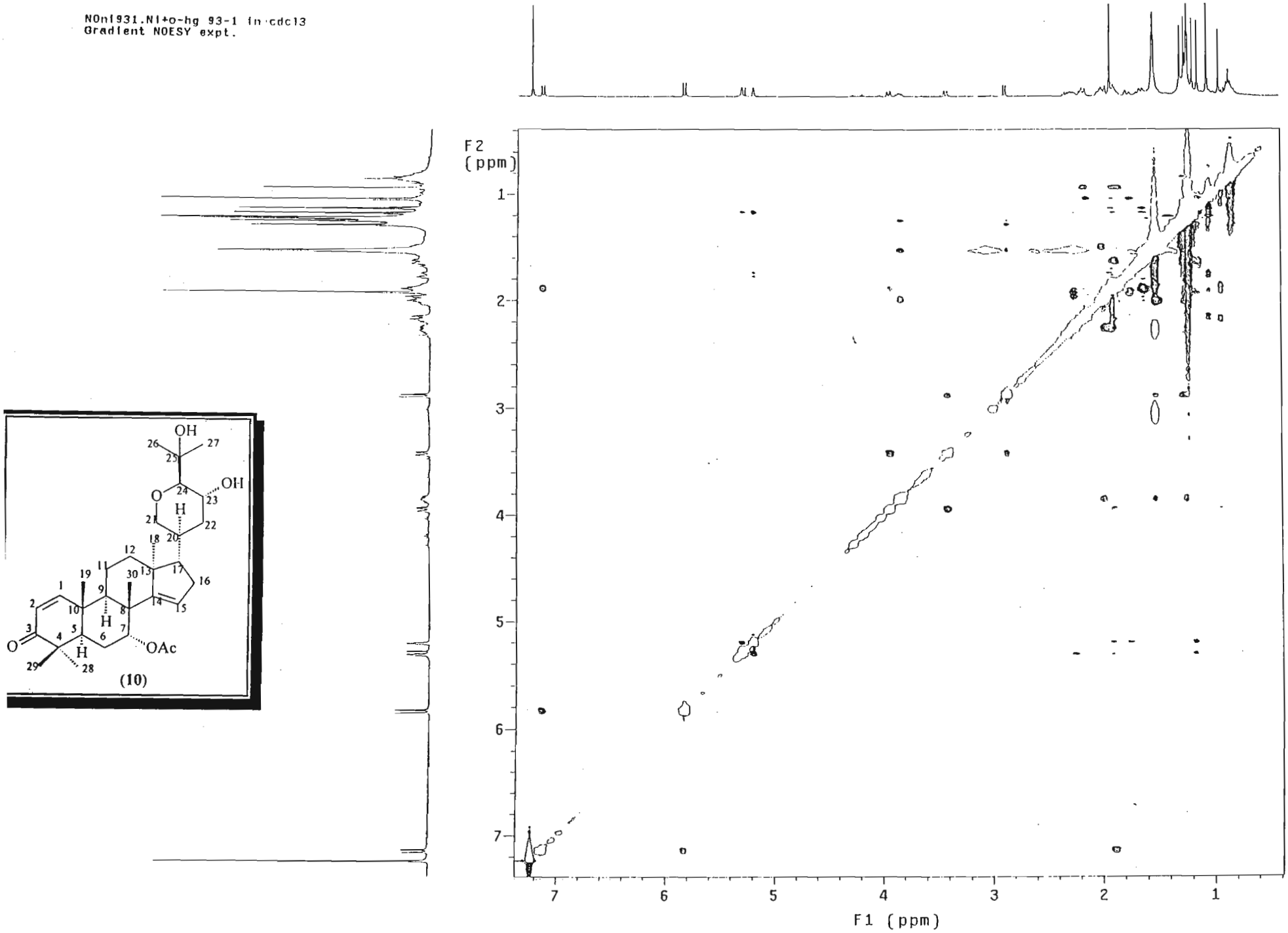

NOESY NMR spectrum of grandifoliolenone (10)